Systematic biology and sexuality in the genus *Scytosiphon* (Scytosiphonaceae, Phaeophyceae)

褐藻カヤモノリ属(カヤモノリ科)における系統分類、生殖隔離、生殖様式について

Masakazu Hoshino

Department of Natural History Sciences
Graduate School of Science
Hokkaido University

March 2021

ABSTRACT

This doctoral thesis focuses on two main themes for the genus *Scytosiphon* (Scytosiphonaceae, Ectocarpales) species: one is its systematic biology (**Part 1**) and the other is sexuality of its field populations (**Part 2**).

Part 1: In brown algae, morphological species identification is often difficult due to their morphological simplicity and plasticity. With the spread of molecular phylogenetic analyses, it has been revealed that many morphospecies include multiple cryptic species, which are often distributed in a narrow geographical scale, sometimes sympatric. It provides us an opportunity to tackle one aspect of the most important 'species problem,' that is, how sympatric, sexually reproducing organisms fall into discrete clusters; however, little is known about reproductive isolating barriers among the species detected by molecular phylogenetic analyses. In **Part 1**, I conducted molecular phylogenetic analyses on the morphospecies of *Scytosiphon lomentaria* and *Planosiphon gracilis* (which formerly belonged to *Scytosiphon*), and performed crossing experiments among the putative species inferred from molecular phylogenetic analyses to examine the existence of reproductive isolating barriers. I showed that morphospecies of both *S. lomentaria* and *Pl. gracilis* included multiple cryptic species with overlapping distributions and gametic incompatibility was often observed as a pre-zygotic barrier among these cryptic species. In *Scytosiphon*, gametic incompatibility was observed more frequently among sympatric species pairs than among allopatric species pairs, suggesting reinforcement–the enhancement of prezygotic isolation in sympatry by natural selection. Here, I demonstrated the concordance of DNA-based species boundaries and reproductive isolating barriers and provided evidence of reproductive isolating barriers in closely related species, for which there were only limited data from macroalga so far. Consequently, I also described four new species in *Scytosiphon* (i.e., *S. shibazakiorum*, *S. tosaensis*, *S. arcanus*, and *S. subtropicus*) and one new species in *Planosiphon* (i.e., *Pl. nakamurae*).

Part 2: Parthenogenesis is a way of asexual reproduction in which an unfused gamete develops into a new individual. In brown algae, this asexual process has been widely observed in laboratory culture conditions, even in sexual taxa. However, little is known about the significance of parthenogenesis in field populations in brown algae. In **Part 2**, I investigated the frequency of parthenogenesis in field and the evolution of parthenogens using three *Scytosiphon* species. I showed that parthenogenesis rarely occurs in the sexual field population of *S. shibazakiorum* with 1:1 sex ratio. While, in *S. lomentraia* and *S. promiscuus*, I found female populations that reproduce parthenogenetically (parthenogenetic populations), in addition to sexual populations including both female and male individuals. In both species, parthenogenetic populations tended to be distributed in colder waters compared with their sexual relatives, and when parthenogenetic populations were parapatric with sexual populations, they inhabited in more wave-exposed area. My data also suggested that, in *S. lomentaria*, parthenogens have a wider distribution area than sexuals. The biased distributions of parthenogens toward a particular environmental setting when compared with their close sexual relatives are known as geographic parthenogenesis. This phenomenon has been frequently reported in land plants and animals, but scarcely in brown algae. Here, I provided novel distribution patterns of brown algal parthenogens. My population genetic and phylogenetic analyses based on genome-wide SNPs data indicated that parthenogens have evolved at least twice in *S. lomentaria* and *S. promiscuus* and parthenogenetic populations had a lower genetic diversity compared with sexual populations. In land plants and animals, inter-species hybridization is known as a major origin of parthenogens. However, my data did not support the hybrid origin of parthenogens although the origin of parthenogens in *Scytosiphon* was unclear. I also showed that female gametes from parthenogenetic populations have reduced sexual traits (sex pheromone production/fertilization ability) and that they have acquired asexual traits (larger gamete size/rapid parthenogenetic development). I got the first

opportunity to discuss the evolution of reproductive traits in the transition to asexuality in brown algae.

ACKNOWLEDGMENTS

I deeply appreciate my supervisor Dr. Kazuhiro Kogame (Hokkaido Univ.) for his support and encouragement for my six years of research activity in Hokkaido University.

I am grateful to Dr. Toru Katoh (Hokkaido Univ), Dr. Ryuichi Masuda (Hokkaido Univ.), Dr. Wilfred J. E. Santiañez (University of the Philippines) and Dr. Davis Iritani for their critical reading and correction of this thesis.

I thank Dr. Kevin C. Wakeman (Hokkaido Univ.) for his indispensable support in sampling trips, lab works, and writing manuscripts.

I appreciate following people who helped collections of samples used in this study: Dr. Masanori Hiraoka (Koch Univ.), Dr. Mitsunobu Kamiya (Tokyo University of Marine Science and Technology), Dr. Shinya Uwai, (Kobe Univ.), Dr. Astuko Tanaka (University of Ryukyus), Dr. Takeaki Hanyuda (Kobe Univ.), Dr. Masahiro Suzuki (Kobe Univ.), Dr. Tsuyoshi Abe (Hokkaido Univ.), Dr. Norishige Yotsukura (Hokkaido Univ.), Dr. Maria E. Croce (Instituto Argentino de Oceanografía), Mr. Takashi Abe (Hokkaido Univ.), Dr. Tadashi Kawai, Dr. Nina Klochkova, Dr. Akira Kurihara (Kyushu Univ.), Mr. Koji Shibazaki, Ms. Kumiko Shibazaki, Mr. Norifumi Sugimoto, and Ms. Takako Sugiyama (Oshoro Marine Station), and the people concerned in Kabushima Shrine (Hachinohe, Aomori Pref.).

I appreciate following people who helped my experiments and data analyses: Dr. Susana M. Coelho and Dr. Agnieszka P. Lipinska (Max Planck Institute) for their help in development of PCR-based sex-check markers; Dr. Shimpei F. Hiruta (National Museum of Nature and Science, Tsukuba) for his help in MIG-seq; Mr. Jun Ishigohoka (Max Planck Institute) for his help in data analyses using SNPs data; Dr. Taizo Motomura (Hokkaido Univ.) for his helpful suggestions on culture experiments; Dr. Masayo Soma (Hokkaido Univ.) for her kind guidance on statistical analyses; Dr. Taiju Kitayama (National Museum of Nature and Science, Tsukuba) for registration of my specimens in TNS; Dr. Tatsufumi Okino, Dr. Toshiyuki Wakimoto, and Mr. Jomori Takahiro (Hokkaido

Univ.) for HPLC and GCMS analyses of sex pheromones; Dr. Ooi Koch Teh (Hokkaido Univ.) for his help in lab works.

I thank lab members of Biodiversity II, Hokkaido University for their tolerance of my research activity.

This work is partly supported by MIKIMOTO FUND FOR MARINE ECOLOGY and JSPS KAKENHI (grant number JP19J10967).

Finally, I am sincerely grateful to my family for their continuous encouragement.

CO-AUTHORSHIP STATEMENT

Part 1

Chapter 1 is based on the following published article:

Hoshino M, Ishikawa S, Kogame K. 2018. Concordance between DNA-based specie boundaries and reproductive isolating barriers in the *Scytosiphon lomentaria* species complex (Ectocarpales, Phaeophyceae). *Phycologia* 57: 232–242.

I conducted DNA extraction, PCR, sequencing, phylogenetic analyses, and crossing experiments. I also wrote the preliminary draft of this manuscript. Mr. Ishikawa conducted a part of crossing experiments. Dr. Kogame conducted a part of crossing experiments and contributed to the writing and interpretation of the final draft.

Chapter 2 is based on the following published article:

Hoshino M, Tanaka A, Kamiya M, Uwai S, Hiraoka M, Kogame K. 2021. Systematics, distribution, and sexual compatibility of six *Scytosiphon* species (Scytosiphonaceae, Ectocarpales) from Japan and the description of four new species. *Journal of Phycology.* https://doi.org/10.1111/jpy.13089.

I conducted fieldwork, microscopy, DNA extraction, sequencing, PCR, phylogenetic analyses, and crossing experiments. I also wrote the preliminary draft of this manuscript. Dr. Tanaka, Dr. Kamiya, Dr. Uwai, Dr. Hiraoka conducted a part of fieldwork and contributed to writing of the final manuscript. Dr. Kogame contributed to the writing and interpretation of the final draft.

Chapter 3 is based on the following published article:

Hoshino M, Croce ME, Hanyuda T, Kogame K. 2020. Species delimitation of *Planosiphon gracilis* morphospecies (Scytosiphonaceae, Phaeophyceae) from Japan and the description of *Pl. nakamurae* sp. nov. *Phycologia* 59: 116–126.

I conducted fieldwork, microscopy, DNA extraction, PCR, sequencing,

phylogenetic analyses, and culture experiments. I also wrote the preliminary draft of this manuscript. Dr. Croce conducted a part of fieldwork and contributed to writing of the final manuscript. Dr. Hanyuda and Dr. Suzuki conducted a part of fieldwork, DNA extraction, PCR, sequencing, and contributed to writing of the final manuscript. Dr. Kogame conducted a part of fieldwork, culture experiments, and contributed to the writing and interpretation of the final draft.

Part2

Chapter 4 is based on the following published article:

Hoshino M, Kogame K. 2019. Parthenogenesis is rare in the reproduction of a sexual field population of the isogamous brown alga *Scytosiphon* (Scytosiphonaceae, Ectocarpales). *Journal of Phycology* 55: 466–472.

I conducted fieldwork, microscopy, DNA extraction, PCR, and culture experiments. I also wrote the preliminary draft of this manuscript. Dr. Kogame conducted a part of fieldwork and culture experiments, and contributed to the writing and interpretation of the final draft.

Chapter 5 is based on the following published article:

Hoshino M, Okino T, Kogame K. 2019. Parthenogenetic female populations in the brown alga *Scytosiphon lomentaria* (Scytosiphonaceae, Ectocarpales): Decay of a sexual trait and acquisition of asexual traits. *Journal of Phycology* 55: 204–213.

I conducted fieldwork, microscopy, DNA extraction, PCR, and culture experiments. I also wrote the preliminary draft of this manuscript. Dr. Okino conducted LCMS analyses of sex pheromone and contributed to writing of the final manuscript. Dr. Coelho and Dr. Lipinska made primers for sex-check PCR. Dr. Kogame conducted a part of fieldwork, culture experiments, and contributed to the writing and interpretation of the final draft.

Chapter 6 is based on the following material:

Hoshino M, Hiruta SF, Jomori T, Kamiya M, Wakimoto T, Croce ME, Kogame K. (in prep). Geographic parthenogenesis in the brown alga *Scytosiphon lomentaria* (Scytosiphonaceae): sexuals in warm waters and parthenogens in cold waters.

I conducted fieldwork, DNA extraction, PCR, sequencing, phylogenetic and population genetic analyses and culture experiments. I and Dr. Hiruta conducted MIG-seq. Dr. Wakimoto conducted GCMS analyses of sex pheromone and Mr. Jomori analyzed the GCMS data. Dr. Kamiya and Dr. Croce conducted a part of fieldwork. Dr. Kogame conducted a part of fieldwork, culture experiments, and contributed to the writing and interpretation of the final draft.

Chapter 7 is based on the following material:

Hoshino M, Hiruta SF, Hiraoka M, Jomori T, Wakimoto T, Kogame K. (in prep). Parthenogens in the brown alga *Scytosiphon promiscuus*: origin, distribution, and evolution of reproductive traits under asexuality.

I conducted fieldwork, DNA extraction, PCR, sequencing, phylogenetic and population genetic analyses and culture experiments. I and Dr. Hiruta conducted MIG-seq. Dr. Wakimoto conducted GCMS analyses of sex pheromone and Mr. Jomori analyzed the GCMS data. Dr. Hiraoka conducted a part of fieldwork. Dr. Kogame conducted a part of fieldwork and contributed to the writing and interpretation of the final draft.

Table of Contents

GENERAL INTRODUCTION

The brown algae (Phaeophyceae, Stramenopiles) are one of few eukaryotic lineages to have evolved complex multicellularity (Cock et al., 2014). It is comprised of approximately 2000 described species and most of these are exclusively marine (Guiry and Guiry, 2020; Lee, 2008). One of the most interesting topics in the brown algae would be its wide variety of life cycles, sexual systems, and reproductive modes (Bringloe et al., 2020). Their life cycles vary; taxa may exhibit 1) isomorphic haplodiplontic life cycles, in which both gametophyte and sporophyte are similar in size (e.g., *Myelophycus* Kjellman); 2) heteromorphic haplodiplontic life cycles, in which either gametophyte or sporophyte is larger (e.g., *Scytosiphon* C.Agardh and kelps); and, 3) diplontic life cycles, where only the diploid generation is multicellular (e.g., *Fucus* Linnaeus).The sexual reproduction in brown algae ranges from isogamy to oogamy. In many cases, sexual reproduction occurs between separate sexes during the haploid stage of the life cycle (dioicy), but several transitions to monoicy have occurred [e.g., *Desmarestia* J.V.Lamouroux (Luthringer et al., 2014)). The order Fucales is the only group having separate sexes during diploid stage (dioecy), and shifts between dioecy and monoecy have occurred multiple times in this group (Cánovas et al., 2011; Bringloe et al., 2020). Genetic bases of sex determination have been revealed in a model species *Ectocarpus* sp., wherein sex is expressed during the haploid stage of the life cycle and sexes are determined after meiosis in the sporophyte, depending on whether the meiospores inherit a U (female) or a V (male) chromosome (Ahmed et al., 2014).

Many species have asexual mode of reproduction, in addition to sexual reproduction. A wide variety of modes of asexual reproduction have been reported so far (Hori, 1993), at least based on what is known in culture condition: parthenogenesis, in which unfused gametes develop into a new gametophyte or sporophyte (parthenosporophyte); clonal reproduction by adventitious branch or propagule; asexual zoids released from gametophytes which develop into a new gametophyte or sporophyte

(unisexual sporophyte); and, zoids released from sporophytes which develop into sporophytes, not gametophytes. Species/populations which are speculated to reproduce only asexually have been also reported. There are numerous species/populations in which sexual reproduction has been never observed in culture (e.g., Wynne, 1969; Peters, 1987; Deshmukhe and Tatewaki, 1993).

The background of Scytosiphonaceae

This doctoral thesis mainly focused on the reproduction, the reproductive isolating barriers among closely related cryptic species and the reproductive mode of populations, of some scytosiphonaceaen species.

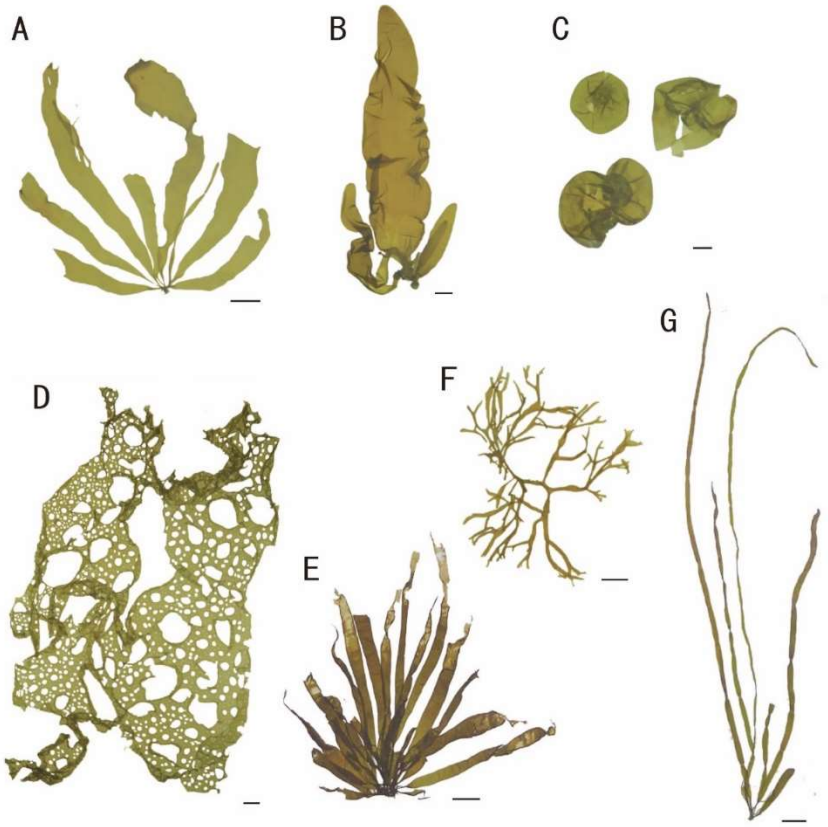

Figure 1. Representatives of the known genera in the Scytosiphonaceae.
A: Erect and leaf-like *Petalonia fascia* (SAP050352). B: Erect, saccate, and elongated *Dactylosiphon bullosus* (SAP059217). C: Saccate *Colpomenia peregrina* (SAP089920). D: Net-like *Hydroclathrus tilesii* (SAP071236). E: Erect and compressed *Planosiphon nakamurae* (SAP115444). F: Erect and branched *Rosenvingea intricata* (SAP046010). G: Erect, cylindrical, and constricted *Scytosiphon subtropicus* (SAP115491). Scale bars = 1 cm.

The family Scytosiphonaceae (Ectocarpales) has a worldwide distribution including tropical and cold waters (Kogame et al., 1999). Members of this group are characterized by having a single plastid with one large pyrenoid. Most of them have a heteromorphic life cycle with a large erect gametophyte alternating with a small prostrate sporophyte (e.g., Wynne, 1969; Nakamura and Tatewaki, 1975; Kogame, 1997). As with other groups of brown algae, the classification and species diversity of Scytosiphonaceae have been significantly revised by recent molecular phylogenetic studies. Generic segregation within the Scytosiphonaceae had traditionally been based on the gross morphology of erect gametophytes (e.g., leaf-like, saccate, net-like, and branched; Fig. 1). However, molecular phylogenetic studies have shown extensive polyphyly among the genera of this group, with a series of taxonomic revisions on genera (e.g., Kogame et al., 1999; McDevit and Saunders, 2017; Santiañez and Kogame, 2017, 2019; Santiañez et al., 2018a, b). Molecular phylogenetic studies have also found the existence of numbers of cryptic species (e.g., Lee et al., 2012; Kogame et al., 2015a, b; McDevit and Saunders, 2017; Hanyuda et al., 2020).

In scytosiphonacean species, sexual reproduction is either isogamous or anisogamous and it occurs between isomorphic dioicous gametophytes (Fig. 2). Female gametes settle on the substratum earlier than male gametes, and secrete sexual pheromones to attract male gametes (Fu et al., 2014). Multiple male gametes attach to the cell surface of the settled female gamete with the anterior flagellar tip and form a clump, and only one of the male gametes fuse with the female gamete. Sexual reproduction is not always observed. For example, in *Scytosiphon* and *Petalonia* Derbès & Solier; sexual reproduction has been reported in the populations of Japan and Australia (Nakamura and Tatewaki, 1975; Clayton, 1980), but not in the populations of North America (Wynne, 1969; Edelstein et al., 1970). So far, there is no clear explanation for this differecnes in sexuality.

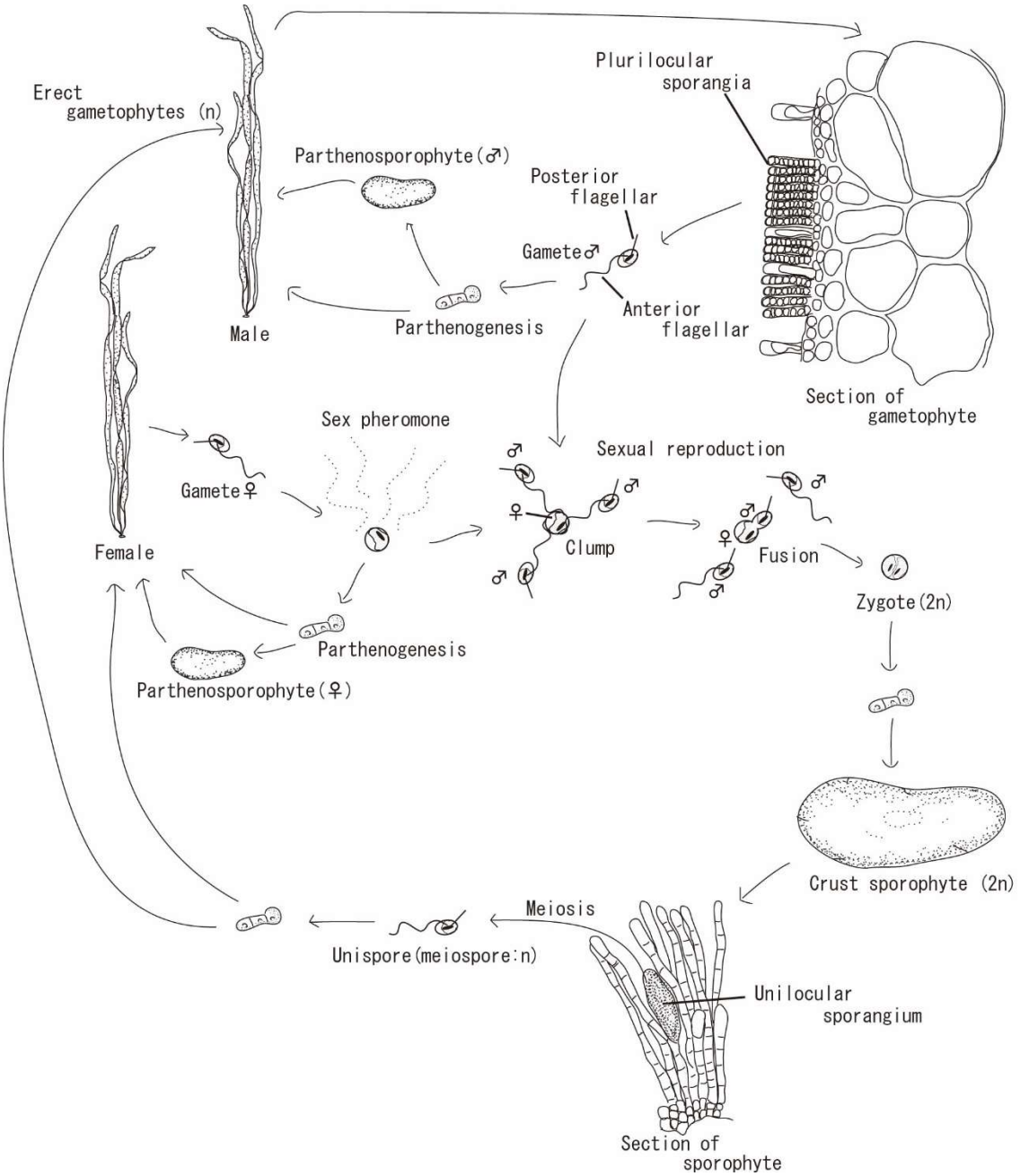

Figure 2. Life cycle of *Scytosiphon*. Isomorphic dioicous gametophytes release isogamous gametes (plurizoids) from plurilocular sporangia (plurilocular zoidangia). Gametes form zygotes if they encounter gametes of the opposite sex or will otherwise undergo parthenogenesis. Sexual sporophytes (zygotic sporophytes; sporophytes originate from zygotes) undergo meiosis in unilocular sporangia (unilocular zoidangia) and produce meiospores which develop into gametophytes.

Aims and outline of the thesis

The thesis comprises two parts: **Part 1** and **Part 2**.

Part 1: Systematic biology of *Scytosiphon*

This part is aimed at investigating species boundaries, systematics, and reproductive isolating barriers in the two scytosiphonacean genera, *Scytosiphon* and *Planosiphon* McDevit & G.W.Saunders. In seaweeds, including brown algae, morphological species identification and classification are often difficult due to their morphological simplicity and plasticity. With the advent of rapid DNA sequencing and development of molecular phylogenetic analyses, DNA-based species delimitation has widely spread since it can detect species boundaries regardless of limitations inherent to morphological datasets (Leliaert et al., 2014). Molecular phylogenetic analyses have detected numbers of cryptic species, even in a narrow geographical scale (e.g., Kogame et al., 2015a; Guillemin et al., 2016; Payo et al., 2013; Montecinos et al., 2017). It reminds us about one aspect of ”species problem,” that is, how sympatric, sexually reproducing organisms fall into discrete clusters (Coyne and Orr, 2004). Although numbers of species recognized have continued to increase, reproductive isolating mechanisms among closely related species are unclear in many cases. In this part, I firstly assessed species diversity of *Scytosiphon* and *Planosiphon* in Japan based on molecular phylogenetic analyses. Then, to examine possible reproductive isolating barriers among the putative species recognized by molecular phylogenetic analyses, I conducted crossing experiments.

Part 1 comprises the following three chapters.

Chapter 1: To estimate the species boundaries in the species complex of *Scytosiphon lomentaria* Lyngbye (Link) from Japan, I conducted multiple DNA-based species delimitation analyses which can automatically estimate species boundaries from a given DNA dataset. Five species (species Ia–Va) with overlapping geographic distributions were estimated by the delimitation analyses. Then, among the five putative species, I performed crossing experiments to verify the estimates of the delimitation

analyses and to investigate the possible reproductive barriers among them. I showed that the DNA-based species boundaries were concordant with biological species barriers; that is, the five species were reproductively isolated from each other by gametic incompatibility and low survival rate of hybrid meiospores.

Chapter 2: In addition to the five *Scytosiphon* species (species Ia–Va) found in **Chapter 1**, one species (species VI) was newly found from Okinawa Island, Japan. Species VI seemed to be geographically isolated from the five species. In *rbc*L phylogenetic analyses, it was recovered as a sister to the five species. My crossing experiments showed that gametic incompatibility (pre-zygotic isolating barrier) was less developed between the allopatric species (i.e., species VI and other species), compared with among the five species having overlapped distributions. These results may suggest that pre-zygotic barriers have evolved among the sympatric species due to reinforcement. In this chapter, taxonomic position and global distribution of each species were also investigated. I concluded that species Ia corresponded to the generitype *S. lomentaria*, species IIIa is *S. promiscuus* McDevit & G.W.Saunders, and the other four species are new species, which were named *S. shibazakiorum* M.Hoshino & Kogame for species IIa, *S. tosaensis* M.Hoshino & Kogame for species IVa, *S. arcanus* M.Hoshino & Kogame for species Va, and *S. subtropicus* M.Hoshino, Ats.Tanaka & Kogame for species VI. *Scytosiphon lomentaria*, *S. shibazakiorum*, and *S. promiscuus* have worldwide distributions, while the other four species are not found outside of Japan.

Chapter 3: Molecular phylogenetic analyses revealed that *Planosiphon gracilis* (Kogame) McDevit & G.W.Saunders from Japan is a complex of three distinct lineages (lineage I–III). Distributions of lineage I and II widely overlapped in Japan including the type locality of *Pl. gracilis*. Crossing experiments showed that lineage I and II reproduce sexually and they are reproductively isolated each other by gametic incompatibility. In lineage III, however, sexual reproduction was not observed. I showed that lineage I was the true *Pl. gracilis* since it included the holotype of *Pl. gracilis*, lineage III was

phylogenetically close to *Pl. complanatus* (Rosenvinge) McDevit & G.W.Saunders from Canada, and lineage II was a new species and was described as *Pl. nakamurae* M.Hoshino, M.E.Croce, Hanyuda & Kogame.

Part 2: Sexuality of field *Scytosiphon* population -parthenogenesis in field-

This part aimed at understanding the sexuality of field populations, especially, the contribution of parthenogenesis to the reproduction of the *Scytosiphon* field populations. Parthenogenesis is a way of asexual reproduction in which an unfused gamete develops into a new individual (Fig. 2). In brown algae, this asexual process has been widely observed in laboratory culture conditions, including *Scytosiphon* (Luthringer et al., 2014). However, little is known about the significance of parthenogenesis in field populations in brown algae. Here, I showed that parthenogenesis is rare in a sexual field population, while some populations are maintained by parthenogenesis (parthenogenetic populations). I also investigated environmental conditions where parthenogenetic populations are distributed and the origin of parthenogenetic populations. **Part 2** comprises the following four chapters.

Chapter 4: The contribution of parthenogenesis to reproduction of a sexual field population was investigated. In a sexual field population with a 1:1 sex ratio of *Scytosiphon shibazakiorum*, 126 field sporophytes were examined if they originated from parthenogenesis or sexual reproduction. I showed that only six sporophytes may originate from parthenogenesis (two female-parthenosporophytes and four male-parthenosporophytes). It indicates that, in the sexual field population, the contribution of parthenogenesis to reproduction is small (≤4.8%) compared to sexual reproduction.

Chapter 5: In *S. lomentaria*, populations in which sexual reproduction cannot be observed have been reported in Japan (asexual population; Kogame et al., 2005). In this chapter, I aimed to reveal the precise reproductive mode of these asexual populations. I firstly examined the genetic sex of the individuals from three asexual and two sexual

populations using PCR-based sex markers. I showed that asexual populations included only females, while sexual populations included both female and males. In culture experiments, I showed that gametes of most strains from asexual populations were able to fuse with male gametes; however, they had less sex pheromone production, larger cell size, and rapid parthenogenetic development compared to female gametes from sexual populations. Furthermore, I found sporophytes, which originated from parthenogenesis of female gametes, in an asexual field population. These results indicate that asexual populations are actually female populations reproducing parthenogenetically and that female gametes in asexual populations are specialized for parthenogenetic reproduction.

Chapter 6: In **Chapter 5**, I showed that *S. lomentaria* has parthenogenetic female populations (parthenogenetic populations) in addition to sexual populations. **Chapter 6** aimed to elucidate the environments in which parthenogenesis is favored over sexual reproduction and the origin of the parthenogenetic populations. To reveal the geographic distributions of parthenogenetic and sexual populations, I examined sex ratio of 33 populations from Japan, four samples from Europe, and two populations from Argentina. Then, to reveal the origin of the parthenogenetic populations, phylogenetic and population genetic analyses were conducted based on mitochondrial *cox*1, nuclear *cetn*-int2, and genome-wide single nucleotide polymorphisms (SNPs). I showed that parthenogenetic populations probably have worldwide distributions, while sexual populations were found only in Japan. In Japan, parthenogenetic populations were biased to cold waters. In localities where parthenogenetic and sexual populations existed closely, parthenogenetic populations occupied the wave-exposed areas while sexual populations grow in relatively protected/calmer areas. The phylogenetic and population genetic analyses showed that the parthenogenetic populations have multiple origin. In land plants and animals, parthenogenetic lineages are often inter-species hybrids (Simon et al., 2003; Kearney, 2005; Hörandl, 2009); however, the analyses did not support the inter-species hybrid origin of the parthenogenetic populations of *S. lomentaria*.

Chapter 7: Three parthenogenetic populations were newly found in *S. promiscuus* in Japan. This chapter aimed to elucidate the origin of the parthenogenetic populations of the species and how reproductive traits of gametes have evolved in the transition to asexuality. Phylogenetic and population genetic analyses based on genome-wide SNPs data suggest that parthenogens have evolved at least twice in *S. promiscuus* and the parthenogens do not originate from inter-species hybridization. In the two parthenogenetic populations which probably evolved independently, two sexual traits (fertilization ability and sex pheromone production) and two asexual traits (gamete size and parthenogenetic ability) were examined. I showed that suppression of sex pheromone production and acquisition of high parthenogenetic capacity have occurred independently in the two parthenogenetic populations, while loss of fertilization ability and enlargement of gamete size have occurred in only one population. Through comparison with previous studies, I also discussed evolutionary pattern of reproductive traits and its importance in the transition to asexuality in brown algae.

Part 1

Systematic biology of *Scytosiphon*

Chapter 1

Concordance between DNA-based species boundaries and reproductive isolating barriers in the *Scytosiphon lomentaria* species complex (Ectocarpales, Phaeophyceae)

INTRODUCTION

Although species are fundamental units of biodiversity, there is considerable disagreement about the way in which species should be defined, and many species concepts have been advocated (Harrison, 1998). This makes species delimitation challenging, because delimitation analyses based on different species concepts may lead to different conclusions (Hausdorf, 2011). Taxonomists have long used morphological data to detect species boundaries: a morphological species concept. However, effectiveness of morphology-based species delimitation is often limited due to morphological plasticity, morphological simplicity, and convergent evolution (Agapow et al., 2004 and included references). With the advent of rapid DNA sequencing and development of molecular phylogenetic analyses, species delimitation based on molecular phylogeny (species delimitation based on phylogenetic species concept) has spread rapidly, because these methods can detect species boundaries regardless limitations inherent to morphological datasets (Agapow et al., 2004; Leliaert et al., 2014).

Recently, a number of DNA-based species delimitation methods, which can automatically estimate species boundaries from a given sequence dataset, have been developed: Generalized Mixed Yule Coalescent (GMYC) (Pons et al., 2006; Monaghan et al., 2009) and Automatic Barcode Gap Discovery (ABGD) (Puillandre et al., 2012) as single-locus based methods, and Bayesian Phylogenetics & Phylogeography (Yang and Rannala, 2010) and SpedeSTEM (Ence and Carstens, 2011) as multi-locus based methods. Among them, single-locus based methods are widely used because of their practicality. These methods can immediately and objectively estimate species boundaries and the number of species even from a large dataset. Thus, these delimitation methods have been used as powerful tools to identify species boundaries in algal taxa in which morphological discrimination is difficult or impossible (Leliaert et al., 2014), and have revealed cryptic species diversity (e.g. Leliaert et al., 2009; Payo et al., 2013; Guillemin et al., 2016; Montecinos et al., 2017). However, it should be noted that every DNA-based species

delimitation method has a potential danger of making an erroneous estimate, because of their simplified evolutionary models and numbers of assumptions (Carstens et al., 2013). Therefore, to place trust in estimates of DNA-based delimitation methods, estimates should be verified with a wide range of data, especially with nongenetic data (e.g. life history, geographical distribution, morphology and reproductive isolation; Carstens et al., 2013), although these kinds of verifications are often skipped.

DNA-based species delimitation methods often estimate the existence of multiple putative cryptic species, even in a narrow geographical scale or sometimes in a sympatric manner (e.g. Payo et al., 2013; Guillemin et al., 2016; Montecinos et al., 2017). Investigation of the isolating mechanism between these putative species is important for following two reasons. First, it verifies estimates of DNA-based species delimitation based on a biological species concept in which reproductive isolation is defined as the species boundaries (Dobzhansky, 1970; Mayr, 1996). In sexual organisms, isolating mechanisms (barriers to gene exchange) generate and maintain biotic discontinuities recognizable as historical partitions in gene genealogies and organismal phylogenies (Avise, 2000). Thus, investigation of isolation mechanisms is effective in verifying species delimitation based on molecular phylogeny. Second, it provides a good opportunity to resolve one aspect of the most important "species problem," namely, how sympatric, sexually reproducing organisms fall into discrete clusters (Coyne and Orr, 2004). Despite this importance, there are only a few casesin which isolation mechanisms among putative species estimated by DNA-based species delimitation methods have been studied (Montecinos et al., 2017).

The brown alga *Scytosiphon lomentaria* (Lyngbye) Link is distributed in cold and warm waters worldwide (Lüning, 1990). This species has a heteromorphic life history with an alternation of generations between the macroscopic dioecious gametophyte (15–50 cm in height) and the microscopic discoid sporophyte (1–5 mm in diameter) (Nakamura and Tatewaki, 1975). Sexual reproduction is nearly isogamous (Tatewaki,

1966). Previous molecular phylogenetic works on this species have suggested that this species is a complex of different entities (Cho et al., 2007; Kogame et al., 2015a, b). Phylogenetic trees inferred from the mitochondrial cytochrome oxidase subunit 3 (*cox*3) gene and the internal transcribed spacer (ITS) region of the nuclear ribosomal cistron separated Pacific and north-eastern Atlantic populations into four clades, P1, P2, A1 and A2 (Kogame et al., 2015b). Populations of *S. lomentaria* in Japan belong to clades P1 and P2. At least three (groups I–III) or possibly five (IV? and V?) putative cryptic species were detected in Japanese samples by examining the combinations of sequence-type groups of four molecular markers (Kogame et al., 2015a). However, meaningful morphological characters distinguishing these putative species have not been found. Individuals within these putative species often grow sympatrically, and their maturation periods overlap. However, no hybrid individuals were detected between them in sequence-type combinations of mitochondrial and nuclear markers, positing the existence of reproductive isolation (Kogame et al., 2015a).

In the present study, I reassessed the diversity of the *S. lomentaria* species complex in Japan using three widely used single-locus based species delimitation methods: GMYC, Poisson Tree Processes (PTP) (Zhang et al., 2013) and ABGD, utilizing a mitochondrial dataset of the cytochrome oxidase subunit 1 (*cox*1) gene and a nuclear dataset of the second intron of the centrin gene (*cetn*-int2) (Nagasato et al., 2004). These delimitation methods predicted multiple cryptic, sometimes sympatric species. Then, to verify the estimates of DNA-based species delimitation methods and to investigate isolation mechanisms among the putative species, crossing experiments were conducted among them using culture isolates.

MATERIALS AND METHODS

Phylogenetic analysis and DNA-based species delimitation

Partial *cox*1 and *cetn*-int2 sequences were generated from 12 cultured isolates (Table S1).

Total genomic DNA was extracted from the cultured thalli using QuickExtract^{TM} FFPE DNA Extraction Kit (epicentre, Madison, U.S.A.). The extracted DNA was used as template DNA in a PCR. The pairs of primers used for PCR and sequencing were: COIS1F and GazR2 (Lane et al., 2007) for *cox*1; Slcen1357F and Slcen2237R for the first round of *cetn*-int2 PCR, and Slcen1377F and Slcen2215R for nested PCR (Kogame et al., 2015a). PCR reactions and DNA sequencing were conducted according to the methods described by Kogame et al. (2015a).

A total of 126 speciemens were included in *cox*1 and *cetn*-int2 datasets (Table S1). Sampling locations of *S. lomentaria* are shown in Fig. 3. For the *cox*1 dataset, 100 sequences of *S. lomentatia* from Japan and 13 sequences from eight scytosiphonacean species were included. For the *cetn*-int2 dataset, 104 sequences of *S. lomentaria* from Japan were included. Except for 13 *cox*1 and four *cetn*-int2 sequences, which were newly sequenced in this study, all seqences were retrieved from GenBank (Table S1). These retrieved sequences of *S. lomentria* were generated in Kogame et al. (2015a). Sequences

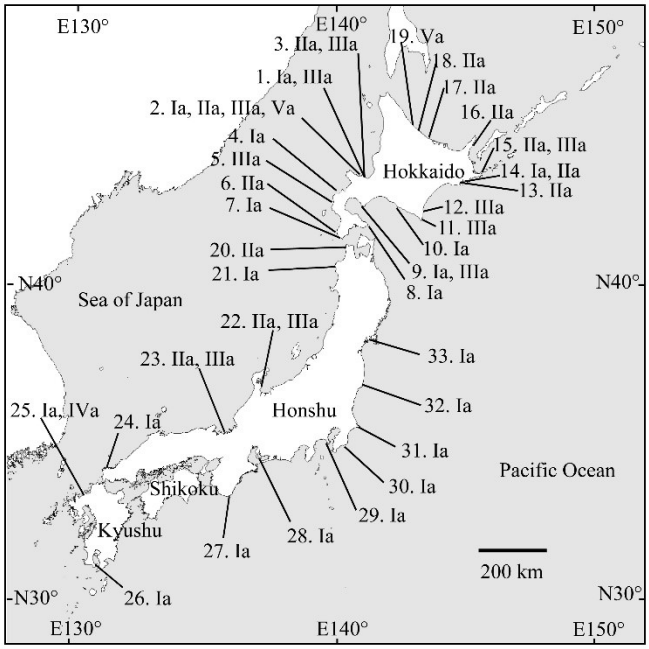

Figure 3. Map of Japan showing sampling locations of *Scytosiphon lomentaria* used in this study. Numerals (1–33) are locality codes, and locality names are listed in Supplemental Table S1. The *cox*1-based putative species (see Fig. 4) found in each locality are shown after the locality codes.

were aligned by CLUSTALW (Thompson et al., 1994) in MEGA v5.2 (Tamura et al., 2011), and the alignments were confirmed by eye.

The best-fit model was estimated by both corrected Akaike Information Criteria (AICc) and Bayesian Information Criteria (BIC) implemented in MEGA v5.2; the HKY+I and K2P + G models were selected for *cox*1 and *cetn*-int2 datasets, respectively. Phylogenetic analyses were performed on the two datasets using the Maximum Likelihood method implemented in RAxML v8.2.10 (Stamatakis, 2014) with the GTR+G model. Bootstrap analyses (Felsenstein, 1985) were performed with 1,000 pseudoreplicates.

Three single-locus based species delimitation methods (GMYC, PTP and ABGD) were performed on unique haplotypes for the *cox*1 and the *cetn*-int2 datasets. Taking a conservative approach, groups of sequences were considered as a final putative species when in at least two analyses their boundaries agreed. For the GMYC analyses, ultrametric trees were constructed by Bayesian analysis in BEAST v2.4.7 (Bouckaert et al., 2014), with the HKY+I model for the *cox*1 and the K2P + G model for the *cetn*-int2. The uncorrelated lognormal relaxed molecular clock model (Drummond et al., 2006) and the constant population size coalescent tree prior were used. Markov Chain Monte Carlo analyses were run for 10 million generations, sampling every 1,000 generations with a 10% burn-in. The outputs were diagnosed for convergence using Tracer v1.6 (Rambaut et al., 2014), and maximum clade credibility trees were calculated with TreeAnnotator v1.8.2. The single-threshold GMYC analyses were performed on maximum clade credibility trees using the SPLITS package (Monaghan et al., 2009) in R 3.3.1 (R Core Team, 2016).

For the PTP analyses, the ML trees were constructed using RAxML v8.2.10 under the GTR+G for both the *cox*1 and the *cetn*-int2 datasets; the analyses were performed on the bPTP web server (http://species.h-its.org/).

The ABGD analyses were performed on the web interface

(http://wwwabi.snv.jussieu.fr/public/abgd/). The K2P distance was selected for the both datasets, and other parameters were set to default. The ABGD analysis yields two partitions: initial and recursive partitions. In general, recursive partitioning defines more groups than initial ones. Although recursive partitions are expected to handle better heterogeneities in the dataset, initial partitions are typically stable on a wider range of prior values and are usually close to the number of groups described by taxonomists (Puillandre et al., 2012). Thus, initial partitions for each intraspecific divergence (*P*) values between 0.001 and 0.100 were recorded.

Crossing experiments among the *cox*1-based putative species

Crossing experiments among the putative species (Ia–Va) suggested by the *cox*1-based species delimitation analyses (Fig. 4) were conducted, using cultured isolates of 16 male and 24 female gametophytes (Table 1), according to methods used by Kato et al. (2006). Cultures were maintained using Petri dishes (90 × 20 mm) with PESI medium (Tatewaki, 1966), at 10, 15, and 20°C in a long day (16:8 h, light:dark) and a short day (8:16 h, light:dark) conditions with fluorescent light of 30–50 μmol m^{-2} s^{-1} photon flux density. Gametophytes grown at 15°C in the short day condition were used for crossing experiments. To examine gametic compatibility, male and female gametes were mixed in a drop of medium on a coverslip (18×18 mm), and gamete interactions were observed using a light microscope in a culture room at 15°C. Because hybrid zygotes were successfully formed between species IIa male and species IIIa female, 11 hybrid zygotes were isolated, and their development was observed to investigate possible post-zygotic barriers. Sporophytic thalli grown from hybrid zygotes formed unilocular sporangia at 15°C, under short day conditions. As a control, 8 zygotes resulting from intraspecific crosses (within species IIa and within species IIIa) were also isolated and cultured. Four to 14 unilocular sporangia were isolated from each zygotic sporophyte and were cultured at 15°C in the short-day condition. The survival rate of seven-day-old germlings of

meiospores (zoospores) released from the isolated unilocular sporangium was recorded.

For the analysis of the survival rate of meiospores between the experimental groups (control/hybrid), a Generalized Linear Mixed Model was adopted with a Binomial distribution using the lme4 package (Bates et al., 2015) in R 3.3.1. (R Core Team, 2016). In this model, unilocular-sporangium identity and sporophyte identity were considered as nested random effects, to deal with non-independence of the data from the same unilocular sporangium or from the same sporophyte.

Table 1. Culture isolates used for crossing experiments. Locality codes correspond to those in Fig. 3.

	Sample code	Locality code	Collection location and date	DNA-based putative species	
				cox 1	*cetn*- int2
Female					
	Asari 8f	1	Asari, Otaru, Hokkkaido, Japan. 11 May 1999	IIIa	IIIb
	Asari 9f	1	Asari, Otaru, Hokkkaido, Japan. 11 May 1999	IIIa	IIIb
	Asari 10f	1	Asari, Otaru, Hokkkaido, Japan. 11 May 1999	IIIa	IIIb
	Oshoro 980407 1f	2	Oshoro, Otaru, Hokkaido, Japan. 7 Apr 1998	Va	Vb
	Oshoro 100406 6f	2	Oshoro, Otaru, Hokkaido, Japan. 6 Apr 2010	IIIa	IIIb
	Oshoro 000510 1f	2	Oshoro, Otaru, Hokkaido, Japan. 10 May 2000	IIa	IIb
	Otamoi 4f	3	Otamoi, Otaru, Hokkaido, Japan. 9 Apr 2011	IIa	IIb
	Otamoi 12f	3	Otamoi, Otaru, Hokkaido, Japan. 9 Apr 2011	IIIa	IIIb
	Otamoi 15f	3	Otamoi, Otaru, Hokkaido, Japan. 9 Apr 2011	IIIa	IIIb
	Muroran 5f	9	Murorann, Hokkaido, Japan. 10 Mar 2000	IIIa	IIIb
	Kakijima 7f	13	Kakijima, Akkeshi, Hokkaido, Japan. 25 Jun 1990	IIa	IIb
	Tappizaki 1f	20	Tappizaki, Aomori Pref., Japan. 29 May 2002	IIa	VIb
	Himi 2f	22	Himi, Toyama Pref., Japan. 26 Feb 2004	IIa	IIb
	Mitsumatsu 2f	23	Mitsumatsu, Takahama, Fukui Pref., Japan. 29 Mar 2005	IIIa	IIIb
	Mitsumatsu 7f	23	Mitsumatsu, Takahama, Fukui Pref., Japan. 29 Mar 2005	IIa	IIb
	Mitsumatsu 8f	23	Mitsumatsu, Takahama, Fukui Pref., Japan. 29 Mar 2005	IIIa	IIIb
	Mitsumatsu 9f	23	Mitsumatsu, Takahama, Fukui Pref., Japan. 29 Mar 2005	IIIa	IIIb
	Kiwado 5f	24	Kiwado, Heki, Yamaguti Pref., Japan. 1 Apr 2000	Ia	Ib
	Tsuyazaki 5f	25	Tsuyazaki, Fukuoka Pref., Japan. 31 Mar 2000	Ia	Ib
	Tsuyazaki 4f	25	Tsuyazaki, Fukuoka Pref., Japan. 31 Mar 2000	Va	Vb
	Sakurajima 2f	26	Sakurajima, Kagoshima Pref., Japan. 3 Mar 2003	Ia	Ib
	Kannonzaki 2f	29	Kannonzaki, Kanagawa Pref., Japan. 2 Apr 2000	Ia	Ib
	Inubouzaki 4f	31	Inubozaki, Chiba Pref., Japan. 4 Mar 2002	Ia	Ib
	Inubouzaki 8f	31	Inubozaki, Chiba Pref., Japan. 4 Mar 2002	Ia	Ib
Male					
	Asari 6m	1	Asari, Otaru, Hokkkaido, Japan. 11 May 1999	IIIa	IIIb
	Oshoro 000510 11m	2	Oshoro, Otaru, Hokkaido, Japan. 10 May 2000	IIa	IIb
	Oshoro 881025 Cr5m	2	Oshoro, Otaru, Hokkaido, Japan. 25 Oct 1988	Va	Vb
	Oshoro 010429 8m	2	Oshoro, Otaru, Hokkaido, Japan. 29 Apr 2001	IIa	IIb
	Oshoro 010429 10m	2	Oshoro, Otaru, Hokkaido, Japan. 29 Apr 2001	IIa	IIb
	Oshoro 010430 1m	2	Oshoro, Otaru, Hokkaido, Japan. 30 Apr 2001	IIa	VIb
	Oshoro 100406 4m	2	Oshoro, Otaru, Hokkaido, Japan. 6 Apr 2010	IIIa	IIIb
	Otamoi 16m	3	Otamoi, Otaru, Hokkaido, Japan. 9 Apr 2011	IIIa	IIIb
	Muroran 8m	9	Murorann, Hokkaido, Japan. 10 Mar 2000	IIIa	IIIb
	Tappizaki 2m	20	Tappizaki, Aomori Pref., Japan. 29 May 2002	IIa	IIb
	Mitsumatsu 1m	23	Mitsumatsu, Takahama, Fukui Pref., Japan. 29 Mar 2005	IIIa	IIIb
	Mitsumatsu 11m	23	Mitsumatsu, Takahama, Fukui Pref., Japan. 29 Mar 2005	IIIa	IIIb
	Sakurajima 3m	26	Sakurajima, Kagoshima Pref., Japan. 3 Mar 2003	Ia	Ib
	Hazumizaki 1m	28	Hazuzaki, Aichi Pref., Japan. 30 Mar 2003	Ia	Ib
	Kannonzaki 4m	29	Kannonzaki, Kanagawa Pref., Japan. 2 Apr 2000	Ia	Ib
	Inubouzaki 6m	31	Inubozaki, Chiba Pref., Japan. 4 Mar 2002	Ia	Ib

RESULTS

*cox*1-based species delimitation

I analyzed 113 *cox*1 sequences (600 bp); 55 unique haplotypes were found. In the ML tree reconstructed from *cox*1 sequences, all sequences of *S. lomentaria* lumped into a clade (Fig. 4). Results of three *cox*1-based species delimitation analyses (GMYC, PTP and ABGD) were broadly congruent (Fig. 4). A conservative approach on the results of the three delimitation analyses detected 14 putative species in the samples of Scytosiphonaceae analyzed, suggesting the existence of cryptic species in *Petalonia fascia* (O.F.Müller) Kuntze and *S. lomentaria*. Five putative cryptic species (Ia–Va) were suggested among *S. lomentaria* from Japan—their geographic distributions are shown in Fig. 3.

GMYC analysis resulted in 14 putative species (confidence interval: 10–24), including six singletons, and detected the existence of five putative species in Japanese *S. lomentaria*. The GMYC model was favored over the null hypothesis that the sequences cannot be differentiated from a single cluster ($P < 0.001$). ABGD analysis yielded two initial partitions: 10 ($P = 0.022$–0.0359) and 14 ($P = 0.0010$–0.0129) putative species. The latter partition was consistent with the delimitation by GMYC analyses. PTP analysis yielded 16 putative species, including nine singletons; six putative species were detected in *S. lomentaria* from Japan.

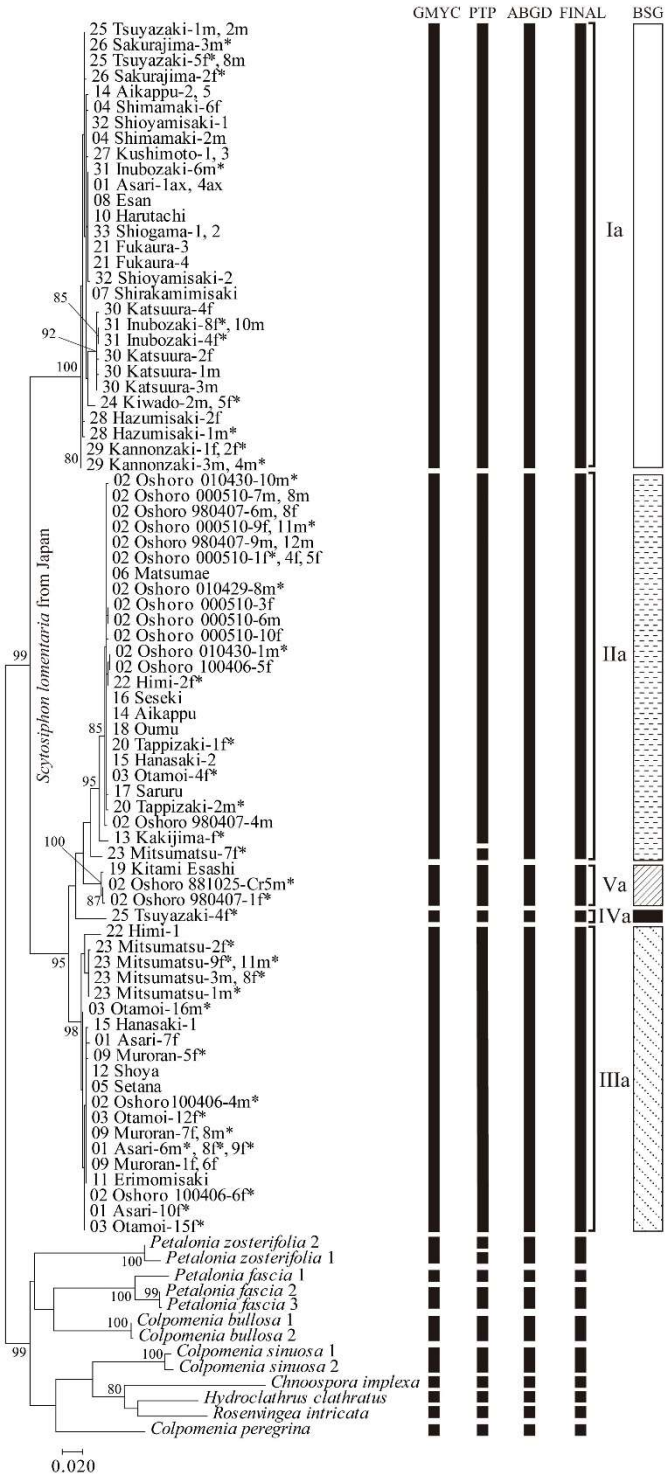

Figure 4. Summarized results from three species delimitation analyses (GMYC, PTP and ABGD) for *Scytosiphon lomentaria* based on the *cox*1 sequences, represented on the ML tree of the full dataset. Bootstrap values (>80) are indicated near branches. The prior intraspecific divergences (*P*) for ABGD are *P* = 0.001–0.0129. FINAL: hypothesized species groupings based on conservative approach; roman numerals are given to each putative sibling species of Japanese *Scytosiphon*. BSG: each pattern represents the Biological Species Group suggested by the crossing experiments. Superscript * on the left of sample code indicates the individuals used in the crossing experiments.

cetn-int2-based species delimitation

The alignment was 774 bp in length with gaps at 32 positions and one microsatellite region consisting of a TCG repeat. The single repeat region was excluded in the analyses. I analyzed 103 *cetn*-int2 sequences (724 bp: without the repeat region); 46 unique haplotypes were found in Japanese samples of *S. lomentaria*.

Results of three *cetn*-int2-based species delimitation analyses (GMYC, PTP and ABGD) were broadly congruent (Fig. 5). A conservative approach on the results of the three delimitation analyses yielded six putative species (Ib–VIb) in Japanese *S. lomentaria* (Fig. 5). Putative species Ib and IIIb–Vb correspond to species Ia and IIIa–Va in *cox*1-based species delimitation. The *cetn*-int2-based delimitation analyses separated *cox*1-based putative species IIa into IIb and VIb.

The GMYC analysis resulted in six putative species (confidence interval: 2–16) including one singleton; the GMYC model was favored over the null hypothesis that the sequences cannot be differentiated from a single cluster ($P = 0.046$) at 5 % significance level. The result of the PTP analysis resulted in seven putative species, including two singletons. ABGD analysis yielded two initial partitions: two ($P = 0.0129$–0.0599) and six ($P = 0.0010$–0.0077) putative species. The latter partition was consistent with the delimitation by GMYC analysis.

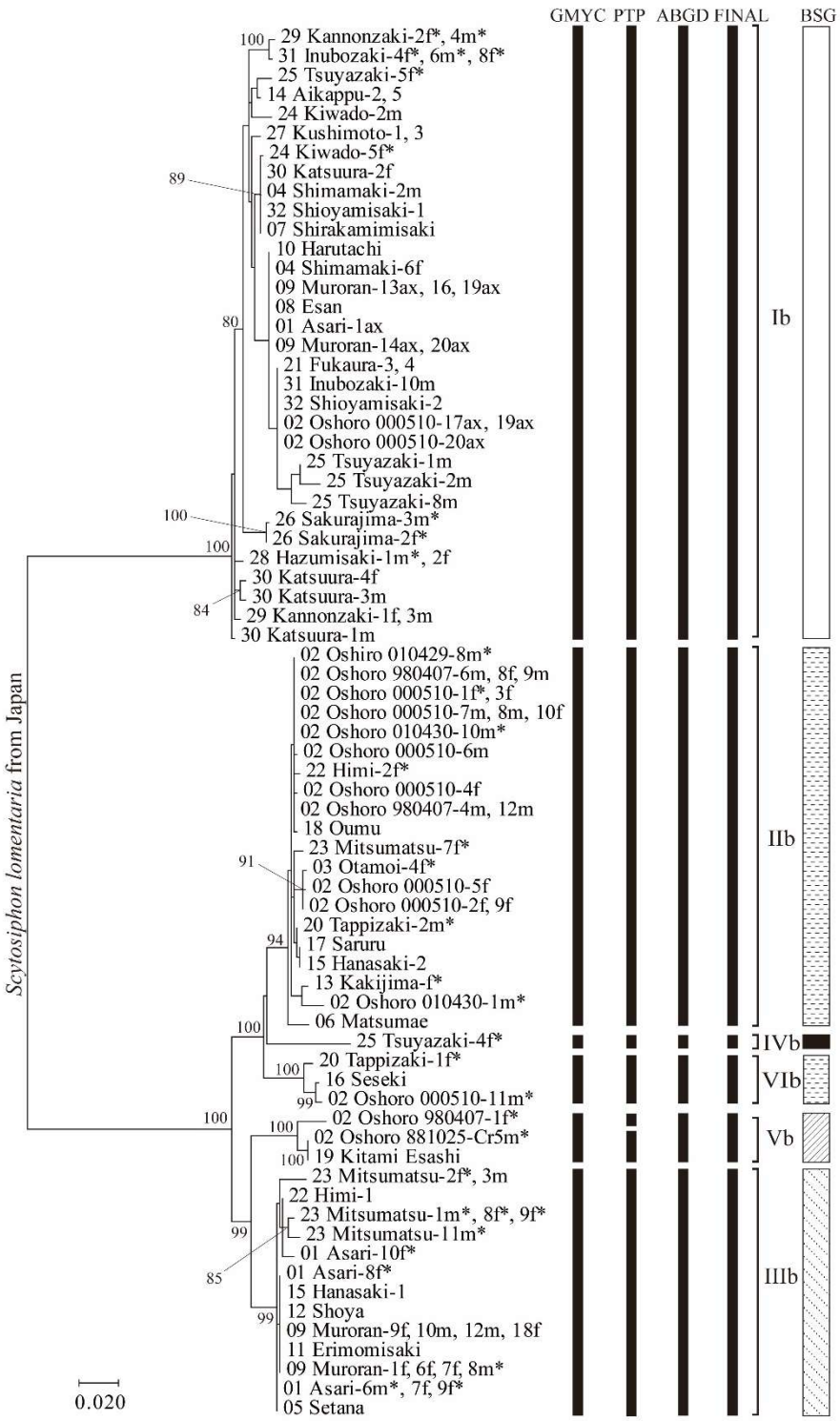

Figure 5. Summarized results from three species delimitation analyses (GMYC, PTP and ABGD) for *Scytosiphon lomentaria* based on the *cetn*-int2 sequences, represented on the ML tree of the full dataset. Bootstrap values (>80) are indicated near branches. The prior intraspecific divergences (*P*) for ABGD are $P = 0.001–0.0077$. See details in Fig. 4.

Crossing experiments

Significant gametic incompatibility was observed among the five *cox*1-based putative species (Ia-Va) except for the cross between IIa male and IIIa female (Fig. 6). Gamete fusion did not occur between Ia and others (IIa–Va). On the other hand, asymmetric hybridizations were observed between IIa and IIIa, and their hybrid zygotes successfully grew.

The process of gamete fusion is shown in Fig. 7. In intraspecific crosses, multiple male gametes attached to the cell surface of the settled female gamete with the anterior flagellar tip (Fig. 7B). Only one of the male gametes was activated and shook violently (Fig. 7C). After this activation, the cell body of the male gamete approached the female gamete, and the pair fused (Fig. 7D–F). Many zygotes were formed in intraspecific crosses (F in Fig. 6): more than 30% of female gametes fused with male gametes. In

♂ \ ♀			Ia						IIa							IIIa									IVa	Va
			Ib						IIb					VIb		IIIb									IVb	Vb
			Inubouzaki-4f	Inubouzaki-8f	Kannonzaki-2f	Tsuyazaki-5f	Sakurajima-2f	Kiwado-5f	Otamoi-4f	Oshoro 000510-1f	Himi-2f	Kakijima-f	Mitsumatsu-7f	Tappizaki-1f	Oshoro 100406-6f**	Asari-8f	Asari-9f	Asari-10f	Otamoi-12 f**	Otamoi-15f**	Muroran-5f**	Mitsumatsu-2f	Mitsumatsu-8f	Mitsumatsu-9f	Tsuyazaki-4f	Oshoro 980407-1f
Ia	Ib	Inubouzaki-6m	F	F	F	F	F	F	N	N				N						N				N	
		Kannonzaki-4m		F	F	F	F	F	N	N	N	N	N	N	N					N	N		N	N	N	N
		Hazumizaki-1m				F	F	F						N						N						
		Sakurajima-3m			F	F	F	F		N	N		N	N						N			N	N	N	N
IIa	IIb	Oshoro 010429-8m						N	F*	F*	F	F	F	F		F	F*			F*	F*	F	F	F	N1	N1
		Oshoro 010430-10m		N		N		N	F	F	F	F	F	F	F	F*	F*			F	F*	F*	F	F	N1	N1
		Tappizaki-2m			N	N	N	N		F	F	F	F	F		F	N1			N1	F	N1	F	F	N1	N1
		Oshoro 010430-1m		N		N		N		F*	F	F	F	F*	F	F*	F*		F*	N1	F	F	F	F*	N1	N1
	VIb	Oshoro 000510-11m					N	N	F	F	F		F	F		F	N1				F	F	N1	N1	N	N1
IIIa	IIIb	Oshoro 100406-4m**				N		N			N	N			F			F		F	F		F	F		
		Asari-6m		N		N	N	N	N	N	N		N	N	F	F	F			F	F*	F	F	F*	N1	N1
		Muroran-8m				N	N	N		N	N	N	N	N		F	F	F		F	F	F	F	F	N1	N1
		Otamoi-16m**													F			F*		F	F*	F	F	F		
		Mitsumatsu-1m				N		N		N	N		N	N	N1	F	F			F	F	F	F	F	N1	N1
		Mitsumatsu-11m				N	N	N		N	N		N	N		F	F			F	F	F	F	F	N1	N1
Va	Vb	Oshoro 881025-Cr5m		N	N	N		N		N1	N	N	N	N	N	N	N			N1	N1	N	N	N	N	F

Figure 6. Results of the crossing experiments among *cox*1-based putative *Scytosiphon* species (Ia–Va). Ib–VIb: *cetn*-int2-based putative species. F: more than 30 % of female gametes fused with male gametes. Superscript * on the left indicates that the zygote was isolated for the analysis of survival rate of the meiospores. N1: male gametes attached to a female gamete with their anterior flagella, but activation of the male gametes rarely occurred, and no more than 1% female gametes fused with male gametes. N: male gametes did not attach to female gametes with their anterior flagella, and no zygotes were formed. Superscript ** on the left of the culture code indicates that sequence of *cetn*-int2 was not determined for that culture.

interspecific crosses, three patterns were observed: 1) male gametes did not attach to female gametes with their anterior flagella, and no zygote was formed (N in Fig. 6), 2) multiple male gametes attached to the female gamete, however, the activation of male gametes rarely occurred. As a result, of the female gametes, not more than 1% fused with male gametes (N1 in Fig. 6), and 3) multiple male gametes attached to the female gametes, and the activation of male gametes and the zygote formation occurred as in the case of intraspecific crosses (F); the third pattern was only observed between species IIa males and species IIIa females.

Development of 11 hybrid (IIa male × IIIa female) and eight control (intraspecific crosses) zygotes was observed in culture. The hybrid zygotes developed into crustose or filamentous thalli and became fertile with unilocular sporangia within two months at 15°C under short day conditions, as did the control zygotes. The unilocular sporangia released meiospores. The hybrid meiospores often stopped growth early in development (one- to three-cell stage) and died. The survival rate of seven-day-old

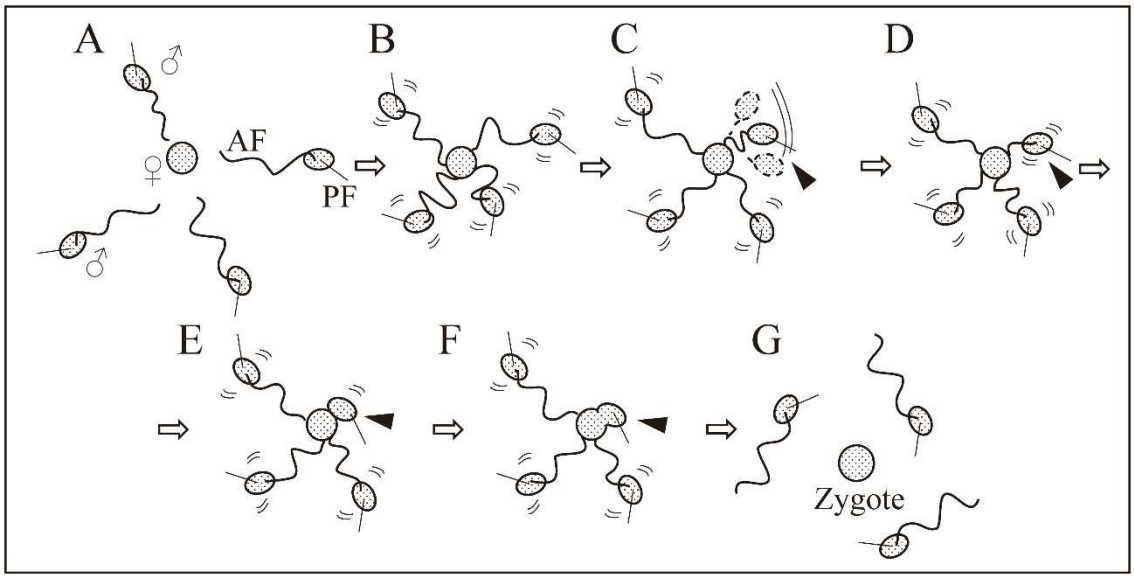

Figure 7. Process of gamete fusion in *Scytosiphon lomentaria*. A: The female gamete (♀) settles on the substratum and then attracts male gametes (♂). AF, anterior flagellum; PF, posterior flagellum. B: The multiple male gametes attach to the cell surface of the settled female gamete with the tips of their anterior flagella. C: One male gamete (arrowhead) is activated and changes its waving of the anterior flagellum aggressive for a moment. D–F: The activated male gamete approaches the female gamete, and then fuses. G: After formation of the zygote, the surplus male gametes detach from the zygote and swim away.

germlings of meiospores was 49.3% among hybrids and was 91.5% among the controls (Fig. 8), and the GLMM predicted that survival rate was significantly lower among hybrids compared to controls (Table 2). Meiospores from hybrids that survived successfully grew into erect thalli (gametophytes) and produced gametes that could backcross with parent species; however, dwarfed morphology was sometimes observed among these hybrid erect thalli (data not shown).

Individuals of *cetn*-int2-based putative species VIb were also used in crossing experiments. Gametes of putative species VIb individuals (Oshoro 000510-11m and Tappizaki-1f) showed identical crossing patterns as that of species IIb (Fig. 6). In the cross, Tappizaki-1f (VIb) × Oshoro 010430-1m (IIb), a zygote successfully grew into a sporophyte. Meiospores from this sporophyte developed normally as did other control meiospores (meiospores between IIb female and IIb male).

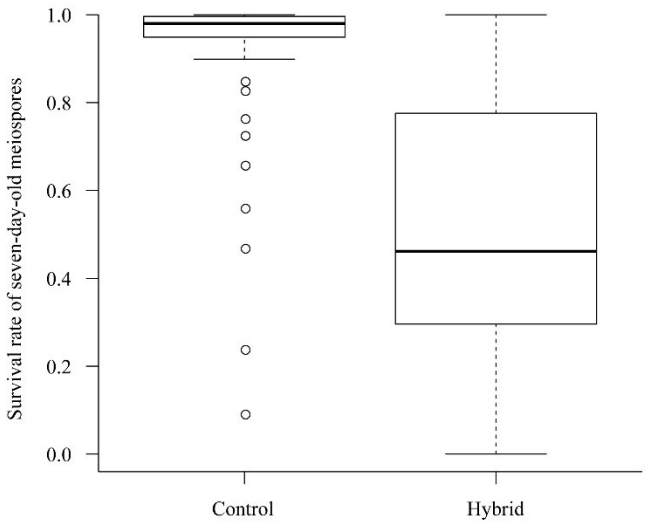

Figure 8. Box-and-whisker plots comparing survival rate of the seven-day-old germlings of meiospores from each unilocular sporangium for control and hybrid groups. The boxes and whiskers represent the interquartile range and the non-outlier ranges, and the band near the middle of the box is the median. Circles represent outliers.

Table 2. Analysis of the generalized linear mixed model for the survival rates of seven-day-old germlings of meiospores in hybrid sporophytes between IIa male × IIa female and controls (sporophytes derived from intra-specific crossings). Estimated coefficient for the group (-4.238) suggests the survival rate is negatively affected in hybrid.

	Coef.	SE	*z*	*p*
Intercept	4.034	0.4692	8.597	< 0.001
Group (Control/Hybrid)	-4.238	0.5953	-7.119	< 0.001

DISCUSSION

In the present study, I tested putative species suggested from DNA-based species delimitation methods (GMYC, PTP and ABGD) by crossing experiments in the Japanese *S. lomentaria* species complex. Although the *cox*1 and the *cetn*-int2 based species delimitations estimated different numbers of species (five and six, respectively), a conservative approach on the estimates of the two species delimitations yielded five putative species: Ia (Ib), IIa (IIb and VIb) and IIIa (IIIb)–Va (Vb). Crossing experiments revealed that the five putative species are reproductively isolated from each other by gametic incompatibility (pre-zygotic barrier) and low survival rate of hybrid meiospores (post-zygotic barrier). Therefore, the species boundaries based on DNA-based species delimitation methods were concordant with biological species boundaries (reproductive isolation barriers). This result supports that these DNA-based species delimitation methods are reliable tools to delimit species, although more verifications are needed in different taxa. The five species in this study correspond to the five genetic groups (Groups I–V) predicted from the combinations of haplotypes of *cox*1, *cox*3, ITS2 and *cetn*-int2 in Kogame et al. (2015a). Therefore, species boundaries predicted by the different DNA-based approach in Kogame et al. (2015a) also agreed with biological species boundaries. The above suggests that at least in the *S. lomentaria* species complex, species boundaries based on molecular data reflect the intrinsic barriers to gene exchange.

In sexual organisms, reproductive isolating mechanisms (barriers to gene exchange) generate and maintain phylogenetic separation and genetic clusters (Harrison, 1998 and included references; Avise, 2000). Thus, concordance between biological

species boundaries and species boundaries predicted from gene genealogies or barcoding gaps is not surprising. In brown algae, concordance between DNA-based species boundaries and reproductive isolating barriers (e.g. a temporal or ecological niche segregation, gametic incompatibility and death of hybrid zygotes) was also reported in *Pylaiella* (Geoffroy et al., 2015) and *Ectocarpus* (Montecinos et al., 2017).

DNA-based species boundaries and biological species boundaries are not always concordant. In the present study, the *cox*1-based analyses suggested species IIa, while the *cetn*-int2-based analyses suggested dividing species IIa into two (IIb and VIb). Individuals of putative species VIb showed the same crossing patterns as individuals of species IIb, and neither pre-zygotic nor post-zygotic barriers were detected between IIb and VIb. Furthermore, individuals of VIb and IIb were found in same locality (locality code 2 and 20 in Fig. 3). Thus, haplotypes delimited as species VIb should not be interpreted as a distinct species but intraspecific variation maintained in populations of species IIa (IIb). Therefore, *cetn*-int2-based species boundaries were partly incongruent with biological species boundaries. It is well known that single-locus based species delimitation cannot accommodate ancestral polymorphism and incomplete lineage sorting, and can fail at species delimitation (Monaghan et al., 2009; Puillandre et al., 2012; Yang, 2014). Although applications of multiple species delimitation methods for a single marker are frequently used to verify the estimates of the delimitation analyses, this approach cannot solve the above problem; species delimitation analyses should be performed using multiple markers. DNA-based species delimitation methods can provide valuable information; however, species delimitation should rely on many kinds of data, such as isolating mechanisms, morphological, geographical, ecological evidence, as the developers of DNA-based delimitation methods themselves mentioned (Monaghan et al., 2009; Yang and Rannala, 2010; Puillandre et al., 2012; Carstens et al., 2013; Zhang et al., 2013).

While DNA-based species delimitation analyses can predict existence of species

boundaries, they cannot tell us the nature of the barriers to genetic exchange. Reproductive isolating barriers are quite important to understand how genetic differences among sympatric species are maintained (Coyne and Orr, 2004). The present crossing experiments demonstrated that gametic incompatibility widely function as a pre-zygotic barrier among the five cryptic species (species Ia–Va) which often grow sympatrically. Two patterns (N and N1) of gametic incompatibilities were observed. N pattern can be considered as a more developed reproductive barrier than the N1 pattern, and N patterns were observed mainly among distantly related species (species Ia and others). In *Ectocarpus*, recognition between male and female gametes involves glycoproteins in the female gamete cell membrane and a glycoprotein-binding structure at the tip of the male's anterior flagellum (Schmid, 1993; Schmid et al., 1994). Defects in such a recognition mechanism may be responsible for the gametic incompatibility among the *S. lomentaria* species complex. In marine free-spawning species, gametic incompatibility plays an important role in speciation, because pre-mating behavioral isolation or mechanical isolation are limited in these taxa (Palumbi, 1994). Gametic incompatibility was previously reported in *Ectocarpus* and *Scytosiphon* (Müller, 1976; Müller, 1979; Müller and Eichenberger, 1995; Kogame, 1998; Peters et al., 2010). In the present study, asymmetric gametic incompatibility was observed in crosses between species IIa and IIIa. Such asymmetric hybridization was also reported in *Ectocarpus* (Müller and Eichenberger, 1995; Peters et al., 2010). In addition to gametic incompatibility, other pre-zygotic barriers in brown algae include: a temporal niche segregation in *Pylaiella* (Geoffroy et al., 2015), an ecological barrier and an asynchronaous gamete release in *Fucus* (Engel et al., 2005; Monteiro et al., 2012).

Although the pre-zygotic barrier between species IIa male and IIIa female was incomplete, low survival rate of hybrid meiospores was detected as a post-zygotic barrier. Hybrid inviability has been reported in many organisms including brown algae (Schnetter et al., 1987; Müller and Eichenberger, 1995; Druehl et al., 2005; Peters et al., 2010). In

general, this kind of post-zygotic barrier is caused by chromosomal rearrangement and Dobzhansky-Muller incompatibility (reviewed in Coyne and Orr, 2004). In the culture of the hybrids between species IIa male and IIIa female, abnormality was observed only after meiosis. Thus, disorder of meiosis in hybrid sporophytes may function as post-zygotic barriers. In my culture experiments, hybrid gametophytes derived from hybrid sporophytes between IIa and IIIa grew and matured. This result suggests an incomplete reproductive barrier between the two species. However, Kogame et al. (2015a) reported that no gametophytic individuals indicative of hybrids between IIa and IIIa were found, even in the locality where the two species sympatrically grow and mature at the same time. This suggests that these two species are reproductively isolated from each other in field. Post-zygotic reproductive isolation after formation of hybrid sporophytes was also reported between *Ectocarpus siliculosus* (Dillwyn) Lyngbye and *E. crouaniorum* Thuret (Montecinos et al., 2017).

McDevit and Saunders (2017) investigated Canadian Scytosiphonaceae using morphological and molecular analyses and recognized five species in *Scytosiphon*: *S. promiscuus* McDevit & G.W.Saunders (Group F), *S. canaliculatus* (Setchell & N.L.Gardner) Kogame (Groups B, C, D, E), *S. lomentaria* (Group I), *Scytosiphon* Atlantic complex (Groups G, H) and *S.* sp. (Group J). From my comparison of the sequence data, the species Ia, IIa and IIIa probably correspond to their *S. lomentaria* (Group I), *S. canaliculatus* (Groups B, C, D, E) and *S. promiscuus* (Group F), respectively. However, the species IIa is morphologically and genetically different from *S. canaliculatus* from Japan (Kogame, 1996; Kogame et al., 1999). McDevit & Saunders (2017) also reported mitochondrial introgression among *S. lomentaria* (Group F), *S. promiscuus* and *S. canaliculatus*, while mitochondrial introgression has not been observed in the *S. lomentaria* species complex from Japan. The present study was conducted using samples from a limited region, i.e. Japan, due to availability of samples. Since the *S. lomentaria* species complex has a worldwide distribution, further studies using more samples from

various regions are required to reveal diversity, distributions and speciation in this species complex.

Chapter 2

Systematics, distribution, and sexual compatibility of six *Scytosiphon* species (Scytosiphonaceae, Phaeophyceae) from Japan and the description of four new species.

INTRODUCTION

In many closely related algal taxa, morphological species discrimination and delimitation are difficult due to their widely overlapping morpho-anatomical characteristics resulting from their morphological plasticity and simplicity. Numbers of cryptic species have been detected by molecular phylogenetic studies, and some of these studies have revealed that a cosmopolitan species is actually a complex of distinct species with more restricted distributions, as seen in *Grateloupia filicina* (De Clerck et al., 2005), *Dictyota crenulata* (Tronholm et al., 2012), and *Lobophora variegata* (Vieira et al., 2016). An understanding of accurate species diversity and geographic distribution of each species is essential for studies on speciation, dispersal capacity of each species, and species conservation.

The brown alga *Scytosiphon lomentaria* Lyngbye (Link) (Scytosiphonaceae, Ectocarpales) is also a species complex that was once considered a single cosmopolitan species (Lüning, 1990). This species was originally described as *Chorda lomentaria* Lyngbye based on material from the Faeroe Is. and Borenholm, Denmark [Fig. 9; syntype localities, but lectotypified for Faeroe Is. in Womersley (1987)], and its thallus was reported as cylindrical, unbranched, and having constrictions (Lyngbye, 1819). It has been reported from cold to warm temperate waters worldwide (Guiry and Guiry, 2020). Many intraspecific taxa and distinct species have been described in *Scytosiphon* based on several characters of erect thalli, such as length, form (cylindrical/compressed/having constrictions or not), and presence/absence of paraphyses (ascocysts) (e.g. Reinke, 1888; Rosenvinge, 1893; Skottsberg, 1907; Setchell and Gardner, 1925; Wynne, 1969). However, most of them are considered as variants induced by environmental factors and maturity (Papenfuss, 1958; Clayton, 1976, 1978). Recent multigene phylogenetic studies have shown that *S. lomentaria* is a complex of multiple lineages (distinct species): Pacific and Atlantic lineages (Cho et al., 2007; Kogame et al. 2015b) and at least five species across the Japanese Islands (Kogame et al., 2015a). However, taxonomic studies remain unfinished. A major obstacle was the lack of clarity regarding to which of these lineages

the type material belongs. Four lineages have been reported around the type locality (north-eastern Atlantic; Kogame et al., 2015b).

The lineage to which the type material belongs was determined by McDevit and Saunders (2017). Their *cox*1-based phylogenetic analyses on Canadian Scytosiphonaceae detected 11 lineages in *Scytosiphon* (genetic groups A–K). The name *S. lomentaria* was applied to group I based on morphological observation. They examined the type material of *S. lomentaria* and found that it has constrictions and phaeophycean hairs and lacked paraphysis; of their lineages, only group I had the same characteristics as those of the type material (McDevit and Saunders, 2017). In addition, they applied the name *S. canaliculatus* (Setchell & N.L.Gardner) Kogame to groups B–E and established a new species, *S. promiscuus* McDevit & G.W.Saunders, for group F. However, Santiañez and Kogame (2018) showed that the true *S. canaliculatus* now belongs to *Hapterophycus*. The two lineages (genetic group G and H), which were endemic to the Atlantic, were named the *Scytosiphon* Atlantic complex (McDevit and Saunders, 2017). As a result of recent taxonomic studies in *Scytosiphon*, and the transfer of four species to other genera [*Planosiphon complanatus* (Rosenvinge) McDevit & G.W.Saunders, *Pl. gracilis* (Kogame) McDevit & G.W.Saunders, *Hapterophycus canaliculatus* Setchell & N.L.Gardner, and *Petalonia tenella* (Kogame) Santiañez & Kogame; McDevit and Saunders, 2017; Santiañez and Kogame, 2019] only four species are currently recognized in this genus: *S. lomentaria*, *S. promiscuus*, *S. dotyi* M.J.Wynne, and *S. crispus* Skottsberg.

In Japan, the *S. lomentaria* complex has been reported from all Japanese Islands. Recent multigene phylogenetic analyses and crossing experiments have recognized five species in the Japanese *S. lomentaria* complex [species Ia–Va; Kogame et al., 2015a; Hoshino et al., 2018 (**Chapter 1)**]. In addition to these five species, a sixth lineage (species VI) was newly detected in this study. In regard to these six Japanese species, I aimed to (1) resolve their phylogenetic relationships with other *Scytosiphon* species, (2) elucidate the taxonomy of each species, (3) estimate the distributions of each species

based on *cox*1 sequences, and (4) examine reproductive isolating barriers (gametic incompatibility) among species VI and others by crossing experiments.

MATERIALS AND METHODS

Specimen collection and morphological observation

More than 200 specimens of *Scytosiphon 'lomentaria'* were collected from various localities in Japan and Far East Russia (Fig. 9, Table S2) and were preserved in salt or silica gel for morphological observations and molecular analyses. Pressed specimens were deposited as vouchers in the Herbarium of Faculty of Science, Hokkaido University, Sapporo, Japan (SAP) and National Museum of Nature and Science, Tsukuba, Japan (TNS); herbarium acronyms follow Thiers (2020). Unialgal culture isolates were established for some samples as previously described by Kogame et al. (2015a). Sections of gametophytic thalli were made by hand with a razor blade and were mounted in seawater or 50% glycerol/seawater containing a small amount of 0.5% cotton blue solution (lactic acid/phenol/glycerol/water 1:1:1:1) for staining. Observations were conducted using a light microscope, and images were taken with a Nikon Digital Sight

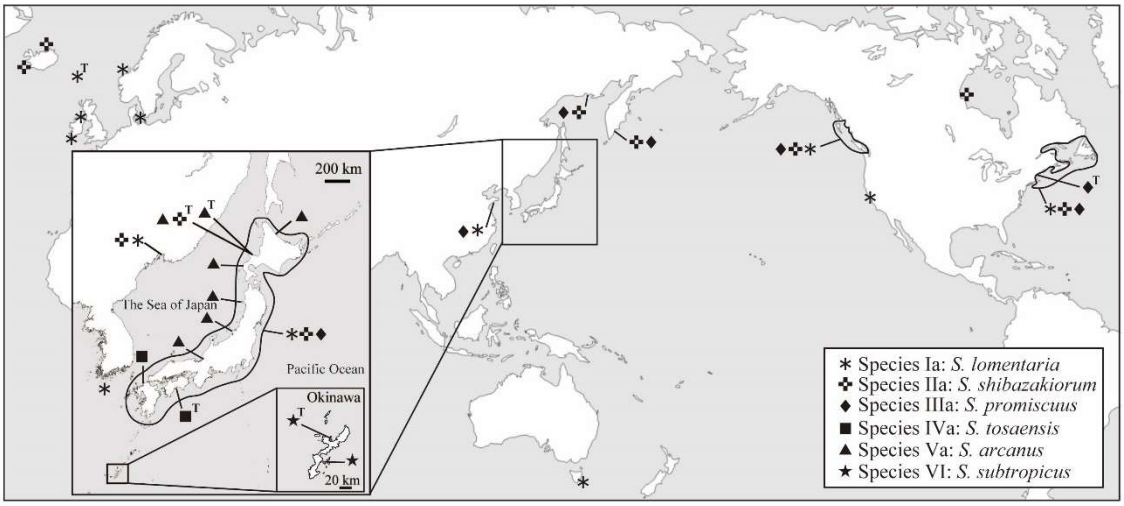

Figure 9. Geographic distributions of six *Scytosiphon* species. Superscript "T" on the right of symbols indicates the type localities of each species. Except for the syntypic localities of *S. lomentaria* (Faeroe Is. and Borenholm, Denmark; Lyngbye 1819), distributional information is based on *cox*1 data (Table S1).

DS-Fi1 (Nikon Corporation, Tokyo). In addition to the newly collected specimens, previously collected specimens and culture isolates (Kogame et al., 2015a, b; Chapter 1 and 5) were also used for morphological observations and molecular analyses (Table S2).

Molecular phylogenetic analyses

Partial sequences of the mitochondrial *cox*1 gene (600 bp) and the chloroplast *rbc*L gene (1084–1467 bp) were used for the molecular phylogenetic analyses. Total genomic DNA was extracted from the cultured or silica gel-dried thalli as previously described (Chapter 1) and used as template DNA for PCR. PCR was performed as previously described [Kogame et al., 1999; Hoshino et al., 2018 (**Chapter 1**)], and DNA sequencing was conducted according to the method described in Kogame et al. (2015a). The resulting sequences were deposited in GenBank (accession numbers are given in Table S2). Newly generated sequences were aligned with the sequences downloaded from GenBank, including previously generated *cox*1 and *rbc*L sequences of *Scytosiphon* species [Cho et al., 2006; Kogame et al., 2015a, b; McDevit and Saunders, 2017; (Hoshino et al., 2018; **Chapter 1**)] and other scytosiphonacean species. These downloaded sequences included the reference sequences of three described *Scytosiphon* species [*cox*1 and *rbc*L sequence from *S. promiscuus* (McDevit and Saunders, 2017), *rbc*L sequence from the specimen of *S. dotyi* collected from near the type locality San Mateo Co., California (Cho et al., 2006), and *cox*1 and *rbc*L sequences from Canadian samples that were identified as *S. lomentaria* by morphological comparison with the type material (McDevit and Saunders 2017)]. Alignment was performed with CLUSTALW (Thompson et al., 1994) in MEGA v. 7 (Kumar et al., 2016) with default parameters. For the *cox*1 dataset, I excluded the sequences less than 600 bp, and duplicate sequences were also excluded using CD-HIT Suite web server (Huang et al., 2010).

Maximum likelihood (ML) and Bayesian inference were used to infer the phylogeny of each gene. The ML analyses were performed using RAxML v. 8.2.10

(Stamatakis, 2014) with 1000 bootstrap pseudoreplicates under the GTR+GAMMA model. Bayesian posterior probabilities were calculated using Mr. Bayes v. 3.2.6 (Huelsenbeck and Ronquist, 2001; Ronquist et al., 2012) using the GTR substitution model with invariable sites over a gamma distribution (lset nst = 6, rates = invgamma) and Monte Carlo Markov Chains (MCMC) ran with the following parameters: 50,000,000 generations, 2 runs, 4 chains, heating parameter of 0.20, sampling frequency of 1000, burn-in fraction of 0.25 and stop value of 0.01. Whether analyses were at stationarity was confirmed by the plot generated by the sump command. Both ML and Bayesian phylogenetic analyses were performed through CIPRES Science Gateway version 3.3 (Miller et al., 2010).

_Cox_1-based species delimitation analyses

To infer species boundaries, Poisson Tree Processes (PTP; Zhang et al., 2013) was conducted for the *cox*1 dataset. PTP models speciation in terms of the number of substitutions and can infer putative species boundaries on the given phylogenetic tree (Zhang et al., 2013). The PTP analysis was performed on the *cox*1 RAxML tree constructed above, using the bPTP web server (https://species.h-its.org/) with default parameters. In addition to the PTP (maximum likelihood based), bPTP (updated version of PTP which is a Bayesian implementation of PTP) was also conducted on the bPTP web server. The bPTP provides Bayesian support values to delimited species on the input tree (i.e., the posterior probability of the taxa forming one species under the PTP model and a flat prior). The convergence of MCMC chains of the bPTP was visually checked by the likelihood plot.

Phylogeographic analyses for three worldwide species, species Ia–IIIa

To reveal the phylogeographic nature of the three worldwide species (species Ia–IIIa), I constructed *cox*1-haplotype networks. The *cox*1 datasets used were 600 bp and 213 sequences in species Ia [97 from Japan, one from Korea, two from Far East Russia, 108

from Canada and USA, two from Norway, two from Ireland, and one from Tasmania], 230 sequences in species IIa (57 from Japan, eight from Far East Russia, 162 from Canada and USA, and three from Iceland), and 126 sequences in species IIIa (52 from Japan, five from Far East Russia, and 69 from Canada and USA). In these datasets, duplicated sequences were not excluded, however, up to 10 sequences were used per locality to avoid sampling bias, and sequences less than 600 bp were excluded. Alignment was conducted by CLUSTALW in MEGA v. 7. Phylogenetic relationships among the *cox*1 haplotypes were reconstructed using median-joining methods (Bandelt et al., 1999) in Network v. 5.0.1.0, and the unnecessary median vectors and links in the networks were identified and cleaned up by MP option (Polzin and Daneshmand, 2003).

For species Ia–IIIa, since many *cox*1 sequences were available from Japan (JPN), the Pacific coast of North America (NAP), and the Atlantic coast of North America (NAA), I compared the genetic diversity of the populations among these regions. Sampling areas of these three regions are roughly shown in Fig. 9 (exact localities are shown in Table S2). Genetic diversity indices [the number of haplotypes (*nH*), the number of polymorphic sites (*nS*), gene diversity (*H*), and nucleotide diversity (π, Nei and Li, 1979)] were calculated; I used sequences from the three regions which were extracted from the alignments used for the network reconstructions. In addition, to examine whether populations of these regions are genetically differentiated or not, pairwise Φ_{st} was also computed (permutations of 1000, significance level of 0.01, compute distance matrix by pairwise difference). All computations were conducted using Arelquin v. 3.5.2.2 (Excoffier and Lischer, 2010).

Crossing experiments

Since my *cox*1-phylogenetic tree detected a new lineage (species VI) which was distinct from previously reported five cryptic species in *Scytosiphon* samples from Japan (Fig. 10; species Ia–Va), I crossed individuals of this lineage with those of species Ia–Va to

examine the possible reproductive isolating barriers among them. The culture isolates used are listed in Table 3. As I did not have male strains of species IVa, species IVa males were not used in the crossing experiments. The crossing experiments were performed following Hoshino et al. (2018; **Chapter 1)**. Since a pre-zygotic barrier (gametic incompatibility) was not observed between species IIIa and VI, hybrid zygotes of species VI female × species IIIa male were isolated and their development were observed at 20°C in long day condition (16 h:8 h, light:dark) and short day condition (10 h:14 h, light:dark) to investigate possible post-zygotic isolation. In addition to the hybrid zygotes, zygotes from an intra-lineage cross in species VI were also observed as control. Development of hybrid zygotes from other inter-specific crosses were not followed.

Table 3. Culture strains of gametophytes used in this study.

Species identity	Sample code	Sex	Collection location and date
Ia: *S. lomentaria*	Kamome-u1f	female	Kamomejima, Hokkaido, Japan; 7 April 2018
	Kannon-3m	male	Kannonzaki, Kanagawa Pref., Japan; 2 April 2000
IIa: *S. shibazakii*	Oshoro 000510-1f	female	Oshoro, Hokkaido, Japan; 10 May 2000
	Oshoro 010430-10m	male	Oshoro, Hokkaido, Japan; 30 April 2001
	Banshozaki-3m	male	Banshozaki, Wakayama Pref., Japan; 28 March 2018
IIIa: *S. promiscuus*	Muroran-5f	female	Muroran, Hokkaido, Japan; 10 March 2000
	Muroran-8m	male	Muroran, Hokkaido, Japan; 10 March 2000
IVa: *S. tosaensis*	Tsuyazaki-4f	female	Tsuyazaki, Fukuoka Pref., Japan; 31 March 2000
Va: *S. arcanus*	Oshoro 980407-1f	female	Oshoro, Hokkaido, Japan; 7 April 1998
	Oshoro 881025-Cr5m	male	Oshoro, Hokkaido, Japan; 25 October 1988
VI: *S. subtropicus*	Yagagi 180123-4f	femle	Yagachi, Okinawa Pref., Japan; 23 January 2018
	Yagagi 180123-3m	male	Yagachi, Okinawa Pref., Japan; 23 January 2018

RESULTS

Molecular phylogenetic and species delimitation analyses

The *cox*1 phylogenetic analyses showed that the *Scytosiphon lomentaria* complex from Japan consists of at least six lineages (Fig. 10): the five previously reported species (species Ia–Va) and one new lineage (species VI). These lineages were also estimated as distinct species by the PTP analysis (Fig. 10). Estimate of bPTP was congruent with that of PTP; however, Bayesian support value for species IIa was low (0.47; Fig. 10),

suggesting the low accuracy of the bPTP estimate for species IIa. Among the six *Scytosiphon* species from Japan, the genetic divergence (*p*-distance) was ca. 3.5–10.0% in *cox*1. In *rbc*L, the relationships among species Ia–Va was not well resolved, due to the low evolutionary rate of *rbc*L (Fig. 11). Species VI was recovered as a sister to the clade of species Ia–Va [bootstrap percentage (BP) = 91%, posterior probability (PP) = 1.0] and genetic divergence of 0.46–0.65% was observed between species VI and species Ia–Va (Fig. 11). The *cox*1 reference sequences of *S. lomentaria* (KF281312, Canada) and *S. promiscuus* (KF281380, USA) belonged to species Ia and IIIa, respectively (Fig. 10). The *rbc*L sequence of *S. dotyi* (DQ239771, USA) was inferred to be the sister group of *Scytosiphon* species Ia–VI (BP = 79%, PP = 0.79; Fig. 11). The Atlantic endemic lineage, i.e., *Scytosiphon* Atlantic complex (as European clade in Cho et al., 2007; McDevit and Saunders, 2017), were also distinct from *Scytosiphon* species Ia–VI both in the *cox*1 and the *rbc*L trees (Figs. 10 and 11). Monophyly of the genus *Scytosiphon* was well supported in *rbc*L (BP = 97%, PP = 1.0; Fig. 11).

My *cox*1 analyses showed that species Ia–IIIa are widely distributed in Japan and also have worldwide distributions (Fig. 9). On the other hand, species IVa, Va, and VI were found only in Japan (Fig. 9). Species IVa was found in two localities, warm regions of West Japan. Species Va was distributed in coastal habitats along the northern portion of the Tsushima warm current (the Sea of Japan side). Species VI was found only in Okinawa Is., subtropical region. In Japan, the geographic distributions of species Ia–Va were overlapped; however, species VI was geographically isolated from others.

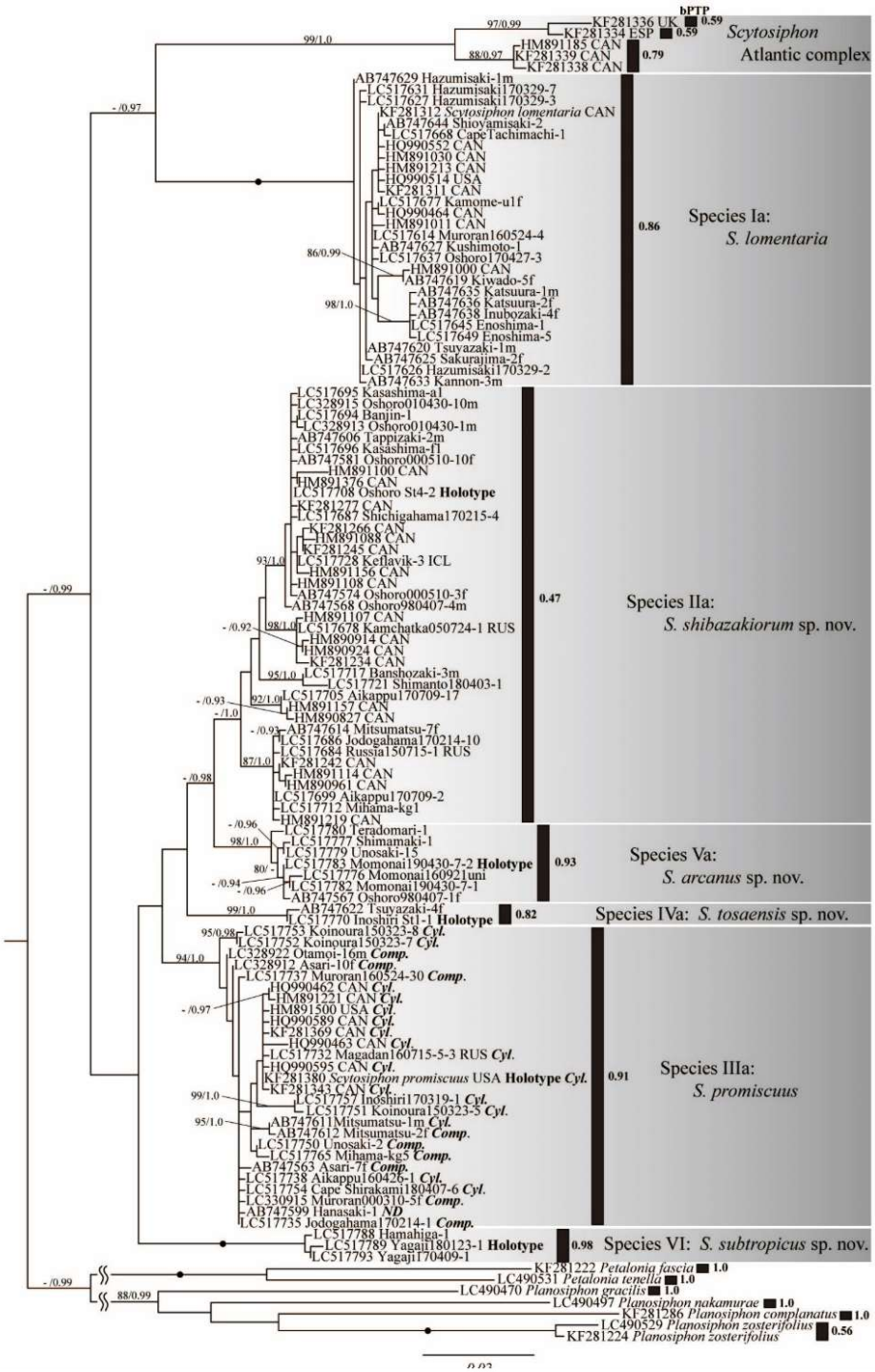

Figure 10. Maximum likelihood tree inferred from a 118 taxa dataset of the mitochondrial cox1 gene (600 bp) and the result of PTP and bPTP species delimitation analyses. Numbers on branches indicate bootstrap percentage from ML analysis (left) and posterior probabilities from Bayesian analysis (right). Only bootstrap percentages ≥ 80% and posterior probabilities ≥ 0.90 are shown. The black dots on branches indicate branches with full support (100/1.0). Black bars represent estimations from the PTP and bPTP analyses. Adjacent numbers indicate Bayesian support values of each delimited species by the bPTP analysis. For Scytosiphon sequences, except for Japanese samples, national code is given. UK: United Kingdom, ESP: Spain, CAN: Canada, USA: United States of America, ICL: Iceland, RUS: Russia. For S. promiscuus, morphotypes (thallus form) of each individual are also indicated: *Cyl*.: cylindrical-type, *Comp*.: complanate-type, *ND*: no data.

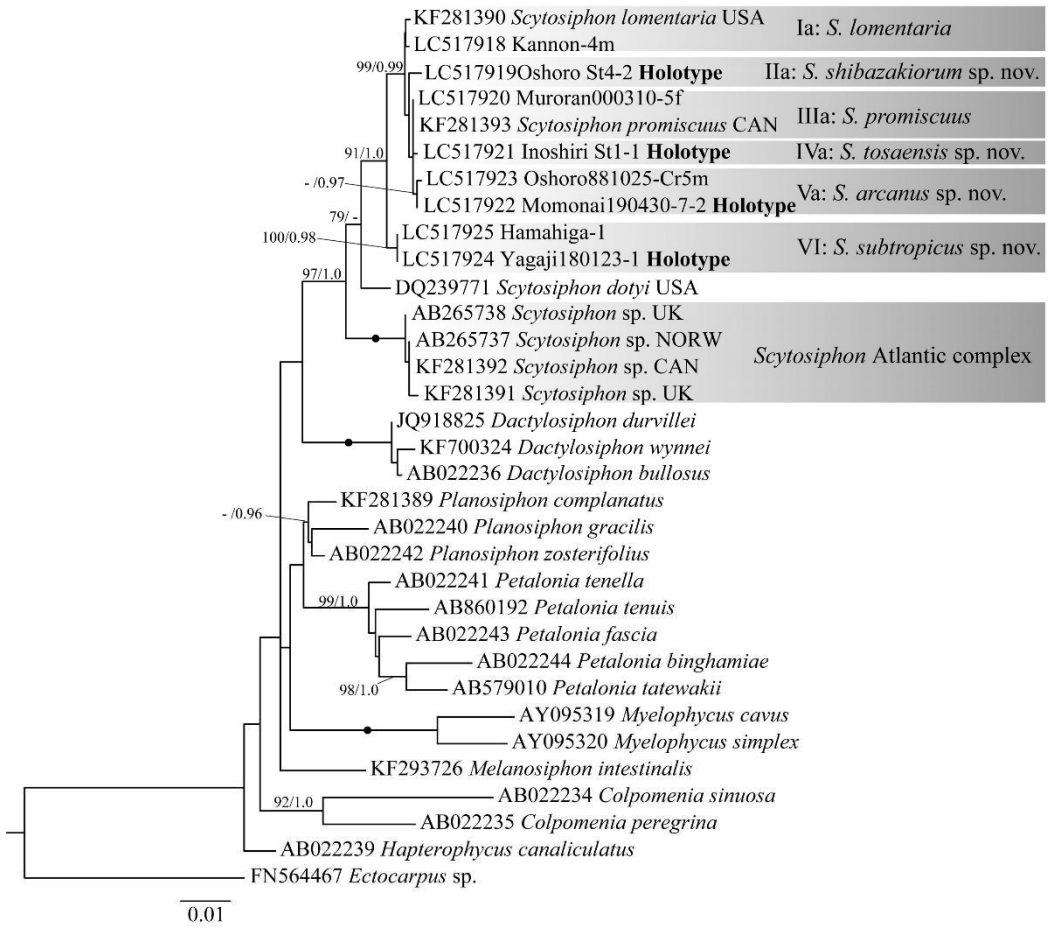

Figure 11. Maximum likelihood tree based on the chloroplast *rbc*L gene (1084–1467 bp). Numbers on branches indicate bootstrap percentage from ML analysis (left) and posterior probabilities from Bayesian analysis (right). Only bootstrap percentages ≥ 70% and posterior probabilities ≥ 0.90 are shown. The black dots on branches indicate branches with full support (100/1.0). For *Scytosiphon* sequences, except for Japanese samples, national code is given. USA: United States of America, CAN: Canada, UK: United Kingdom, NOR: Norway.

*Cox*1 haplotype networks and genetic diversity of the worldwide species, species Ia–IIIa

All species Ia–IIIa were widely distributed in the mid to high latitude region of Northern Hemisphere. However, genetic diversity and the degree of genetic differentiation among Japan (JPN), the Pacific coast of North America (NAP), and the Atlantic coast of North America (NAA) were different in each species. *Cox*1 haplotypes of species Ia were obtained from Japan, South Korea, Far East Russia, North America, Ireland, Norway, and Tasmania (Figs. 9 and 12A). In total, 28 haplotypes were identified and intraspecific

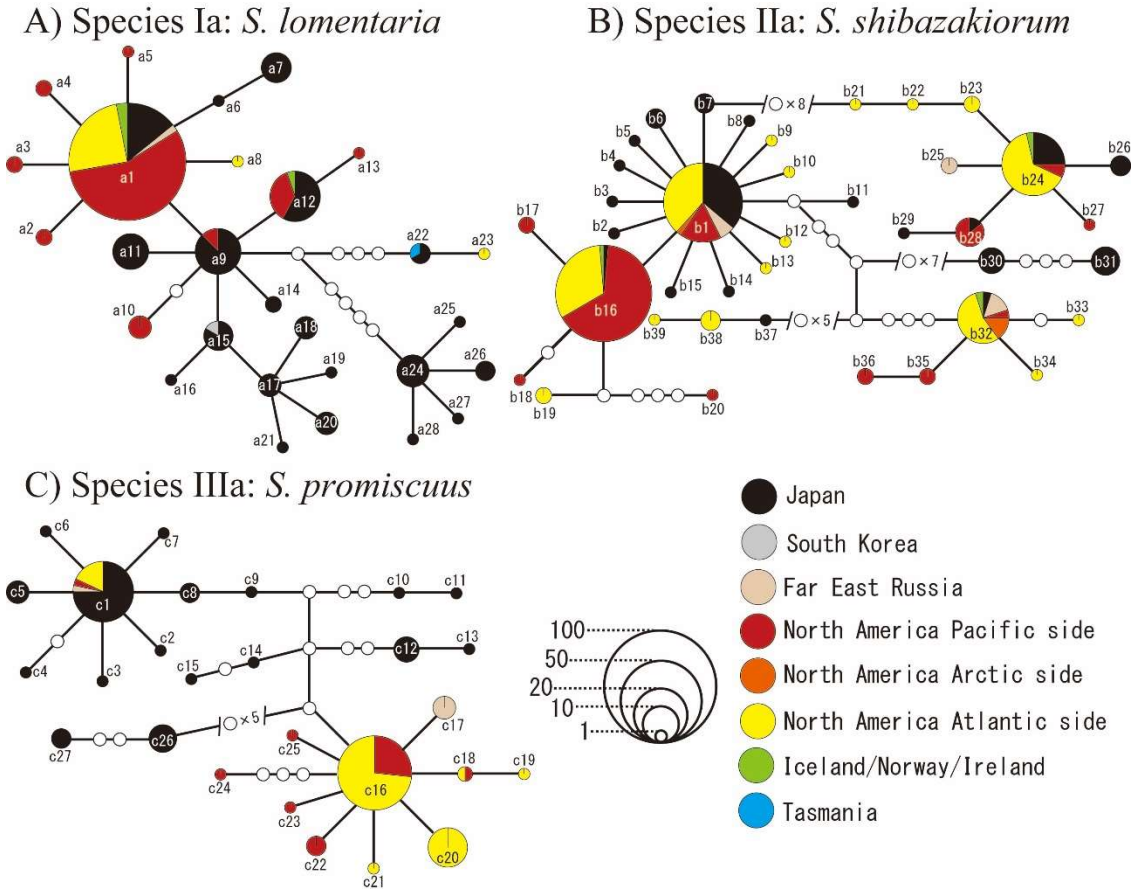

Figure 12. Haplotype networks of *cox*1 for three worldwide *Scytosiphon* species. One of the shortest trees is shown: (A) species Ia: *S. lomentaria*, (B) species IIa: *S. shibazakiorum*, and (C) species IIIa: *S. promiscuus*. Geographic region of origin of the samples are represented as different colors. Codes are given to each haplotype (e.g. a1, b1, and c1). Each colored circle represents a haplotype and its size is proportional to its frequency. White circles represent hypothetical unsampled haplotypes.

Table 4. *Cox*1-genetic diversity indices of species Ia (*S. lomentaria*), species IIa (*S. shibazakiorum*), and species IIIa (*S. promiscuus*) for three regions: JPN (Japan), NAP (Pacific coast of North America), NAA (Atlantic coast of North America). *N*, the number of individuals; *nH*, the number of haplotypes; *nS*, the number of polymorphic sites; *H*, gene diversity; π, nucleotide diversity (Nei and Li, 1979).

	Scytosiphon lomentaria			*Scytosiphon shibazakiorum*			*Scytosiphon promiscuus*		
	JPN	NAP	NAA	JPN	NAP	NAA	JPN	NAP	NAA
N	97	80	28	57	72	86	52	19	50
nH	20	9	3	20	11	16	17	7	6
nS	26	8	8	39	29	32	27	12	8
H	0.92 ± 0.01	0.45 ± 0.07	0.14 ± 0.09	0.88 ± 0.03	0.56 ± 0.07	0.83 ± 0.02	0.82 ± 0.05	0.66 ± 0.11	0.58 ± 0.06
π	3.69 ± 2.10	0.86 ± 0.68	0.57 ± 0.53	8.96 ± 4.65	4.64 ± 2.55	7.98 ± 4.15	4.72 ± 2.60	1.44 ± 1.02	1.27 ± 0.90

divergence was up to 1.8% in *p*-distance. The haplotype network showed that various haplotypes appeared at relatively similar frequency in Japan (Fig. 12A). In North America, a star-like network pattern (i.e. one frequent haplotype together with several less frequent haplotypes) was observed (haplotypes a1–a9; Fig. 12A). This pattern is usually associated with a recent population expansion (population expansions lead to star-shaped genealogies; Slatkin and Hudson, 1991). Haplotypes from Far East Russia, Ireland, and Norway were identical to the haplotypes found in Japan and North America, and a haplotype from Tasmania was identical to the haplotype from Japan in the Sea of Japan. A Korean haplotype was identical to those from Kyushu Is., Japan, the closest of the islands to South Korea. Among the three regions (JPN, NAP, and NAA), JPN showed the highest genetic diversity than others [$nH = 20$, $nS = 26$, $H = 0.92 \pm 0.01$ (± SD), $\pi = 3.69 \pm 2.10$ (± SD); Table 4]. The population pairwise Φ_{st} suggested that JPN population is significantly differentiated statistically from those of NAP ($\Phi_{st} = 0.19$, $p < 0.001$) and NAA ($\Phi_{st} = 0.19$, $p < 0.001$), but there was no significant differentiation between NAP and NAA ($\Phi_{st} = 0.03$, $p = 0.061$).

*Cox*1 haplotypes of species IIa were obtained from Japan, Far East Russia, North America, and Iceland (Figs 9 and 12B). In total, 39 haplotypes were identified and intraspecific divergence was up to 3.5% in *p*-distance. The haplotype network consisted of several haplogroups, including one big star-like haplogroup (haplotypes b1–b15; Fig. 12B), and they were distantly related to each other. Most of these haplogroups were commonly detected in Japan and North America with some difference in their frequencies. Haplotypes from Far East Russia and Iceland were identical to those of Japan and North America, except for one haplotype from Far East Russia (haplotype b25; Fig. 12B). Among the three regions (JPN, NAP, and NAA), JPN showed the highest genetic diversity ($nH = 20$, $nS = 39$, $H = 0.88 \pm 0.03$, $\pi = 8.96 \pm 4.65$; Table 4). The population pairwise Φ_{st} suggested statistically significant differentiation between JPN and NAP ($\Phi_{st} = 0.13$, p

< 0.001), and NAP and NAA (Φ_{st} = 0.09, p < 0.001), but there was no significant differentiation between JPN and NAA (Φ_{st} = 0.03, p = 0.023).

*Cox*1 haplotypes of species IIIa were obtained from Japan, Far East Russia, and North America (Figs. 9 and12C). In total, 27 haplotypes were identified and intraspecific divergence was up to 2.3% in *p*-distance. The haplotype network included two star-like haplogroups; one haplogroup consisted of mainly Japanese specimens (haplotypes c1–c9; Fig. 12C), but the other included haplotypes from NAP and NAA but no Japanese specimens (haplotypes c16–c25; Fig. 12C). From Far East Russia, haplotypes of both star-like haplogroups were detected. Among the three regions (JPN, NAP, and NAA), JPN showed the highest genetic diversity (nH = 17, nS = 27, H = 0.82 ± 0.05, π = 4.72 ± 2.60; Table 4). The population pairwise Φ_{st} suggested that JPN population is significantly differentiated statistically from those of NAP (Φ_{st} = 0.38, p < 0.001) and NAA (Φ_{st} = 0.42, p < 0.001), but there was no significant differentiation between NAP and NAA (Φ_{st} = 0.04, p = 0.07).

Crossing experiments

Although gametic incompatibility (pre-zygotic barrier) was incomplete between species VI and others, crossing patterns of species VI were different from those of others (Fig. 13). In intra-species crosses, multiple male gametes attached to the cell surface of the settled female gamete with the anterior flagellar tip and formed a clump, and only one of the male gametes fused with the female gametes. In inter-species crosses, female gametes of species VI fused with male gametes of species IIa, IIIa, and Va, but never fused with male gametes of species Ia. Male gametes of species VI fused with female gametes of species IIIa and IVa, but never fused with female gametes of species Ia, IIa and Va. Although gametic incompatibility was not observed between species IIIa and species VI, these two species showed the different crossing pattern with species IVa and Va (Fig. 13).

♂ \ ♀		Ia		IIa	IIIa	IVa	Va	VI
		Kamomejima-ura-1f	Kiwado-5f	Oshoro 000510-1f	Muroran-5f	Tsuyazaki-4f	Oshoro 980407-1f	Yagaji 180123-4f
Ia: *S. lomentaria*	Kannon-4m	-	F	N	N	N	N	-
	Kannon-3m	F	-	-	-	-	-	N
IIa: *S. shibazakiorum*	Oshoro 010430-10m	-	N	F	F	N	N1	F
	Banshozaki-3m	-	-	F	F	-	N1	F
IIIa: *S. promiscuus*	Muroran-8m	-	N	N	F	N1	N1	F*
Va: *S. occultus*	Oshoro 881025-Cr5m	-	N	N1	N1	N	F	F
VI: *S. subtropicus*	Yagaji 180123-3m	N	-	N	F	F	N1	F*

Figure 13. Results of the crossing experiments among six *Scytosiphon* species. Results from this study are indicated with a gray background and results with a white background are from Hoshino et al. 2018. F: more than 30% of female gametes fused with male gametes. Superscript asterisks on the right indicates that the development of zygotes was observed. N1: male gametes attached to a female gamete with their anterior flagella but gamete fusion was rare (no more than 1%) or not observed. N: male gametes did not attach to a female gametes and gamete fusion was not observed. -: no data.

Hybrid and control zygotes isolated (F* in Fig. 13) developed into sporophytes (discoid or filamentous thalli). Hybrid sporophytes (species VI female × species IIIa male) produced many unilocular sporangia. Ten unilocular sporangia were isolated (Uni1–10). Each unilocular sporangium released approximately 40–150 zoospores and these were cultured at 20°C in short day condition. After two weeks, some germlings (zoospores) developed well, and the number of cells of these germlings were uncountable at the light microscopy level (Fig. 14). However, the majority were less than 5-celled, and these poorly grown germlings usually had significantly shrunken chloroplasts and appeared to be dead (Fig. 14). The frequency of the germlings which were less than 5-celled was different among the unilocular sporangia [Uni1: 33/47 (70.2%), Uni2: 85/162 (52.5%), Uni3: 64/78 (82.1%), Uni4: 29/54 (53.7%), Uni5: 30/41 (73.2%), Uni6: 62/63 (98.4%), Uni7: 91/105 (86.7%), Uni8: 31/51 (60.8%), Uni9: 154/155 (99.4%), Uni10: 74/76 (97.4%)]. On average, among the unilocular sporangia, 77.4 ± 18.1 (SD)% of germlings were less than 5-celled and seemed to be dead; survival rate of the hybrid zoospores was approximately 22.6% after the two weeks cultivation. Erect (gametophytic), filamentous, or discoid thalli were observed after two months in the cultures of six unilocular sporangia (Uni1, 2, 4, 5, 8, 9). Surviving germlings were not observed in the cultures from the other four unilocular sporangia. The control sporophytes

(intra-species cross in species VI) seemed to mature, since I observed germlings and gametophytic thalli that probably originated from zoospores released from unilocular sporangia. However, unilocular sporangia were never observed. These control sporophytes probably produced few sporangia.

Figure 14. Two-week-old germlings of hybrid zoospores (species VI female × IIIa male). Poorly grown germlings with shrunk chloroplasts (arrowheads) and successfully grown one with normal chloroplasts (asterisk).

Taxonomic observations

Species Ia: *Scytosiphon lomentaria* (Lyngbye) Link 1833, nom. cons.

(Fig. 15A–E; Table 5).

BASIONYM: *Chorda lomentaria* Lyngbye.

TYPE LOCALITY: Quvig, Faeroe Is., Denmark (Womersley 1987, p. 295).

LECTOTYPE SPECIMEN: deposited in Herb. Lyngbye, C.

DISTRIBUTION: Japan, Korea, China, Far East Russia, Ireland, Norway, Denmark, Canada, USA, New Zealand and Tasmania (Cho et al. 2007, Fig. 9).

HABITAT AND PHENOLOGY: Erect thalli grow on rocks, boulders, and concrete blocks in intertidal to upper subtidal zones; found in late winter to spring in Japan.

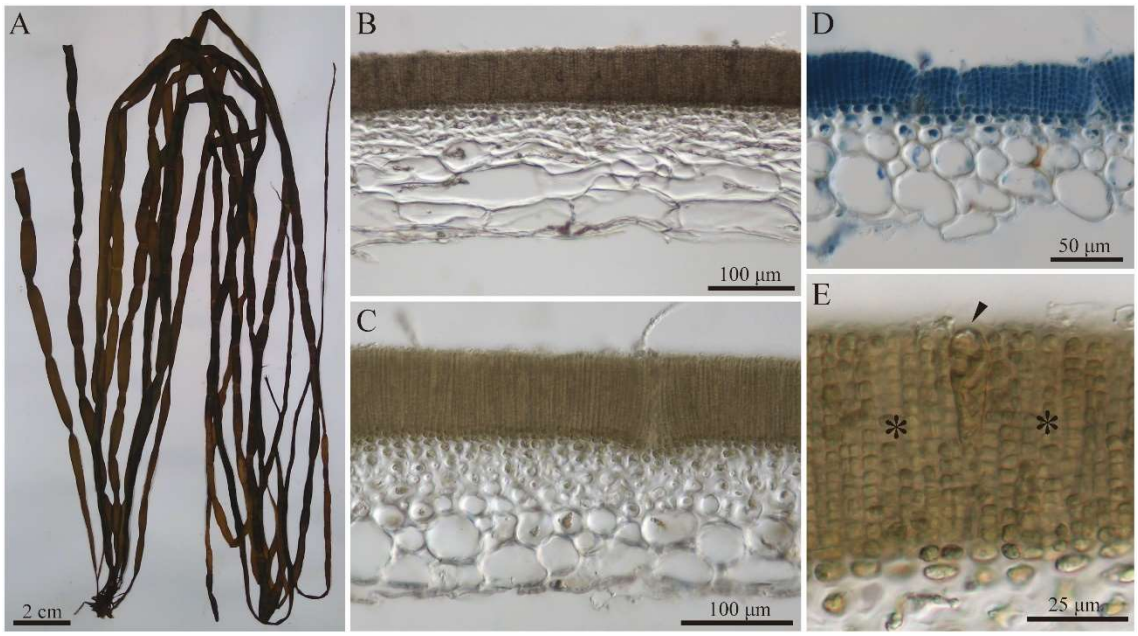

Figure 15. Morphology of gametophytes of species Ia, *Scytosiphon lomentaria*. (A) Gametophyte showing constrictions at a regular interval (SAP115551-3). (B) Longitudinal section of SAP115551-3. (C) Cross-section of SAP115551-3, displaying the medulla consisting of 6–7 cell layers. (D) Cross-section of SAP115552-1, displaying the medulla consisting of 3–4 cell layers. (E) Plurilocular sporangia (asterisk) and a paraphysis (arrowhead) of SAP115551-3

JAPANESE NAME: Kayamonori

SPECIMENS EXAMINED: SAP115417-6, -7, -9–11, -13, -19, -21, Aikappu, Hokkaido, Japan, 9 July 2017; SAP115553-1–8, -10, Cape Tachimachi, Hokkaido, Japan, 6 April 2018; SAP115552-1–3, -8, -10, -13, Cape Shirakami, Hokkaido, Japan, 7 April 2018; SAP115555-1, Kamomejima-Ura, Hokkaido, Japan, 7 April 2018; SAP 115551-3, Muroran, Hokkaido, Japan, 17 May 2018; SAP115416-1–10, Oshoro, Hokkaido, Japan, 27 April 2017; SAP115420-2–10, 29 March 2017, Hazumisaki, Aichi Prefecture, Japan; SAP115419-1–8, -12, Enoshima, Kanagawa Prefecture, Japan, 18 February 2017; SAP114730-2, Portrush, Co. Antrim, Ireland, 30 May 2004; SAP114742-1, Ona, Møre og Romsdal County, Norway, 28 June 2004.

MORPHOLOGY OF GAMETOPHYTES: The external morphology of 70 specimens from 12 populations and internal anatomy of 12 specimens from seven populations were examined. Thalli were yellowish brown when young, becoming darker when fertile, cylindrical to flattened, hollow, commonly gregarious, arising from a small holdfast.

Thalli were simple and unconstricted when young, but usually constricted at regular intervals when fertile (Fig.15A). Thallus size was varied among populations. For example, fertile thalli at the Cape Tachimachi were short and narrow (up to 30 cm in length; ca. 1–2 mm in width; n = 30); while, those at Muroran were long and wide (up to 60 cm in length; ca. 5–8 mm in width; n = 7). In longitudinal section, medullary cells were longer in inner portions, to 270 μm in length (Fig.15B). In cross section, the cortex was comprised of 2–3 layers of small pigmented cells (4.5–10.0 μm × 3–6 μm) and the medulla was comprised of 3–7 layers of large colorless cells. The appearance of the medulla was varied among the localities. Specimens from Muroran had the medulla consisting of 6–7 cell layers and outer four layers were dense with small cells (Fig.15C). However, such dense cell layers were not observed in specimens from Cape Shirakami (Fig.15D). Phaeophycean hairs were variable in number and usually grouped. Plurilocular sprorangia were produced by cortical cells on the entire surface of the thallus, uni- or biseriate, consisting of up to 22 chambers, and were loosely coherent without a cuticular layer covering them (Fig.15E). The unicellular paraphyses were associated with plurilocular sporangia (Fig.15E). Paraphyses were varied in number; rarely observed or absent in some specimens, but frequent in others.

REMARKS: *Scytosiphon lomentaria* is morphologically distinguished from other *Scytosiphon* species except for *S. shibazakiorum* by having a thicker medulla which is usually more than three cell layers. This species corresponds to clade A in Cho et al. (2007), group I in Kogame et al. (2015a), clade P1 in Kogame et al. (2015b), group I in McDevit and Saunders (2017) and species Ia in Hoshino et al. (2018) and **Chapter 1**.

Species IIa: ***Scytosiphon shibazakiorum*** M.Hoshino & Kogame

in Hoshino et al. (2020c)

(Fig. 16A–E; Table 5).

DESCRIPTION: Erect thalli are yellowish-brown when young, becoming darker when fertile, simple, cylindrical to somewhat flattened, hollow, usually having constrictions, to 70 cm long and 0.7 cm wide, gregarious, arising from a small holdfast; the cortex is composed of 2–3 layers of small pigmented cells; the medulla is composed of 2–7 layers of large, round or polygonal colorless cells; plurilocular sporangia are produced by cortical cells on the entire surface of the thallus, uni- or biseriate, up to 17 chambers, and loosely coherent without a covering cuticular layer; paraphyses and phaeophycean hairs present. Mitochondrial–encoded *cox*1 sequence = GenBank accession LC517708; chloroplast–encoded *rbc*L sequences LC517919.

TYPE LOCALITY: Oshoro, Otaru, Hokkaido, Japan, (43°12'50.4" N, 140°51'28.4" E).

HOLOTYPE: SAP115515 (Fig. 16A), attached on a rock in intertidal zone, collected by M. Hoshino on 28 February 2018.

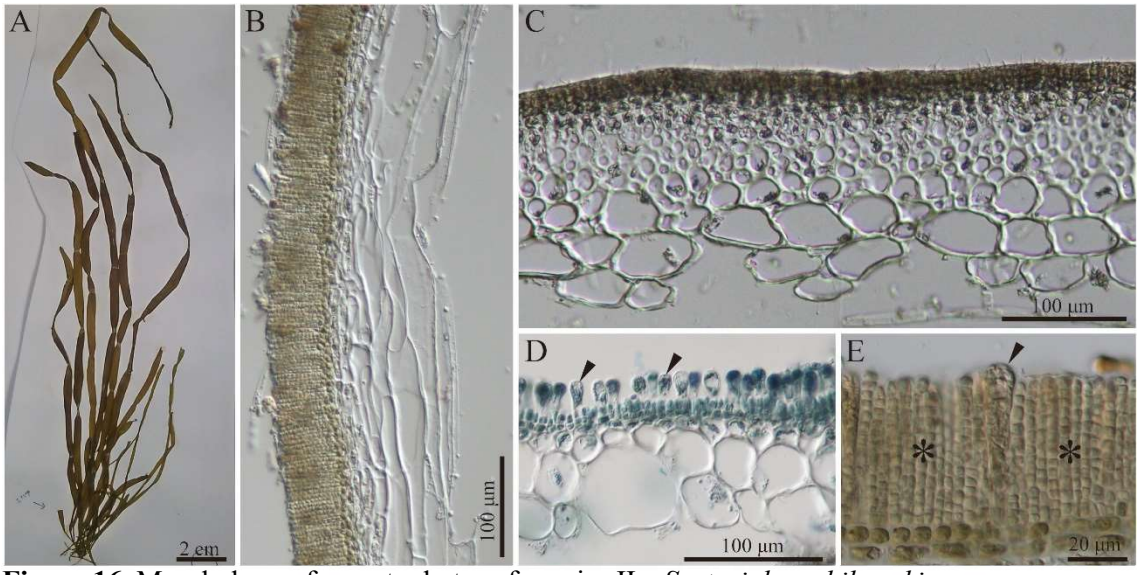

Figure 16. Morphology of gametophytes of species IIa, *Scytosiphon shibazakiorum* sp. nov. (A) Holotype specimen, SAP115515. (B) Longitudinal section of SAP115517. (C) Cross-section of SAP115525-2, displaying the medulla consisting of 6–7 cell layers. (D) Cross-section of SAP115529-2, displaying the medulla consisting of 2–3 cell layers. (E) Plurilocular sporangia (asterisk) and a paraphysis (arrowhead) of SAP115517.

ISOTYPE: SAP115517–115518, TNS-AL213451, and TNS-AL213452; deposited in SAP and TNS.

DISTRIBUTION: Japan, Korea, Far East Russia, Iceland, Canada, USA (Fig. 9).

HABITAT AND PHENOLOGY: Erect thalli grow on rocks, boulders, and concrete blocks in intertidal to upper subtidal zones; found in late winter to spring.

ETYMOLOGY: This species is in honor of Mr. Koji Shibazaki, a former employee at Oshoro Marine Station, and his wife Ms. Kumiko Shibazaki, for their indispensable support during the sampling at Oshoro (the type locality of this species).

JAPANESE NAME: Shibazaki-kayamonori (Hoshino et al., 2020c).

ADDITIONAL SPECIMENS EXAMINED: SAP115521, Jodogahama, Iwate Prefecture, Japan, 14 February 2017; SAP115522, Shichigahama, Miyagi Prefecture, Japan, 15 February 2017; SAP115523, Unosaki, Akita Prefecture, Japan, 6 April 2017; SAP115524, Atsumi, Yamagata Prefecture, Japan, 5 April 2017; SAP115532, SAP115525-2, -3, Fukaura, Aomori Prefecture, Japan, 14 April 2018; SAP115526, Teradomari, Niigata Prefecture, Japan, 17 April 2018; SAP115527, Banjin, Niigata Prefecture, Japan, 17 April 2018; SAP115528, SAP115529-1–3, Kasashima, Niigata Prefecture, Japan, 10 April 2018; SAP115530-2–4, -8, -15–17, Aikappu, Akkeshi, Hokkaido, Japan, 9 July 2017; SAP115531, Kamomejima, Esashi, Hokkaido, Japan, 7 April 2018; SAP115533-1–4, Mihama, Fukui Prefecture, Japan, 18 March 2018; SAP115534-1, -3–5, -10, Banshozaki, Wakayama Prefecture, Japan, 28 March 2018; SAP115535, SAP115535-1–4, -6, Shimanto, Kochi Prefecture, Japan, 3 April 2018, 19 February 2019; SAP114762-1, -3, Keflavik, Reykjanes, Iceland, 15 September 2004; SAP114760-5, Köpasker, Norðurland eystra, Iceland, 12 Sep. 2004; SAP115562-1, -2, SAP115564, SAP115565, Petropavlovsk-Kamchatskii, Russia, July 2005; SAP115559-19, Vesyolaya Bay, Magadan, Russia, 9 July 2016; SAP115561-1, -5, Vladivostok, Russia, 15 July 2015.

MORPHOLOGY OF GAMETOPHYTES: The external morphology of 51 specimens from 19 populations and internal anatomy of 16 specimens from nine populations were examined. The morphology of thalli seemed to be varied depending on the wave strength of habitat. In exposed areas/the upper intertidal zones, thalli were somewhat short and narrow, and tended to have clear constrictions. In protected areas/the subtidal zones, thalli were relatively long and wide, and had unclear constrictions. In cross section, the cortex was composed of 2–3 layers of small pigmented cells (5–12 μm × 4–6 μm) and the medulla is composed of large colorless cells. Thalli grown in exposed areas had thick medullary cell layers (3–7 cell layers) consisting of relatively small cells (Fig. 16C), while thalli grown in protected areas/subtidal zones seem to have thin medullas (2–3 cell layers) consisting of relatively large cells (Fig. 16D). In longitudinal section, medullary cells were longer in inner portions, to 300 μm in length (Fig. 16B). Phaeophycean hairs and unicellular paraphyses were always present (Fig. 16E).

REMARKS: This species belongs to clade B in Cho et al. (2007) and clade P2 in Kogame et al. (2015b) and corresponds to group II in Kogame et al. (2015), groups B–E in McDevit and Saunders (2017), and species IIa in Hoshino et al. (2020) and **Chapter 1**.

Species IIIa: *Scytosiphon promiscuus* McDevit & G.W.Saunders 2017

(Fig. 17A–E; Table 5)

TYPE LOCALITY: Narragansett, Rhode Island, USA (41°24'52.2"N, 71°27'09.3"W).

HOLOTYPE: UNB GWS006024.

DISTRIBUTION: Japan, Korea, China, Far East Russia, Canada, USA., Australia and New Zealand (Kogame at al. 2015a, Fig. 9).

HABITAT AND PHENOLOGY: Erect thalli grow on rocks, boulders, and concrete blocks in intertidal to upper subtidal zone; found in late winter to spring in Japan.

JAPANESE NAME: Kita-kayamonori (Hoshino et al., 2020c).

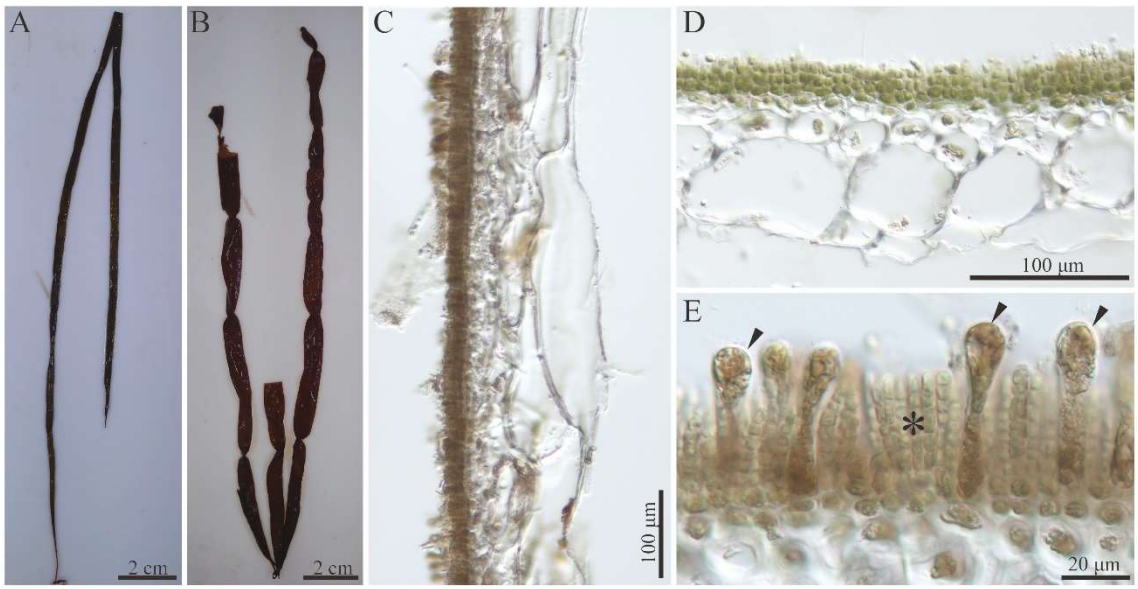

Figure 17. Morphology of gametophytes of species IIIa, *Scytosiphon promiscuus*.
(A) complanate-type thallus, SAP115544. (B) Cylindrical-type thallus, SAP115546-1. (C) Longitudinal section of cylindrical-type thallus, SAP115546-1. (D) Cross-section of complanate-type thalli, SAP115544, displaying the medulla consisting of 2–3 cell layers. (E) Plurilocular sporangia (asterisk) and a paraphysis (arrowhead) of SAP115546-1.

SPECIMENS EXAMINED: SAP115537, Jodogahama, Iwate Prefecture, Japan, 14 February 2017; SAP115538, Muroran, Hokkaido, Japan, 24 May 2016; SAP115539-1–11, Aikappu, Akkeshi, Hokkaido, Japan, 26 April 2016; SAP115540, Shiranohana, Usa, Kochi Prefecture, 19 March 2017; SAP115541, Unosaki, Akita Prefecture, Japan, 6 April 2017; SAP115542, Cape Shirakami, Hokkaido, 7 April 2018; SAP115543, Kamomejima, Esashi, Hokkaido, Japan, 7 April 2018; SAP115544, Oshoro, Hokkaido, Japan, 21 March 2018; SAP115545-1, -6, SAP115546-1, -3–5, SAP115547-1, SAP115548-1, Inoshiri, Usa, Kochi Prefecture, Japan, 19 March 2017, 29 March 2018, 20, 21 February 2019; SAP115549, Mihama, Fukui Prefecture, Japan, 18 March 2018; SAP115550, Shioyazaki, Fukushima Prefecture, Japan, 25 March 2018; SAP115563, Vilkova, Petropavlovsk-Kamchatsky, Russia, 22 July 2005; SAP115560, Svetlaya Bay, Magadan, Russia, 15 July 2016.

MORPHOLOGY OF GAMETOPHYTES: The external morphology of 43 specimens from 15 populations and the internal anatomy of 12 specimens from five populations were

examined. Two morphotypes, complanate-type and cylindrical-type were observed. The complanate-type had highly compressed thalli and its constrictions were sometimes not clear (Fig. 17A), whereas the cylindrical-type thalli were strongly constricted (Fig. 17B). Except for the three populations in which cylindrical-type was dominant (Koinoura, Inoshiri, and Svetlaya Bay, Magadan; Table S2), the complanate-type was mainly observed. However, even in the complanate-type populations, somewhat cylindrical individuals were observed. In *cox*1 phylogenetic analyses, specimens having haplotypes c1–c9 and c12–c15 often had complanate thalli, and specimens having haplotypes c10, c11 and c16–c27 had cylindrical thalli (Figs. 10 and 12C). Both morphotypes were yellowish-brown when young, becoming darker when fertile, hollow, commonly gregarious, arising from a small holdfast. No significant difference was detected in internal anatomy between these morphotypes. In longitudinal section, medullary cells were longer in inner portions, to 320 μm in length (Fig. 17C). In cross section, the cortex was composed of roughly two layers of small pigmented cells and the medulla was composed of 2–4 layers of large colorless cells (Fig. 17D). Plurilocular sporangia were uni- or biseriate, were produced basipetally on the entire surface of the thallus consisted of up to 16 chambers, and were loosely coherent without a covering cuticular layer. Phaeophycean hairs and unicellular paraphyses were always present (Fig. 17E).

REMARKS: *Scytosiphon promiscuus* is distinguished from other *Scytosiphon* species when it has a complanate habit. This species belongs to clade B in Cho et al. (2007) and clade P2 in Kogame et al. (2015b) and corresponds to group III in Kogame et al. (2015a), and species IIIa in Hoshino et al. (2020c) and **Chapter 1**.

Species IVa: *Scytosiphon tosaensis* M.Hoshino & Kogame **in Hoshino et al. (2020c)**

(Fig. 18A–F; Table 5)

DESCRIPTION: Erect thalli are yellowish-brown when young, becoming darker when fertile, simple, cylindrical to somewhat flattened, hollow, often lack constrictions, to 50 cm long and 0.4 cm wide, gregarious, arising from small holdfasts; the cortex is composed of two layers of small pigmented cells; the medulla is composed of two layers of large, round or polygonal colorless cells; plurilocular sporangia are produced by cortical cells on the entire surface of the thallus, uni- or biseriate, consisted of up to 5 chambers, loosely coherent without a covering cuticular layer; paraphyses and phaeophycean hairs present. Mitochondrial–encoded *cox*1 sequence = GenBank accession LC517770; chloroplast–encoded *rbc*L sequences LC517921.

TYPE LOCALITY: Inoshiri, Usa, Tosa, Kochi Prefecture, Japan (33°26'06.7" N, 133°26'29.8" E).

HOLOTYPE: SAP 115506 (Fig. 18A), attached on a rock in intertidal zone, collected by M. Hoshino on 29 March 2018

ISOTYPE: SAP115509–115513, TNS-AL213453, and TNS-AL213454; deposited in

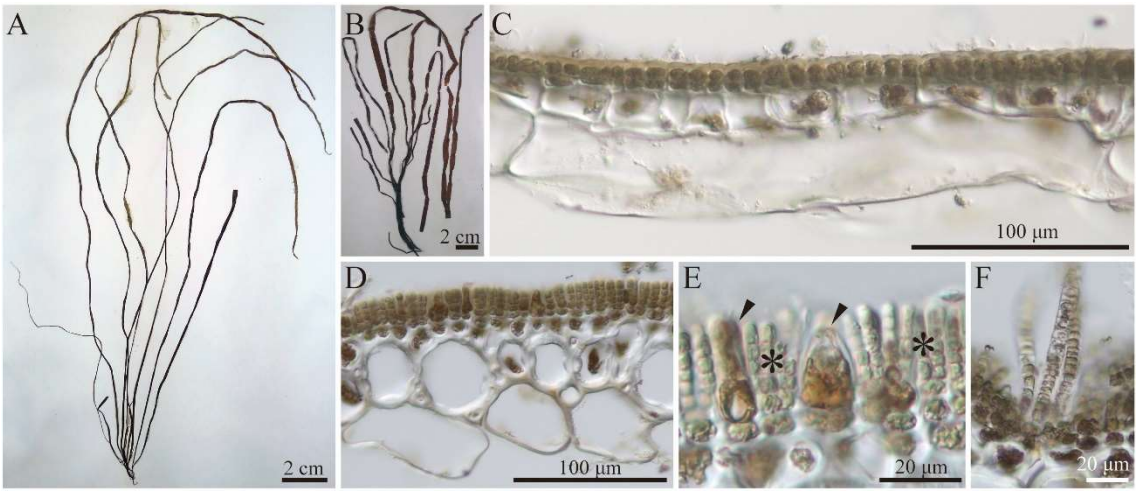

Figure 18. Morphology of gametophytes of species IVa, *Scytosiphon tosaensis* sp. nov. (A) Holotype specimen, SAP115506. Constructions are not clear. (B) Isotype specimen, SAP115513. Constructions are clear. (C) Longitudinal section of SAP115506. (D) Cross-section of SAP115506, displaying the medulla consisting of two cell layers. (E) Plurilocular sporangia (asterisk) and a paraphysis (arrowhead) of SAP115506. (F) Phaeophycean hair of SAP115506.

SAP and TNS.

DISTRIBUTION: This species has been found in two localities in Japan (Fig. 9).

HABITAT AND PHENOLOGY: Erect thalli grow on rocks, boulders, and concrete blocks in the intertidal zone; found in spring.

ETYMOLOGY: This species is named after its type locality, Tosa city.

JAPANESE NAME: Nankai-kayamonori (Hoshino et al., 2020c).

ADDITIONAL SPECIMENS EXAMINED: SAP115514-21, -30, -31, Inoshiri, Usa, Kochi Prefecture, Japan, 19 March 2017.

MORPHOLOGY OF GAMETOPHYTES: Gametophytes from the type locality were observed; the external morphology of nine specimens and internal anatomy of seven specimens were examined. At the type locality, thalli growing in protected areas lacked constrictions (Fig. 18A); while, thalli in exposed areas had clear constrictions (Fig. 18B). In longitudinal section, medullary cells were longer in inner portions, to 300 μm in length (Fig. 18C). In cross section, the cortex was composed of 2–3 layers of small pigmented cells (5–8 μm × 3–8 μm) and the medulla was composed of roughly two layers of colorless large cells (Fig. 18D). Phaeophycean hairs and unicellular paraphyses were always present (Fig. 18E and F).

REMARKS: This species corresponds to group IV in Kogame et al. (2015a) and species IVa in Hoshino et al. (2020c) and Hoshino et al. (2020c) and **Chapter 1**.

Species Va: *Scytosiphon arcanus* M.Hoshino & Kogame **in Hoshino et al. (2020c)**

(Fig. 19A–E; Table 5)

DESCRIPTION: Erect thalli are yellowish-brown when young, becoming darker when fertile, simple, cylindrical to somewhat flattened, hollow, usually constricted, to 45 cm long and 0.6 cm wide, gregarious, arising from a small holdfast; the cortex is composed of roughly two layers of small pigmented cells; the medulla is composed of 3–4 layers of large, round or polygonal colorless cells; plurilocular sporangia are produced by cortical

cells on the entire surface of the thallus, uni- or biseriate, consisted of up to 7 chambers, loosely coherent without a covering cuticular layer; paraphyses and phaeophycean hairs present. Mitochondrial–encoded *cox*1 sequence = GenBank accession LC517783; chloroplast–encoded *rbc*L sequences LC517922.

TYPE LOCALITY: Momonai, Otaru, Hokkaido, Japan, (43°12'37.4" N, 140°53'42.7" E).

HOLOTYPE: SAP 115499 (Fig. 19A), attached on a boulder in intertidal zone, collected by M. Hoshino on 30 April 2019.

ISOTYPE: TNS-AL 213455; deposited in TNS.

DISTRIBUTION: Japan. This species is distributed in coastal habitats along the northern portion of the Tsushima warm current (Fig. 9).

HABITAT AND PHENOLOGY: Erect thalli grow on rocks, boulders, and concrete blocks in the intertidal zone; and found in spring.

ETYMOLOGY: This name comes from a Latin word *arcanus* meaning hidden (secret), for the rarity of this species.

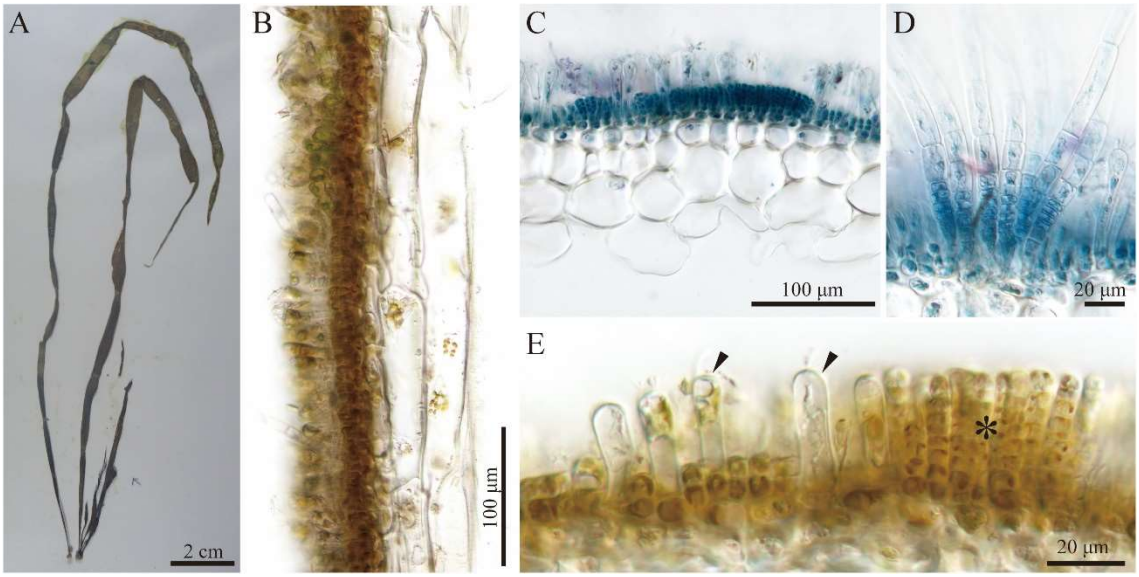

Figure 19. Morphology of a gametophyte of species Va, *Scytosiphon arcanus* sp. nov.
(A) Holotype specimen, SAP115499. (B) Longitudinal section of TNS-AL213455. (C) Cross-section of SAP115502 displaying medulla consisting of 3–4 cell layers. (D) Phaeophycean hairs of SAP115502. (E) Plurilocular sporangia (asterisk) and paraphyses (arrowhead) of SAP115499.

JAPANESE NAME: Kakure-kayamonori (Hoshino et al., 2020c).

ADDITIONAL SPECIMENS EXAMINED: SAP 115501, Unosaki. Akita Prefecture, Japan, 6 April 2017; SAP 115502, Teradomari, Niigata Prefecture, Japan, 17 April 2018; SAP 115503, Mihama, Fukui Prefecture, Japan, 18 March 2018; SAP 115404-2–5, Cape Kamui, Kitami-Esashi, Hokkaido, Japan, 30 April 2014; SAP 115405-5, -12, Oshoro, Hokkaido, Japan, 21 March 2018.

MORPHOLOGY OF GAMETOPHYTES: The external morphology of six specimens from five populations and the internal anatomy of five specimens from four populations were examined. Fertile thalli usually had constriction at regular intervals. In longitudinal section, medullary cells were longer in inner portions, to 350 μm in length (Fig. 19B). In cross section, the cortex was composed of 2–3 layers of small pigmented cells (5– 9.5 μm × 4.5–7 μm). The medulla was composed of 3–4 layers of colorless cells (Fig. 19C). Phaeophycean hairs and unicellular paraphyses were always present (Fig. 19E and D).

REMARKS: This species was extremely rare compared with other *Scytosiphon* species in Japan. It corresponds to group V in Kogame et al. (2015a) and species Va in Hoshino et al. (2020c) and **Chapter 1**.

Species VI: *Scytosiphon subtropicus* M.Hoshino, Ats.Tanaka & Kogame **in Hoshino et al. (2020c)**

(Fig. 20A–F; Table 5)

DESCRIPTION: Erect thalli are yellowish-brown when young, becoming darker when fertile, cylindrical, hollow, constricted, to 40 cm long and 3.5 mm wide, gregarious, arising from small holdfasts; the cortex is composed of two layers of small pigmented cells; the medulla is composed of 2–3 layers of large, round or polygonal colorless cells; plurilocular sporangia are produced by cortical cells on the entire surface of the thallus, uni- or biseriate and consisting of up to 10 chambers, loosely coherent without a covering cuticular layer; paraphyses and phaeophycean hairs present. Mitochondrial–encoded *cox*1

sequence = GenBank accession LC517789; chloroplast–encoded *rbc*L sequences LC517924.

TYPE LOCALITY: Yagaji, Okinawa Prefecture, Japan, (26°38'48.5" N, 128°02'03.5" E).

HOLOTYPE: SAP115491 (Fig. 20A), attached on a rock in intertidal zone, collected by A. Tanaka on 23 January 2018.

ISOTYPE: SAP115492, SAP115495–115497, TNS-AL213456, and TNS-AL213457; deposited in SAP and TNS.

DISTRIBUTION: Okinawa Is., Japan (Fig. 9).

HABITAT AND PHENOLOGY: Erect thalli grow on rocks, boulders, and concrete blocks in the intertidal zone; found in late winter to spring.

ETYMOLOGY: This name comes from the subtropical habitats of this species.

JAPANESE NAME: Ryukyu-kayamonori (Hoshino et al., 2020c).

ADDITIONAL SPECIMENS EXAMINED: SAP115490, Hamahiga, Okinawa

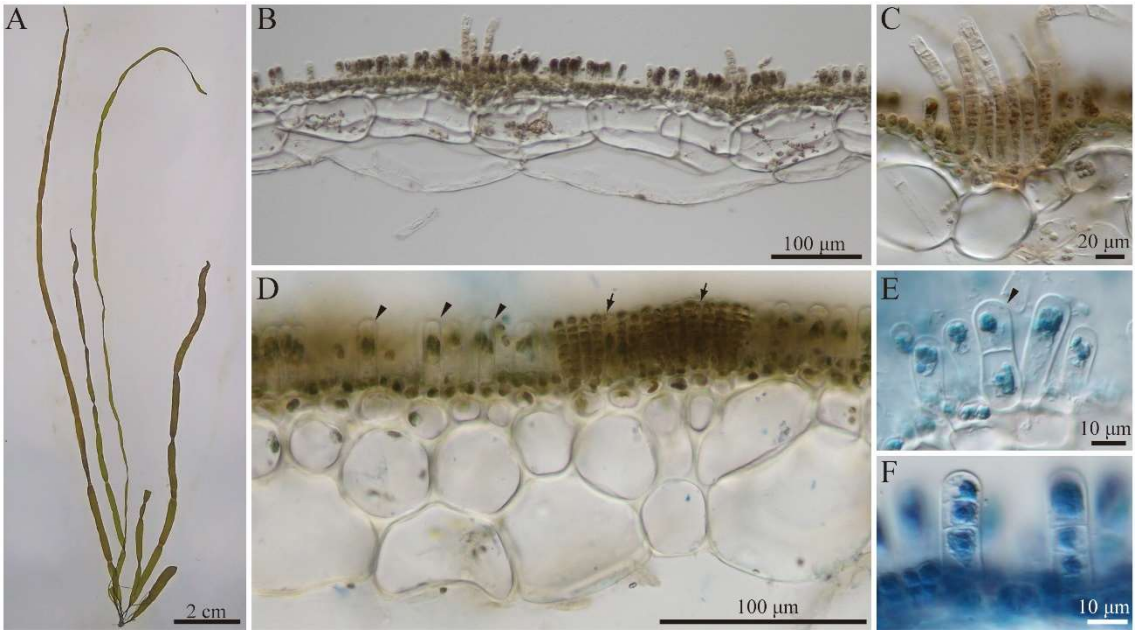

Figure 20. Morphology of gametophytes of species VI, *Scytosiphon subtropicus* sp. nov.
(A) Holotype specimen, SAP115491. (B) Longitudinal section of SAP115491. (C) Phaeophycean hairs of SAP115491. (D) Cross-section of SAP115491, displaying the medulla consisting of 2–3 cell layers, paraphyses (arrowhead), and plurilocular sporangia (arrow). (E)Two-celled paraphysis (arrowhead) of SAP 115491. (F) Three-celled paraphysis of SAP115491.

Prefecture, Japan, 19 February 2018; SAP115498-1, -2, Yagaji, Okinawa Prefecture, Japan, 9 April 2017.

MORPHOLOGY OF GAMETOPHYTES: Gametophytes from two localities (Yagaji, Hamahiga) were observed; external and internal morphology of 8 specimens were examined. In cross section, the cortex was composed of two layers of small pigmented cells (6–10 μm × 3.5–6.5 μm). In longitudinal section, medullary cells were longer in inner portions, to 300 μm in length (Fig. 20B). The medulla was composed of 2–3 layers of colorless large cells (Fig. 20D). Phaeophyceaen hairs and paraphyses were always present (Fig. 20C–F). The paraphyses were usually unicellular, but rarely 2–3 celled (Fig. 20D–F).

REMARKS: *Scytosiphon subtropicus* can be distinguished from other *Scytosiphon* species by having multicellular paraphyses. However, since the multicellular paraphyses are extremely rare, this character may not be useful to identify this species.

Table 5. Comparison of erect thalli of recognized *Scytosiphon* species.

	Species Ia *S. lomentaria*	Species IIa *S. shibazakiorum*	Species IIIa *S. promiscuus*	Species IVa *S. tosaensis*	Species Va *S. occultus*	Species VI *S. subtropicus*	*S. lomentaria* [a, b]	*S. dotyi* [c, d]	*S. crispus* [d, e]	*S.* Atlantic complex[f]
Shape	Cylindrical	Cylindrical	Cylindrical/ Flattene	Cylindrical	Cylindrical	Cylindrical	Cylindrical	Cylindrical to flattened[c]	Slightly flattened[e]	Cylindrical
Constrictions	+	+/-	+/-	+/-	+	+	+[a, b]	-[c]	-[e]	+
Length (cm)	–65	–70	–55	–50	–35	–40	–8[a]	–12	–1[e]	–9
Width (mm)	–7–(10)	–7	–6–(8)	–4	–4	–3.5	?	–1	–0.3[e]	–5
Medulla cell layers (n)	3–7	2–7	2–4	2	2–4	2–3	4–5[b]	2–3	2–3[d]	2
Paraphyses	+/-	+	+	+	+	+ (rarely multicellular)	-[b]	-[c]	-[d]	+
Cuticular layer	-	-	-	-	-	-	-[b]	+[d]	+[d]	?

Data from: [a] Lyngbye (1819); [b] observation of the *S. lomentaria* type material by McDevit and Saunders (2017); [c] Wynne (1969); [d] Kogame (1998); [e] Skottsberg (1907); [f] McDevit and Saunders (2017).

DISCUSSION

Species delimitation and taxonomy of the *S. lomentaria* complex from Japan

Multigene-based species delimitation and crossing experiments have shown that *Scytosiphon 'lomentaria'* from Japan is a species complex of five species [species Ia–Va; Kogame et al., 2015a; Hoshino et al., 2018 (**Chapter 1**)]. Herein, I report the sixth species (*S. subtropicus*) from the subtropical area, Okinawa Is. In my crossing experiments, *S. subtropicus* easily formed hybrid zygotes with species *S. shibazakiorum*, *S. promiscuus*, *S. tosaensis*, and *S. arcanus*. Thus, based on gametic incompatibility alone, the recognition of *S. subtropicus* as a new species was not clear. Particularly, gametic incompatibility was not observed between *S. subtropicus* and *S. promiscuus*, and their hybrid zygotes developed into sporophytes and produced zoospores showing the survival rate of ca. 22.6% after the two weeks cultivation. Although I could not examine the survival rate of zoospores from the control sporophytes (intra-species crossing in *S. subtropicus*), in my previous study, zoospores from intraspecific crosses in *S. shibazakiorum* and *S. promiscuus* showed the survival rate of ca. 90% in different culture condition [Hoshino et al., 2018 (**Chapter 1**)]. Considering this, survival rate of the hybrid zoospores from *S. subtropicus* female × *S. promiscuus* male might be low. In any case, pre- and post-zygotic barriers between *S. subtropicus* and other species were not always complete in the culture experiments. However, my phylogenetic analyses and the unique distribution highly support its distinctness. Therefore, I conclude that the Japanese *S. 'lomentaria'* is a species complex of six species.

Four species are currently recognized in *Scytosiphon*: *S. lomentaria*, *S. promiscuus*, *S. dotyi*, and *S. crispus*. The latter two species are morphologically distinguishable from the Japanese six species. The gametophytic thalli of these two species are much shorter and narrower, and their plurilocular sporangia are firmly coherent with a cuticular layer (Skottsberg, 1907; Wynne, 1969; Kogame, 1998) whereas those of Japanese species are loosely coherent without a cuticular layer (Table 5). My

*cox*1 and *rbc*L phylogenetic analyses also supported *S. dotyi* as distinct from all of the species now known from Japan. In addition, phylogenetic analyses showed that species IIIa clade includes the holotype of *S. promiscuus*, and the clade for species Ia includes Canadian specimens of *S. lomentaria* (genetic group I in McDevit and Saunders, 2017; Fig. 10). McDevit and Saunders (2017) attributed the genetic group I to *S. lomentaria* since it had constrictions, phaeophycean hairs, and no paraphyses, like the type material of *S. lomentaria*. My morphological observations in specimens in species Ia had some differences from those of McDevit and Saunders (2017). In the present study, paraphyses were clearly present in most of specimens, and I considered that the presence or absence of paraphyses is a morphologically variable character in species Ia. However, despite these differences, my observations suggest that only those specimens from species Ia may have the same characters as the *S. lomentaria* type material (Table 5), supporting McDevit and Saunders (2017).

Since *S. lomentaria* turned out to be a species complex, all previous heterotypic synonyms must be reviewed. Seven species rank-heterotypic synonyms are listed in AlgaeBase (Guiry and Guiry, 2020) and their type localities are in Europe: *Ulva simplicissima* Clemente was originally described from Andalsia, Spain (Cremades and Pérez-Cirera, 1990), *Asperococcus castaneus* W.J.Hooker from England (Hooker, 1833), *Chlorosiphon shuttleworthianus* Kützing from Ireland (Papenfuss, 1958), *Chorda fistulosa* Zanardini from Dalmatia (Zanardini, 1843), *Chorda autumnalis* Areschoug from Scandinavia (Guiry and Guiry, 2020), *Chorda attenuata* Foslie from Norway (Wynne, 1969), and *S. pygmaeus* Reinke from Germany (Reinke, 1888). Molecular phylogenetic studies have shown that *Scytosiphon* Atlantic complex has a wide distribution in Europe (Greece, Italy, Spain, UK, Ireland, Norway), *S. lomentaria* is in Ireland and Norway, and *S. shibazakiorum* is in Iceland (Cho et al., 2007; Kogame et al., 2015b; McDevit and Saunders, 2017; this study). Considering the distributional patterns mentioned above, the type material of the heterotypic synonyms should be included in the *Scytosiphon* Atlantic

complex or *S. lomentaria*, but not in my four new species.

The six *Scytosiphon* species I observed had some morphological differences (Table 5). *Scytosiphon lomentaria* and *S. shibazakiorum* can have a thicker medulla (more than three cell layers) compared with the other four species. Complanate habit and multicellular paraphyses were observed only in *S. promiscuus* and *S. subtropicus*, respectively. However, morphology-based species discrimination was often unreliable. Previously reported interspecific differences (e.g., thallus size, presence or absence of constrictions, cylindrical or complanate thallus form, presence or absence of paraphyses, and thickness of medullary layers of erect thalli; Clayton 1976, 1978; Kogame 1998; McDevit and Saunders 2017) often fell within the range of intraspecific variation. In *S. shibazakiorum*, Canadian specimens lack constrictions and have three-cell-layered medulla (group B–E; McDevit and Saunders, 2017). However, in Japan, specimens from exposed areas tend to have clear constrictions and thick medullary layers (up to 7 cell layers), while specimens from protected areas tend to have unclear constrictions and thin medullary layers (2–3 cell layers). The former is indistinguishable from *S. lomentaria* and the latter was often also indistinguishable from *S. promiscuus* and *S. arcanus*. In *S. lomentaria*, the presence or absence of paraphyses might demonstrate intraspecific variation, but it was reported that Canadian specimens lack paraphyses (McDevit and Saunders, 2017). The abundance of paraphyses was variable among Japanese specimens I observed (not detectable to abundant). In *S. promiscuus*, the complanate-type and cylindrical-type were observed. In *Scytosiphon*, the complanate habit has been used as a taxonomic characteristic (Rosenvinge, 1893; Doty, 1947) or has been regarded as just one of the stages of life history (Clayton, 1976). In *S. promiscuus*, the two morphotypes did not show a clear phylogenetic relationship (Fig. 10 and the complanate form seems to be a morphological polymorphism. In conclusion, DNA barcoding analysis is indispensable for accurate species identification of Japanese *Scytosiphon*.

Relatively large intraspecific variations were observed in the *cox*1 analyses of *S.*

shibazakiorum (up to 3.5 % in *p*-distance) and *S. promiscuus* (up to 2.3%). DNA barcoding studies using *cox*1 (5'-COI) on brown algae have inferred that species-level cut-off is a K2P divergence of 1.2% for the Laminariales and the Desmarestiales (Yang et al., 2014) and of 1.8% for the Ectocarpales (where *Scytosiphon* belongs; Peters et al., 2015). Considering this, these two species possibly include multiple species. Moreover, the bPTP support value for *S. shibazakiorum* was much lower than other species. Since these two species were supported by previous multigene species delimitation analyses and no reproductive barriers have been detected in each species so far [Kogame et al., 2015a; Hoshino et al., 2018 (**Chapter 1**), this Chapter], further species delimitation on them was suspended in this study.

Geographic distribution of *Scytosiphon* species

Although the *S. lomentaria* complex has been reported from all over the world except in the tropics (Guiry and Guiry, 2020), the geographic range of each species in the growing complex of segregated species is unclear. The species composition of *Scytosiphon* differs in the Pacific and Atlantic Oceans: Pacific species also appear in the North Atlantic, but the Atlantic species do not appear in the Pacific (Cho et al., 2007; Kogame et al., 2015b; McDevit and Saunders, 2017). *Scytosiphon lomentaria*, *S. shibazakiorum*, *S. promiscuus*, *S. tosaensis*, *S. arcanus*, *S. subtropicus*, and *S. dotyi* are found in the Pacific (Wynne, 1969; this study). In the Atlantic, in addition to some endemic undescribed species (at least two species in the *Scytosiphon* Atlantic complex; McDevit and Saunders 2017), *S. crispus*, *S. lomentaria*, *S. shibazakiorum*, and *S. promiscuus* are known (Skottsberg, 1907; Kogame et al., 2015b; McDevit and Saunders 2017, this study).

I have shown that *S. tosaensis*, *S. arcanus*, and *S. subtropicus* are presently endemic to Japan, whereas *S. lomentaria*, *S. shibazakiorum*, and *S. promiscuus* are widely distributed in the mid-high latitudinal area of northern hemisphere. Worldwide distributions of the latter three species have also been reported by previous studies based on ITS region of ribosomal RNA: *S. lomentaria* in North Pacific, Australia, New Zealand

and Chile, *S. shibazakiorum* in Japan, Korea, USA and Russia, and *S. promiscuus* in Japan, Korea, Australia, New Zealand (Kogame et al., 2015a and references therein). Cho et al. (2007) pointed out that these worldwide distributions might be partly due to recent artificial introductions, since identical ITS haplotypes were found in localities far from each other. The same situation was also observed in my *cox*1 analyses, for example, *S. lomentaria* in Japan and Tasmania (Fig. 12A). These data may suggest that Tasmanian population was introduced. However, distributions of the three worldwide species in the northern hemisphere (at least in Japan and North America) are probably not due to artificial introduction alone. The *cox*1 haplotype networks showed that these species had haplotypes/haplogroups that are specific to Japan and North America (and Far East Russia in *S. shibazakiorum* and *S. promiscuus*). Furthermore, these three species showed a certain degree of genetic diversity in JPN, NAP, and NAA (Table 4). These facts are difficult to explain away only as artificial introductions. The common haplotypes among JPN, NAP and NAA, and the low Φ_{st} values (i.e. genetic homogeneity) between NAP and NAA in the three species may suggest gene flow through high latitudinal areas, such as the Aleutian Islands and the Arctic Ocean. *Scytosiphon dotyi* was reported to be distributed between Oregon to Baja California (North America) and possibly distributed in the Kurile Islands and Sakhaline Northwest Pacific) according to its original description (Wynne, 1969). However, *S. dotyi* was not detected among the specimens collected from the Northwest Pacific including Sakhaline and Kamchatka. Thus, the northerly distribution of this species is unproven, and it is only verified from its type locality, California. *Scytosiphon crispus* has been reported from the South Atlantic, Falkland Islands (type locality) and Argentina (Skottsberg, 1907; Papenfuss, 1964; Boraso de Zaixso, 2013). Undescribed species in the Atlantic (Atlantic species complex) have been reported from Europe, Bermuda and the Atlantic coast of Canada (Cho et al., 2007; Kogame et al., 2015b; McDevit and Saunders, 2017).

Reinforcement in *Scytosiphon*?

Undeveloped pre-zygotic isolation (here, gametic incompatibility) between *S. subtropicus* and *S. shibazakiorum*, *S. promiscuus*, *S. tosaensis*, and *S. arcanus* might be due to the geographic isolating barrier between them. *Scytosiphon subtropicus* has a relatively large genetic distance from others. It was estimated as a sister group of *S. lomentaria*, *S. shibazakiorum*, *S. promiscuus*, *S. tosaensis*, and *S. arcanus* in the *rbc*L tree. However, gametic incompatibility between *S. subtropicus* and others seemed to be undeveloped compared to that among the other five species. This circumstance can be explained by the theory of reinforcement–natural selection enhancing pre-zygotic isolation as a response to maladaptive hybridization (i.e., unfit hybrid) between sympatric diverging species (Coyne and Orr, 2004). That is, pre-zygotic isolation may have developed more rapidly among *S. lomentaria*, *S. shibazakiorum*, *S. promiscuus*, *S. tosaensis*, and *S. arcanus* those showed overlapped geographic distributions [Fig. 1; Hoshino et al., 2018 (**Chapter 1**)] than between *S. subtropicus* and others where hybridization never occurs due to no overlapping distributions. This pattern of greater pre-zygotic isolation in sympatry relative to allopatry has been reported in various organisms including brown algae (Hoarau et al., 2015) and often considered evidence of reinforcement (Coyne and Orr, 2004). Although I have no clear evidence of reinforcement among the sympatric five species, low survival rate of hybrid zoospores between species *S. shibazakiorum* and *S. promiscuus* [Hoshino et al., 2018 (**Chapter 1**)] and between species *S. promiscuus* and *S. subtropicus* indicates the high possibility of selection against hybridization (i.e., possibility of reinforcement of pre-zygotic isolation).

Chapter 3

Species delimitation of *Planosiphon gracilis* morphospecies (Scytosiphonaceae, Phaeophyceae) from Japan and the description of *Pl. nakamurae* sp. nov.

INTRODUCTION

The brown algal family Scytosiphonaceae (Ectocarpales) has a worldwide distribution including tropical and cold waters (Kogame et al., 1999). Members of this group are characterized by having a single plastid with one large pyrenoid. In addition, they have a heteromorphic life cycle with an erect gametophyte alternating with a small prostrate sporophyte (e.g., Wynne, 1969; Nakamura and Tatewaki, 1975; Kogame, 1997) except for *Melanosiphon* Wynne and *Myelophycus* Kjellman which has an isomorphic life cycle (Wynne, 1969; Tanaka and Chihara, 1984; Kawai et al., 1994). Generic segregation within the Scytosiphonaceae has traditionally been based on the external morphology and structure of erect thalli. However, subsequent molecular phylogenetic studies showed extensive polyphyly among the genera of this group (Kogame et al., 1999; Cho et al., 2006). To deal with this taxonomic problem, several new genera and combinations have been proposed based on molecular phylogenetic analyses (McDevit and Saunders, 2017; Santiañez et al., 2018a, b).

McDevit and Saunders (2017) conducted molecular phylogenetic analyses on Canadian Scytosiphonaceae and proposed the new genus *Planosiphon* McDevit & G.W.Saunders. It was made to accommodate a highly supported clade consisting of species from the genus *Scytosiphon* C.Agardh and *Petalonia* Derbès & Solier with flattened thalli that are hollow to partially hollow [*S. complanatus* (Rosenvinge) Doty, *S. gracilis* Kogame and *Pet. zosterifolia* (Reinke) Kuntze]. Typically, erect thalli of *Planosiphon* species are linear, compressed to flattened and non-constricted, and lack paraphyses (ascocysts) amongst their plurilocular sporangia (McDevit and Saunders, 2017). Santiañez and Kogame (2017) pointed out that *Planosiphon* species have *Compsonema*-like sporophytic thalli which are distinct from *Ralfsia* or *Stragularia*-like sporophytes of *Scytosiphon* and *Petalonia*, and proposed the transfer of *Pet. filiformis* (Batters) Kuntze, which has *Compsonema*-like sporophytes, to the genus *Planosiphon*. One the other hand, *Pl. complanatus* (Rosenvinge) McDevit & G.W.Saunders [as *S.*

lomentaria (Lyngbye) Link var. *complanatus* Rosenvinge] was reported to have *Ralfsia*-like sporophytic thalli in culture conditions (Pedersen, 1980).

Four species are currently recognized in the genus *Planosiphon*: *Pl. complanatus*, *Pl. gracilis* (Kogame) McDevit & G.W.Saunders, *Pl. zosterifolius* (Reinke) McDevit & G.W.Saunders and *Pl. filiformis* (Batters) Santiañez & Kogame. These species have the following distributions: *Pl. complanatus* in Greenland and the northwest Atlantic (Rosenvinge, 1893; McDevit and Saunders, 2017); *Pl. gracilis* in Japan, South Korea, Mexico and Chile (Kogame, 1998; Cho et al., 2002; Aguilar-Rosas et al., 2006; Contreras et al., 2007); *Pl. zosterifolius* in the North Atlantic and the Northwestern Pacific (Vinogradova, 1973; Fletcher, 1987; Kogame and Kawai, 1993; Cho et al., 2002; McDevit and Saunders, 2017); and *Pl. filiformis* in Europe (Fletcher, 1987).

In Japan, two *Planosiphon* species, *Pl. gracilis* and *Pl. zosterifolius*, have been reported based on morphological observations (Kogame and Kawai, 1993; Kogame, 1998). In the present study, I reassessed the species diversity of *Planosiphon*, especially of the *Pl. gracilis* morphospecies from Japan, by morphological observation, molecular phylogenetic analyses, and crossing experiments. Based on this study, I described in Hoshino et al. (2020a) a new species of *Planosiphon*, which is mostly morphologically indistinguishable from *Pl. gracilis*, but is phylogenetically and biologically distinct.

MATERIALS AND METHODS

Specimen collection

In total, 56 *Pl. gracilis-like* specimens and two *Pl. zosterifolius*-like specimens were collected from various localities in Japan (Fig. 21, Table S3). In addition to these Japanese samples, nine *Pl. gracilis*-like specimens were collected from three localities in Argentina: San Antonio Oeste (SAO; 40°43'31.0"S, 64°56'39.0"W), Bahia Blanca Harbor (BBH; 38°47'21.0"S, 62°16'22"W) and Puerto Madryn (PM; 42°45'56.6"S 65°01'55.7"W ; Table S3). Specimens were preserved in 5% formalin-seawater or salt for

morphological observations and a fragment of each thallus was preserved in a silica-gel for molecular analyses. Pressed specimens were also made and deposited as vouchers in the Herbarium of Faculty of Science, Hokkaido University, Sapporo, Japan (SAP) or in the Herbarium of Universidad Nacional der Sur, Bahia Blanca, Argentina (BBB) or in Kobe University Research Center for Inland Seas. Unialgal culture isolates were established for some samples as previously described in Kogame et al. (2015a).

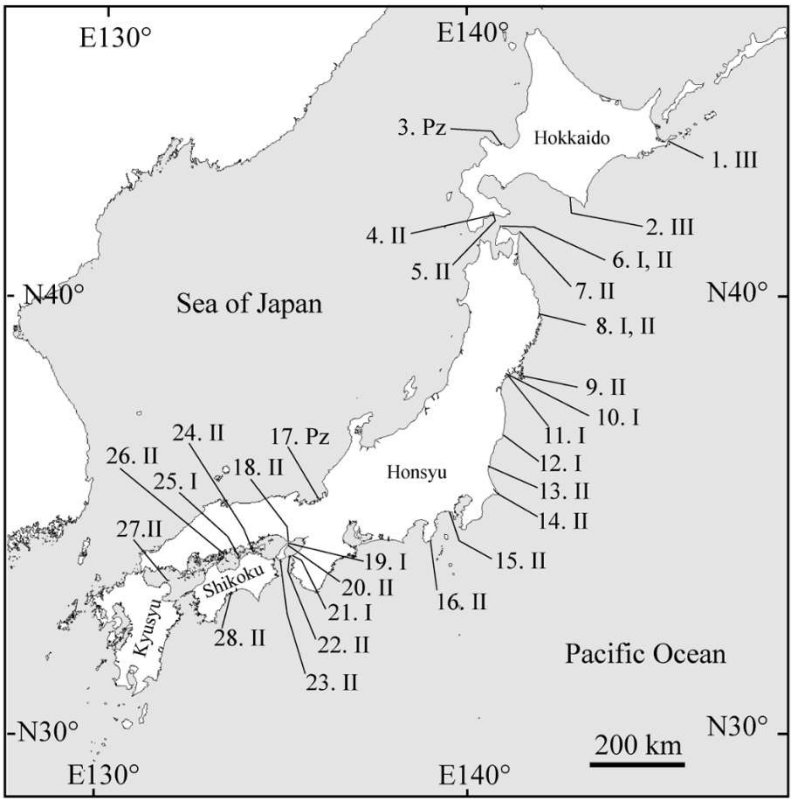

Figure 21. Map of Japan showing collection localities of samples used in this study. Arabic numerals (1–28) are locality codes: 1, Hanasaki; 2, Samani; 3, Oshoro; 4, Anama; 5, Tachimachi; 6, Ohma; 7, Shiriya; 8, Jodogahama; 9, Kitsunezaki; 10, Sabusawa; 11, Shichigahama; 12, Shioyazaki; 13, Oarai; 14, Inubosaki; 15, Enoshima; 16, Nabeta; 17, Mihama; 18, Tarumi; 19, Tanoshiro; 20, Ooiso; 21, Misakimachi; 22, Kada; 23, Karimo; 24, Megishima; 25, Awashima; 26, Innoshima; 27, Himeshima; 28, Inoshiri. Lineages (species) found in each locality are shown after the locality codes: I, lineage I (*Planosiphon gracilis*); II, lineage II (*Pl. nakamurae*); III, lineage III; Pz, *Pl. zosterifolius*.

Molecular analyses

Partial sequences of the mitochondrial *cox*1 and *cox*3 genes and complete sequences of the chloroplast *rbc*L gene were used for the phylogenetic analyses. Total genomic DNA

was extracted from cultured or silica gel-dried thalli as previously described (**Chapter 1**) and used as template DNA for polymerase chain reaction (PCR). The primers used were GazF2 and GazR2 (Lane et al., 2007) or cox1-P1.2, cox1-P5.2 and trnI-P1 (Kawai et al., 2013) for *cox*1, F49 and CAR4A (Kogame et al., 2005; Boo et al., 2010) or trnY-P2, trnY-P1 and cox3-P2 (Ni-Ni-Win et al., 2008; Kawai et al., 2012) for *cox*3, and PRB-F0, PRBF2, PRBF3, PRBR1A, PRBR2 and RSPR (Kogame et al., 1999) or rbcL-P2.2, rbcL-P2, rbcL-Rh3 and rbcS-P1 (Hanyuda et al., 2004; Kawai et al., 2007; Kawai et al., 2012) for *rbc*L. The polymerases I used were AmpliTaq Gold 360 Master Mix (Thermo Fisher Scientific) or TaKaRa Ex Taq (Takara Bio Inc., Otsu, Japan). The PCR program included a denaturation step at 94°C for 10 min (for AmpliTaq Gold) or 1 min (for TaKaRa Ex Taq), followed by 35 cycles of 94°C for 30 sec, 50°C (for *cox*1 and *cox*3) or 55°C (for *rbc*L) for 30 sec and 72°C for 30 sec, and a final elongation step at 72°C for 7 min. DNA sequencing was conducted according to the method described in Kogame *et al.* (2015a).

*Cox*1 and *cox*3 sequences were also obtained from 28 to 32-year-old pressed specimens (SAP059717, SAP059720, and SAP115482), including the holotype of *Pl. gracilis* (SAP059720). Total genomic DNA was extracted from a small fragment of the specimens using GenCheck® DNA Extraction Reagent (FASMAC, Atsugi, Japan) following the manufacturer's instruction. For PCR, primers targeting short segments (ca. 200 bp; Table S4) and KOD FX polymerase (TOYOBO, Osaka, Japan) were used. Amplifications were performed as follows: a denaturation step at 94°C for 2 min, followed by 25 cycles of 98°C for 10 sec, 50°C for 30 sec and 68°C for 1 min, and a final elongation step at 68°C for 7 min. Using 0.5 µl of the product obtained from this initial reaction, a second round of PCR was conducted under identical conditions to increase the concentration of target sequences. DNA sequencing was conducted as in Kogame et al. (2015a) with the primers used in the PCR and 487 bp of *cox*1 and ca. 480 bp of *cox*3 sequences were obtained.

Sequences obtained for each gene (Table S3), together with available sequence

data downloaded from GenBank, were aligned using Clustal W (Thompson et al., 1994) in MEGA v. 7 (Kumar et al., 2016) with default parameters. The *cox*1 and *cox*3 sequences of specimens, which were collected from Japanese tsunami marine debris drifted to the U.S.A and identified as *Scytosiphon* sp. in Hanyuda et al. (2018), were also included in the alignment.

Maximum likelihood (ML) and Bayesian inference were used to infer the phylogeny for each gene. The ML analyses were performed using RAxML v. 8.2.10 (Stamatakis, 2014) with 1000 bootstrap pseudoreplicates under GTRGAMMA. Bayesian posterior probabilities were calculated using Mr. Bayes version 3.2.6 (Huelsenbeck and Ronquist, 2001; Ronquist et al., 2012) using the GTR substitution model with invariable sites over a gamma distribution (lset nst = 6, rates = invgamma) and Monte Carlo Markov Chains (MCMC) ran with the following parameters: 50,000,000 generations, 2 runs, 4 chains, heating parameter of 0.20, sampling frequency of 1000, burn-in fraction of 0.25 and stop value of 0.01. Whether the analyses are at stationarity was confirmed by the plot generated by the sump command. Both ML and Bayesian phylogenetic analyses were performed through Cipres Science Gateway version 3.3 (Miller et al., 2010). For the *rbc*L analyses, *Ectocarpus sp.* (FN564467) was specified as an outgroup.

Morphological observations

Sections of gametophytic thalli were made by hand with a razor blade and were mounted in seawater or a mixture of 50% glycerol/seawater /and 0.5% cotton blue solution (lactic acid/phenol/glycerol/water 1:1:1:1). Observations were made using a light microscope and images were taken with a Nikon Digital Sight DS-Fi1 (Nikon Corporation, Tokyo).

Life cycles in culture and crossing experiments

Life cycles of *Planosiphon* species were investigated in culture. Culture strains used are shown in Table 6. For lineage III, seven field gametophytes collected at Samani (locality

code 2 in Fig. 21) in 2019 were also used. Culture experiments were conducted using plastic Petri dishes (90 × 20 mm) and PESI medium (Tatewaki, 1966) at 10, 15, and 20°C in LD (long day; 16h:8h, light:dark) and SD (short day; 8h:16h, light:dark) conditions with fluorescent lighting of 30–50 μmol m^{-2} s^{-1} photon flux density.

My molecular phylogenetic analyses indicated that the *Pl. gracilis* morphospecies consists of three distinct species (lineage I–III). Since sexual reproduction was observed in lineage I and II and their geographic distribution mostly overlapped (Fig. 21), I conducted crossing experiments to investigate the possible reproductive isolating barriers among them. Four strains of lineage I and three strains of lineage II were used for crossing experiments (Table 6). The crossing experiments were performed as previously described in Hoshino et al., (2018; **Chapter 1**).

Table 6. Culture strains used in this study.

DNA-based species identity	Strain code	Sex	Collection location and date
Lineage I: *Planosiphon gracilis*	Netanai-1	male	Ohma; 2 Feb. 1990
	Netanai-3	female	Ohma; 2 Feb. 1990
	Ohma-3	female	Ohma; 14 Feb. 1994
	Sabusawa-A	female	Sabusawa; 12 Apr. 1994
Lineage II: *Planosiphon nakamurae*	Shimoda-2	male	Shimoda; 20 Feb. 2018
	Anama	female	Anama; 30 Mar. 2002
	Enoshima180219-7	female	Enoshima; 19 Feb. 2018
Lineage III	Samani-1	?	Samani; 19 May 1991
	Samani-2	?	Samani; 19 May 1991
	Hanasaki	?	Hanasaki; 18 May 1991
Petalonia fasia	G259[a]	?	Greenland; 2 Aug. 1977

[a] Culture strain established as *Planosiphon complanatus* (*Scytosiphon lomentaria* var. *complanatus*) by Pedersen (1980).

RESULTS

Molecular phylogenetic analyses

A total of 110 sequences were newly generated (*cox*1: –658 bp, n = 69; *cox*3: –621 bp n = 36; *rbc*L: –1467 bp, n = 5; Table S3). My phylogenetic analyses based on *cox*1, *cox*3, and *rbc*L sequence data did not resolve the phylogenetic relationships among the *Planosiphon* species and support for the monophyly of the genus *Planosiphon* was not always high [bootstrap percentage (BP) = 65%, posterior probability (PP) = 0.99 in *cox*1 (Fig. 22); BP = 57%, PP = 0.96 in *rbc*L (Fig. 23); BP = 99%, PP = 0.99 in *cox*3 (Fig. 24)]. However, in Japanese *Pl. gracilis* morphospecies, three lineages (lineages I–III) were highly supported in all the analyses. The inter-lineage divergences (*p*-distances) among the three lineages were ranged 10.4–11.6% in *cox*1, 9.1–10.3% in *cox*3, and 1.4–1.5% in *rbc*L. In lineage II, intra-lineage divergences were relatively large compared to others: up to 1.7% in *cox*1 and 1.8% in *cox*3. Lineage I contained the holotype specimen of *Pl. gracilis* (Figs. 22, 24). Lineage III formed a clade with *Pl. complanatus* from Canada with high support, but sequence divergence between them was relatively large (ca. 4.1% in *cox*1 and 0.5% in *rbc*L; Figs. 22, 23). Lineages I and II were commonly found in Japan. Their geographic distributions widely overlapped and they were sympatric even in the type locality of *Pl. gracilis* (Ohma, locality code 6 in Fig. 21). Lineage III was found only in Hokkaido, Japan (Fig. 21).

The *cox*1 and *cox*3 sequences of specimens which were collected from Japanese tsunami marine debris drifted to the U.S.A. and identified as *Scytosiphon* sp. in Hanyuda et al. (2018) belonged to lineage II (OR USA; Figs 22, 24). All Argentinean specimens were lineage II (Fig. 22). The *cox*1 sequence of the *Pl. complanatus* strain, G259, established by Pedersen (1980) was almost identical to those of *Pet. fascia* (Fig. 22). In *Pl. zosterifolius*, 1.1% divergence was observed in *cox*1 between Canadian and Japanese specimens (Fig. 22).

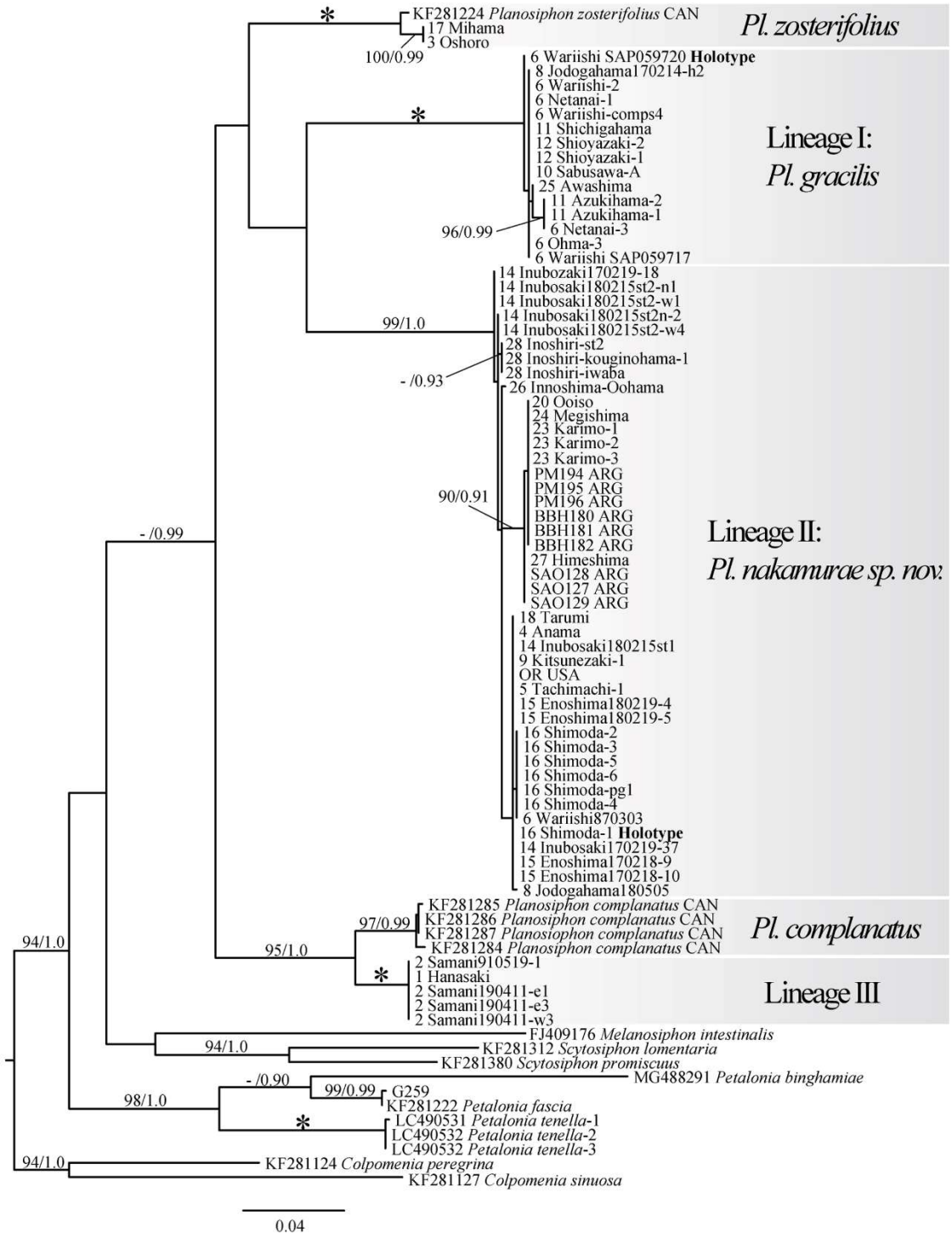

Figure 22. Maximum likelihood tree based on the mitochondrial *cox*1 gene (–658 bp). Numbers on branches indicate bootstrap values (%) from ML analysis (left) and posterior probabilities from Bayesian analysis (right). Only bootstrap values ≥ 90% and posterior probabilities ≥ 0.90 are shown. The asterisks indicate branches with full support (100/1.0). For Japanese samples, numbers indicating the locality code (Fig. 21) are given on the right of the sample code. CAN: Canada, ARG: Argentina.

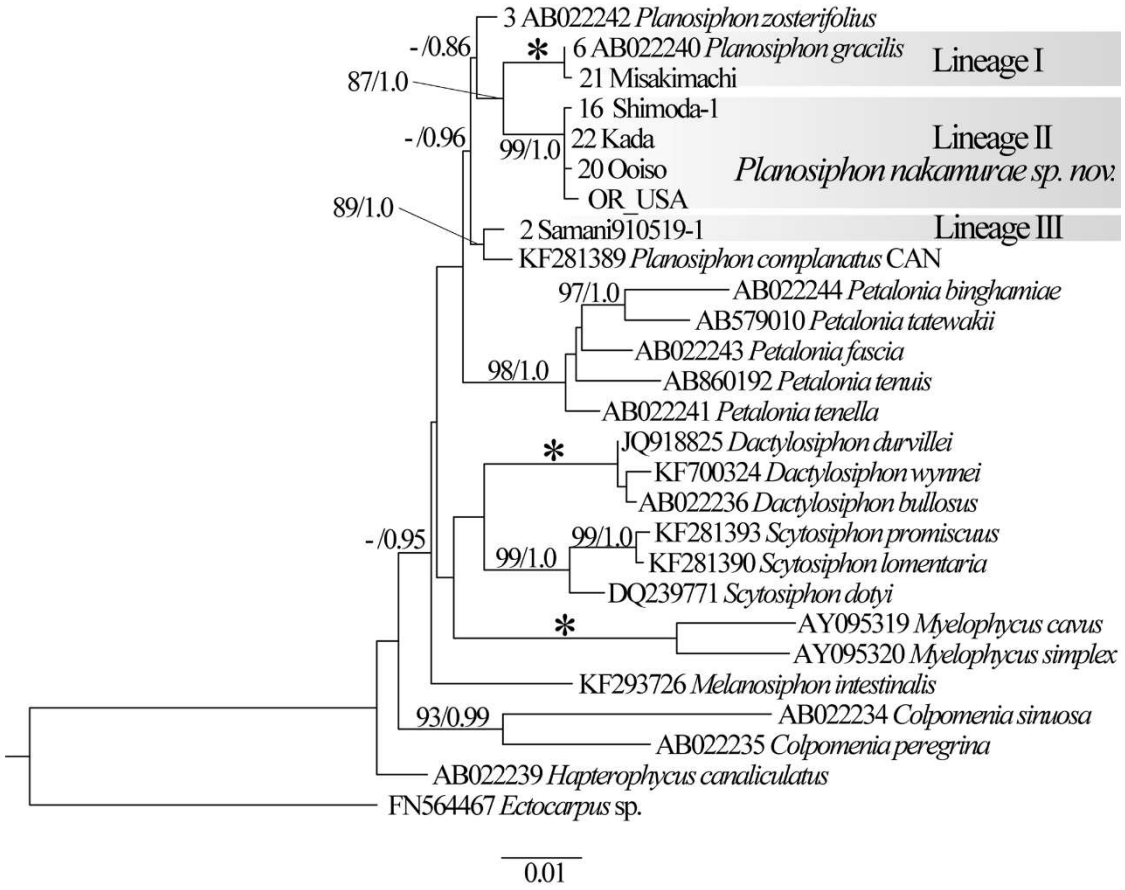

Figure 23. Maximum likelihood tree based on the chloroplast *rbc*L gene (–1467 bp). Numbers on branches indicate bootstrap values (%) from ML analysis (left) and posterior probabilities from Bayesian analysis (right). Only bootstrap values ≥ 80% and posterior probabilities ≥ 0.80 are shown. See the details in Fig. 22.

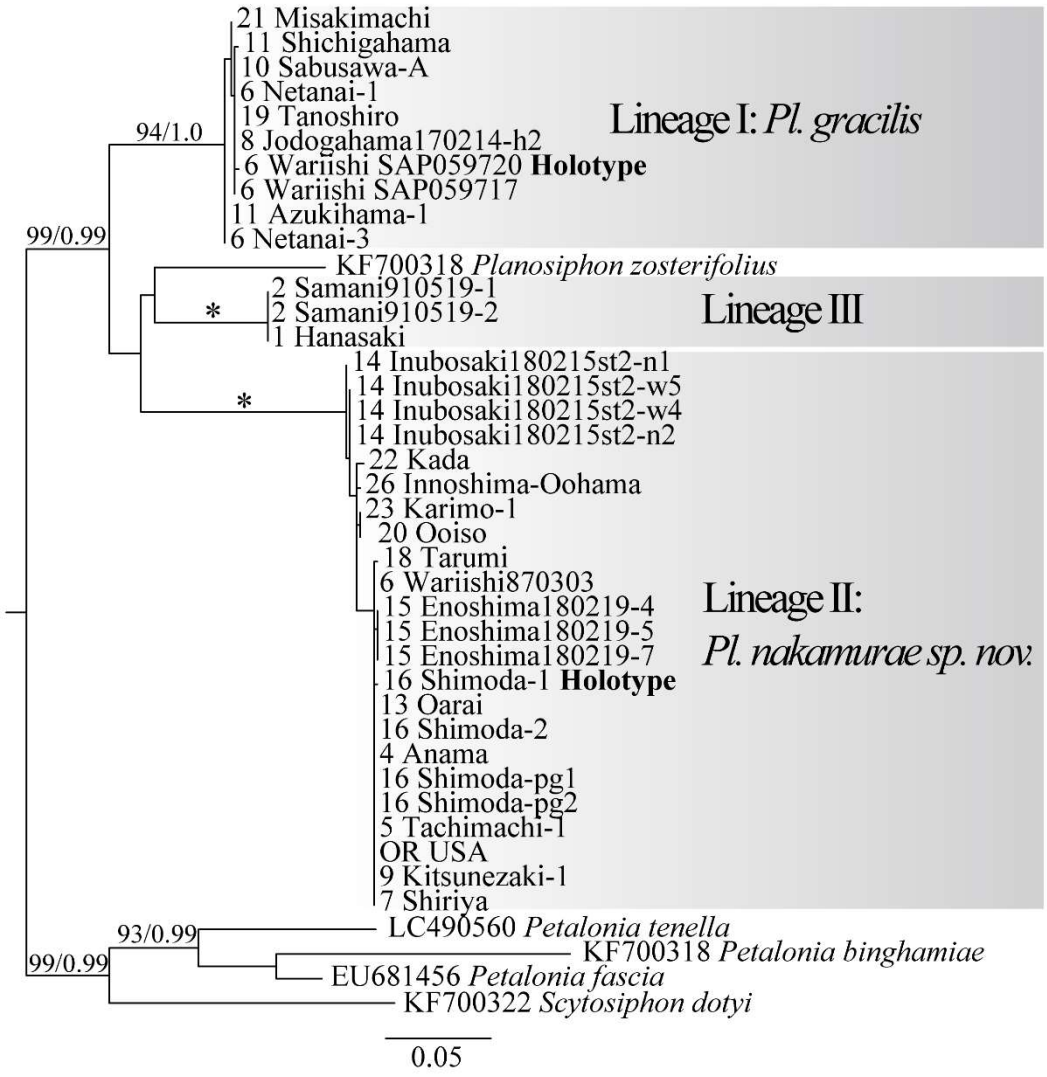

Figure 24. Maximum likelihood tree based on the mitochondrial *cox*3 gene (–621 bp). Numbers on branches indicate bootstrap values (%) from ML analysis (left) and posterior probabilities from Bayesian analysis (right). Only bootstrap values ≥ 80% and posterior probabilities ≥ 0.80 are shown. See the details in Fig. 22.

Taxonomic observation

Lineage I: *Planosiphon gracilis* (Kogame) McDevit & G.W.Saunders

BASIONYM: *Scytosiphon gracilis* Kogame 1998.

HOLOTYPE: SAP059720; *cox*1 sequence = Genbank accession LC504290; *cox*3 sequence = Genbank accession LC504291.

TYPE LOCALITY: Ohma (locality code 6 in Fig. 21), Aomori Prefecture, Japan.

DISTRIBUTION: Japan; South Korea; Mexico; Chile (Kogame, 1998; Cho et al., 2002; Aguilar-Rosas et al., 2006; Contreras et al., 2007)

SPECIMENS EXAMINED: SAP059716–SAP059721 (holotype and isotype), 1 February 1990, Ohma, Aomori Prefecture, Japan; SAP115440, 14 February 2017, Jodogahama, Iwate Prefecture, Japan; SAP115441 and SAP115442, 14 February 2018, Azukihama, Miyagi Prefecture, Japan; SAP115443, 25 March 2018, Shioyazaki, Fukushima Prefecture, Japan; SAP059699, 5 April 1989, Awashima, Kagawa Prefecture, Japan.

MORPHOLOGY OF GAMETOPHYTES: External morphology was examined in eight specimens from five populations and internal anatomy was examined in four specimens from two populations. Thalli are yellowish brown to dark brown, cylindrical to flattened, hollow, up to 35 cm in length and 3 mm in width, commonly gregarious, arising from a small holdfast. In cross section, the cortex composed of 2–3 layers of small pigmented cells. The medulla composed of 1–3 layers of colourless cells. Phaeophycean hairs were variable in number and usually grouped. Plurilocular zoidangia are produced basipetally on the entire surface of the thallus, covered with a cuticular layer even when mature. Since pigmented cells in the cortical layer usually become plurilocular zoidangia, portions of thalli from which plurizoids (gametes) have been released are colourless. Paraphyses are absent.

Lineage II: *Planosiphon nakamurae* M.Hoshino, M.E.Croce, Hanyuda & Kogame **in Hoshino et al. (2020a)**

Figs 25 and 26

DESCRIPTION: Erect thalli, yellowish brown to dark brown, flattened, sometimes cylindrical, hollow, up to 45 cm long and 0.5–8 mm wide, commonly gregarious, and arising from a small holdfast; the cortex is composed of two layers of small pigmented cells; the medulla is composed of 2–3(–4) layers of large, round or polygonal colourless cells; plurilocular zoidangia firmly coherent with a covering cuticular layer; paraphysis absent; *cox*1 sequence = Genbank accession LC490497; *cox*3 sequence = Genbank accession LC490550; *rbc*L sequence = Genbank accession LC490561.

HOLOTYPE: SAP115444 (Fig. 25A), collected by M. Hoshino at Nabeta, Shimoda, Shizuoka Prefecture, Japan, on 20 February 2018, deposited in SAP.

ISOTYPE: SAP115445–SAP115451 (Fig. 25B), collected by M. Hoshino at Nabeta, Shimoda, Shizuoka Prefecture, Japan, on 20 February 2018, deposited in SAP.

TYPE LOCALITY: Nabeta (34°39'58.6" N, 138°56'09.1" E; locality code 16 in Fig. 21), Shimoda, Shizuoka Prefecture, Japan; intertidal, attached on rocks.

ETYMOLOGY: This species is named after Prof. Yositeru Nakamura for his substantial contribution to phycology including the life-history studies of the family Scytosiphonaceae.

JAPANESE NAME: Nami-usukayamo (Hoshino et al., 2020b).

DISTRIBUTION: Japan; Argentina.

ADDITIONAL SPECIMENS EXAMINED (GAMETOPHYTE): SAP115482, 3 March 1987, Ohma, Aomori Prefecture, Japan; SAP115459, 6 April 2018, Cape Tachimachi, Hakodate, Hokkaido, Japan; SAP115460, 26 March 2018, Kitsunezaki, Miyagi Prefecture, Japan; SAP115454–SAP115457, 19 February 2017 and 15 February 2018, Inubosaki, Chiba Prefecture, Japan; SAP 115452 and SAP115453, 18 February 2017 and 19 February 2018, Enoshima, Kanagawa Prefecture, Japan; SAP115458, 5 May

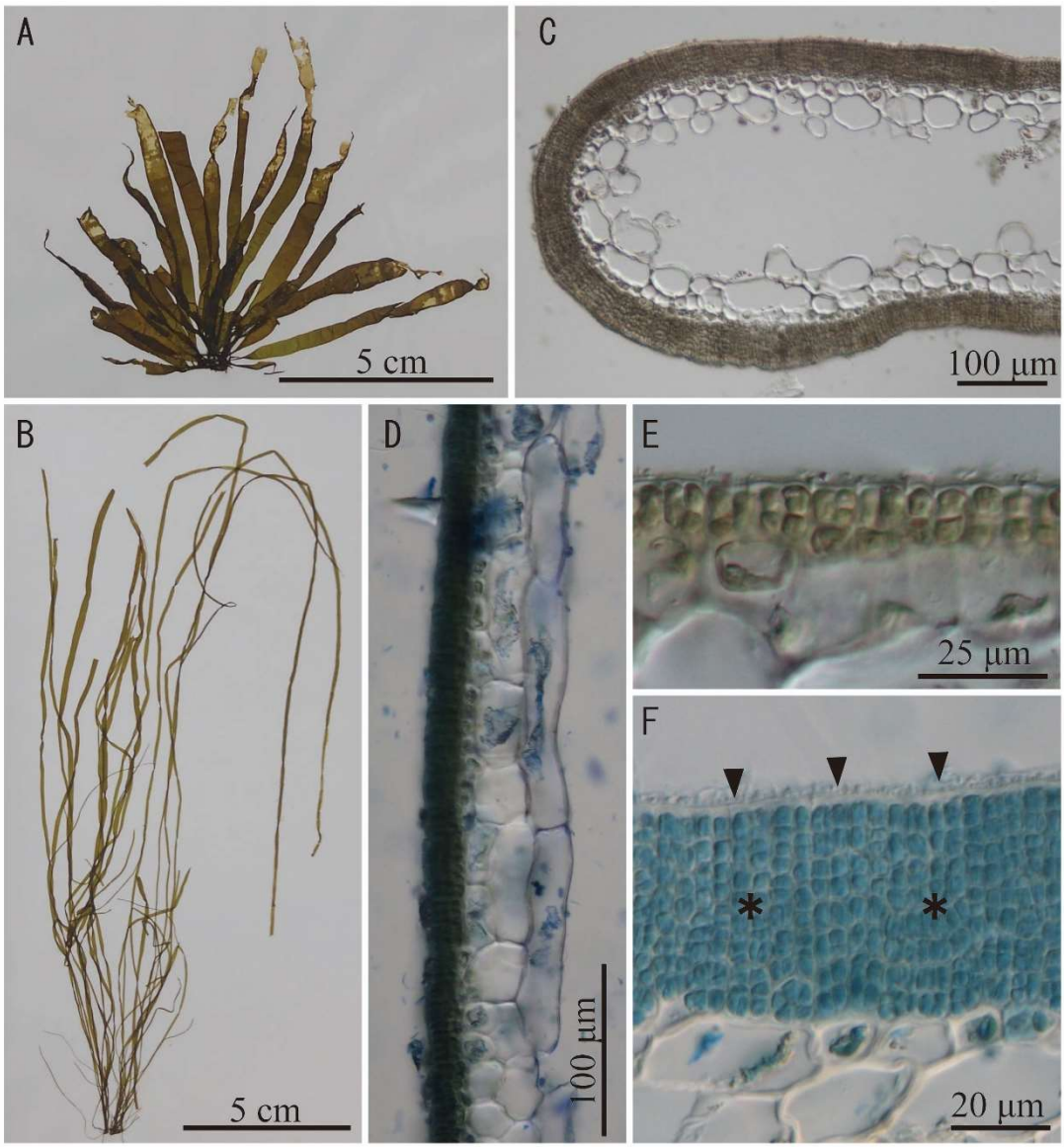

Figure 25. Morphology of erect thalli of lineage II, *Planosiphon nakamurae sp. nov.*
(A) Holotype specimen (SAP115444) showing wide thalli and colorless portions (arrowheads) which released plurizoids. (B) Isotype specimen (SAP115450) showing narrow thalli. (C) Cross section of the thallus. (D) Longitudinal section of the thallus. (E) Cortical layer of the immature portion in cross section of the thallus. (F) Mature plurilocular zoidangia (asterisks) covered with a cuticular layer (arrowheads) in cross section of the thallus.

2018, Jodogahama, Iwate Prefecture, Japan; SAP059701, Karimo, Hyogo Prefecture, Japan, 31 March 1990; SAP059704, Megishima, Kagawa Prefecture, Japan, 6 April 1989; SAP115461 and SAP115462, Inoshiri, Kochi Prefecture, Japan; MEC127–MEC129, 8 August 2018, San Antonio Oeste, Rio Negro, Argentina; MEC180– MEC182, 28 August 2018, Bahía Blanca, Buenos Aires, Argentina; MEC194–MEC196, 10 September 2018, Puerto Madryn, Argentina.

OBSERVATION OF GAMETOPHYTES: External morphology was examined in 44 specimens from 15 localities and internal anatomy was examined in 26 specimens from nine localities. Thalli are soft, and wide thalli are wrinkled (Fig. 25A). In cross-section, cortex cells are 3–7 × 3–6 μm and medullary cells are 10–40 × 10–90 μm in size (Figs. 25C, D). In longitudinal section, medullary cells are elongated and longer in inner portions, up to 300 μm long (Fig. 25D). The number of phaeophycean hairs is variable among samples. The characters of plurilocular zoidangia are the same as those of *Pl. gracilis* (Figs 25C, F). Paraphyses are absent.

LIFE CYCLE IN CULTURE: Gamete fusions were observed among gametophyte strains. Gametes were pear-shaped, laterally biflagellate with one plastid and one eyespot. Female and male gametes were isogamous (Figs. 26A, B); female gametes were 6.2 ± 0.5 × 3.9 ± 0.4 (Avg. ± SD) μm and male gametes were 6.0 ± 0.6 × 3.8 ± 0.4 μm. Female gametes settled to substratum earlier than male gametes and then became spherical. Multiple male gametes attached to the surface of the settled female gamete using the anterior flagellar tip and only one of them fused with the female gamete.

Zygotes cultured at 15°C (SD) developed into *Compsonema*-like sporophytes; those were filamentous prostrate thalli composed of branched, occasionally pluriseriate filaments bearing simple, uniseriate upright filaments (Figs. 26D–F). No discoid thalli were formed. Two months after germination, sporophytes grew to 7 mm in diameter and produced oval to pyriform unilocular sporangia and erect thalli (Fig. 26F). A unilocular sporangium was isolated, and unispores released were cultured at 10 °C (LD). Unispores

developed into filamentous prostrate thalli, and multiple erect thalli were formed on these prostrate thalli (Fig. 26G). Erect thalli matured with plurilocular zoidangia (Fig. 26H).

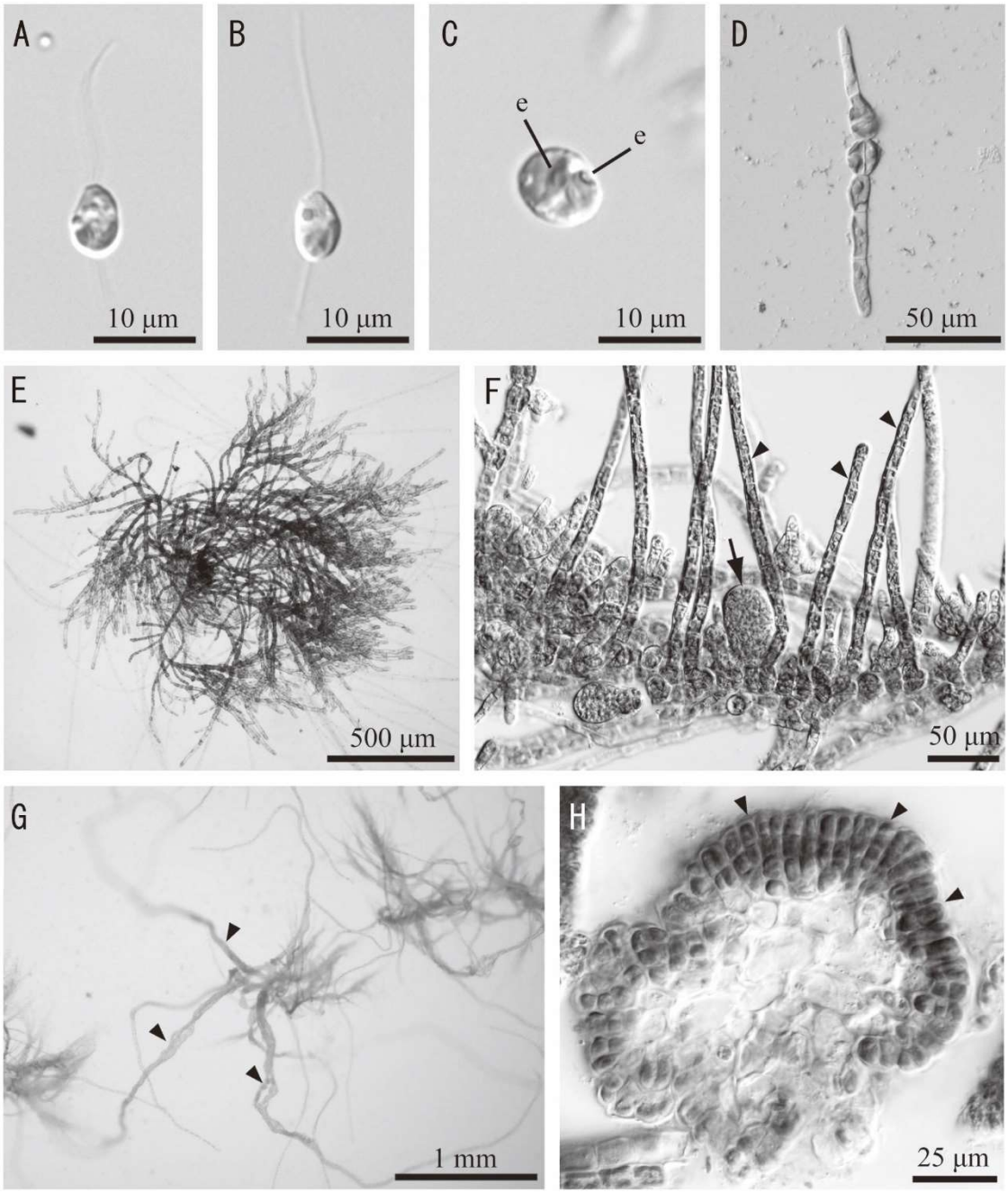

Figure 26. Life cycle of *Planosiphon nakamurae* in culture conditions.
(A) Female gamete. (B) Male gamete. (C) Zygote showing two eyespots (e). (D) Six-day-old germling at 20°C, LD. (E) 19-day-old sporophyte (prostrate thallus) at 20°C, LD. (F) Mature sporophyte showing unilocular zoidangia (arrow) and uniseriate upright filaments (arrowhead). (G) Erect thalli (arrowhead) derived from zoids from unilocular zoidangia. (H) Cross section of erect thalli with plurilocular zoidangia (arrowhead).

Lineage III

Fig. 27

DISTRIBUTION: Hokkaido, Japan.

SPECIMENS EXAMINED: SAP115465-e1–e5, e10, w3–5 and w8, 11 April 2019, Samani, Hokkaido, Japan.

MORPHOLOGY OF GAMETOPHYTES: External morphology and internal anatomy were examined in 10 specimens from Samani. Thalli are yellowish brown to dark brown, flattened, hollow, up to 45 cm in length and 9 mm in width, commonly gregarious, arising from a small holdfast (Figs. 27A, B). They are soft and wide thalli are wrinkled. In cross section, the cortex is composed of 2 layers of small pigmented cells and the medulla composed of 2–3 layers of colorless cells (Figs .27B, D). Phaeophycean hairs are present. Plurilocular zoidangia are produced basipetally on the entire surface of the thallus, covered with a cuticular layer even when mature (Fig. 27D). The characters of plurilocular zoidangia are the same as those of *Pl. gracilis* (Figs. 27A, D). Paraphyses are absent.

LIFE CYCLE: No sexual fusion (gamete fusion) was observed among seven individuals collected from Samani on 11 April 2019 and three culture strains I used (Table 6). No sex pheromone was detectable by olfaction from plurizoids in all individuals. Plurizoids from a strain Samani910519-1 were cultured at 15 °C (SD), and they developed into erect thalli or *Compsonema*-like prostrate thalli (Fig. 27E).

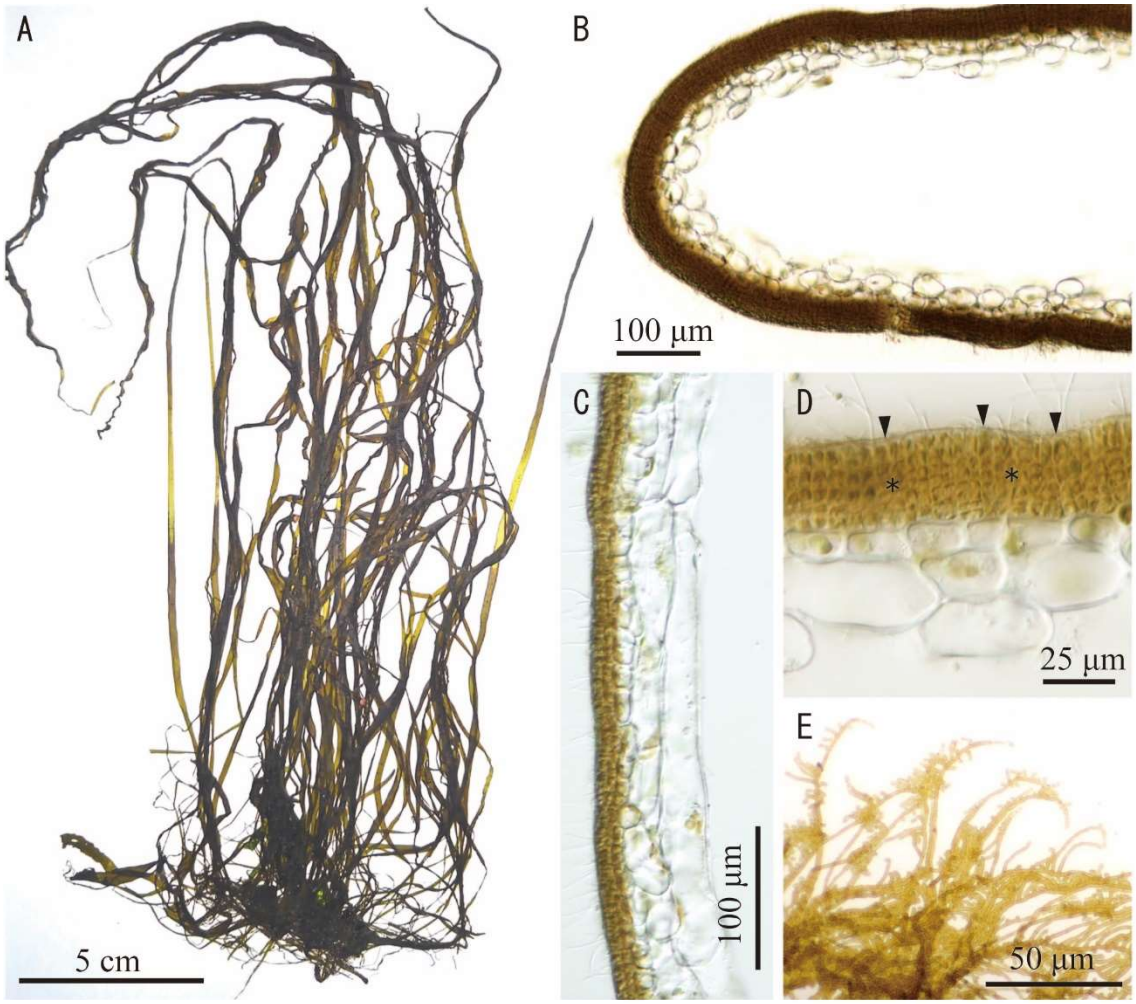

Figure 27. Morphology of lineage III.
(A) Field erect thalli (SAP115465-e3). Colourless portions which released plurizoids (arrowheads). (B) Cross section of the thallus. (C) Longitudinal section of the thallus. (D) Mature plurilocular zoidangia (asterisks) covered with a cuticular layer (arrowheads) in cross section of the thallus. (E) *Compsonema*-like prostrate thallus derived from a plurizoid.

Observation of culture strain G259

A culture strain of *Pl. complanatus*, G259, established by Pedersen (1980) developed flat erect thalli and released plurizoids. These plurizoids developed into erect thalli or discoid thalli (Figs 28A, B) as reported in Pedersen (1980).

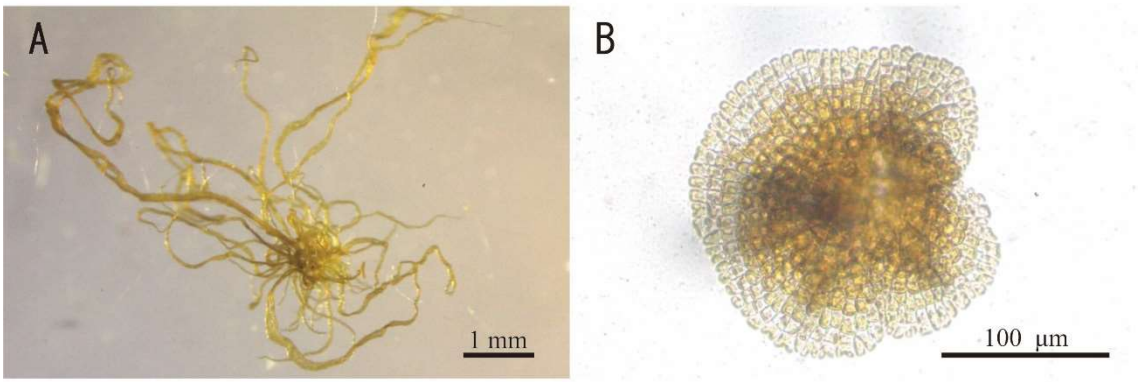

Figure 28. Morphology of the culture strain G259, established as *Planosiphon complanatus* (*Scytosiphon lomentaria* var. *complanatus*) by Pedersen (1980).
(A) Flattened erect thalli. (B) Discoid thallus derived from a plurizoid.

Crossing experiments

The result of the crossing experiments is shown in Figure 29. Gametic incompatibility was observed between lineages I (*Pl. gracilis*) and II (*Pl. nakamurae*). In intra-specific crosses, multiple male gametes attached to a settled female gamete with the anterior flagellar tip and formed a clump around the settled female gamete, and only one male gamete fused with the female gamete. In the cross between a lineage II female × lineage I male, male gametes formed clumps, but no gamete fusion was observed. Between a lineage I female and lineage II male, neither clumps nor gamete fusion were observed. Since sexual reproduction was not observed in lineage III, crossings between lineage III and others was not attempted.

♂ \ ♀		Lineage I: *P. gracilis*			Lineage II: *P. nakamurae*	
		Netanai-3	Ohma-3	Sabusawa-A	Anama	Enoshima180219-7
Lineage I	Netanai-1	-	F	F	N1	N1
Lineage II	Shimoda-2	N	N	N	F	F

Figure 29. Results from crossing experiments between *Planosiphon gracilis* (lineage I) and *Pl. nakamurae* (lineage II). F: gamete fusion was observed. N1: male gametes attached to a female gamete with their anterior flagella, but no gamete fusion occurred. N: male gametes did not attach to female gametes with their anterior flagella and no gamete fusion occurred.

DISCUSSION

This study revealed that *Planosiphon gracilis* morphospecies from Japan is a complex of three distinct lineages (lineages I–III). All phylogenetic analyses of *cox*1, *cox*3, and *rbc*L sequences consistently demonstrated the distinctness of lineages I–III and the crossing experiment showed that two lineages (lineages I and II), of which geographic distributions overlapped, were reproductively isolated from each other. These results demonstrate that these three lineages are distinct species. Since lineage I included the holotype of *Pl. gracilis* in my molecular analyses, I concluded that this lineage is *Pl. gracilis*. In addition, my molecular analyses demonstrated that lineage III was closely related to *Pl. complanatus* from Canada. Currently accepted species having hollow thalli in this genus are only *Pl. gracilis* and *Pl. complanatus* (Rosenvinge, 1893; Kogame, 1998; McDevit and Saunders, 2017; Santiañez and Kogame, 2017), thus lineage II is a third species having hollow thalli. Therefore, I concluded that lineage II is a new species and named the lineage *Pl. nakamurae* (Hoshino et al., 2020b).

Table 7. Morphological comparisons of *Planosiphon* species having hollow erect thalli.

	Lineage I: *Pl. gracilis*	Lineage II: *Pl. nakamurae*	Lineage III	*Pl. complanatus*
Erect thallus				
Shape	Flattened, sometimes cylindrical	Flattened, sometimes cylindrical	Flattened	Flattened[a,c]
Length (cm)	Up to 35	Up to 45	Up to 45	Up to 50[a]
Width (mm)	Up to 3	Up to 8	Up to 9	Up to 5[c]
Thickness of medullary layer	2–3 cells	2–3(–4) cells	2–3 cells	2–3 cells[b]/3–4 cells[c]
Phaeophycean hairs	Present	Present, but sometimes not detectable	Present	Absent[c]
Paraphysis	Absent	Absent	Absent	Absent[a–c]
Plurilocular zoidangia	Coherent	Coherent	Coherent	Coherent[b]

Data from: [a] Rosenvinge (1893), [b] Kogame (1998), [c] McDevit and Saunders (2017).

Between lineage III and Canadian *Pl. complanatus*, a relatively large divergence (ca. 4.1% in *cox*1) was observed. *Cox*1 (COI-5P) has been used as a DNA barcode marker for species differentiation among brown algae (e.g., Lane et al., 2007; McDevit and Saunders, 2017; Montecions et al., 2017) and McDevit and Saunders (2017) suggested that, typically, intra-specific divergence levels for *cox*1 are below 0.5% and inter-specific divergence levels greater than 4%. Indeed, reproductive isolating barriers were observed among the lineages in the *Scytosiphon lomentaria* species complex which diverged around 4.0–5.0% in *cox*1 [Hoshino et al., 2018 (**Chapter 1**)]. Thus, lineage III and Canadian *Pl. complanatus* could be different species from each other. However, further investigation is needed to reveal the certain relationship between lineage III and *Pl. complanatus*, using more samples from various localities. Therefore, I have left lineage III unnamed in the present study.

Three hollow *Planosiphon* species (*Pl. gracilis*, *Pl. nakamurae* and *Pl. complanatus*) are almost indistinguishable in morphology of erect thalli (Table 7). Since the specimens examined in the original description of *Pl. gracilis* in Kogame (1998) appeared to contain a significant number of potentially *Pl. nakamurae* specimens, I re-examined the morphology of *Pl. gracilis* here based on the type specimens and the specimens identified as *Pl. gracilis* (lineage I) by molecular phylogenetic analyses. Based on this re-examination, the range of width of erect thalli was changed from 0.5–4 (8) mm (Kogame, 1998) to 0.5–3 mm. Although *Pl. nakamurae* and *Pl. complanatus* can have wider thalli than *Pl. gracilis* (Table 7), specimens showing such wide thalli were only found in some populations and there was considerable variation in width of thalli. Thus, in many cases, it is difficult to identify the three species by morphology of erect thalli. Kogame (1998) distinguished *Pl. complanatus* and *Pl. gracilis* based on the morphology of microscopic phase: discoid prostrate thalli were reported in *Pl. complanatus* (Pedersen, 1980), while *Compsonema*-like filamentous prostrate thalli were observed in *Pl. gracilis* (Kogame, 1998). Although in my culture observation, I confirmed that the strain G259

used as *Pl. complanatus* in Pedersen (1980) formed discoid prostrate thalli, my *cox*1 phylogenetic analysis showed that the strain G259 is not *Pl. complanatus*, but *Petalonia fascia*, suggesting misidentification by Pedersen (1980). Furthermore, in the culture of lineage III that is closely related to *Pl. complanatus*, I observed *Compsonema*-like prostrate thalli, which were similar to those of *Pl. gracilis* (Kogame, 1998) and *Pl. nakamurae*. Considering the above, *Compsonema*-like prostrate thalli is common in the genus *Planosiphon* as pointed out by Santiañez and Kogame (2017), and morphological discrimination of the three hollow *Planosiphon* species is also difficult based on prostrate thalli. Although the statistical support for the monophyly of the genus *Planosiphon* was not always high in my phylogenetic analyses, the character "*Compsonema*-like prostrate thalli" supports the monophyly of this genus as a synapomorphy.

Planosiphon nakamurae was found in the Pacific coast of North America, Argentina, as well as Japan. Hanyuda et al. (2018) reported *Scytosiphon* sp. from Japanese tsunami marine debris (JTMD), which were caused by the 2011 Great East Japan Earthquake and Tsunami and arrived on the northeastern Pacific coast. I confirmed that their *Scytosiphon* sp. is *Pl. nakamurae* based on *cox*1 and *cox*3 sequences. Identical *cox*1 and *cox*3 haplotypes to those from JTMD were found in several localities of Japan including Tohoku area (Kitsunezaki-1) where the tsunami hit. From Argentinean specimens (nine specimens from three localities), two *cox*1 haplotypes (one mutation was observed between them) were found and they were identical to those of specimens from Seto Inland Sea, Japan (locality code 20, 23, 24, and 27 in Fig. 21; Fig. 22). This genetic homogeneity may suggest a recent introduction of *Pl. nakamurae* from Japan to Argentina. The three localities in Argentina where *Pl. nakamurae* was found have commercial or touristic ports and no historical reports of a "complanate *Scytosiphon*" suggestive of hollow *Planosiphon* species are found in these regions. There are several algae in Argentina that are considered introduced from Asia, mainly Japan: *Undaria pinnatifida* (Casas and Piriz, 1996; Martin and Cuevas, 2006; Meretta et al., 2012), *Melanothamnus*

harveyi (Raffo et al., 2014a, as *Neosiphonia harveyi*), *Polysiphonia morrowii* (Croce and Parodi, 2014; Raffo et al., 2014b), *Anotrichium furcellatum* (Boraso de Zaixso and Akselman, 2005), *Sporochnus pedunculatus* (Boraso de Zaixso and Negri, 1997), and *Schizymenia dubyi* (Ramirez et al., 2012). Some of these introductions have been attributed to the transport on transoceanic vessels, either on ballast water or as fouling organisms because of a high transit of fishing vessels and cargo ships in the Atlantic Patagonian coast (Oresanz et al., 2002). However other vectors have been suggested, for example, the macroalgae may have been transported as epibionts of the Japanese oyster *Crassostrea gigas* and *Undaria pinnatifida* (Croce and Parodi, 2014; Raffo et al., 2014a). There are many oyster farms in Seto Inland Sea in Japan, and the oysters were exported overseas for aquaculture purposes (Cheang et al., 2010). It is then plausible that *Pl. nakamurae* was introduced to Argentina as a hitchhiker on *C. gigas*. In the present study, I used a limited number of specimens from only three localities of Argentina. To elucidate whether the Argentinean populations of *Pl. nakamurae* are native or exotic, further investigation using specimens from more localities is needed.

Part 2

Sexuality of field *Scytosiphon* populations

parthenogenesis in field

Chapter 4

Parthenogenesis is rare in the reproduction of a sexual field population of the isogamous brown alga *Scytosiphon shibazakiorum* (Scytosiphonaceae, Ectocarpales)

INTRODUCTION

Parthenogenesis is a form of asexual reproduction in which an unfertilized gamete develops into a new individual. In laboratory culture, this asexual process has been commonly observed in various taxa of Phaeophyceae and Ulvophyceae (Brawley and Johnson, 1992; Luthringer et al., 2014 and references therein). In these taxa, gametes form zygotes if they encounter gametes of the opposite sex or will otherwise undergo parthenogenesis. If such parthenogenesis also functions in the field, it would increase reproductive efficiency because it would avoid some cost of sexual reproduction in that unfused gametes are not wasted. However, there is little information regarding whether the parthenogenesis observed in culture conditions contributes to the reproduction of field populations (De Wreede and Klinger, 1988).

In brown algae, the frequency of parthenogenesis seems to vary from population to population. In some populations in which sexual reproduction is unlikely to occur, parthenogenesis undoubtedly functions as the main method of reproduction. For example, populations showing a significant female-biased sex ratio have been reported in *Colpomenia peregrina* Sauvageau and *Scytosiphon lomentaria* [Yamagishi and Kogame, 1998; Hoshino et al., 2019 (**Chapter 5**)]. In these populations, most of the field sporophytes are unisexual females originating from parthenogenesis of female gametes [Yamagishi and Kogame, 1998; Hoshino et al., 2019 (**Chapter 5**)]. Female-dominant populations which are likely maintained by parthenogenesis have been also reported in *Mutimo cylindricus* H.Kawai & Kitayama (Kitayama et al., 1992).

Parthenogenesis seems to be rare in populations in which sexual reproduction likely occurs (such as populations showing 1:1 sex ratio). In *Lessonia nigrescens* Bory (Laminariales), unfertilized eggs form parthenosporophytes under culture conditions. However, in the field, only one out of 45 sporophytic thalli was determined as a parthenosporophyte (Oppliger et al., 2007). In *Dictyosiphon foeniculaceus* (Hudson) Greville (Ectocarpales), although parthenogenetic development of both female and male

gametes was observed in culture, no parthenosporophytes were found among 34 field sporophytic thalli collected (Peters and Müller, 1985). Parthenogenesis is also prevalent in *Ectocarpus* (Ectocarpales) in the laboratory. However, no parthenosporophytes were detected among nearly 200 field sporophytic thalli examined (Couceiro et al., 2015). Therefore, I hypothesized that parthenogenesis rarely contributes to reproduction in sexual populations, even if it can be observed under culture conditions.

The isogamous brown alga *Scytosiphon* is distributed in cold and warm waters worldwide [Hoshino et al., 2020c (**Chapter 2**)]. It has macroscopic dioicous isomorphic gametophytes. Sexual reproduction is nearly isogamous: male gametes are slightly smaller than female gametes. Zygotes develop into microscopic discoid sporophytes (Nakamura and Tatewaki, 1975). The sporophytes produce unilocular sporangia in which meiosis occurs. In laboratory cultures, both female and male gametes undergo parthenogenesis and develop into either parthenosporophytes (discoid or filamentous thalli) or gametophytes depending on temperature and daylength (Nakamura and Tatewaki, 1975; tom Dieck, 1987). *Scytosiphon* in Japan include at least six cryptic species [i.e., *S. lomentaria*, *S. shibazakiorum*, *S. promiscuus*, *S. tosaensis*, *S. arcanus*, and *S. subtropicus*; Hoshino et al., 2020c (**Chapter 2**)]. *Scytosiphon lomentaria* includes parthenogenetic female-dominant populations in addition to populations consisting of both female and male gametophytes [sexual populations; Kogame et al. 2015a; Hoshino et al., 2019 (**Chapter 5**)]. In *S. shibazakiorum*, *S. promiscuus*, *S. arcanus*, and *S. subtropicus*, only sexual populations have been found.

In this study, to test the hypothesis that parthenogenesis is a rare event in sexual field populations, I focused on a population of *S. shibazakiorum* in Oshoro Bay, Hokkaido, Japan. In this population, I found a sex ratio of approximately 1:1 and gamete fusion is observable in the laboratory. Using this population, I investigated the parthenogenesis of female and male gametes compared to development of zygotes in culture and the frequency of female and male parthenosporophytes and zygotic sporophytes in field.

MATERIALS AND METHODS

Sex ratio of the field gametophyte population

To examine the sexuality of the population, gametophytes of *S. shibazakiorum* were collected in Oshoro Bay, Otaru, Hokkaido, Japan (43°12'54.8"N, 140°51'19.2"E) on 21 March 2018 (Table S5). Each individual served to make a herbarium specimen and total genomic DNA was extracted from a fragment for molecular experiments as described in Hoshino et al. (2018; **Chapter 1**). The sex of each gametophyte was examined using PCR-based sex markers. Partial sequences of the sex-specific non-recombining regions in the female and male sex-determining regions (Lipinska et al., 2017) were amplified and used as the sex markers [Hoshino et al., 2019 (**Chapter 5**)]. The presence/absence of PCR products was determined by 1% agarose-gel electrophoresis.

Parthenogenetic development in laboratory culture

To examine the parthenogenetic capacity of gametes, parthenogenetic development was observed in culture. The culture isolates used are listed in Table 8. Culture experiments were conducted using plastic Petri dishes (90 × 20 mm) and PESI medium (Tatewaki, 1966) with fluorescent lighting of 30–50 μmol $m^{-2}s^{-1}$ photon flux density. Gametophytes and their gametes were cultured in two conditions: 3°C short day (9.5:14.5 LD) and 10°C long day (16:8 LD). These culture conditions roughly correspond to the water temperatures and the daylengths of February and May in Oshoro Bay, respectively, where mature gametophytes were observed during these months.

Gametes were cultured at 3°C for 12 weeks and at 10°C for eight weeks. Zygotes were cultured at 3°C for four weeks and at 10°C for two weeks. The cell numbers of each four-week-old germling (gametes/zygotes) at 3°C and one-week-old germling at 10°C were recorded (30–100 germlings were observed for each gametophyte strain and five germlings were observed for each zygote strain). For the statistical analysis of the cell

number of the germlings among experimental groups (female/male/zygote), a generalized linear mixed model (GLMM) was adopted with a Poisson distribution. In this model, the experimental groups (female/male/zygote) were considered as fixed effects and the identity of each strain was considered as a random effect to deal with non-independence of the data from the same culture strain. The GLMM analyses were conducted using the lme4 package (Bates et al. 2015) in R ver. 3.3.1. (R Core Team, 2016).

Subsequent to making the above observations, I examined whether the germlings of unfused gametes develop into gametophytic or sporophytic thalli. For each culture strain, 80–400 germlings were examined for 12-week-old thalli at 3°C and eight-week-old thalli at 10°C.

Table 8. Culture strains used in experiments at 3°C and 10°C, respectively.
-: not used. Cultures of female and male gametophytes were established from the sporophytes collected in Oshoro on 6 October 2017.

	Culture strain	3 °C	10 °C
Female	F1: Oshoro-171006-Cr2B	used	used
	F2: Oshoro-171006-Cr2E	-	used
	F3: Oshoro-171006-Cr3D	-	used
	F4: Oshoro-171006-Cr5A	used	used
	F5: Oshoro-171006-Cr5C	used	used
Male	M1: Oshoro-171006-Cr1B	-	used
	M2: Oshoro-171006-Cr3A	used	used
	M3: Oshoro-171006-Cr5B	used	used
	M4: Oshoro-171006-Cr5D	used	used
Zygote	Z1: Oshoro-171006-Cr5A×Oshoro-171006-Cr5D	-	used
	Z2: Oshoro-171006-Cr2B×Oshoro-171006-Cr5D	used	used
	Z3: Oshoro-171006-Cr5C×Oshoro-171006-Cr5B	-	used
	Z4: Oshoro-171006-Cr3A×Oshoro-171006-Cr5A	used	-
	Z5: Oshoro-171006-Cr5A×Oshoro-171006-Cr5B	used	-
	Z6: Oshoro-171006-Cr5C×Oshoro-171006-Cr5D	used	-

Parthenosporophytes in the field

Sporophytic thalli (Fig. 30A) were collected in Oshoro Bay from August to December of 2016 and 2017 (Table S6). Zygotic sporophytes (originating from sexual reproduction) produce both male and female gametophytes in the offspring from a unilocular sporangium (Fig. 31). On the other hand, parthenosporophytes (originating from parthenogenesis of gametes) produce unisexual gametophytes (Fig. 31; Nakamura and Tatewaki, 1975). Therefore, gamete fusion (zygotes) should be observed among the gametophytes derived from a sexually formed sporophyte, but not observed among the gametophytes derived from a parthenosporophyte.

Single unilocular sporangium (Fig. 30B) was isolated from each sporophytic thallus and was cultured at 10°C in short-day condition. Spores from a unilocular sporangium grew up to gametophytes (Fig. 30C) and produced gametes in four months.

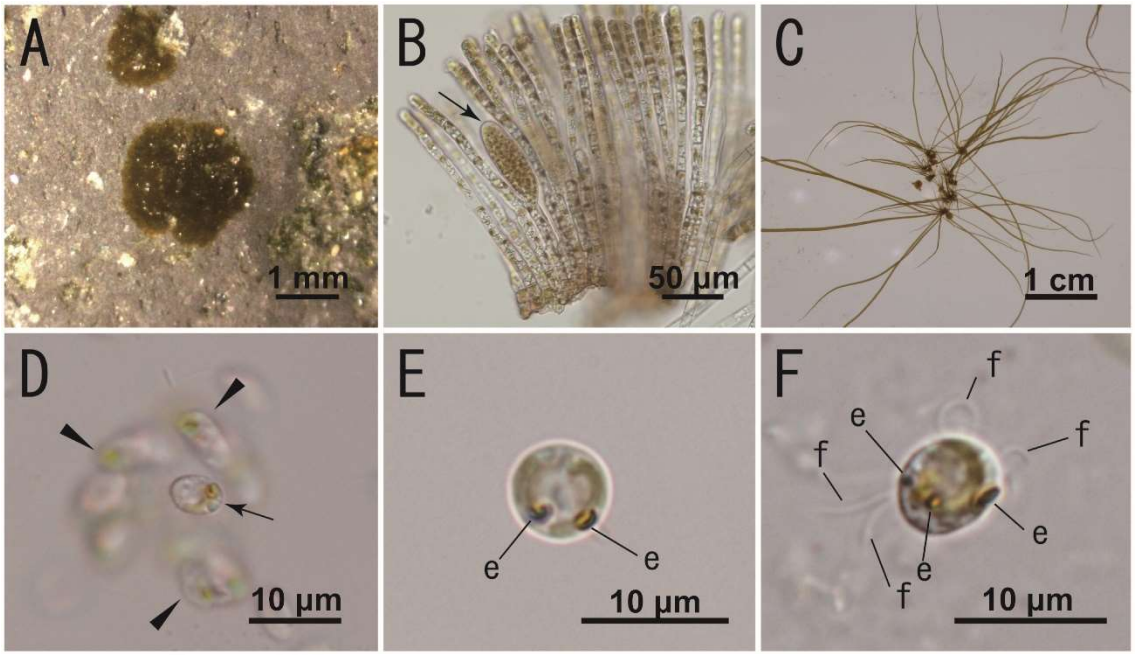

Figure 30. Field sporophytic thalli and observations of the cultures established from their unilocular sporangia. (A) Field sporophytic thallus on a rock. (B) Cross-section of a sporophytic thallus showing a unilocular sporangium (arrow). (C) Gametophytes derived from an isolated unilocular sporangium. (D) Fertilization observed in a culture. Multiple male gametes (arrow head) gather around a female gamete (arrow). (E) Zygote observed in a culture, two eyespots (e) are visible. (F) Abnormal gamete showing multiple eyespots (e) and more than two flagella (f).

The presence or absence of gamete fusion or numerous zygotes (settled cells showing two eyespots; Fig. 30E) was checked in each culture from a single unilocular sporangium using a light microscope. For cultures in which the presence of gamete fusion or zygotes could not be confirmed (e.g., due to insufficient fertility/growth of gametophytes or a small number of zygotes), the PCR-based sex markers were used to check whether the culture includes both sexes. In unisexual samples, PCRs were repeated once to verify reproducibility.

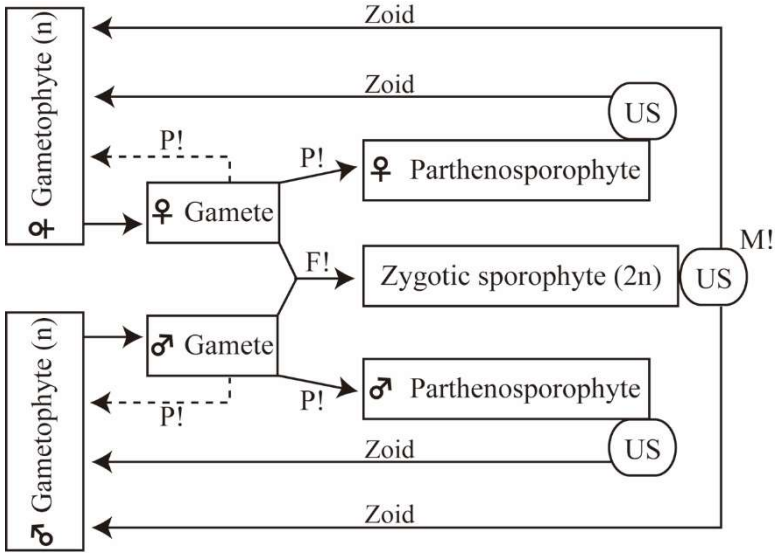

Figure 31. Schematic figure of the life cycle of Scytosiphon in culture. Fusion of female and male gametes (F!) produces a zygote which develops into a zygotic sporophyte. The zygotic sporophyte produces unilocular sporangia (US) in which meiosis (M!) occurs and zoids (meiospores) develop into female or male gametophytes. Unfused gametes can undergo parthenogenesis (P!) and mainly develop into parthenosporophytes, not gametophytes. Unilocular sporangia of parthenosporophytes produce unisexual gametophytes.

RESULTS

Sex ratio in the field population

The sex of 27 gametophytes was identified with the sex markers. The ratio between female and male gametophytes was 12:15 (Table S5) and not significantly different from 1:1 (G test, $G = 0.334$; df = 1, $P = 0.563$).

Parthenogenetic development in laboratory culture

Unfused gametes showed higher mortality and slower development than zygotes (Fig. 32). The GLMM predicted that the cell numbers of germlings of female gametes would be significantly larger than those of male gametes and significantly smaller than that of zygotes (Table 9). I followed the development of 20 zygotes (four zygote strains) at 3°C and 15 zygotes (three zygote strains) at 10°C. Except for one zygote of strain Z2, which died at 3°C, they developed into discoid sporophytes (which were 20–100-celled after four weeks culture at 3°C and 9–15-celled after one week culture at 10°C; Fig. 32). In female strains, most gametes showed slower development compared to zygotes although in some exceptions the gametes developed at the same rate (see non-outlier ranges and outliers in Fig. 32). In male strains, most gametes stayed 1–3-celled both at 3°C (four weeks) and at 10°C (one week; Fig. 32).

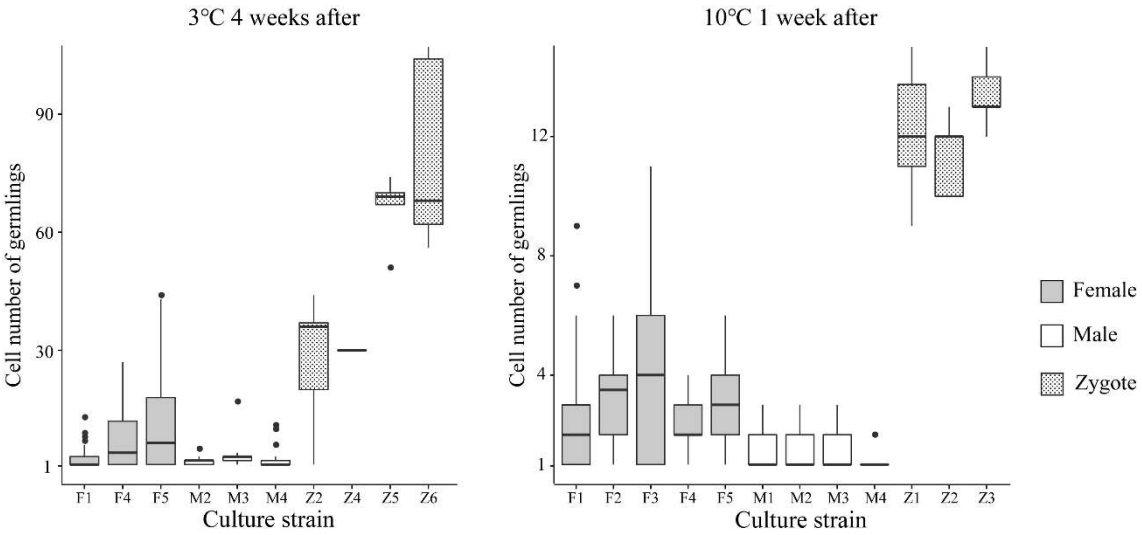

Figure 32. Cell numbers of germlings (4-week-old germlings at 3°C and 1-week-old germlings at 10°C) of gametes and zygotes. The gametes/zygotes that failed to germinate and aborted during development are also included (bursted gametes are excluded since they were impossible to count). Codes of culture strains are listed in Table 8. The boxes and whiskers represent the interquartile range and the non-outlier ranges. The horizontal band in the box is the median. Black dots represent outliers.

Table 9. The effects of the experimental groups (female/male/zygote) on the cell numbers of germlings at 3°C and 10°C. Coefficients of the experimental groups (female/male and female/zygote) indicate that cell numbers of germlings from female gametes are larger than that of male gametes, but smaller than that of zygotes at a 5% significance level.

	Cell number of germination							
	3°C 4 weeks after				10°C 1 week after			
	Coef.	SE	z value	*p*	Coef.	SE	z value	*p*
Intercept	1.71	0.28	6.14	< 0.0001	1.03	0.07	14.11	< 0.0001
Group(female/male)	-1.01	0.39	-2.56	0.0103	-0.76	0.11	-6.72	< 0.0001
Group(female/zygote)	2.11	0.37	5.75	< 0.0001	1.48	0.13	11.23	< 0.0001

The parthenogenetic development was different between female and male gametes. Although the germination rate of female gametes was lower than male gametes, survival rates seemed to be higher in female gametes than male gametes. In all female strains, 20–60% (varied across the strains) of gametes swelled unusually without germination in both 3°C and 10°C conditions (Figs. 33B and 34) and these swollen gametes frequently bursted and died. However, female gametes rarely died once they successfully germinated (Fig. 33A). In male strains, swollen gametes were rarely observed, except for strain M4 at 3°C where nearly 30% of gametes were swollen (Fig. 34). Male gametes showed higher germination rates than female gametes (Fig. 34); however, 94–97% of them stopped their development before the 5-celled stage (Figs. 33C and 34) and died in several weeks.

In both 3°C and 10°C conditions, surviving gametes usually developed into parthenosporophytes (discoid or filamentous thalli) and rarely formed erect thalli (gametophytes). The ratio of thalli that formed erect thalli were 0.8 ± 0.3 (Avg. ± SD) % in female strains and 0.4 ± 0.4% in male strains at 3°C, and 2.9 ± 4.1% in female strains and 1.6 ± 0.9% in male strains at 10°C (Table S7).

Parthenosporophytes in field. In total, 126 unilocular sporangia were isolated from 126 different field-collected sporophytic thalli and were cultured. The presence of gamete fusion or numerous zygotes (Figs. 30D, E) was confirmed in 104 cultures of unilocular sporangia. The remaining 22 cultures were the followings: 1) two cultures in

which spores did not develop into gametophytes; 2) seven cultures in which some gametes had multiple eyespots and more than two flagella (possibly twins; Fig. 30F) and confirmation of zygotes was impossible since these zoids were hardly distinguishable from zygotes; and 3) 11 cultures in which neither gamete fusion nor zygotes were not observed. In the sex marker PCRs, out of these 22 cultures, both female and male markers were amplified in 16 cultures, only female markers were amplified in two cultures, and only male markers were amplified in four cultures (Table S6).

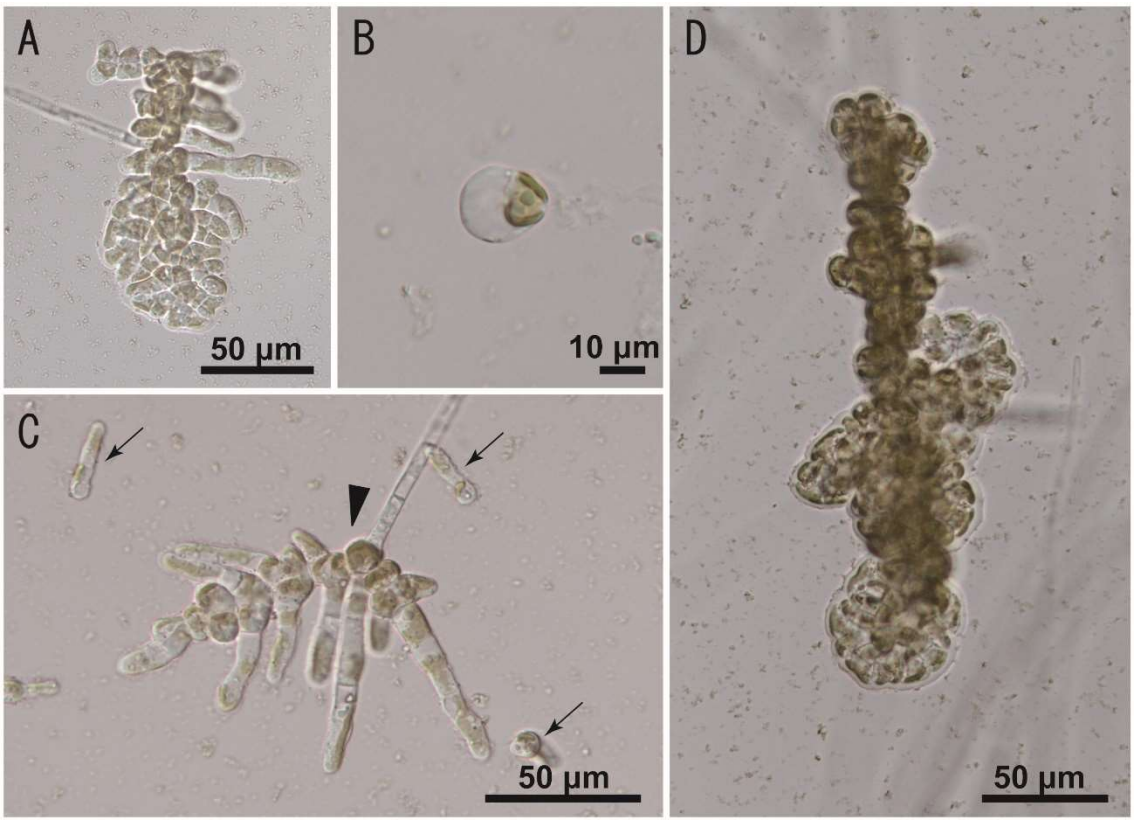

Figure 33. Two-week-old germlings of gametes and zygotes at 10°C. (A) Germling of a female gamete forming discoid thalli. (B) Unusually swollen female gamete. (C) Germlings of male gametes, which stopped their development at 2-celled-stage (arrow). Large one (arrowhead) is a germling that successfully grew (filamentous). (D) Germling of a zygote which developed a discoid part.

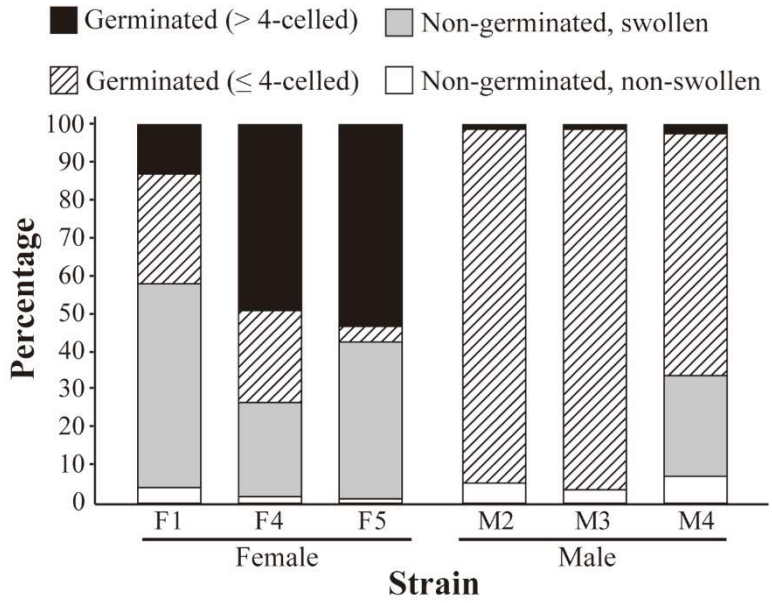

Figure 34. Percentage of four phenotypes (non-germinated and non-swollen; non-germinated and swollen; germlings less than 5-celled; germlings more than 4-celled) observed in four-week-old gametes at 3°C. Bursted gametes are not included.

DISCUSSION

I demonstrated that the contribution of parthenogenesis to reproduction is small in the sexual population of *S. shibazakiorum*, being consistent with my hypothesis that parthenogenesis is a rare event in sexual field populations. Out of 126 field sporophytic thalli, only six (4.8%) showed no evidence of a zygotic origin, but rather a parthenogenetic origin (Table 10). In culture, more than 90% of partheno-germlings that survived and grew developed into sporophytic thalli irrespective of the culture conditions examined. This suggests that if parthenogenesis occurs in the field, most of them would form parthenosporophytes. Therefore, the rarity of field parthenosporophytes in my results indicates that parthenogenesis seldom occurs compared to sexual reproduction in the field.

Table 10. The percentage of zygotic sporophytes, unisexual female sporophytes, and unisexual male sporophytes in field sporophytic thalli.

Total number of unilocular sporangia examined	Discrimination result		
	Sexual origin	Parthenogenesis of female	Parthenogenesis of male
126	120 (95.2%)	2 (1.6%)	4 (3.2%)

A dominance of zygotic sporophytes (i.e., rare parthenosporophytes) has also been reported in the sexual populations of *Laminaria digitata* (Hudson) J.V. Lamouroux, *Lessonia nigrescens*, *Dictyosiphon foeniculaceus* and *Ectocarpus* (Peters and Müller, 1985; Oppliger et al., 2007, 2014; Couceiro et al., 2015). Several causes can be considered for explaining the rare occurrence of parthenogenesis. High fertilization success (i.e., few unfused gametes) has been proposed as the cause of the rare parthenosporophytes (Peters and Müller, 1985; Couceiro et al., 2015). It is well known that brown algae have various mechanisms that enhance the probability of gamete encounter, such as synchronous gamete release, phototaxis, and attraction of male gametes by sexual pheromones (Brawley and Johnson, 1992). Although the fertilization rates of natural populations are largely unknown, it is noteworthy that high fertilization values (70–100%) have been

reported in fucoids (reviewed in Santelices, 2002). Another possible cause is the reduced viability of parthenogenetic germlings (Peters and Müller, 1985). I showed that the survival rate and growth rate of unfused gametes were much lower than those of zygotes. In the field, biotic interactions should also be considered as a contributing factor to the rarity of parthenosporophytes. For instance, gametes may have various predators in the field. Additionally, unfused gametes are probably more vulnerable to grazing or predation than zygotes which rapidly start development and are protected by a cell wall and body size. Unfused gametes need to stay naked for some time to wait/look for their mating partner and even if they started parthenogenetic development, its development is much slower than that of zygotes.

Previous reports of parthenogenesis under culture conditions should be treated with caution. Most studies described only the occurrence of parthenogenesis and did not compare its survival rate and development with those of zygotes. The studies, which compared the development of unfused gametes and that of zygotes, often show that unfused gametes have high mortality and slow/abnormal development compared to zygotes [e.g., Berthold, 1881; Kemp and Cole, 1961; Nakahara, 1984; Peters and Müller, 1985; Hoshino et al., 2019 (**Chapter 5**)]. In such cases, parthenogenesis is unlikely to function in the field. Interestingly, female gametes from the parthenogenetic populations of *S. lomentaria* show parthenogenetic development that is as rapid as zygotic development in culture [Hoshino et al., 2019 (**Chapter 5**)].

It has been considered that both female and male gametes are capable of parthenogenesis in brown algal isogamous taxa (Oppliger et al., 2007, Luthringer et al., 2014). However, in my culture experiments, parthenogenetic capacity (i.e., germination rate and survival rate) was significantly different depending on sex. Such sex-based differences in parthenogenetic development have also been reported in the other isogamous taxa including *Ectocarpus siliculosus* and several *Scytosiphon* species [Berthold, 1881; Han et al. 2014; Hoshino et al., 2019 (**Chapter 5**)]. Differences between

the sexes in parthenogenetic capacity, despite their isogamous nature, may be attributable to differences in subcellular components such as mitochondria and centrioles (Nagasato et al., 1998; Kimura et al., 2010; Han et al., 2014). In *Scytosiphon*, to detect the high mortality of male gametes, observation for several weeks was essential since most male gametes normally develop up to the 4-celled stage [Han et al., 2014; Hoshino et al., 2019 (**Chapter 5**)]. Thus, the high mortality of male gametes may have been overlooked in previous studies. In spite of the high mortality of male gametes in culture, I detected more male parthenosporophytes than female ones in field. Although it may have been accidentally caused owing to such a small number of parthenosporophytes detected (six individuals), I cannot offer any explanation for this phenomenon in the current study.

Chapter 5

Parthenogenetic female populations in the brown alga *Scytosiphon lomentaria* (Scytosiphonaceae, Ectocarpales): decay of a sexual trait and acquisition of asexual traits

INTRODUCTION

While sex is the predominant mode of reproduction in nearly all multicellular organisms, the occurrence of asexuals is widespread in nature (Kramer and Templeton, 2001). Parthenogenesis is a form of asexual reproduction in which an unfertilized gamete develops into a new individual. In land plants and animals, numerous examples of asexual populations/species reproducing parthenogenetically have been reported (Kearney, 2005 and references therein). Comparative studies between these parthenogens and their close sexual relatives have provided important insight for understanding the costs and benefits of sex and have been considered as an important topic in evolutionary biology (Maynard Smith, 1986; Lehtonen et al., 2012).

In brown algae, reports of parthenogenetic asexual populations are scarce, although parthenogenetic development of unfused gametes has been reported in culture studies of various taxa (e.g., Nakamura and Tatewaki, 1975; Nakahara, 1984; Clayton, 1987). The scarcity of reports of parthenogenetic asexual populations in this group seem to stem from difficulties in investigating the reproductive mode of a population. The reproductive mode (sexual/asexual) of isogamous brown algal populations has been confirmed by observations of the presence or absence of gamete fusion in the laboratory (e.g., Peters, 1987 and included references) because morphological sex-determination of gametophytes is impossible. However, crossing experiments have a fundamental problem. The presence of gamete fusion serves as absolute evidence for the sexuality of a population (presence of both male and female individuals), but the absence of gamete fusion in the laboratory is not absolute evidence for the asexuality of a population since sexual reproduction may have been missed for reasons including technical problems with cultivation and observation (Peters, 1987). Furthermore, Clayton (1982) hypothesized that the production of sexual gametes might be a transient and seasonal phenomenon (i.e., gamete fusion is not observable since asexual zoids are usually produced). There is also a possibility that individuals of the population have lost sexuality and produce asexual

zoids for asexual reproduction. Thus, although there are numerous reports of populations/species in which gamete fusion cannot be observed in the laboratory (e.g., Wynne, 1969; Müller, 1977; Peters, 1987; Kogame and Kawai, 1993), their precise reproductive mode is unclear. For the accurate understanding of reproductive strategy in brown algae, it is important to reveal the reproductive mode of populations with no sign of sexuality in the laboratory.

The brown alga *Scytosiphon lomentaria* includes populations in which gamete fusion cannot be observed and these populations have been referred to as asexual populations (Kogame et al., 2005). These asexual populations are closely related to sexual populations; they cannot be distinguished by molecular phylogenetic analyses based on the mitochondrial *cox*1 gene (Kogame et al., 2015a). In sexual populations, isogamous gamete fusion can be observed between isomorphic female and male gametophytes. Female gametes settle on the substratum earlier than male gametes, secrete a sexual pheromone to attract male gametes, and gamete fusion occurs (Fu et al., 2014). Their life history has been reported to be heteromorphic: an alternation of generation between the macroscopic gametophyte (15–50 cm in height) and the microscopic discoid sporophyte (1–5 mm in diameter) (Nakamura and Tatewaki, 1975). The sporophytes produce unilocular sporangia within which meiosis occurs. In asexual populations, no fusion can be observed between gametes produced from different gametophytes originating from the same field population (Kogame et al., 2005). Gametes of asexual populations tend to settle more rapidly than female gametes from sexual populations and do not have detectable smells of a sexual pheromone (Kogame et al., 2005). These asexual populations have been reported from colder waters compared to sexual populations (Kogame et al., 2015a).

In this study, I aimed at understanding the precise reproductive mode of the asexual populations in *S. lomentaria*. Sex ratios (i.e., the ratio of male and female gametophytes in field populations) were compared between two sexual and three asexual

populations. To determine the sex of the gametophytes, I developed PCR-based sex markers adapted from Lipinska et al. (2017). I show that sexual populations include both males and females while all individuals from asexual populations are female which strongly suggests that the asexual populations of *S. lomentaria* are exclusively composed of female individuals that reproduce parthenogenetically. I examined the life cycle of "female" individuals in the asexual population in the field, focusing on whether females in the asexual populations have a sporophytic stage in their life cycle. In addition, in transitioning from sexual reproduction involving both females and males to asexual reproduction involving only females, the asexual populations of *S. lomentaria* have simultaneously reduced formerly adaptive sexual traits and acquired new adaptive asexual traits. Therefore, potentially adaptive traits in sexual populations (sexual pheromone production and fertilization ability) and in asexual populations (gamete size, and parthenogenesis ability) were compared between "female" gametes from asexual populations and female gametes from sexual populations.

MATERIALS AND METHODS

Sampling and taxonomic identity

Sampling was conducted at five localities in Japan (Fig. 35). A total of 238 individuals of *Scytosiphon* gametophytes were collected. Each individual was dried as a voucher pressed specimen and a fragment was preserved in silica gel for molecular analyses. Unialgal culture isolates were established for some samples as previously described by Kogame et al. (2015a).

In Japan, four cryptic species closely related to *S. lomentaria* have been reported around the sampling localities [Hoshino et al., 2020c (**Chapter 2**)]. Thus, I screened all samples using PCR with species-specific PCR markers. I designed *S. lomentaria*-specific primers based on two specific polymorphic sites in *S. lomentaria* which were detected in an alignment of *cox*1 sequences of *Scytosiphon* species in Hoshino et al. (2018; **Chapter**

1): Slom_sp1F (5'-CAGGTAATCAGTTTTTAGGTGGT-3': forward) and Slom_sp1R (5'-TGTTGATACAATACCGGATCT-3': reverse). Using these primers, the partial *cox*1 gene was amplified. Total genomic DNA was extracted from the cultured and silica gel-dried thalli as previously described [Hoshino et al., 2018 (**Chapter 1**)] and used as template DNA. PCRs were performed using TaKaRa Ex Taq DNA Polymerase (Takara Bio Inc., Otsu, Japan) with dimethylsulfoxide (5% in reaction volume). The PCR program included a denaturation step at 94°C for 1 min, followed by 35 cycles of 94°C for 30 sec, 59°C for 30 sec, 74°C for 30 sec, and a final elongation step at 74°C for 7 min. Under these conditions, amplification occurs only in *S. lomentaria* but not in other species. The

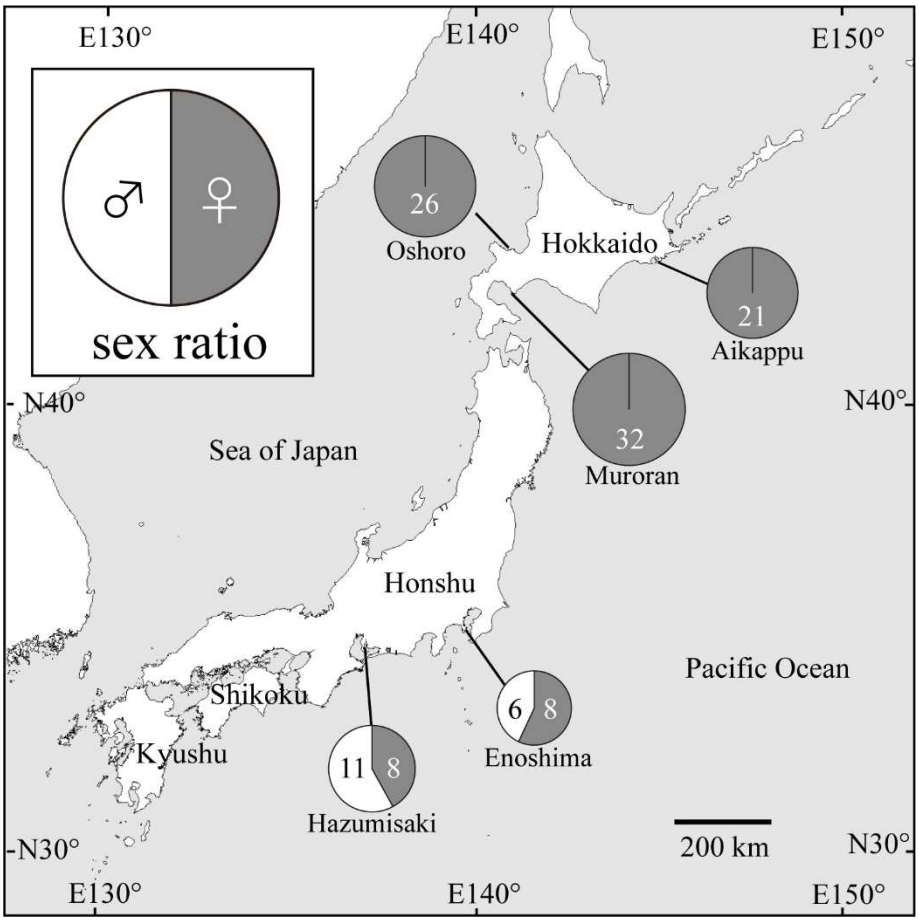

Figure 35. Sex ratios of three asexual (Oshoro, Muroran, and Aikappu) and two sexual populations (Enoshima and Hazumisaki). The number of gametophytes of each sex is given in each circle. The name of each locality is given under each circle. Oshoro, 43°12'53.9"N 140°51'12.6"E; Muroran, 42°18'20.3"N 140°59'00.9"E; Aikappu, 43°00'54.9"N 144°49'59.5"E; Enoshima, 35°17'52.1"N 139°28'47.0"E; Hazumisaki, 34°41'51.3"N 136°58'11.6"E.

presence/absence of PCR products was determined by 1% agarose-gel electrophoresis.

Sex ratio investigation of the field populations

Sex ratios were investigated in three asexual (Oshoro, Muroran, and Aikappu in Hokkaido) and two sexual populations (Enoshima and Hazumisaki in Honshu) using PCR-based sex markers. Partial sequences of the sex-specific non-recombining region on the sex chromosome of *S. lomentaria* were used as sex markers and were amplified using two pairs of primers: Slom-13_14102F (5'-CCCGGAAAGTCTGTTTTGAG-3': forward) and Slom13_14102R (5'-CCCTCCAAGACTCGAGATGA-3': reverse) for the female marker and Slom-13_1840F (5'-CGGGACGTGAATAAGTTCGT -3': forward) and Slom-13_1840R (5'-TCTCCATTTTCACCGTCCTC-3': reverse) for the male marker (Lipinska et al., 2017). PCRs were performed using TaKaRa Ex Taq DNA Polymerase with dimethylsulfoxide (5% in reaction volume). The PCR program included a denaturation step at 94°C for 1 min, followed by 50 cycles of 94°C for 30 sec, 59°C for 30 sec, 74°C for 30 sec, and a final elongation step at 74°C for 7 min. Under this condition, I confirmed that sex determination by the PCR-based markers is congruent with that of crossing experiments and both sex markers are amplified in zygotic sporophytes. The presence/absence of PCR products was checked by 1% agarose-gel electrophoresis.

Life cycle of a representative asexual population

To reveal the life cycle of asexual populations, I conducted field observations in Oshoro (Fig. 35) and investigated whether alternation of the gametophytic stage and the sporophytic stage occurs. In Oshoro, asexual gametophytes (i.e., gametophytes of the asexual population) were observed from January to May and mature sporophytic thalli with unilocular sporangia were observed from September to December. Sporophytic thalli collected at Oshoro on 20 October 2017 were used for molecular analyses. A single unilocular sporangium was isolated from each of the 48 sporophytic thalli. DNA was

extracted from each unilocular sporangium using 10 μl of QuickExtract™ FFPE DNA Extraction Kit (epicentre, Madison, U.S.A.). Their taxonomic identity was checked by PCR with *S. lomentaria*-specific primers.

Sporophytes which originate from sexual reproduction produce both female and male gametophytes from their unilocular sporangia while sporophytes originating from parthenogenesis of female (male) gametes produce only female (male) gametophytes from their unilocular sporangia (Nakamura and Tatewaki, 1975). Thus, for the unilocular sporangia identified as *S. lomentaria*, sex markers were additionally used to determine whether the collected sporophytes originate from sexual reproduction or parthenogenesis.

Cell size and parthenogenetic capacity of gametes

Cell size and parthenogenetic growth rate of gametes were compared among asexual, female, and male gametophytes under culture conditions. The cultured strains of gametophytes are shown in Tables 11 and S8. Culture experiments were conducted using plastic Petri dishes (90 × 20 mm) and PESI medium (Tatewaki, 1966) at 10 and 15°C in long day (16h:8h, light:dark) and short day (8h:16h, light:dark) conditions with fluorescent lighting of 30–50 μmol $m^{-2}s^{-1}$ photon flux density. Gametes released from the gametophytes grown at 15°C under the short day condition were used for each experiment. Zygotes were also made by crossing (Table S8) and their cell size and growth rate were measured for comparison with those of the gametes. Zygotes were easily distinguishable from unfused gametes by having two eyespots.

Several minutes after liberation, gametes lose their motility and settle to the substratum and then change their shape from pear-shaped to spherical. Images of these spherical gametes were taken with a Nikon Digital Sight DS-Fi1 (Nikon Corporation, Tokyo) and their diameter was measured using ImageJ software (Schneider et al., 2012). Thirty to a hundred gametes were measured for each cultured strain. The diameter of the zygotes was also measured. For statistical analysis of the diameter of gametes/zygotes

among the experimental groups (asexual/male/female/zygote), a generalized linear mixed model (GLMM) was adopted with a normal distribution. In this model, gametophyte identity (strain) and replication for each gametophyte were considered as nested random effects to deal with non-independence of the data from the same culture strain.

Gametes and zygotes were cultured in long day conditions at 10°C for seven days and at 15°C for five days. The number of germinated gametes, non-germinated gametes, and the number of cells in each germling (gamete) were recorded; 50–100 germlings (gametes) were observed for each culture strain every day. For the statistical analysis of the germination rate (the number of germinated gametes and non-germinated gametes) and the cell division rate (the cell numbers of the germlings) of gametes/zygotes among the experimental groups (asexual/male/female/zygote), a GLMM was adopted with a binominal distribution and with a Poisson distribution, respectively. In these models, the experimental groups (asexual/male/female/zygote) and the number of days in culture were considered as fixed effects, and gametophyte identity (strain) was considered as the random effect to deal with non-independence of the data from the same cultured strain.

All statistical analyses were conducted using the lme4 package (Bates et al. 2015) and the lmerTest package (Kuznetsova et al., 2016) in R 3.3.1. (R Core Team, 2016).

Analysis of sexual pheromone production by a liquid chromatography/mass spectrometry (LC/MS).

Using a LC/MS, I examined if a sexual pheromone is detectable in *S. lomentaria* asexual gametophytes. I also examined the female and male gametes of *S. shibazakiorum* and *S. promiscuus*; in female gametes of these two species, the smell of a sexual pheromone is detectable. For the LC/MS analyses, field gametophytes were used because I could not obtain enough gametes from culture samples. Since sexual populations of *S. lomentaria* were not found in shores near the laboratory, I analyzed *S. shibazakiorum* and *S.*

promiscuus instead. All materials were collected at Oshoro on February to April in 2018. The sex of each thallus of *S. shibazakiorum* and *S. promiscuus* was checked by a sex marker PCR or crossing experiments.

Gametophytes were kept in filtered seawater (300 ml) in a 500 ml flask at 10°C and gametes were released in the flask. Volatile secretions (sexual pheromone) were trapped on activated carbon (10 mg) by a closed-loop-stripping system at 10°C. After looping 20 hours, absorbed volatile compounds were eluted with 50 µl of CH_2Cl_2. The eluate was dissolved in 100 µl of MeCN and analyzed by LCMS on a micrOTOF focus (Bruker Daltonics, UK) equipped with APCI source (positive mode) and coupled with an agilent 1100 series HPLC system (CAPCELL PAK C18 column 2.0 × 100 mm with a gradient from MeCN/H_2O 80/20 to MeCN/H_2O 100/0 over 20 min, followed by isocratic elution of MeCN/H_2O 100/0 for 10 min, at a flow rate of 0.2 ml/min).

To estimate the amount of gametes released during the absorption of volatile compounds, chlorophyll *a* was extracted from gametes and quantified for each sample. After the looping, gametophytic thalli were removed from the flask, and the seawater inside was filtered using a Whatman filter paper (Grade GF/C). Pigments were extracted with 40 ml of 90% acetone from the gametes attached on the filter paper and the inside of the flask. The eluate was centrifuged at 3000 rpm for five mins at room temperature and the supernatant was analyzed with a UV-1200 spectrophotometer (Shimazu, Kyoto, Japan). The absorbance at 630 and 664 nm were measured and the proportion of chlorophyll *a* (solvent 90% aceton) was calculated following the equation: chlorophyll *a* = $11.47*A_{664} - 0.40*A_{630}$ (the symbol A_x denotes the absorbance at wavelength x; Jeffrey and Humphrey, 1975).

Fertilization capacity of asexual gametes

To examine fertilization capacity of asexual gametes (i.e., gametes from asexual populations), they were crossed with male and female gametes from sexual populations

using culture strains listed in Table 11. Asexual gametes were mixed with male or female gametes in a drop of medium and gamete behavior was observed using a light microscope in a culture room at 15°C. One zygote from the cross, A1 (asexual) × M2 (male) was isolated and cultured at 15°C under the short day condition and the zygote developed into a sporophyte and matured with unilocular sporangia. Hybrid gametophytes originating from a single unilocular sporangium (Table S8) were cultured at 10°C and parthenogenetic development of their gametes was observed.

Table 11. Culture strains of gametophytes used in this study.

	Culture strains	Collection location and date
Male		
	M1: Kannonzaki -3m	Kannonzaki, Kanagawa Pref., Japan. 2 Apr. 2000
	M2: Kannonzaki-4m	Kannonzaki, Kanagawa Pref., Japan. 2 Apr. 2000
	M3: Koinoura-1m	Koinoura, Fukuoka Pref., Japan. 31 Mar. 2000
	M4: Hazumisaki-1m	Hazumisaki, Aichi Pref., Japan. 30 Mar. 2003
	M5: Sakurajima-5m	Sakurajima, Kagoshima Pref., Japan. 3 Mar. 2003
	M6: Inubouzaki-6m	Inubouzaki, Chiba Pref., Japan. 4 Mar. 2002
Female		
	F1: Inubouzaki-8f	Inubouzaki, Chiba Pref., Japan. 4 Mar. 2002
	F2: Tsuyazaki-5f	Tsuyazaki, Fukuoka Pref., Japan. 31 Mar. 2000
	F3: Kiwado-5f	Kiwado, Heki, Yamaguchi Pref., Japan. 1 Apr. 2000
	F4: Sakurajima-4f	Sakurajima, Kagoshima Pref., Japan. 3 Mar. 2003
	F5: Kannonzaki-2f	Kannonzaki, Kanagawa Pref., Japan. 2 Apr. 2000
Asexual		
	A1: Oshoro-000510-17ax	Oshoro, Otaru, Hokkaido, Japan. 10 May 2000
	A2: Asari-2ax	Asari, Otaru, Hokkaido, Japan. 11 May 1999
	A3: Asari-3ax	Asari, Otaru, Hokkaido, Japan. 11 May 1999
	A4: Oshoro-000510-19ax	Oshoro, Otaru, Hokkaido, Japan. 10 May 2000
	A5: Muroran-20ax	Muroran, Hokkaido, Japan. 10 Mar. 2000
	A6: Muroran-13ax	Muroran, Hokkaido, Japan. 10 Mar. 2000
	A7: Muroran-15ax	Muroran, Hokkaido, Japan. 10 Mar. 2000

RESULTS

Sex ratio of field population

In total, 134 gametophytes were identified as *S. lomentaria* and the sex of 112 individuals was successfully determined using the sex markers (neither female nor male markers were amplified in some individuals; see Table S9). The sex ratio of each population is shown in Fig. 35. In the three asexual populations (Oshoro, Muroran and Aikappu, in Hokkaido), all asexual gametophytes were scored as "female." In the two sexual populations, both female and male gametophytes were detected: eight females and six males in Enoshima and eight females and 11 males in Hazumisaki.

Life cycle of an asexual population in Oshoro

In total, 16 sporophytic thalli were identified as *S. lomentaria* by the species-check PCR. PCR of the sex markers succeeded in 11 individuals and only the female marker was amplified, indicating that these 11 sporophytic thalli originated from parthenogenesis of asexual "female" gametes.

Asexual gametes were larger and had an increased parthenogenetic capacity compared with sexual gametes

All asexual, female, and male gametes showed negative phototaxis and asexual and female gametes had a shorter period of motility than male gametes and settled on the substratum (data not shown). Settled asexual gametes were ca. 5.0–6.0 μm in diameter, whereas settled female and male gametes were ca. 3.5–4.5 μm in diameter (Figs. 36 A–C and 37). Zygotes ranged 5.5–7.0 μm in diameter (Figs. 36D and 37). The GLMM predicted that the diameter of asexual gametes was significantly larger than that of female and male gametes and smaller than that of zygotes at the 1% significance level (Table 12).

Asexual gametes exhibited more rapid germination and cell division than female and male gametes, and the parthenogenetic development of asexual gametes was nearly

as rapid as the development of zygotes (Figs. 36E–H, 38, and 39). The ability of parthenogenetic development of male gametes was inferior to asexual and female gametes and 92–95% of 2-week-old germlings of male gametes remained at 1–3 cell stages and these germlings died within a month. The GLMM predicted that both germination rate and cell division rate were significantly larger in parthenogenesis of asexual gametes than in female and male gametes, and no significant difference was predicted between asexual gametes and zygotes at the 1 % significance level, except for the germination rate at 10°C in which the germination rate of zygotes was significantly larger than that of asexual gametes (Tables 13 and 14).

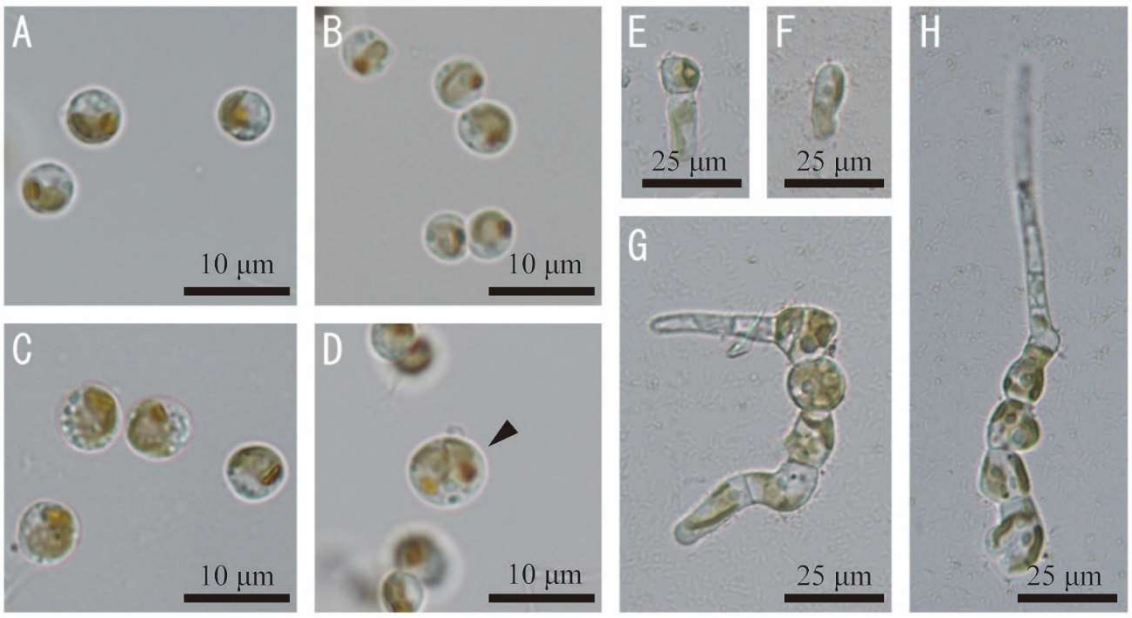

Figure 36. Gametes, zygote, and their 7-day-old germlings under a 10°C long day condition. (A) Female gametes from a strain, F3. (B) Male gametes from a strain, M6. (C) Asexual gametes from a strain, A6. (D) Zygote (arrowhead) formed by the cross F1 × M2. (E) 7-day-old germling of a female gamete from a strain, F3. (F) 7-day-old germling of a male gamete from a strain, M6. (G) 7-day-old germling of an asexual gamete from a strain, A4. (H) 7-day-old germling of a zygote formed by the cross, F1 × M2.

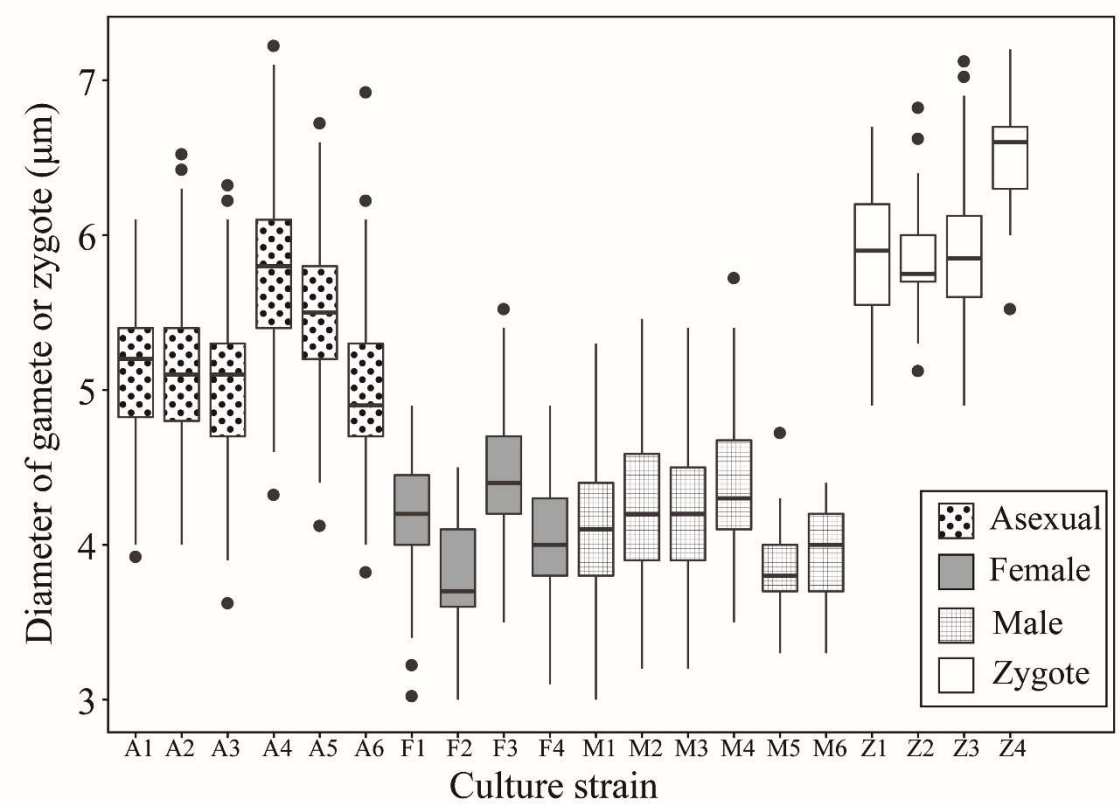

Figure 37. Box-and-whisker plots of diameters of gametes and zygotes from each strain and cross. Asexual gametes, female gametes, male gametes and zygotes are color-coded respectively. Codes for culture strains are listed in Table 11 and Table S8 The boxes and whiskers represent the interquartile range and the non-outlier ranges and the band near the middle of the box is the median. Black dots represent outliers.

Table 12. The effects of the experimental groups (asexual/male/female/zygote) on gamete/zygote size. Negative values for the coefficients of the experimental groups (asexual/male and asexual/female) indicate that male and female gametes were predicted as smaller than asexual gametes. Positive value for the coefficient of the experimental group, asexual/zygote, indicates that zygotes were predicted as larger than asexual gametes.

Diameter (gamete/zygote size)					
	Coef.	SE	df	*t* value	*p*
Intercept	5.29	0.1	14	51.3	< 0.001
Group (asex/male)	-1.15	0.17	14.7	-6.9	< 0.001
Group (asex/female)	-1.16	0.15	14.7	-7.9	< 0.001
Group (asex/zygote)	0.74	0.18	20.4	4.1	< 0.001

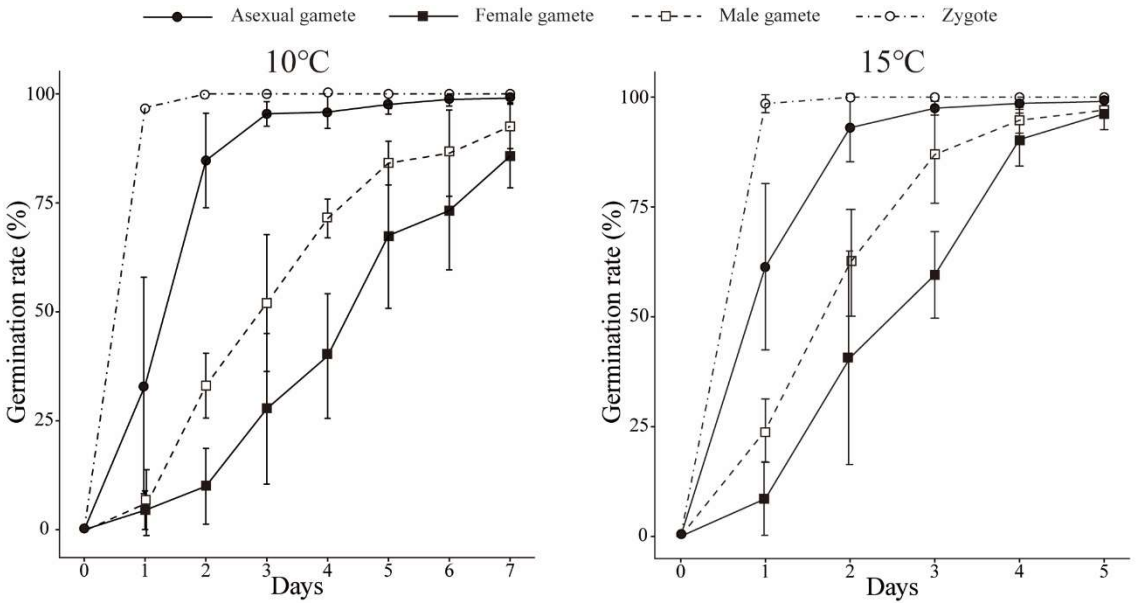

Figure 38. Line graphs displaying the germination rate (± SD) of gametes and zygotes at 10°C and 15°C.

Table 13. The effects of the days and the experimental groups (asexual/male/female/zygote) on the germination rate of gametes and zygotes at 10 and 15°C. Negative values for the coefficients of the experimental groups (asexual/male and asexual/female) indicate that germination rate of male and female gametes was predicted as lower than that of asexual gametes.

Germination rate								
	10°C				15°C			
	Coef.	SE	z value	*p*	Coef.	SE	z value	*p*
Intercept	-1.36	0.20	-6.7	< 0.001	-1.72	0.23	-7.5	< 0.001
Day	1.02	0.02	57.8	< 0.001	1.78	0.04	48.7	< 0.001
Group (asex/male)	-3.21	0.30	-10.7	< 0.001	-2.85	0.34	-8.4	< 0.001
Group (asex/female)	-1.93	0.28	-6.8	< 0.001	-1.55	0.32	-4.9	< 0.001
Group (asex/zygote)	0.79	0.38	2.1	0.04	0.80	0.42	1.9	0.06

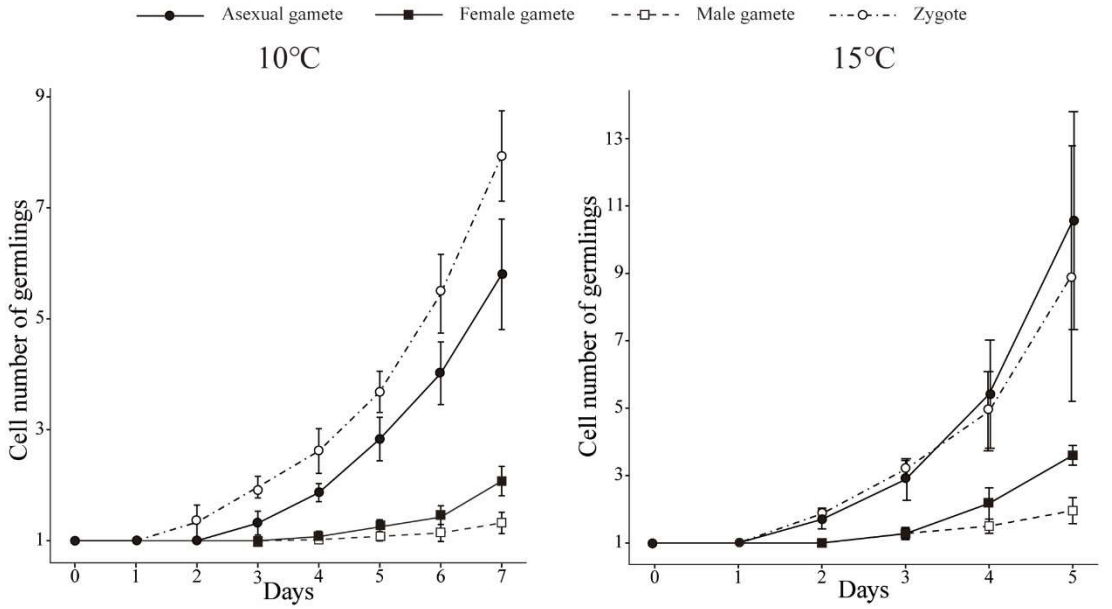

Figure 39. Line graphs displaying cell division rate (± SD) of germlings of gametes and zygotes at 10°C and 15°C.

Table 14. The effects of the days and the experimental groups (asexual/male/female/zygote) on cell division rate of gametes and zygotes at 10 and 15°C. Negative values for the coefficients of the experimental groups (asexual/male and asexual/female) indicate that asexual gametes showed higher cell division rate compared from male and female gametes.

Growth rate								
	10°C				15°C			
	Coef.	SE	z value	*p*	Coef.	SE	z value	*p*
Intercept	-0.05	0.04	-1.3	0.19	-0.09	0.07	-1.3	0.21
Day	0.22	0.00	57.5	< 0.001	0.45	0.01	81.5	< 0.001
Group (asex/male)	-0.76	0.05	-14.0	< 0.001	-0.85	0.11	-7.5	< 0.001
Group (asex/female)	-0.94	0.05	-18.2	< 0.001	-1.17	0.11	-10.9	< 0.001
Group (asex/zygote)	0.25	0.06	4.3	< 0.001	-0.06	0.11	-0.6	0.55

Sexual pheromone production and fertilization capacity of asexual gametes

The smell of the sexual pheromones was always detectable in cultures where female gametes were released, while little to no smell was detectable in cultures where asexual gametes were released. In the LC/MS analyses, the compound, of which molecular formula was predicted as $C_{11}H_{16}$ (same molecular formula as ectocarpene and hormosirene; see Maier and Müller, 1986), was detected with high intensity in female gametes of *S. shibazakiorum* and *S. promiscuus*, but neither in *S. lomentaria* asexual gametophytes nor males of *S. shibazakiorum* and *S. promiscuus* (Fig. 40). The amount of chlorophyll *a* extracted from gametes was 78.5 µg in *S. lomentaria* asexual gametophytes, 25.7 µg in *S. shibazakiorum* females, 51.7 µg in *S. shibazakiorum* males and 134.4 µg in *S. promiscuus* females (I failed to examine *S. promiscuus* males). This indicates that,

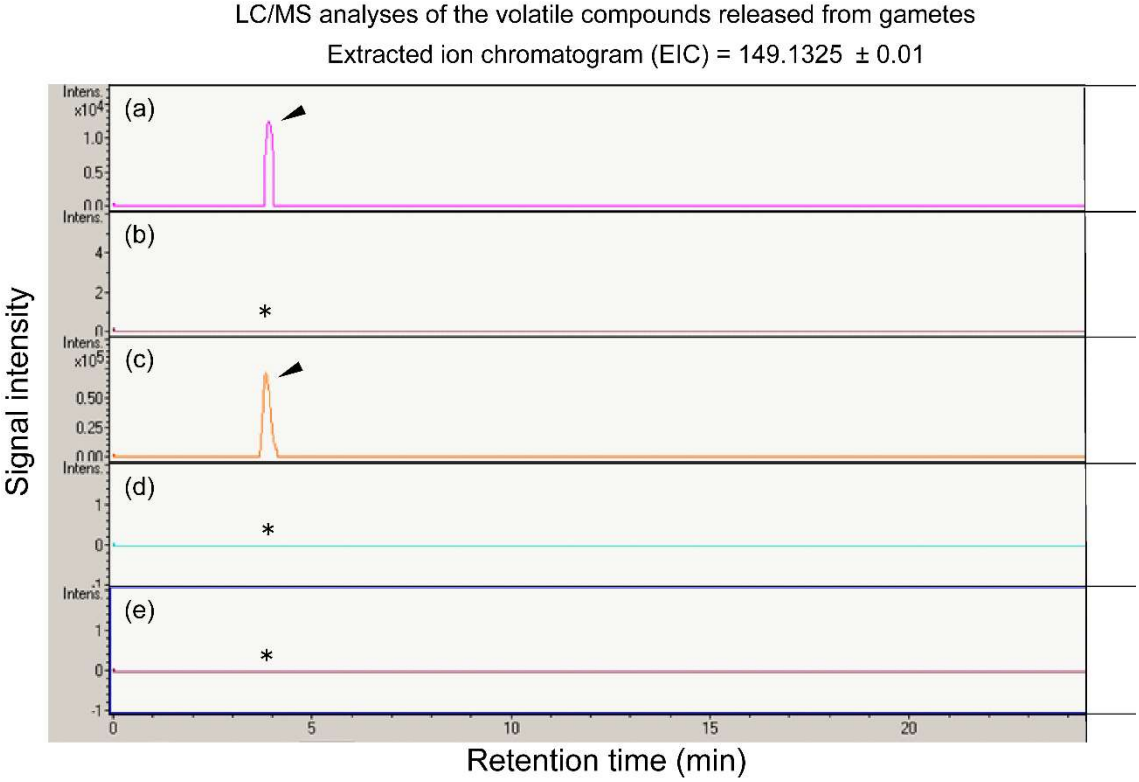

Figure 40. Results of the LC/MS analyses of the volatile compounds released from gametes: extracted ion chromatograms for the expected ion, $[C_{11}H_{16} + H]^+$ (*m/z*; 149.1325 ± 0.01). The compound predicted as $C_{11}H_{16}$ was detected with high intensity at around 3.9 min from the female gametes of *S. shibazakiorum* and *S. promiscuus* (arrowhead), but neither from asexual gametes of *S. lomentaria* nor male gametes of *S. shibazakiorum* and *S. promiscuus* (asterisk). (a) *S. shibazakiorum* female gametes. (b) *S. lomentaria* asexual gametes. (c) *S. promiscuus* female gametes. (d) *S. shibazakiorum* male gametes. (e) *S. promiscuus* male gametes.

although *S. lomentaria* asexual gametophytes released much gametes than *S. shibazakiorum* females, their gametes did not secrete enough sexual pheromones to be detected by the LC/MS.

Gametes from six out of seven asexual strains fused with male gametes, but not with female gametes. Zygotes originated from the cross A1 (asexual) × M2 (male) developed into sporophytes and at maturity produced unilocular sporangia. Zoospores from a single unilocular sporangium developed into both male and female gametophytes. These F_1 hybrid female gametophytes (Table S8) released gametes which do not have a detectable smell of the sexual pheromone, similar to the parental asexual gametophytes. Gametes from the F_1 hybrid gametophytes showed an intermediate cell division rate in their parthenogenetic development compared with those of their parental strains (Fig. 41). Furthermore, gametes from F1 hybrid male gametophytes did not show high mortality which was observed in those from their parental male strain. One asexual strain, A5, which had been determined as female by the sex-marker PCR, produced gametes that neither fused with female nor male gametes.

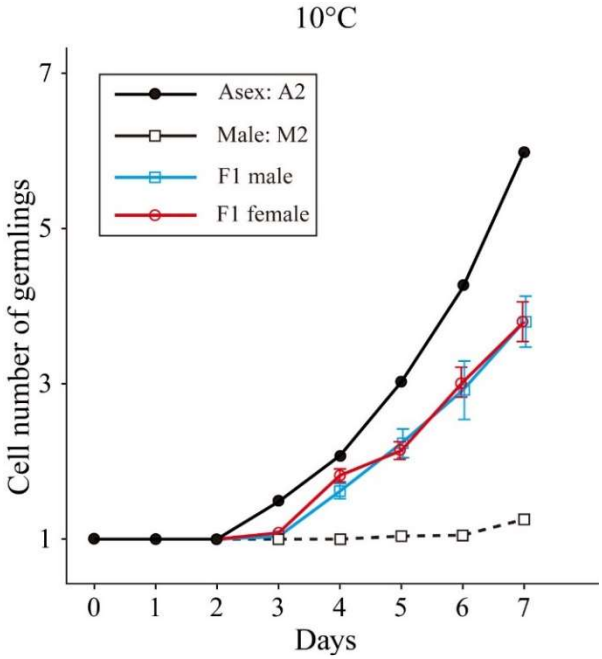

Figure 41. Line graphs displaying growth rate of germlings (±SD of the strains) of gametes from parental strains (asexual strain A2 and male strain M2) and their F1 hybrid strains (F1 male strains and F1 female strains) at 10°C.

DISCUSSION

Reproductive mode of the *S. lomentaria* species Ia asexual populations

I demonstrated that the asexual populations of *S. lomentaria* consist of only "female" individuals and that these "females" reproduce asexually through parthenogenesis and undergo the alternation of a gametophytic stage and a sporophytic stage in the life cycle. Thus, in the case of asexual populations of *S. lomentaria*, the absence of gamete fusion is not due to the previously hypothesized factors such as unsuitable culture conditions (Peters, 1987) or transient production of sexual gametes (Clayton, 1982), but instead due to their completely female-biased sex ratio. Female dominant populations have also been reported in anisogamous brown algae in which the sex of gametophytes is distinguishable by size of their gametangia: *Mutimo cylindricus* (as *Cutleria cylindrica* Okamura; Kitayama et al., 1992) and *Colpomenia peregrina* (Yamagishi and Kogame, 1998). In isogamous taxa including *S. lomentaria*, the sexes of the gametophytes are morphologically indistinguishable. Thus, although reports of populations with no sign of sexuality are not scarce in isogamous brown alga, the sex of gametophytes in those populations has been unclear such as in the following cases: e.g., *Petalonia binghamiae* (J.Agardh) K.L.Vinogradova (as *Endarachne binghamiae* J. Agardh; Wynne, 1969), *Ectocarpus siliculosus* (Müller, 1977), *Leathesia marina* (Lyngbye) Decaisne (as *Leathesia difformis* Areschoug; Peters, 1987), *Eudesme virescens* (Carmichael ex Berkeley) J.Agardh (Peters, 1987). Interestingly, Müller (1977) reported that his asexual strains of *E. siliculosus* produced larger zoids and a detectable smell of the sexual pheromone. Although he hypothesized contamination of females in his asexual strains (Müller, 1977), there is a possibility that his asexual strains were also "female" and still retained sexual pheromone production. Sex ratio investigation using PCR-based sex markers may be able to provide insightful information in reproductive mode of isogamous brown algae including the previously mentioned taxa.

In *S. lometaria*, the evolution of the asexual populations is possibly the response

to a cold environment. The asexual populations have been only found in the cold waters of Hokkaido (Kogame et al., 2015a) and the geographic distribution of asexuals seems to be biased towards colder environments compared with that of sexuals (Fig. 35; Kogame et al. 2015a). At present, I have no clear idea of how environment and the reproductive mode of this species interact. Interestingly, in the green alga *Ulva mutabilis*, abortive mating reportedly increased with decreasing temperature, and it has been theoretically predicted that populations in cold environment will tend to quit sexual reproduction and rely on parthenogenesis (Løvlie and Bryhni, 1976, 1978). Examination of the relationships between fertilization success and temperature, and further sex ratio investigation through the whole distribution area are needed to understand the origin of the parthenogenetic populations in *S. lomentaria*.

Effectiveness of PCR-based sex markers and the importance of molecular phylogenetic analyses

This study showed that PCR-based sex markers can be a powerful approach to investigate the sex ratio of isogamous brown algal populations in which morphological sex determination is impossible. In brown algae, PCR-based sex markers have been developed and used in *Ectocarpus* (Couceiro et al., 2015) and in kelps (Lipinska et al., 2015) with the recent identification of sex specific regions in brown algal genomes (Ahmed et al., 2014). PCR-based sex markers can rapidly determine sex if DNA of sufficient quality can be extracted. This is quite advantageous compared to the time-consuming sex determination method of crossing experiments and makes large-scale investigations of sex ratio feasible.

Molecular phylogenetic analysis is also essential for the accurate understanding of reproductive strategies of populations. In many algal taxa, species level delimitation is often difficult due to their morphological simplicity and plasticity (Leliaert et al., 2014). With the advent of rapid DNA sequencing and development of phylogenetic analyses, unexpected cryptic species diversity has been revealed, and in some cases, these cryptic

species have been found in a sympatric manner (e.g., Montecinos et al., 2017; **Chapter 1**). If multiple cryptic species having different reproductive strategies exist sympatrically, there is a possibility of misunderstanding reproductive strategies of populations. For example, Han et al. (2014) mentioned that the gametophytes of *S. lomentaria* at Muroran produce gametes in late winter and spring and produce asexual zoids in late spring. However, the thalli reproducing sexual gametes and the thalli reproducing asexual zoids actually belong to distinct species which have slightly different seasonal occurrence (*S. promiscuus* and *S. lomentaria*, respectively; personal communication with Dr. T. Motomura and unpublished observation). In the present study, sexually reproducing cryptic species were also found sympatrically with the *S. lomentaria* asexual populations (at Oshoro, Muroran, Aikappu): *S. shibazakiorum* and *S. promiscuus* at Oshoro, *S. promiscuus* at Muroran and *S. shibazakiorum* at Aikappu.

Decay of a sexual trait and acquisition of asexual traits

Sexual pheromones of brown algae have been known to have a detectable, fragrant smell (Maier and Müller, 1986). However, I detected little/no smell of a sexual pheromone in "female" gametes from the asexual populations and the LC/MS analyses also failed to detect sexual pheromones from them. In the crossing experiments, the F_1 hybrid female gametophytes between the asexual "female" and the male gametophyte had no detectable smell of a sexual pheromone. This indicates that decreased pheromone production is a heritable trait and "females" in asexual populations have reduced their sexual pheromone production. In brown algae, sexual pheromones play an important role to attract conspecific male gametes (Peters, 1987; Fu et al., 2014). Therefore, sexual pheromone production is certainly an adaptive trait in sexual populations. In asexual populations, on the other hand, pheromone production is unlikely to be an adaptive trait because there are no male gametes to attract and the energy cost to produce sexual pheromone is wasteful. It has been suggested that a formerly adaptive trait can be reduced, when that trait is neutral or maladaptive in the new selective environment (Hall and Colegrave, 2008; van

der Kooi and Schwander, 2014). Although I am not sure whether the pheromone production is neutral or maladaptive in the asexual population, it is likely that pheromone production has reduced in all-female asexual populations. Decay of sexual pheromone production in parthenogenetic all-female lineages has been also reported in insects (reviewed in van der Kooi and Schwander, 2014). In brown algae, it has been reported that zoids from some asexual species do not produce pheromones, although the sex of the individuals of these asexual species has not been examined (Peters, 1987).

Crossing experiments also showed that one culture isolate of an asexual "female" gametophyte, A5, lacked fertilization capacity. Loss of fertilization capacity of eggs is a common phenomenon in asexual lineages of animal species (van der Kooi and Schwander, 2014). Low fertilization capacity of female gametes from female-dominant populations has been reported also in anisogamous brown alga *Mutimo cylindricus* (Kitayama et al., 1992). Unfortunately, quantitative analysis of fertilization rate of female gametes is difficult in isogamous *S. lomentaria* because unfused female gametes and male gametes are morphologically indistinguishable. It is unclear whether "female" gametes from the asexual populations also have low fertilization capacity in the present study.

While "females" in the asexual populations might have reduced a sexual trait (i.e., sexual pheromone production), they have acquired some possibly adaptive traits in the no-male environment: larger gamete size and high parthenogenetic capacity (rapid germination and cell division). Gamete size may reflect a change in resource allocation for early development. A gamete has only half of an initial resource of a zygote. Therefore, in asexual populations, it would be adaptive to produce larger gametes, although production of larger gametes may result in a reduction of the total number of gametes. Crossing experiments between asexual "female" and male gametophytes showed that the capacity of rapid parthenogenetic development is also a heritable trait. Apparently "female" gametes have acquired some genetic change that enhances parthenogenetic capacity. Further investigation of the inheritance pattern of high parthenogenetic capacity

is required to reveal the genetic bases of this asexual trait.

Chapter 6

Geographic parthenogenesis in the brown alga *Scytosiphon lomentaria* (Scytosiphonaceae): sexuals in warm waters and parthenogens in cold waters.

INTRODUCTION

Parthenogenesis is a way of asexual reproduction in which an unfertilized gamete develops into a new individual. Although sex is the predominant mode of reproduction in nearly all multicellular organisms, organisms reproducing only by parthenogenesis (obligate parthenogens) are numerous across the tree of life. An important ecological pattern is geographic parthenogenesis, a phenomenon where parthenogens and their close sexual relatives have distinct geographic areas. Parthenogens often have a biased distribution toward particular environmental settings (e.g., high latitude, high altitude, deserts, islands and 'marginal', 'disturbed' or 'ecotonal' environment) when compared with close sexual relatives (Kearney, 2005; Tilquin and Kokko, 2016). The loss of sex (or success of parthenogens) in particular environmental settings has been an interesting topic in evolutionary biology, shedding light on the cost and benefit of sex, adaptation to marginal habitats, role of hybridization and polyploidy in evolution (e.g., Lynch, 1984; Bierzychudek, 1985; Kearney, 2005; Hörandl, 2009).

In brown algae (Phaeophyceae), parthenogenesis is a common phenomenon. Even in sexual lineages, parthenogenetic development of unfused gametes is common in laboratory culture (Luthringer et al., 2014), and it has been also detected from sexual field populations at low frequency [e.g., Oppliger et al., 2007; Klochkova et al., 2017; Hoshino and Kogame, 2019 (**Chapter 4**)]. There are numerous reports of populations speculated to have an obligate parthenogenetic life cycle [i.e., populations in which sexual reproduction cannot be observed in culture conditions; e.g., Wynne, 1969; Müller, 1977; Peters, 1987; Kogame and Kawai, 1993; Hoshino et al., 2020a (**Chapter 3**)]. However, there are only few reports in which these populations were compared with their close sexual relatives and it remains largely unclear in what kind of environment parthenogenesis is favored and how parthenogens arise.

To the best of my knowledge, there are only three cases in which brown algal asexuals have been compared with close sexual relatives in detail. The first example is

Fucus radicans L.Bergström & L.Kautsky, a species endemic to the brackish water of the Baltic Sea (Bergström et al., 2005). Although parthenogenesis is not known in this species, it has asexual populations that are maintained by clonal reproduction using adventitious branches (as dwarf morphotype of *F. vesiculosus* Linnaeus; Tatarenkov et al., 2005). In this species, asexual populations tend to be distributed in lower salinity area than sexual populations (Ardehed et al., 2015). It has been posited that low salinity restricts sexual reproduction due to lysis of the egg cell or polyspermy (Serrão et al., 1999), which could favor a switch to asexual reproduction (Tatarenkov et al., 2005; Ardehed et al., 2015). Although this is a convincing and interesting hypothesis for the evolutionary process of asexual lineages, it cannot be applied to asexuals living in saline environments where the majority of brown algal asexuals occur. The second example is *Mutimo cylindricus* (Okamura) H.Kawai & Kitayama in the Japanese Islands. In *M. cylindricus*, female-dominant parthenogenetic populations were parapatric with sexual populations in the Tsugaru Strait (Fig. 42; the strait between Hokkaido and Honshu), the northern limit of this species (as *Cutleria cylindrica* in Kitayama et al., 1992). However, since sex ratio investigations over the entire distributional area in Japan has not been conducted yet (Kitayama et al., 1992; Kogishi et al., 2010), it is unclear if the parthenogens exist only in its northern limit. The last example is *Scytosiphon lomentaria* [Hoshino et al., 2019 (**Chapter 5**)].

Scytosiphon lomentaria (Scytosiphonaceae) is distributed in warm and cold temperate waters worldwide and, in Japan, it has been reported from Hokkaido to Kyushu [Fig. 42; Hoshino et al., 2020c (**Chapter 2**)]. It has a heteromorphic life history: an alternation of generation between the macroscopic dioicous isomorphic gametophytes and the microscopic discoid sporophyte (Nakamura and Tatewaki, 1975). Its sexual reproduction is isogamous; female gametes settle on the substratum sooner than male gametes and secrete sex pheromones that attract male gametes (Fu et al., 2014). In Japanese population, in addition to sexual populations including both females and males,

parthenogenetic populations consisting of only females are known [Hoshino et al., 2019; (**Chapter 5**)]. So far, parthenogenetic populations have been found only in Hokkaido, and sexual populations have been reported in southern Honshu [Hoshino et al., 2019 (**Chapter 5**)]. Females in the parthenogenetic populations release gametes that are larger in size, produce lesser sex pheromones, and their parthenogenetic development is rapid, compared with females in the sexual populations [Hoshino et al., 2019 (**Chapter 5**)].

In the present study, I focused on *S. lomentraia* and aimed to reveal in what kind of environments parthenogenesis is favored over sexual reproduction and how parthenogens have arisen. Using the samples from nearly the whole distributional area of *S. lomentaria* (33 localities in Japan, three localities in Europe, and two localities in Argentina), I conducted (i) sex ratio investigations, (ii) phylogenetic and population

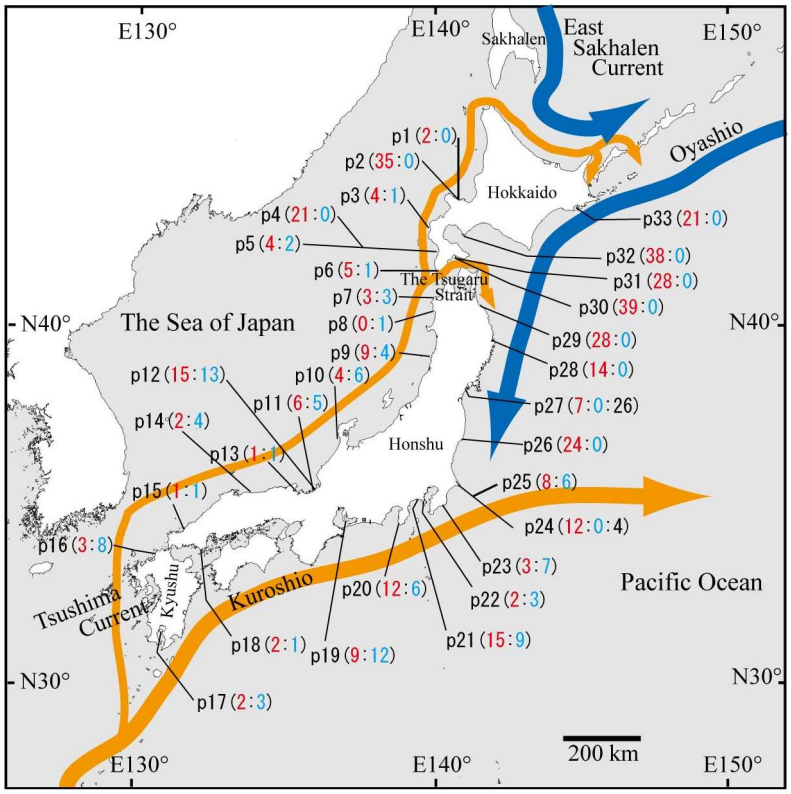

Figure 42. Map of Japan showing collection localities of samples used in this study. A population code (p1–p33) is given to each population. The sex ratio of each population is given in parenthesis: the number of females is represented in red color, males in blue, and samples having both female and male markers are in black. Warm ocean currents (Kuroshio and Tsushima currents) are presented in orange color and cold ocean currents (Oyashio and East Sakhalen currents) are in blue.

genetic analyses based on mitochondrial *cox*1, nuclear *cetn*-int2, and genome-wide SNP markers, (iii) crossing experiments, karyotype observations, and analyses of sex pheromone production.

MATERIALS AND METHODS

Sampling, DNA extraction, and taxonomic identity

Scytosiphon lomentaria gametophytes examined in this study were collected from 33 localities in Japan (Fig. 42; population code p1–p33), two localities in Argentina [Puerto Madryn (PM) and San Antonio Oeste (SAO)], and three localities in Europe (Slea Head, Portrush, Ona; Table 15). These samples included previously collected specimens [Kogame et al., 2005, 2015a, 2015b; Hoshino et al., 2019 (**Chapter 5**), 2020c (**Chapter 2**)]. For newly collected samples, a fragment of each sample was preserved in a silica-gel for molecular analyses and unialgal culture isolates were also established for same samples as previously described by Kogame et al. (2015a). Pressed specimens were made for all samples and deposited as vouchers in the Herbarium of Faculty of Science, Hokkaido University, Sapporo, Japan (SAP) or in the Herbarium of Universidad Nacional der Sur, Bahia Blanca, Argentina (BBB). For molecular analyses, total genomic DNA was extracted from the cultured and silica gel-dried thalli as previously described (Hoshino et al., 2020b) and used as template DNA for PCR.

Since six cryptic species of *S. lomentaria* have been reported in Japan [Hoshino et al., 2020c (**Chapter 2**)], all samples were screened by species-check PCR [primers and PCR conditions are in Hoshino et al., 2019 (**Chapter 5**)]. In this PCR, the partial mitochondria *cox*1 gene are amplified only in *S. lomentaria*. The presence/absence of PCR products was determined by 1% agarose-gel electrophoresis.

Sex ratio investigation

To reveal the geographical distribution of parthenogenetic populations (female-dominant

populations) and sexual populations, sex ratios of 38 populations (localities) were investigated. Since sex of *S. lomentaria* gametophytes is morphologically indistinguishable, sex of each sample was identified by sex-check PCR or crossing experiments. In the sex-check PCR, partial sequences of the sex-specific non-recombining region on the sex chromosome (female U chromosome and male V chromosome) of *S. lomentaria* were used as sex markers and were amplified as in Hoshino et al. (2019; **Chapter 5**). The sex of each samples was confirmed by the presence/absence of PCR products in 1% agarose-gel electrophoresis. In the crossing experiments, gametes of each sample were crossed with male and female gametes from sexual populations using culture strains following the methods outlined in Hoshino et al. (2018; **Chapter 1**).

Phylogenetic analyses of mitochondrial and nuclear markers

To roughly understand the genetic structure of parthenogenetic populations, I conducted phylogenetic analyses using 5' end of cytochrome oxidase I (*cox*1) gene as a mitochondrial marker and the second intron of centrin gene (*cetn*-int2) which is a single copy nuclear gene in *S. lomentaria* (Nagasato et al., 2004). PCRs and sequencing were performed as in Kogame et al. (2015a). In the samples from p24 and p27, I observed double peaks in the whole region of *cetn*-int2 suggesting that these samples had multiple *cetn*-int2 haplotypes. Therefore, fusion cloning (Fu et al., 2014) was performed to obtain each sequence. Newly generated sequences (Table Sl0; *cox*1: 208 sequences from 26 populations; *cetn*-int2: 99 sequences from 34 populations) were aligned with the previously generated sequences including those of related *Scytosiphon* species (Table S10; Kogame et al., 2015; McDevit and Saunders, 2017; Hoshino et al., 2018, 2020c; **Chapter 1**; **2**) using CLUSTAL W (Thompson et al., 1994) in MEGA v. 7 (Kumar et al., 2016) with default parameters. *Cox*1 dataset was 600 bp and the sequences less than 600 bp were excluded. For *cetn*-int2 dataset, gaps and highly variable regions were omitted

using Gblocks web server (http://molevol.cmima.csic.es/castresana/Gblocks_server.html; Castresana, 2000) and the final dataset consisted of 604 bp.

For *cox*1 dataset, phylogenetic relationships among the *cox*1 haplotypes were reconstructed using median-joining methods (Bandelt et al., 1999) in Network v. 5.0.1.0. For *cetn*-int2 dataset, a maximum likelihood tree was constructed using RAxML version 8.2.10 (Stamatakis, 2014) with 1000 bootstrap pseudoreplicates under the GTR-GAMMA, through Cipres Science Gateway version 3.3 (Miller et al., 2010).

Population genetic analyses based on genome-wide SNPs

Library preparation and data processing

For the discovery of single nucleotide polymorphisms (SNPs), multiplexed ISSR genotyping by sequencing (MIG-seq) was conducted following the procedure by Suyama and Matsuki (2015) with a slight modification: annealing temperature of the first PCR was changed from 48°C to 38°C. Both ends of fragments were obtained by paired-end sequencing (read 1 and 2), but only read 1 was used for the following analyses. Low-quality reads were removed by FASTX-Toolkit (http://hannonlab.cshl.edu/fastx_toolkit/) using *quality_filter* option under the setting of q = 30 and p = 40. To remove the reads derived from extremely short library entries, the sequence primer regions in the sequences were searched and the reads which had the primer sequence were removed by FASTX-Toolkit using *fastx_clipper* option.

De novo assembly was performed using Stacks v. 2.53 (Catchen et al., 2013). Since my samples are gametophytes, they should be haploid. However, some samples had both female and male markers or two haplotypes of nuclear marker *cetn*-int2 suggesting their diploidy. Therefore, at first, I performed assembly with the following parameters assuming that all samples are diploid: minimum number of identical reads required to create a stack (m = 3), the nucleotide mismatches between loci within a single individual

(M = 2), the mismatches between loci when building the catalogue (n = 1), and other parameters were set default. The SNP genotype for each individual was exported using the '*populations*' command; only the first SNP was extracted from each putative locus using the flags --*write_single_snp*. As I expected, samples having some heterozygous loci were found (all samples from p24, p27, and one samples from Ona). Then, without these samples, the second assembly was performed with the following parameters assuming that all samples are haploid. The minimum number of identical reads required to create a stack (m = 3). The maximum number of mismatches to create putative loci was set to zero (M = 0). Furthermore, since calling stacks from the secondary reads (reads that are not distinguishable from sequencing error) produced heterozygosity within individuals, it was disabled using the flags -N (set to zero) and -H. The maximum number of mismatches between loci when building the catalogue was set to one (n = 1). The SNP genotype for each individual was exported using the '*populations*' command; only the first SNP was extracted from each putative locus using the flags --*write_single_snp*.

Both diploid and haploid datasets were processed using PLINK v. 2.00 (Chang et al., 2015; www.cog-genomics.org/plink/2.0/). SNPs with a minor allele frequency < 0.03, loci with a missing individual rate > 0.7, and individuals with a missing locus rate > 0.7 were filtered out. The diploid dataset included 237 samples from 36 populations, 818 SNPs (loci), and the mean genotyping rate was 50.2%. The haploid dataset included 212 samples from 34 populations, 865 SNPs (loci), and the mean genotyping rate was 48.8%. Format of the output files of PLINK was converted using PGDSpider2 (Lischer and Excoffier, 2012) for subsequent analyses.

Gene diversity and clonal diversity

Gene diversity (expected heterozygosity: *He*) of each population was calculated using '*genetic diversity*' function of GenoDive v. 3.04 (Meirmans and Van Tienderen, 2004; Meirmans, 2020). To examine clonal diversity, the number of clonal lineages was assessed using '*assign clone*' function of GenoDive. The function works by first

calculating a matrix of genetic distances, and then choosing a threshold distance (Meirmans, 2020). If the distance between a pair of individuals is below the threshold, they are deemed to belong to the same clonal lineage (Meirmans, 2020). I calculated a matrix of genetic distances using an infinite allele model (in this calculation, missing data were discarded) and determined the threshold distance. Each clonal lineage was treated as a single genotype and Nei's (1987) genetic diversity corrected for samples size (*Div*) was calculated for each population using '*clonal diversity*' function. Clonal diversity index *R* (Dorken and Eckert, 2001) was also calculated. The index *R* was calculated by the equation: $R = (G\text{-}1)/(N\text{-}1)$, where *G* is the number of distinct genotypes and *N* is the total number of sampled individuals.

Population genetic structure

To assess population genetic structure, Bayesian clustering analysis and principal component analysis (PCA) were conducted for both haploid and diploid datasets. Bayesian clustering analysis was performed using STRUCTURE v. 2.3.4 (Pritchard et al., 2000). The number of clusters (*K*) of 1–10 was tested by running 10 simulations for each *K*, with 100,000 Markov chain Monte Carlo steps and a burn-in of 100,000, using the model with admixture and correlated allele frequencies. The meaningful number of *K* was determined based on the mean estimated Ln probability of the data [LnP(*K*)] and the second-order rate of change in the log probability of the data (ΔK; Evanno et al., 2005). The ΔK values were calculated using STRUCTURE HARVESTER v. 0.6.94 (Earl and vonHoldt, 2012). Principal component analysis was performed using PLINK and the results were visualized using R software v. 3.6.0 (R Core Team, 2019). To reveal phylogenetic relationships between parthenogenetic and sexual populations, a phylogenetic network was constructed based on uncorrected *P* distances using NeighborNet method (Bryant and Moulton, 2004) in SplitsTree v. 4.15.1 (Huson and Bryant, 2006).

Chromosome observation

To examine ploidy level of individuals in parthenogenetic and sexual populations, the number of chromosomes was counted in two females from parthenogenetic populations (p2 and p32) and two females from sexual populations (p15 and p22). Small pieces of cultured gametophytes were fixed in a 3:1 mixture of ethanol and glacial acetic acid at 2 h after the light-period of the culture chamber, and chromosomes were stained by aceto-iron-haematoxylin-chloral hydrate methods (Yabu and Tokida, 1966).

Sex pheromone production

Molecular data suggested that the Pacific coast parthenogenetic populations are genetically distinct from the Sea of Japan coast parthenogenetic populations which include p2 of which sex pheromone production was analyzed in Hoshino et al., (2019; **Chapter 5**). Thus, the parthenogens in the Pacific side were newly examined whether they produce sexual pheromone using a gas chromatography/mass spectrometry (GCMS). Females from parthenogenetic populations p28 were used for GCMS. Cultured gametophytes were kept in 300 mL of sterilized seawater in a 500 mL flask at 15°C and gametes were released in the flask. Volatile secretions were trapped on Mono Trap RCC18 (GL science, Tokyo, Japan) using a closed-loop-stripping system at 15°C. After looping 15 h, absorbed volatile compounds were eluted with 50 μL of CH_2Cl_2 and immediately analyzed by GCMS. [Zebron ZB-wax (phenomenex) 30 m × 0.25 μm; He as the carrier gas; program rate: 45-200°C at 5°C/min]. Compounds were identified by using the NIST MS library and similarity search program. A female gametophyte from sexual population p15 was also analyzed as positive control.

RESULTS

Sex ratio and geographic distribution of sexual and parthenogenetic populations

Results of sex check by sex-check PCR and crossing experiments were almost concordant.

However, in sex-check PCR, some samples from p24, p27, and Argentina had both female and male markers. In crossing experiments, samples from p27 released gametes fused with male gametes of p22 (Table S10) and did not function as male gametes. Therefore, the samples having both markers were considered female (at least, phenotypically).

In the Sea of Japan coast, populations including males (sexual populations) were found from Kyushu to Hokkaido, and distributions of the sexual populations and populations without males (parthenogenetic populations) overlapped in the west coast of Hokkaido (Fig. 42). In the Pacific coast, sexual populations were limited to the south of

Figure 43. Sampling localities of the parapatric sexual and parthenogenetic populations.
(A) Parthenogenetic population p4 and sexual population p5 at Esashi, Hokkaido.
(B) Parthenogenetic population p24 and sexual population p25 at Choshi, Chiba Prefecture.

Choshi, Chiba Pref. (the sampling locality of p24 and p25) and parthenogenetic populations were found to the north of Choshi (Fig. 42). Sexual and parthenogenetic populations were parapatric in these two localities: Esashi, the west coast of Hokkaido (p4 and p5) and Choshi (p24 and p25). At these localities, the two types of populations were 1 km and 0.3 km apart along the coast, respectively (Fig. 43). In both localities, parthenogenetic populations were found in upper intertidal zone in wave-exposed area, and sexual populations were found in lower intertidal zone of relatively protected area. No males were found from European and Argentinean samples (four and 17 samples, respectively; Table S10).

*Cox*1 haplotype network

A total of 37 haplotypes were detected in *S. lomentaria*, and these haplotypes formed

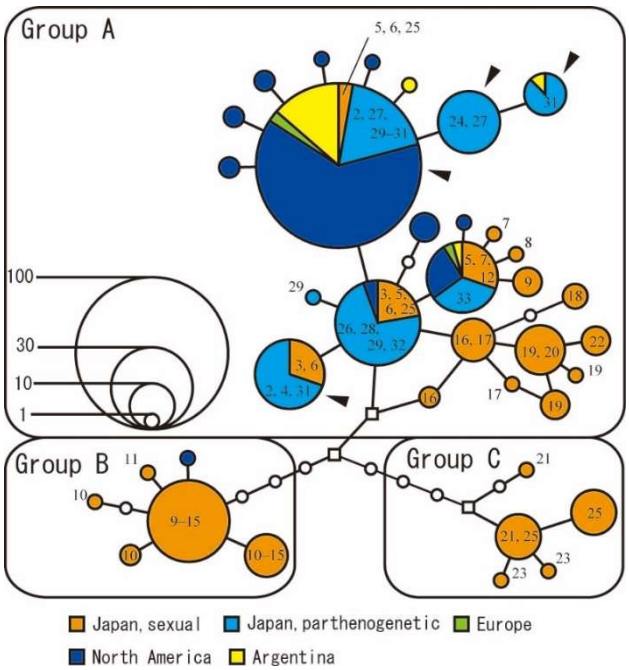

Figure 44. *Cox*1-haplotype network. Population codes [1–33 (without 'p')] are given to the haplotypes of Japanese samples. Sampling region of samples is represented as different colors. For the samples from Japan, samples from sexual and parthenogenetic populations were represented in different colors. Each colored circle represents a haplotype and its size is proportional to its frequency. White circles represent hypothetical unsampled haplotypes. White squares represent median vectors. Haplotypes indicated by arrowheads were found in 6–45 samples of which sex was identified, but none of these samples were identified as male (female or samples having both female and male markers).

three haplogroups (group A–C; Fig. 44). Group A had 26 haplotypes and was detected from all over Japan, Europe, North America (both Pacific and Atlantic sides), and Argentina. Group B had six haplotypes and was detected from the Sea of Japan side of southern Honshu and North America. Group C had five haplotypes and was detected from the Pacific side of central Honshu. Samples of parthenogenetic populations from Japan had group A haplotypes without exception. Most haplotypes from Europe, North America, and Argentina were identical or close to those from parthenogenetic populations from Japan, and formed a big star-like network pattern (i.e., one frequent haplotype together with several less frequent haplotypes). Group A included haplotypes which did not found in male samples (haplotypes indicated by arrowheads in Fig. 44). Although these haplotypes were found in 6–45 samples of which sex was identified, but none of these samples were identified as male.

cetn-int2 molecular phylogeny

Populations from the Pacific coast and the Sea of Japan coast tended to have different haplotypes, but this tendency was not clear in the populations from Kyushu and Tsugaru Strait (p16, p30, and p31) where the two seas meet (Fig. 42). Samples from parthenogenetic populations p24 and p27 had two *cetn*-int2 haplotypes; the one haplotype was common in the Pacific coast parthenogenetic populations and the other was common in the Sea of Japan coast sexual populations (Fig. 45).

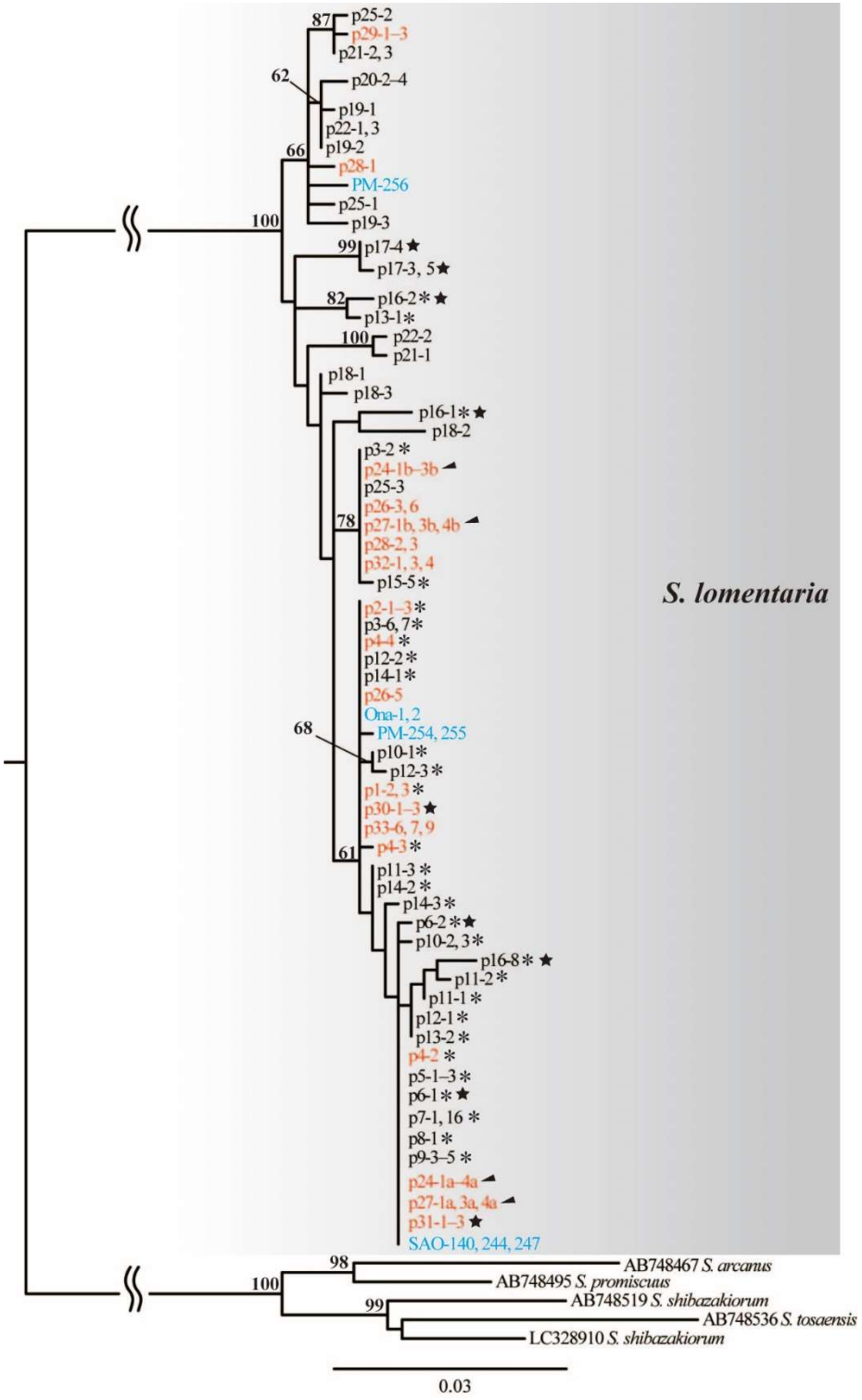

Figure 45. Maximum likelihood tree based on the nuclear *cetn*-int2 (604 bp). Numbers on branches indicate bootstrap percentage from ML analysis. Only bootstrap percentages ≥ 60% are shown. The labels of samples from parthenogenetic populations are indicated in red color, those from sexual populations are in black, and those from Argentina and Europe are in blue. Asterisks are given to the samples from the Sea of Japan coast (p1–p16). Stars are given to the samples from the Tsugaru Strait and Kyushu (p6, p16, p17, p30, and p31). Arrowheads indicate the two haplotypes found in samples from p24 and p27.

SNPs data analyses

Genetic diversity and clonal diversity

Parthenogenetic populations tended to have lower gene diversity (*He*; Table 15). Gene diversity was around 0.10 in most sexual populations, while that of parthenogenetic populations was often below 0.05. Although parthenogenetic populations p24 and p27 showed high gene diversity, it is probably because individuals in these populations have two distinct genomes.

Genetic distances between individuals showed that parthenogenetic populations included more genetically identical/nearly identical individuals than sexual populations (Fig. 46). Histograms of the genetic distances based on haploid and diploid datasets were similar in shape, except for that the genetic distances based on the diploid dataset were double of those of the haploid dataset (Fig. 46). Histograms based on haploid dataset showed that pairs of individuals having genetic distance of less than 11 were rare in sexual populations (i.e., seven pairs), but abundant in parthenogenetic populations (i.e., 221 pairs). In Hoshino and Kogame (2019; **Chapter 4**), I showed that parthenogenesis rarely occurs in a sexual population of *Scytosiphon shibazakiorum*. Therefore, I considered that

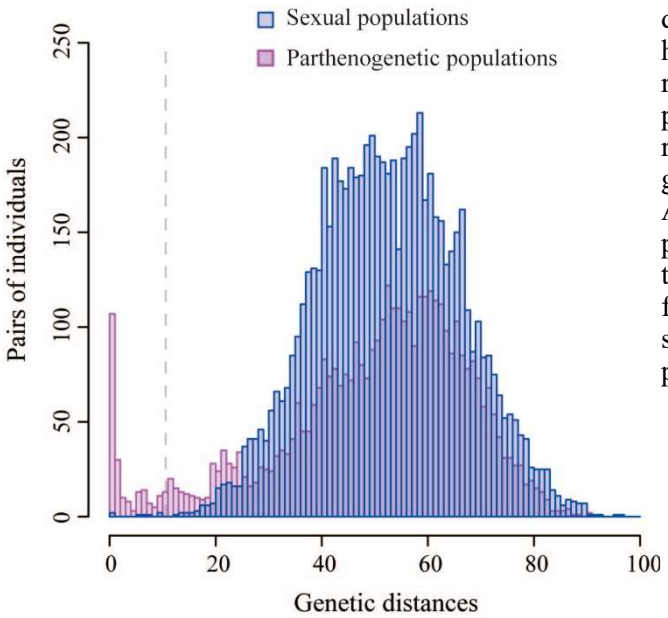

Figure 46. Histograms showing genetic distances between samples based on the haploid dataset. Different colored bars represent sexual and parthenogenetic populations. The threshold distances (10) to recognize clonal lineages is indicated by a grey broken line. Samples from Europe and Argentina are included in the histogram for parthenogenetic populations. Note that, in the actual calculation in '*assign clone*' function of GenoDive, the dataset was not separated into sexual and parthenogenetic populations.

the genetic distances observed in sexual populations (larger than 11) are genetic distances mostly between sexually produced individuals, and the genetic distances between individuals belonging to the same clone are smaller than those. Thus, a threshold distance distinguishing whether pairs of individuals belonging to the same clone was set to 10 (shown in Fig. 46 as a grey broken line). For the diploid dataset, a threshold distance was set to 20. In the haploid dataset, 27 clones were assumed from 93 parthenogenetic population individuals, 114 clones were assumed from 119 sexual population individuals, and 138 clones were assumed in total (three clonal lineages c5, c28, and c53 were shared by both parthenogenetic and sexual populations; Table 15). In the diploid dataset, 33 clones were assumed from 118 parthenogenetic population individuals, 115 clones were assumed from 119 sexual population individuals, and 145 clones were assumed in total (three clonal lineages were shared by both parthenogenetic and sexual populations).

Most sexual populations had genetic diversity (*Div*) and clonal diversity index (*R*) of nearly 1.0, while those of parthenogenetic populations were usually below 0.5 (Table 15). Each parthenogenetic population usually had unique clonal lineages, but several clonal lineages were shared by several populations. For examples, lineage c5 was found in three parthenogenetic populations (p28, p29, and p32) and also in a sexual population p6 (Table 15), possibly suggesting that the population p6 includes parthenogenetic individuals. Argentinean populations had clonal lineages (c44 and c98) which were found from Japanese parthenogenetic populations p2 and p29.

Table 15. Sample information and genetic diversity of each populations. *N*, the number of samples from which SNPs data was successfully obtained; *G*, the number of distinct genotypes (distinct clonal lineages); *He*, gene diversity; *Div*, genetic diversity corrected for samples size; *R*, clonal diversity index. Green color indicates high value of *He* (≥0.1), *Div* and *R* (≥0.9). Orange color indicates low value of *He* (≤0.05), *Div* and *R* (≤0.5). Clone codes are given to each clonal lineage; the clonal lineages found in multiple populations are indicated in bold and those from diploid samples are in underline. For clonal lineages which found in multiple individuals in one population, the number of individuals is shown in parentheses. Values of genetic diversity indices are based on calculations using the haploid dataset, except for p24 and p27.

Population code	Locality	Locality	Sexual mode	*N*	*G*	Clone code	*He*	*Div*	*R*
p1	Asari, Hokkaido	43°10'35.5"N 141°04'00.1"E	Parthenogenetic	2	1	c4	0.002	0.00	0.00
p2	Oshoro, Hokkaido	43°12'54.0"N 140°51'12.3"E	Parthenogenetic	8	5	c94(2),c95–c97,**c98**(2)	0.065	0.86	0.57
p3	Shimamaki, Hokkaido	42°42'46.2"N 140°03'50.6"E	Sexual	5	2	c118(4), c119	0.064	0.40	0.25
p4	Eshashi, Hokkaido	41°52'06.3"N 140°06'43.6"E	Parthenogenetic	8	1	**c53**	0.028	0.00	0.00
p5	Eshashi, Hokkaido	41°51'58.3"N 140°06'49.0"E	Sexual	6	6	c54-59	0.159	1.00	1.00
p6	Shirakami, Hokkaido	41°23'52.1"N 140°11'56.0"E	Sexual	6	6	**c5**,**c53**,c121-c124	0.175	1.00	1.00
p7	Fukaura, Aomori Pref.	40°46'08.6"N 140°03'09.9"E	Sexual	6	6	c14-c19	0.089	1.00	1.00
p8	Akita-shirakami, Akita Pref.	40°23'05.7"N 139°59'05.6"E	Sexual	1	1	c3	NA	NA	NA
p9	Kosagawa, Akita Pref.	39°08'04.0"N 139°53'02.9"E	Sexual	8	8	c64-c71	0.111	1.00	1.00
p10	Nagatejima, Ishikawa Pref.	36°57'03.7"N 136°45'23.2"E	Sexual	8	8	c84-c91	0.130	1.00	1.00
p11	Mihama, Fukui Pref.	35°36'43.2"N 135°53'30.8"E	Sexual	8	7	c73–c77,c78(2),c79	0.125	0.96	0.86
p12	Shikimi, Fukui Pref.	35°33'46.6"N 135°50'11.3"E	Sexual	8	8	c101-c108	0.122	1.00	1.00
p13	Miyatsu, Kyoto Pref.	35°32'N 135°11'E	Sexual	2	2	c80,c81	0.094	1.00	1.00
p14	Yurihama, Tottori Pref.	35°30'N 133°54'E	Sexual	7	7	c132-c138	0.100	1.00	1.00
p15	Kiwado, Yamaguchi Pref.	34°23'12.4"N 131°08'31.2"E	Sexual	1	1	c72	NA	NA	NA
p16	Koinoura, Fukuoka Pref.	33°47'49.6"N 130°26'54.7"E	Sexual	8	8	c45-c52	0.120	1.00	1.00
p17	Sakurajima, Kagoshima Pref.	31°34'49.0"N 130°35'36.1"E	Sexual	2	1	c109	0.038	0.00	0.00
p18	Murozumi,	33°55'N 131°58E	Sexual	0	NA	NA	NA	NA	NA
p19	Hazumisaki, Nagoya Pref.	34°41'51.4"N 136°58'11.6"E	Sexual	8	8	c20-c27	0.084	1.00	1.00
p20	Shimoda, Shizuoka Pref.	34°39'58.4"N 138°56'09.2"E	Sexual	8	8	c110-c117	0.069	1.00	1.00
p21	Enoshima, Kanagawa Pref.	35°17'52.4"N 139°28'46.2"E	Sexual	8	8	c6-c13	0.107	1.00	1.00
p22	Kannonzaki, Kanagawa Pref.	35°15'22.9"N 139°44'45.7"E	Sexual	4	4	c60-c63	0.096	1.00	1.00
p23	Katsuura, Chiba Pref.	35°08'01.8"N 140°17'02.4"E	Sexual	0	NA	NA	NA	NA	NA
p24	Choshi, Chiba Pref.	35°42'19.5"N 140°51'52.6"E	Parthenogenetic	16	1	**c139**	0.097	0.00	0.00
p25	Choshi, Chiba Pref.	35°42'22.8"N 140°52'02.7"E	Sexual	15	15	**c28**-c42	0.146	1.00	1.00
p26	Shioyazaki, Fukushima Pref.	36°59'50.8"N 140°58'53.6"E	Parthenogenetic	8	2	**c28**(7),c120	0.044	0.25	0.14
p27	Azukihama, Miyagi Pref.	38°17'41.9"N 141°04'29.8"E	Parthenogenetic	8	2	**c139**(5),c140(3)	0.101	0.25	0.14
p28	Miyako, Iwate Pref.	39°39'01.6"N 141°58'48.7"E	Parthenogenetic	8	2	**c5**(7),c43	0.039	0.25	0.14
p29	Kabushima, Aomori Pref.	40°32'19.4"N 141°33'30.9"E	Parthenogenetic	8	2	**c5**,**c44**(7)	0.040	0.25	0.14
p30	Nanae, Hokkaido	41°48'42.8"N 140°42'12.2"E	Parthenogenetic	7	2	**c83**(2),c92(5)	0.026	0.48	0.17
p31	Cape Tachimachi, Hokkaido	41°44'40.6"N 140°43'18.1"E	Parthenogenetic	8	7	c125(2),c126–c131	0.112	0.96	0.86
p32	Muroran, Hokkaido	42°18'20.9"N 140°59'01.0"E	Parthenogenetic	10	3	**c5**(8),c82,**c83**	0.072	0.38	0.22
p33	Aikappu, Hokkaido	43°00'54.4"N 144°49'58.8"E	Parthenogenetic	8	2	c1(6), c2(2)	0.047	0.43	0.14
Argentina	PM	42°43'S, 64°57'W	Parthenogenetic?	7	3	**c44**,**c98**(4),c99(2)	0.132	0.57	0.33
Argentina	SAO	40°43'S, 64°56'W	Parthenogenetic?	8	1	**c98**	0.004	0.00	0.00
Ireland	Slea Head	52°06'33"N, 10°27'54"W	?	1	1	**c100**	NA	NA	NA
Ireland	Portrush	55°12'37"N, 6°39'18"W	?	1	1	**c100**	NA	NA	NA
Norway	Ona	62°51'46"N, 6°32'50"E	?	2	2	c93,c141	NA	NA	1.00

Population genetic structure

Three different analyses revealed that populations of *S. lomentaria* in Japan falls into two genetically differentiated groups, the Pacific coast populations and the Sea of Japan coast populations, regardless of the reproductive mode of the populations (Figs. 47–49). Populations around Kyushu and the Tsugaru Strait were intermediates connecting the two groups of populations. Samples from Argentina and Europe were genetically close to those from parthenogenetic populations in Japan.

In the STRUCTURE analysis based on the diploid dataset, the log-likelihood of the data, LnP(K), increased with increasing K until K = 7 and the ideal number of clusters determined by the Evanno method (Evanno et al., 2005) was K = 2 (the ΔK value showed a single peak at K =2). At K = 2, in the all runs, clear genetic differentiation was observed between the Pacific coast populations and the Sea of Japan coast populations (although p33 was from the Pacific coast, it was clustered with the Sea of Japan coast populations; Fig. 47). An admixture between the two genetic clusters was observed in the populations from Kyushu and the Tsugaru Strait, suggesting the gene flow there. Although sex-check PCR, *cetn*-int2 data, and SNPs data suggested that p24 and p27 had two distinct genomes, an admixture of two clusters was not estimated in them, except for two runs at K = 3. In

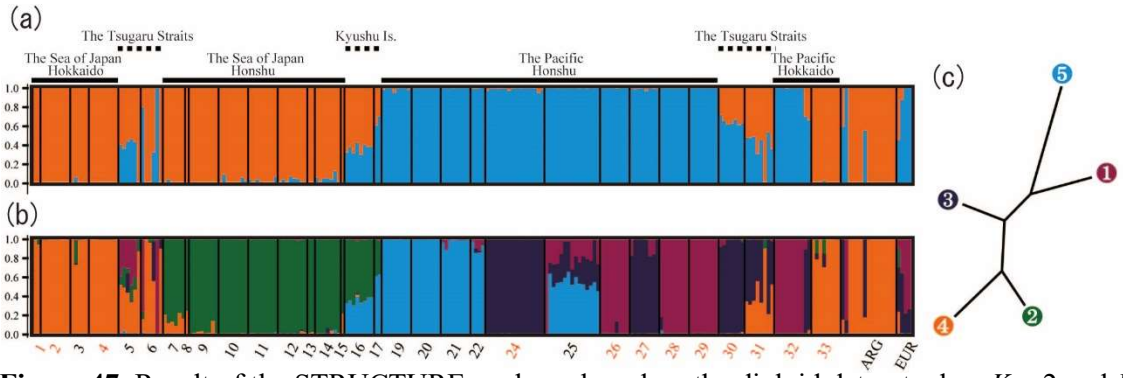

Figure 47. Result of the STRUCTURE analyses based on the diploid dataset when K = 2 and K =5. The frequency of each cluster in each sample is shown by the bar plot. Sampling region in the Japanese Islands are shown above the bar plot, and population codes [1–33 (without 'p'), ARG: Argentina, EUR: Europe; parthenogenetic populations from Japan are indicated in red] are shown below the bar plot. (a) The genetic clusters estimated in the all runs at K = 2; (b) The genetic clusters estimated in five of 10 runs at K = 5; (c) The Neighbor Joining tree for the five clusters at K = 5 shown in (b). Color for each cluster is consistent in the bar plot of (b) and the NJ tree.

the two runs at $K = 3$, the cluster of the Sea of Japan coast populations in $K = 2$ were divided into the west coast of Hokkaido populations (p1–p6) and the Honshu populations (p7–p16), and an admixture between the west coast of Hokkaido populations and the Pacific coast populations were observed in p24 and p27 and also in p30 and p31. In other runs at $K = 3$, p24 and p27 formed a cluster with the sexual or parthenogenetic populations from the Pacific coast. In the runs at $K > 3$, p24 and p27 formed an independent cluster with or without p30. At $K = 5$, in five of 10 runs, the Sea of Japan populations were divided into two clusters (west coast of Hokkaido populations and the Honshu populations) and the Pacific coast populations were divided into three clusters (a cluster of sexual populations and two clusters of parthenogenetic populations; Fig. 47).

In the PCA (Fig. 48), PC1 roughly divided the Japanese populations into the group of Pacific side and the group of Sea of Japan side and explained 26.6% of the variance, and PC2 captured north-south variation along it in each group and explained 15.9% of the variance. The PCA appeared as if the individuals were plotted in a ring along the coast of the Japanese Islands; individuals from Kyushu (p16 and p17) and near the Tsugaru Strait (p5, p6, p30, p31) connected the edges of the two groups (Fig. 48). Each group was roughly divided into sexual and parthenogenetic populations along PC3 which explained 11.5% of the variance (Fig. 48). Samples from parthenogenetic populations p24 and p27, which were likely to be polyploid, were close to those from parthenogenetic populations around the Tsugaru Strait (p30–p32). In parthenogenetic populations (p1, p2, p4, p24, and p26–p33), the plots tended to be more densely clustered, relative to the sexual populations. This is probably due to the lower genetic variance of each parthenogenetic population.

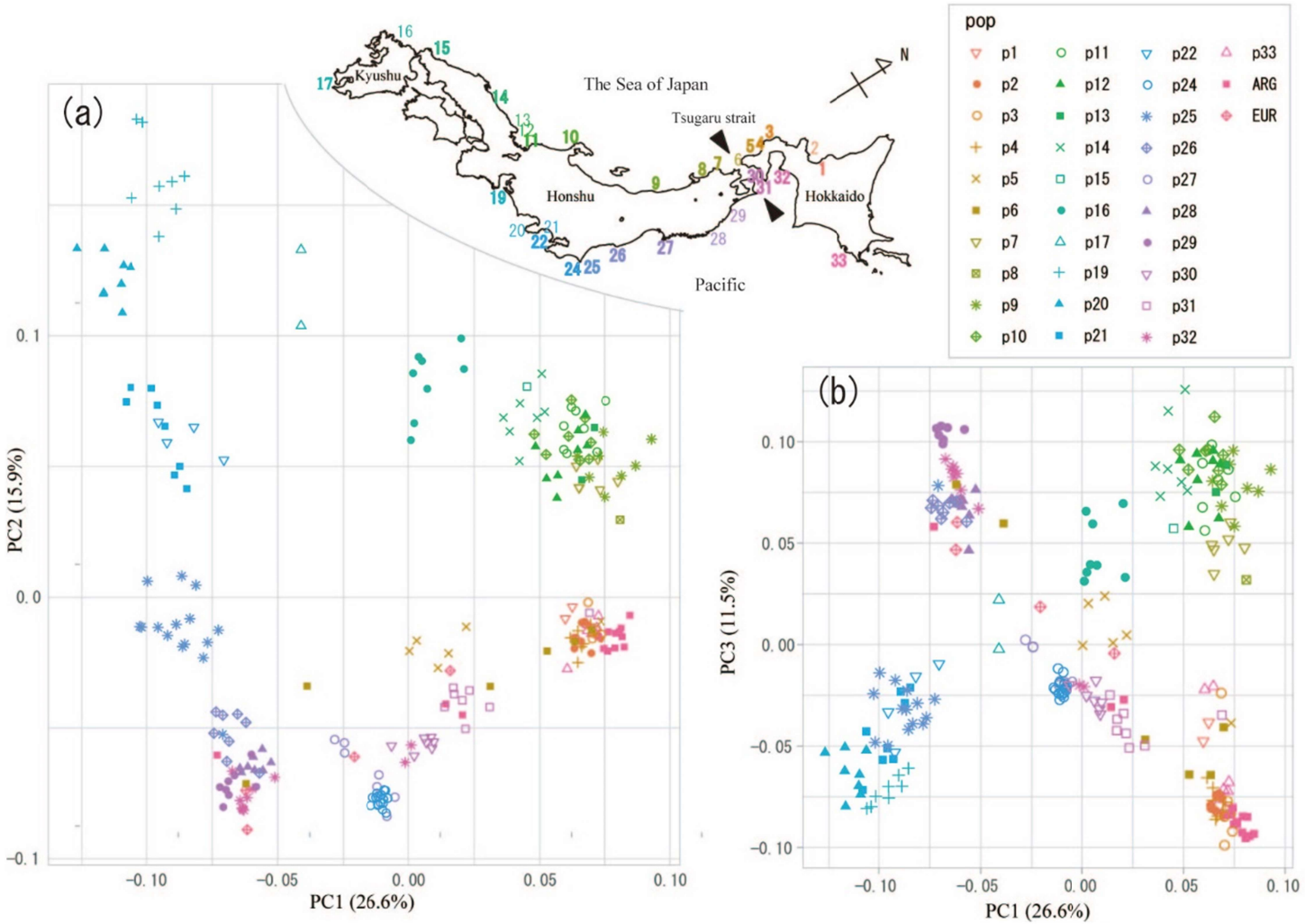

Figure 48. Result of the PCA based on the diploid dataset showing the locations of each individual on the first three principal components (PC1–PC3), which describe 54% of the genetic variation. Sampling localities of each Japanese population are shown in the map of Japan (Fig. 42). Colors for each population are consistent in the PCA plots and the map.

The NeighborNet network showed polyphyly of parthenogenetic populations (Fig. 49). The network also supported the genetic differentiation between the Pacific coast group and the Sea of Japan coast group. Populations around Kyushu (p15–p17) and the Tsugaru Strait (p5, p6, p30, p31) were intermediates connecting the two groups.

In the above three analyses, no significant difference was observed between diploid and haploid dataset.

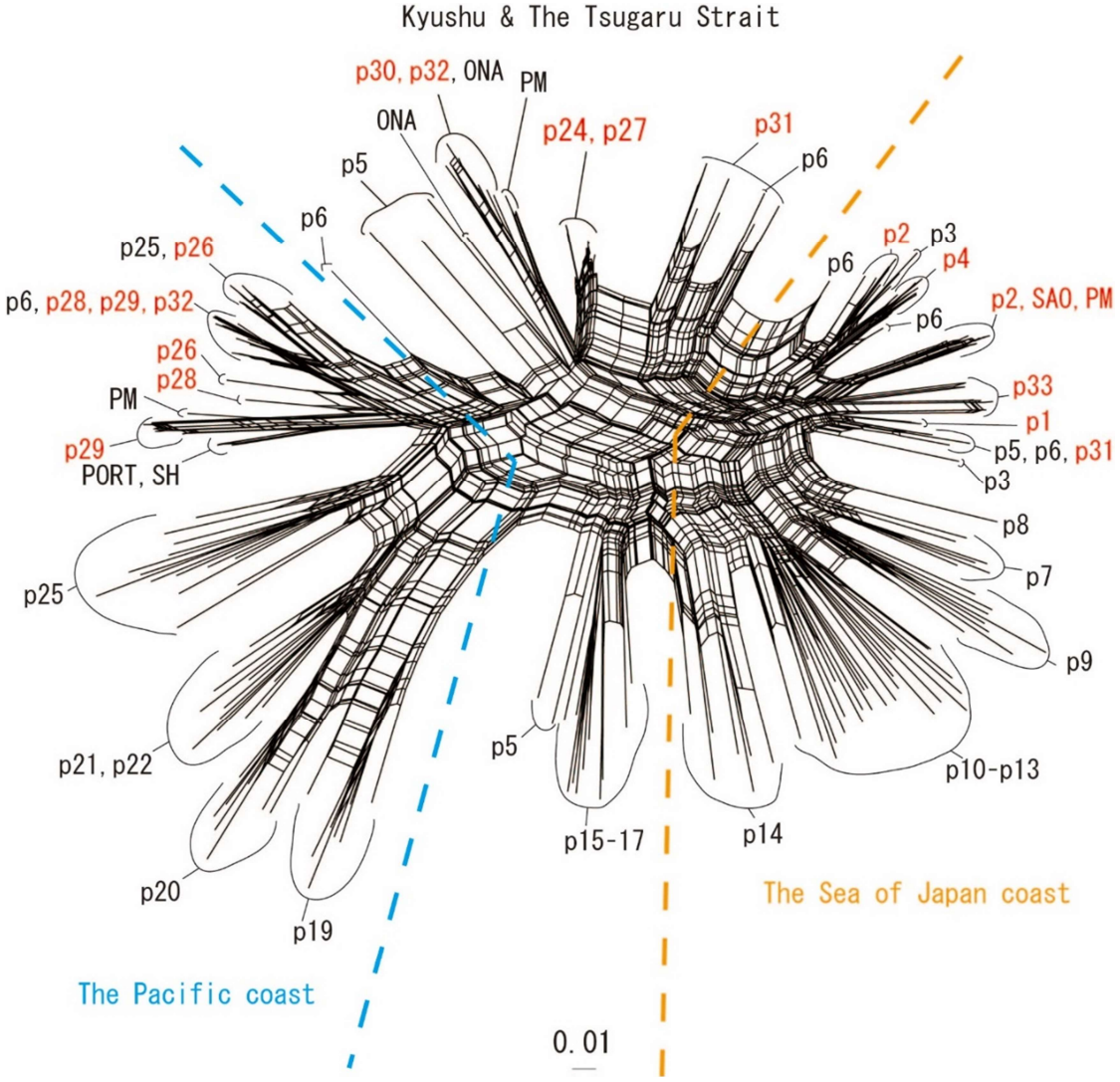

Figure 49. The NeighborNet tree based on the diploid dataset, showing the polyphyly of parthenogenetic populations. Population codes of parthenogenetic populations from Japan are indicated by red color. Blue and orange broken lines roughly separete Japanese populations into those from the Pacific coast, Kyushu and the Tsugaru Strait, and The Sea of Japan.

Chromosome observation

No difference was observed in the number of chromosomes between individuals from parthenogenetic populations (p2 and p32) and sexual populations (p15 and p22). Gametophytes from both parthenogenetic and sexual populations had ca. 22 chromosomes (14 nuclei were examined in each; Fig. 50)

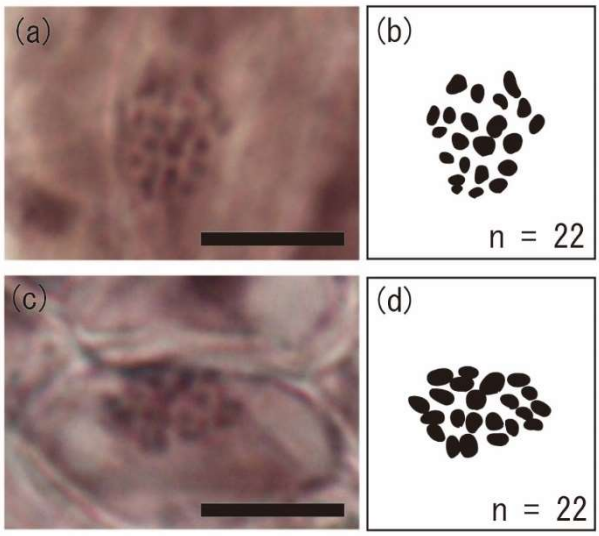

Figure 50. Aceto-iron-haematoxylin-chloral hydrate staining of chromosomes of gametophytes at metaphase.
(a & b) Chromosomes, n = 22, of gametophyte from sexual population p15.
(c & d) Chromosomes, n = 22, of gametophyte from parthenogenetic population p32.
Scale bars = 5 μm

Sex pheromone production

GCMS analyses did not detect sex pheromones from the female gametes of parthenogenetic population p28 (Fig. 8). The compounds predicted as brown algal sex pheromones were detected only from the positive control (female gametes from sexual populations p15) with high intensity at around 12.1 and 14.6 min (Fig. 8). In similarity search for the first compound, the first candidate was 6-[(1*Z*)-1-butenyl]-1,4-cycloheptadiene (ectocarpene; similarity value = 97%) and the second candidate was 6-[(1*E*)-1-butenyl]-1,4-cycloheptadiene (the *cis-trans* isomer of ectocarpene; similarity value = 93%). For the second compound, the first candidate was ectocarpene (similarity value = 95%) and the second candidate was (3*E*,5*E*,8*E*)-1,3,5,8-undecatetraene (similarity value = 91%).

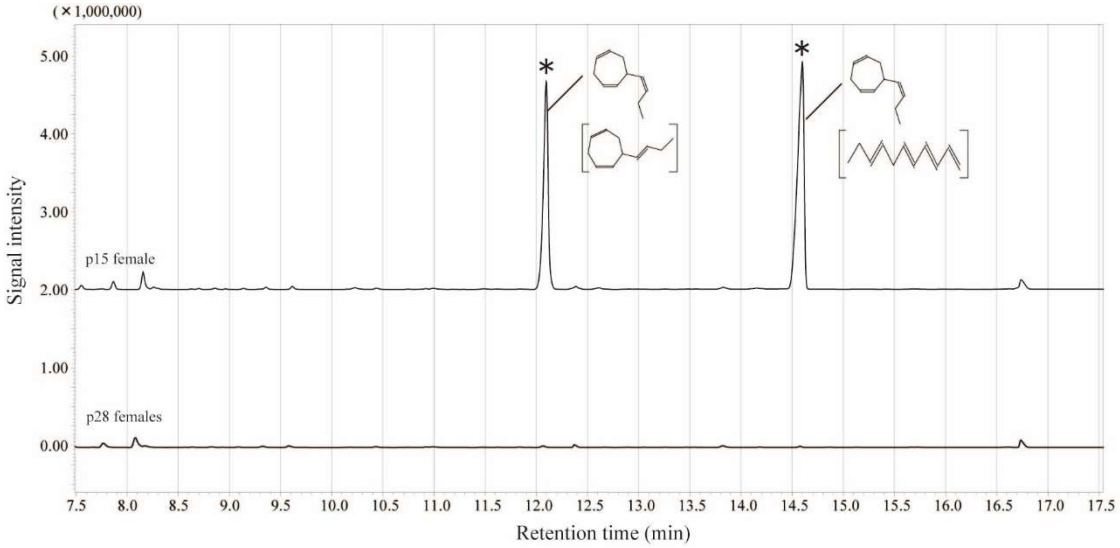

Figure 51. Results of the GCMS analyses of the volatile compounds released from gametes: extracted ion chromatograms = 148–149 *m/z*. The compound predicted as ectocarpene (6-[(*Z*)-1-butenyl]-1,4-cycloheptadiene) was detected with high intensity at around 12.1 and 14.6 min from female gametes of a sexual population (p15; asterisks), not from those of parthenogenetic population p28.

DISCUSSION

In brown algae, populations speculated to be parthenogenetic populations are numerous and parthenogenesis seems to be an important reproductive strategy. However, almost nothing is known as to the distribution pattern of parthenogens and sexuals and how parthenogens arise. The present study shed light on biogeographic and evolutionary questions involving the parthenogens in the brown alga *S. lomentaria*. I showed that distribution of parthenogens was biased to cold waters in the Japanese Islands, and parthenogens probably had a worldwide distribution. Second, results of this study demonstrated that parthenogens have evolved at least twice in *S. lomentaria* and these parthenogens did not originate from inter-species hybridization, which is common in animals and land plants. Third, my results suggested that parthenogens have become genetically diverse through backcrosses with their ancestral sexuals.

Geographic parthenogenesis in *S. lomentaria*

In *S. lomentaria*, parthenogenetic populations were distributed in cold waters. In previous

studies, parthenogenetic populations were only reported from Hokkaido and sexual populations were only reported from south of central Honshu [Hoshino et al., 2019 (**Chapter 5**)]. The present study revealed that, in the Sea of Japan coast, sexuals were distributed from Kyushu to the west coast of Hokkaido and overlapped with parthenogens in the west coast of Hokkaido, whereas, in the Pacific coast, sexuals were distributed in south of Choshi (the sampling locality of p24 and p25) and parthenogens were distributed in north of Choshi. This distributional pattern fits well with the division of seaweed flora/ecoregions in the Japanese Islands proposed so far (Okamura, 1931; Yoshizaki, 1979; Yoshizaki and Tanaka, 1986; Spalding et al., 2007). The seaweed flora in Japan is influenced by the water temperature associated with prevailing ocean currents along its coast (Fig. 42; Okamura, 1931). Choshi is known as one of the boundaries of the seaweed flora in the Pacific coast; it is the southern limit of cold waters species (Okamura, 1931; Yoshizaki, 1979). The northern limit of subtropical species, the Cape Taito (35°18'N, 140°24'E), is also near Choshi (Okamura, 1931; Yoshizaki, 1979). Furthermore, a ddRAD-seq based phylogeographic study on the brown alga *Sargassum thunbergii* (Mertens ex Roth) Kuntze, which is widely distributed along the Japanese coast, has also indicated the existence of a barrier for gene flow around Choshi (Kobayashi et al., 2018). Clearly, a dispersal barrier, which probably generated by the cold Oyashio and warm Kuroshio Currents, exists around Choshi, at least in some species. On the other hand, the seaweed flora along the Sea of Japan coast is generally warm temperate due to the Tsushima Current, a relatively smaller warm current that bifurcated from the Kuroshio Current, although the Tsugaru Strait has been suggested as a boundary of seaweed floras (Okamura, 1931; Yoshizaki and Tanaka, 1986).

Differences in the distribution between parthenogens and sexuals were also found in a smaller scale. Parthenogenetic populations and sexual populations were parapatric in the west coast of Hokkaido (p4 and p5) and in Choshi (p24 and p25). In both localities, parthenogens grew in the upper-intertidal zone exposed to waves while sexuals

occurred in the lower-intertidal zone and were relatively protected from waves. In intertidal zone, seaweed species often grow in specific vertical or horizontal “zones” or “bands” along environmental gradients such as wave exposure and environment conditions affected by tidal level (e.g., temperature, salinity, dehydration, light), partly due to interspecies differences in the tolerance to the environmental stress (Hurd et al., 2014 and the references therein). The above habitat differentiation between parthenogenetic and sexual populations likely indicates their niche differentiation.

It has been often suggested that parthenogenetic organisms tend to be biased toward marginal and disturbed environments, when compared with their close sexual relatives (Tilquin and Kokko, 2016 and the references therein). Lynch (1984) speculated that the association of parthenogens with marginal habitats may be as a consequence of selection pressure for parthenogens to use habitat not occupied by the parental sexuals. That is, since one of the most stringent requirements for the establishment and maintenance of a parthenogen will be the avoidance of backcrosses and competition with parental sexuals, incipient clones that tend to use habitats not normally occupied by the parental sexuals will have an initial selective advantage over other clones (Lynch, 1984). In *S. lomentaria*, parthenogens and sexuals clearly occupied different ecological niche. However, it is unclear whether the cold waters and the wave-exposed areas, where parthenogens existed, are the marginal/disturbed habitats for sexuals. Although I have performed culture experiments in 10, 15, and 20°C, at least in gametophytic phase, no difference was observed in growth and maturity between the samples from parthenogenetic and sexual populations. Wave-exposed areas, on the other hand, are possibly unsuitable habitats for sexuals since waves can disturb interaction between male and female gametes. In some brown algae, laboratory experiments have shown that gamete release is enhanced in calm/no-flow conditions and is inhibited in shaken/high-flow conditions (Gordon and Brawley, 2004; Pearson and Serrão, 2006). Strong waves can also be physical stress for seaweeds (Hurd et al., 2014). Gametophytic thalli of

parthenogenetic populations p4 and p24 which were found in wave-exposed areas tended to be smaller than those of parapatric sexual populations p5 and p25 which were found in wave-protected area.

Parthenogens have larger distributions?

Parthenogens often occupy larger distribution areas than their sexual relatives (Bierzychudek, 1985; Hörandl, 2009). Perhaps that is also the case with *S. lomentaria*. I showed that populations from Argentina and Europe included no males and they were genetically close/identical to parthenogenetic populations in Japan. Regarding populations in North America, although only *cox*1 data was available, most of them had haplotypes which were close/identical to those from the parthenogenetic populations in Japan. Furthermore, sexual reproduction (gamete fusions) has not been reported from *S. lomentaria* in North America (Wynne, 1969). These facts suggest that the populations in Argentina, Europe, and North America are parthenogenetic and parthenogens are more widely distributed than sexuals.

To explain a larger distribution of parthenogens, two hypotheses that focus on a selection among genetically diverse parthenogenetic clones (clonal selection) are often cited: the "general-purpose genotype" (GPG) and "frozen niche-variation" (FNV) hypotheses. The GPG hypothesis supposes that clonal selection will promote the evolution of highly generalized (or general-purpose) genotypes, which are characterized by both broad tolerance ranges and low fitness variance for relevant environmental gradients; it expects a widespread distribution of a parthenogen has resulted from the dispersal of a single (several) highly generalized clone(s) (Lynch, 1984). The FNV hypothesis, on the other hand, expects a widespread distribution of a parthenogen has resulted from the joint distribution of many locally adapted (specialist) clones (Vrijenhoek, 1984; Hörandl, 2009). In *S. lomentaria*, several parthenogenetic clones (or clonal lineages) were found in multiple populations and had wide distributions, as GPG hypothesis expects. However, the whole parthenogenetic populations consisted of about

30 polyphyletic clones and the major clone in each parthenogenetic population was often different. Although it is unclear if each clone is locally adapted, this high clonal diversity seems to fit the FNV hypothesis.

Another important factor to explain a wide distribution of parthenogens is superior colonization ability. Parthenogens should have a significant advantage over bi-sexual parents in colonization, since they can initiate a new colony by a single individual and its potential increase in numbers per generation is double that of a bi-sexual parent (Cuellar, 1977). Considering that parthenogens are commonly biased towards previously glaciated areas (Kearney, 2005), it is likely that parthenogens have occupied these areas after the glaciation as a consequence of their superior colonization ability. It is known that the last glacial maximum also impacted the distribution of seaweeds. Some seaweeds show shallow population structure probably due to postglacial northward recolonization from southern glacial refugia (e.g., Provan et al., 2005; Hoarau et al., 2007; Coyer et al., 2011; Neiva et al., 2014). A star-like network pattern observed in the *cox*1-haplogroup, group A, may suggest the recent population expansion (i.e., postglacial recolonization) of *S. lomentaria* parthenogens.

Origin of parthenogens

Molecular analyses demonstrated that parthenogens have evolved at least twice in *S. lomentaria*. Parthenogens in the Sea of Japan coast and those in the Pacific coast probably have independent origins. Parthenogens in the Sea of Japan coast (p1, p2, and p4) likely have evolved from the sexuals in the west coast of Hokkaido (p3, p5, and p6) which are the closest sexual relatives. Although p33 is in the Pacific coast, it was genetically close to parthenogens from the Sea of Japan. It may suggest that parthenogens in the Sea of Japan coast have spread to the Pacific coast along Tsushima current (Fig. 42). Parthenogens in the Pacific coast (p26, p28, p29, and p32) were the genetically closest to the sexuals in the Pacific coast (p19–p22 and p25), suggesting that the parthenogens have evolved around the northern limit of sexuals in the Pacific coast. In

the NeighborNet, parthenogens in p24 and p27 and those around the Tsugaru Strait (p30–p32) appeared to distinct lineages from those in the Sea of Japan (p1, p2, and p4) and the Pacific coast (p26, p28, p29, and p32). However, judging from the results of STRUCTURE and PCA, they probably originated from hybridization between sexuals from the Sea of Japan coast and existing parthenogens from the Pacific coast, rather than newly arose parthenogens. Polyploidy of parthenogens in p24 and p27 may indicate that meiosis was disturbed for some reason after the hybridization. Although a backcross with their parental sexuals has been considered a taboo for the maintenance of parthenogens (Lynch, 1984), it might have occurred multiple times in *S. lomentaria* and provided genetic diversity in parthenogens. Parthenogens of organisms having a haploid generation like *S. lomentaria* are expected to be more susceptible to the accumulation of deleterious mutations compared with parthenogens having diploid or higher ploidy. In *S. lomentaria* parthenogens, backcrosses with sexual relatives may have the benefits of eliminating accumulated mutations and acquiring a new genome.

Although the origins of parthenogens are not always known, inter-specific hybridization and polyploidy are seen as major triggers for parthenogenesis in animals and flowering plants (Simon et al., 2003; Kearney, 2005; Hörandl, 2009). But it is probably not the case for *S. lomentaria*. The parthenogenetic populations did not show evidence for inter-specific hybridization, such as mitochondrial introgression. Some parthenogenetic individuals seemed to be polyploid; however, *cetn*-int2 analysis showed that these polyploid samples from p24 and p27 originated from intra-specific crossing, not inter-specific hybridization as I mentioned above.

The most possible candidate for the origin of *S. lomentaria* parthenogens might be spontaneous origin, that is, spontaneous loss of sexuality or acquisition of asexuality through mutation (Simon et al., 2003). In *S. lomentaria*, parthenogenesis of unfused gametes is common in culture condition, even in individuals from sexual populations [Hoshino et al., 2019 (**Chapter 5**)]. Thus, I expect if sexual reproduction is somehow

disturbed (e.g., due to environmental factors or loss of sexual traits), parthenogenetic ability will be under strong selection and individuals with high parthenogenetic ability will easily arise in *S. lomentaria*. I have shown parallel suppression/loss of sex pheromone production in parthenogens in the Sea of Japan coast and the Pacific coast [Hoshino et al., 2019 (**Chapter 5**); this study]. Although it is unclear whether the suppression/loss of sex pheromone production occurred before the evolution of parthenogens, if they occurred before, they could have triggered the evolution of parthenogens. If they occurred after the evolution of parthenogens, they can be considered regressive evolution. In asexual life cycles, sex pheromone production can be considered neutral or maladaptive traits depending on the amount of energy cost required for their expression. It has been suggested that a formerly adaptive trait can be reduced, when that trait is neutral or maladaptive in the new selective environment (Lynch, 1984; Lahti et al., 2009; van der Kooi and Schwander, 2014). In animal parthenogens, decay of female sexual traits has been widely reported (van der Kooi and Schwander, 2014).

Chapter 7

Parthenogens in the brown alga *Scytosiphon promiscuus*: their origin, distribution, and evolution of reproductive traits under asexuality.

INTRODUCTION

Although sex is the predominant mode of reproduction in nearly all multicellular organisms, secondary loss of sex (i.e., evolution of obligate asexuals) is numerous across the tree of life. In animals and land plants, comparative studies between obligate asexuals and their close sexual relatives have shed light on several important topics in evolutionary biology, such as problem of the maintenance of sex (Lynch, 1984), adaptation to marginal habitats (Kawecki, 2008; Tilquin and Kokko, 2016), and trait evolution (Lahti et al., 2009; van der Kooi and Schwander 2014).

Brown algae (Phaeophyceae) are a group of multicellular heterokonts and a key source of productivity along the coast (Bringloe et al., 2020). Parthenogenesis is a way of asexual reproduction in which an unfertilized gamete develops into a new individual. In brown algae, parthenogenesis is a common phenomenon. Even in sexual taxa, parthenogenetic development of unfused gametes is common in laboratory culture, and it has been also detected from field populations at low frequency [e.g., Oppliger et al., 2007; Klochkova et al., 2017; Hoshino and Kogame, 2019 (**Chapter 4**)]. Reports of species/populations that probably maintained by obligate parthenogenesis (i.e., species/populations in which sexual reproduction cannot be observed in culture conditions) are numerous (e.g., Wynne, 1969; Peters, 1987; Kogame and Kawai, 1993). However, reports that go beyond the mere description of life history are rare, and the nature of obligate parthenogens in brown algae remains unclear.

The brown alga *Scytosiphon promiscuus* is commonly distributed in the northern hemisphere [Hoshino et al., 2020c (**Chapter 2**)]. It has a heteromorphic life history: an alternation of generation between the macroscopic dioicous isomorphic gametophytes and the microscopic discoid sporophyte (Nakamura and Tatewaki, 1975). Its sexual reproduction is isogamous; female gametes settle on the substratum sooner than male gametes and secrete sexual pheromones that attract male gametes (Fu et al., 2014). In Japan, sexual reproduction is common in *S. promiscuus*. However, I found three possibly

parthenogenetic populations [populations in which sexual reproduction (gamete fusions) is not observable]. In the present study, using these parthenogenetic populations and the two sexual populations having the identical mitochondrial *cox*1 haplotypes with the parthenogenetic populations, I conducted the following three comparative approaches: (1) sex ratio investigation using sex-check PCR to reveal the genetic sex of parthenogens; (2) phylogenetic and population genetic analyses based on genome-wide SNPs to reveal the phylogenetic relationships between sexuals and parthenogens, and to compare the genetic diversity; and, (3) comparison of four reproductive traits of female gametes (sex pheromone production, fertilization rate, gamete size, and parthenogenetic ability) to reveal how reproductive traits have evolved in the transition to asexuality. Based on my observations and previous studies, here I discuss the potential rules of evolution of brown algal parthenogens.

MATERIALS AND METHODS

Specimen collection, DNA extraction and sex ratio investigation

In total, 205 gametophyte individuals of *Scytosiphon promiscuus* were used, including samples previously collected [Kogame et al., 2015; Hoshino et al., 2020c (**Chapter 2**)]. Sampling localities are shown in Fig. 52. Collected gametophytes were preserved in salt, but some fresh, living samples were also transported back to the laboratory and subsequently used for experiments. A fragment of the thallus was preserved in a silica gel for molecular analyses. Unialgal culture isolates were established for some samples as previously described in Kogame et al. (2015a). Pressed specimens were also made and deposited as vouchers in the Herbarium of Faculty of Sciences, Hokkaido University, Sapporo, Japan (SAP).

Sex ratios were investigated in five closely related populations [Hoshino et al., 2020c (**Chapter 2**)]: three parthenogenetic populations (p14–p16; Fig. 52) and two sexual populations (p12 and p13). Their sex ratio were followed for 1–3 years. Sex of each

individuals was examined by crossing experiments and sex-check PCR. For sex-check PCR, partial sequences of the sex-specific nonrecombining region on the sex chromosome of *S. lomentaria* (Lipinska et al., 2017) were amplified as the sex markers. Total genomic DNA was extracted from a small fragment of silica gel-dried specimens or living samples, using Gencheck® DNA Extraction Reagent (FASMAC, Atsugi, Japan) as described in Hoshino et al. (2020b; **Chapter 3**). Amplifications of the sex markers were performed as in Hoshino et al. (2019; **Chapter 5**).

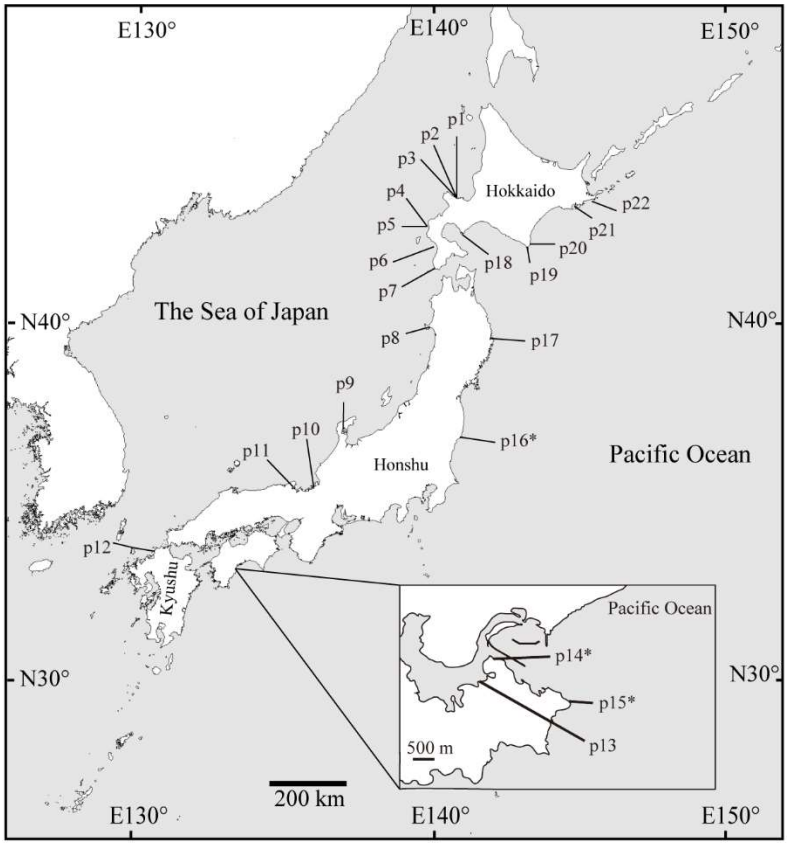

Figure 52. Map of Japan showing collection localities of samples used in this study. A population code (p1–p22) is given to each population. For parthenogenetic populations, superscript asterisk is given on the right of population code.

Mitochondrial *cox*1 haplotype network

To roughly understand genetic structure of the parthenogenetic populations, a haplotype network was constructed using the mitochondrial *cox*1 gene. In total, 79 sequences of *cox*1(–617 bp) were newly generated as previously described in Kogame et al. (2015a).

The sequences obtained were combined with an alignment of *S. promiscuus* used in Hoshino et al. (2020c; **Chapter 2**) and aligned using CLUSTALW in MEGA v. 7 (Kumar et al., 2016). The dataset used was 600 bp and 203 individuals (sequences less than 600 bp were excluded). Phylogenetic relationships among the haplotypes were reconstructed using median-joining methods (Bandelt et al., 1999) in Network version 5.0.1.0, and the unnecessary median vectors and links in the networks were identified and cleaned up by MP option (Polzin and Daneshmand, 2003).

Population genetic analyses based on genome-wide SNPs

Library preparation and data processing

For the discovery of SNPs (single nucleotide polymorphisms), multiplexed ISSR genotyping by sequencing (MIG-seq) was conducted following the procedure by Suyama and Matsuki (2015) with a slight modification: annealing temperature of the first PCR was changed from 48°C to 38°C. Both ends of fragments were obtained by paired-end sequencing (read 1and 2), but only read 1 was used for the following analyses. Low-quality reads and the primer regions in the sequences were removed by FASTX-Toolkit (http://hannonlab.cshl.edu/fastx_toolkit/) as described in **Chapter 6**.

De novo assembly was performed using Stacks v. 2.53 (Catchen et al., 2013) with the following parameters. The minimum number of identical reads to create unique stacks within each individual was set to three (m = 3) and other parameters were set following **Chapter 6** (M = 0, -N 0, -H, and n = 1) to accommodate the haploidy of my samples. The SNP genotype for each individual was exported using the '*populations*' command; only the first SNP was extracted from each putative locus using the flags --*write_single_snp*. The exported genotype data was processed using PLINK v. 2.00 (Chang et al., 2015; www.cog-genomics.org/plink/2.0/). SNPs with a minor allele frequency < 0.03, locus with a missing individual rate > 0.5, and individuals with a missing locus rate > 0.5 were filtered out. Format of the output files of PLINK was

converted using PGDSpider2 (Lischer and Excoffier, 2012) for subsequent analyses.

Gene diversity and clonal diversity

Gene diversity (expected heterozygosity: *He*) of each population was calculated using '*genetic diversity*' function of GenoDive v. 3.04 (Meirmans, 2020). To examine clonal diversity, the number of clonal lineages was assessed using '*assign clone*' function of GenoDive. Using this function, I calculated a matrix of genetic distances using an infinite allele model (in this calculation, missing data were discarded) and chose a threshold distance as in **Chapter 6**. A pair of individuals, of which genetic distance is below the threshold distance, were considered to belong to the same clonal lineage. Each clonal lineage was treated as a single genotype and Nei's (1987) genetic diversity corrected for samples size (*Div*) was calculated for each population using '*clonal diversity*' function (Meirmans and Van Tienderen, 2004). Clonal diversity index *R* (Dorken and Eckert, 2001) was also calculated manually by the equation: $R = (G\text{-}1)/(N\text{-}1)$, where *G* is the number of distinct genotypes and *N* is the total number of sampled individuals.

Population genetic structure

Population genetic structure was examined by three different methods as in **Chapter 6**: Bayesian clustering analysis, principal component analysis (PCA), and phylogenetic network reconstruction. Bayesian clustering analysis was conducted using STRUCTURE v. 2.3.4 (Pritchard et al., 2000). The number of clusters (*K*) of 1–10 was tested by running 20 simulations for each *K*, with 100,000 Markov chain Monte Carlo steps and a burn-in of 100,000, using the model with admixture and correlated allele frequencies. The meaningful number of *K* was determined based on the second-order rate of change in the log probability of the data (ΔK; Evanno et al., 2005). The ΔK values were calculated using STRUCTURE HARVESTER v. 0.6.94 (Earl and vonHoldt, 2012). Principal component analyses were performed using PLINK and the results were visualized using R software v. 3.6.0 (R Core Team, 2019). To reveal phylogenetic relationships between parthenogenetic and sexual populations, a phylogenetic network was constructed based

on uncorrected *P* distances using NeighborNet method (Bryant and Moulton, 2004) in SplitsTree v. 4.15.1 (Huson and Bryant, 2006).

Sexual and asexual traits in parthenogenetic populations

Materials and culture conditions

Four reproductive traits of gametes were observed: fertilization rate, sex pheromone production, gamete size, and parthenogenetic development. These traits were examined in two parthenogenetic populations, p14 and p16, and they were compared with those of sexual populations which were inferred as the closest relatives by the above SNPs-based phylogenetic analyses (Figs. 55–57). That is, p14 was compared with p13, and p16 was compared with p12. For p13 and p14, gametophytes collected from field were used. In other cases, culture stains were used. Culture strains were maintained using plastic Petri dishes (90 × 20 mm) and PESI medium (Tatewaki, 1966) at 15 and 10°C in long day (16h:8h, light:dark) and short day (8h:16h, light:dark) conditions with fluorescent lighting of 30–50 μmol $m^{-2}s^{-1}$ photon flux density. Field gametophytes and culture stains used are shown in Table S11.

Fertilization rate

To examine fertilization rates of gametes from parthenogenetic populations, they were crossed with male and female gametes from sexual populations. Crossing was performed following the methods outlined in Hoshino et al. (2018; **Chapter 1**). Male gametes were added to female gametes that settled in the microscopic field of view. Female gametes were directly observed over a period of 5 minutes to see which formed zygotes. As a control, crossing between female and male gametes from sexual populations was also performed.

Sex pheromone production

Brown algal female gametes release sex pheromones to attract male gametes. The sex pheromones are volatile, lipophilic, more or less unsaturated C_8- or C_{11}-hydorocarbons,

and detectable by olfaction (Maier and Müller, 1986). Females from sexual populations p11 and p12 had smell of sex pheromones. However, most females from parthenogenetic populations p13 and p15 released gametes having no smell of sex pheromones. Thus, their sex pheromone production was examined using a gas chromatography/mass spectrometry (GCMS). Females from parthenogenetic populations which do not have smell of sex pheromones were used for GCMS. Cultured gametophytes or field collected gametophytes were kept in 300 mL of sterilized seawater in a 500 mL flask at 15°C and gametes were released in the flask. Volatile secretions were trapped on Mono Trap RCC18 (GL science, Tokyo, Japan) using a closed-loop-stripping system at 15°C as described in **Chapter 6**. After looping 12 h, absorbed volatile compounds were eluted with 50 μL of CH_2Cl_2 and immediately analyzed by GCMS as described in **Chapter 6**. Compounds were identified by using the NIST MS library and similarity search program. Females and males from sexual populations were also analyzed as positive and negative controls, respectively. Since female strains of p11 did not release gametes when GCMS was conducted, female strains from p1 and p13 were used instead.

Gamete size and parthenogenetic development

Several minutes after gametes release, gametes lose their motility and settle to the substratum and then change their shape from pear-shaped to spherical. To examine gamete size, the diameter of these spherical gametes was measured. Images of spherical gametes were taken with a Nikon Digital Sight DS-Fi1 (Nikon Corporation, Tokyo) and measured their diameter using ImageJ software (Schneider et al., 2012). Sixteen to fifty gametes were measured for each individual.

To examine parthenogenetic development, gametes were cultured at 15°C under long day condition. The number of germinated gametes and nongerminated gametes were counted after 24 h cultivation (germination rate). The number of cells in each germling (gamete) after five-day cultivation was also examined. For each individual, 16–170 gametes (germlings) were observed.

For the statistical analysis of the diameter of gametes, germination rate, and the cell numbers of germlings, a generalized linear mixed model (GLMM) was adopted with a normal distribution, a binominal distribution, and a Poisson distribution, respectively. In these models, the experimental groups (gametes from parthenogenetic population/ female gametes from sexual population/ male gametes from sexual population) were considered as the fixed effects, and gametophyte identity was considered as the random effect. All statistical analyses were conducted using R software package lmer (Bates et al., 2015) and lmerTest (Kuznetsova et al., 2017) in R.

RESULTS

Sex ratio

In total, the sex of 139 individuals from p12–p16 was identified by the PCR-based sex markers (Table 16). The sex-check PCR detected both female and male individuals from sexual populations p12 and p13, and detected only females from parthenogenetic populations p15 and p16. However, contrary to my expectations, two male individuals were found in parthenogenetic populations p14. The results of the sex-check PCR agreed with those by crossing experiments except for those two males from p14. Although they were identified as male by sex-check PCR, their gametes did not fuse with either female or male gametes, indicating that they do not function as male.

Table 16. Results of the sex ratio investigation.

Population code	Collection date	Sex ratio (♀:♂)
p12 (sexual)		
	23 and 24 March 2015	5:1
p13 (sexual)		
	21 Feb. 2019	3:3
	7 Mar. 2019	13:8
	13 Feb. 2020	8:12
p14 (parthenogenetic)		
	20 Feb. 2019	20:0
	7 Mar. 2019	11:0
	14 Feb. 2020	22:2[†]
p15 (parthenogenetic)		
	26 Mar. 2017	6:0
p16 (parthenogenetic)		
	16 Feb. 2017	5:0
	25 Mar. 2018	2:0
	21 Mar. 2019	18:0

[†] These two males were identified as male by sex-check PCR, but their crossing pattern were that of females, rather than that of males.

*Cox*1 haplotype network

In parthenogenetic populations (p14–16), three closely related mitotypes were detected: Mt. a–c (Fig. 53). These three mitotypes had some distance (more than six mutations) from other mitotypes found in *S. promiscuus*. Individuals from parthenogenetic population p14 and p15 mainly had mitotype Mt. a. In p14, one individual had mitotype Mt. c and two individuals which were identified as male by the sex markers had mitotype Mt. b. Individuals from parthenogenetic population p16 mainly had mitotype Mt. c, but one individual had mitotype Mt. a. Individuals from sexual populations p12 and p13 had mitotypes Mt. c and Mt. a, respectively.

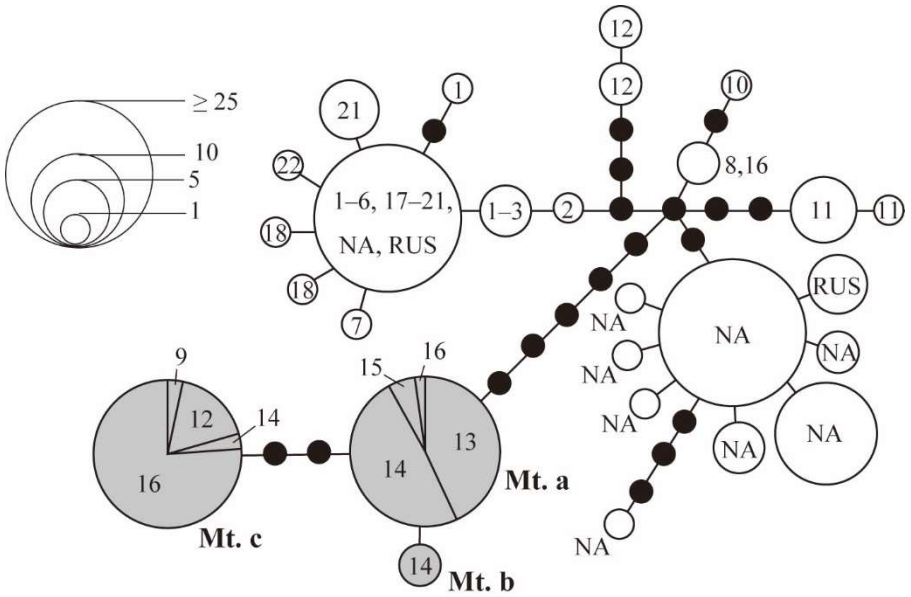

Figure 53. *Cox*1-haplotype network (one of the shortest trees). Population codes [1–22 (without 'p')] are given to the haplotypes of Japanese samples. Each white and grey circle represents a haplotype and its size is proportional to its frequency. Black circles represent hypothetical unsampled haplotypes. The haplotypes found in parthenogenetic populations are indicated in grey color (Mt. a–c). NA: North America. RUS: Far East Russia.

SNPs analyses

SNPs dataset

A total of 75 samples from p12–p16 were genotyped at 522 SNPs (loci) and the mean genotyping rate was 70.7%. In the filtering procedure, individuals which did not have mitotypes Mt. a–c were filtered out, since they had few common SNPs (loci) with the individuals having mitotypes Mt. a–c.

Gene diversity and clonal diversity

Parthenogenetic populations p13 and p14 showed lower Gene diversity (*He*) than others, but that of parthenogenetic population p16 was as high as those of sexual populations p12 and p13 (Table 17). Calculation of genetic distances between individuals showed that parthenogenetic populations included genetically completely/almost identical individuals: genetic distances of nearly 250 pairs of individuals was 0–4 (Fig. 54). While, the minimum genetic distances between individuals was 22 in sexual populations (Fig. 54). In Hoshino and Kogame (2019; **Chapter 4**), I showed that parthenogenesis rarely occurs in a sexual population of *Scytosiphon*. Therefore, I considered that the genetic distances observed in sexuals populations (more than 21) are genetic distances mostly between sexually produced individuals, and the genetic distances between individuals belong to the same clone are less than those, as in **Chapter 6**. Thus, a threshold distance distinguishing whether pairs of individuals belong to the same clonal lineage was set to

Table 17. Genetic diversity of each population. *N*, the number of samples from which SNPs data was successfully obtained; *G*, the number of distinct genotypes (distinct clonal lineages); *He*, gene diversity; *Div*, genetic diversity corrected for samples size; *R*, clonal diversity index. Clone codes are given to each clonal lineage; the clonal lineages found in multiple populations are indicated in bold. For clonal lineages which found in multiple individuals in one population, the number of individuals is shown in parentheses.

Population code	*N*	*G*	Clone code (genotype code)	*Div*	*R*	*He*
p12, sexual	4	4	c26-c29	1.000	1.000	0.122
p13, sexual	21	21	c5-25	1.000	1.000	0.153
p14, parthenogenetic	24	4	c1(21),**c2**,**c3**,c4	0.239	0.130	0.078
p15, parthenogenetic	5	2	**c3**(4),c38	0.400	0.250	0.028
p16, parthenogenetic	21	9	**c2**,c30(3),c31(3),c32(4),c33(2),c34,c35,c36,c37	0.890	0.400	0.124

10 (broken lines in Fig. 54), and based on this value, clonal lineages were recognized. Both genetic diversity (*Div*) and clonal diversity index (*R*) were lower in parthenogenetic populations (Table 17), supporting that these populations are maintained by parthenogenesis. In parthenogenetic populations p14 and p15, one dominant clonal lineage was detected in each (c1 and c3 respectively), but in p15, such dominant clonal lineage was not found (Table 17). Each clonal lineage was specific to each population, except for c2 and c3 which were shared by two parthenogenetic populations (Table 17).

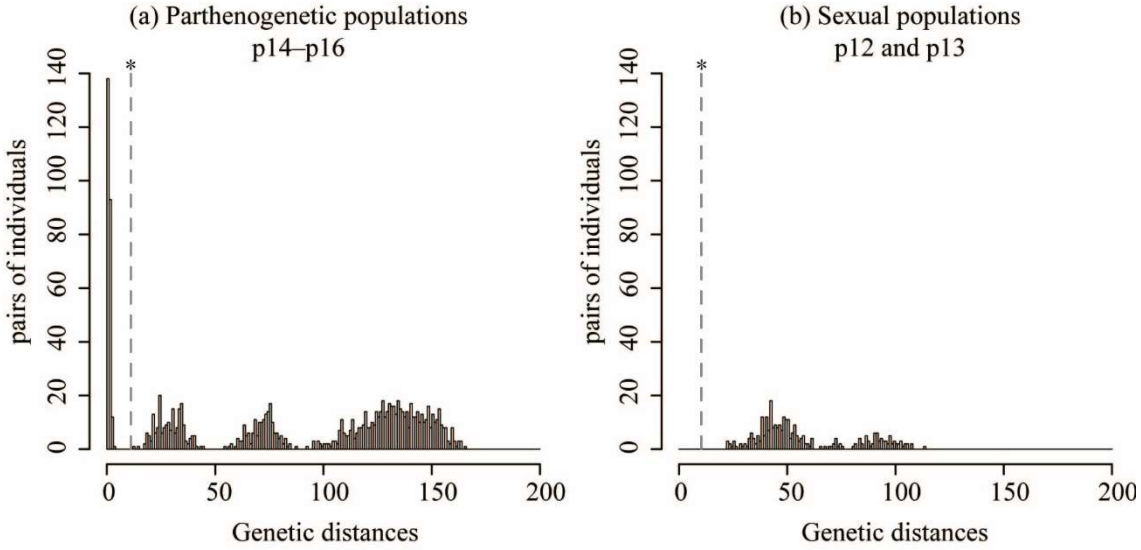

Figure 54. Histograms showing genetic distances between individuals. The threshold distances (10) to recognize clonal lineages are indicated by broken lines. Note that, in the actual calculation in 'assign clone' function of GenoDive, the dataset was not separated into sexual and parthenogenetic populations.

Population genetic structure

Three different analyses revealed that five populations examined fall into two genetically differentiated groups: individuals having *cox*1 haplotype Mt. a (mainly p13–p15) and individuals having Mt. c (mainly p12 and p16; Figs. 55–57). These analyses showed that parthenogens of *S. promiscuus* are not monophyletic.

In the STRUCTURE analyses, the ideal number of clusters determined by the Evanno method (Evanno et al., 2005) was $K = 2$ (ΔK value was the largest when $K = 2$). At $K = 2$, clear genetic differentiation between individuals having Mt. a and those having

Mt. c (Fig. 55). In the PCA (Fig. 56), PC1 divided populations into the group of the individuals having Mt. a and the group of the individuals having Mt. c and explained 43.5% of the variance, and PC2 captured variation among the individuals having Mt. a along it and explained 17.9% of the variance. The NeighborNet also separated individuals broadly into two groups which corresponded to the mitotypes of individuals (Fig. 57). In the PCA, plots of individuals tended to be more densely clustered in parthenogenetic populations, relative to the sexual populations (Fig. 56). External branches of the NeighborNet also tended to be shorter in the parthenogenetic populations (Fig. 57). This is probably due to the lower genetic variance of each parthenogenetic population.

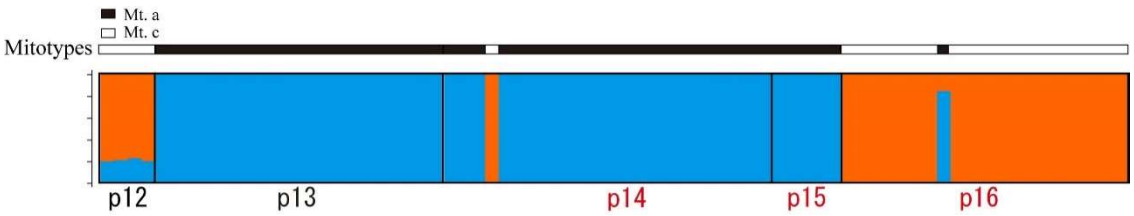

Figure 55. Result of the STRUCTURE analyses when $K = 2$. The frequency of each cluster in each sample is shown by the bar plot. Population codes (p11–p15) are shown below the bar plot. The population codes of parthenogenetic populations are indicated in red. The mitotype of each individual is indicated above the bar plot.

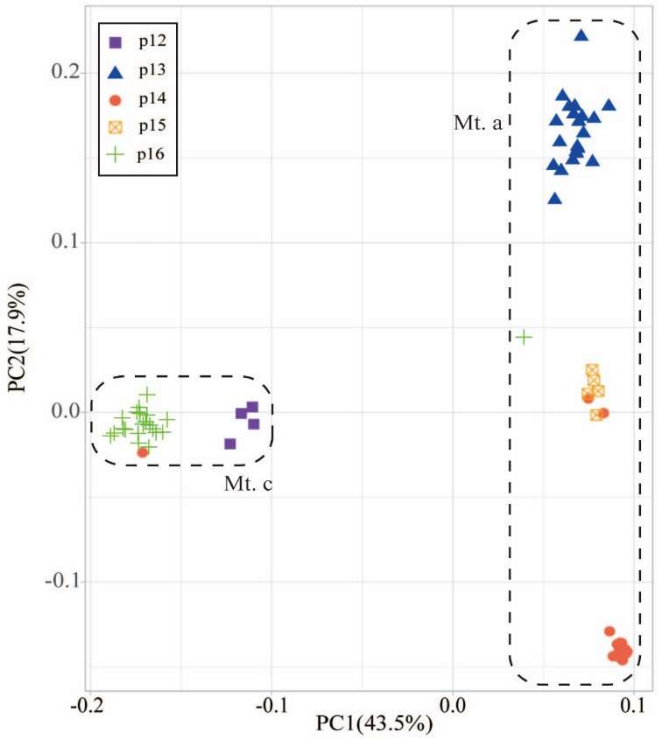

Figure 56. Result of the PCA showing the locations of each individual on the first two principal component (PC1 and PC2), which describe 61.44% of the genetic variation. Individuals are separated by broken lines depending on their mitotypes (Mt. a or Mt. c).

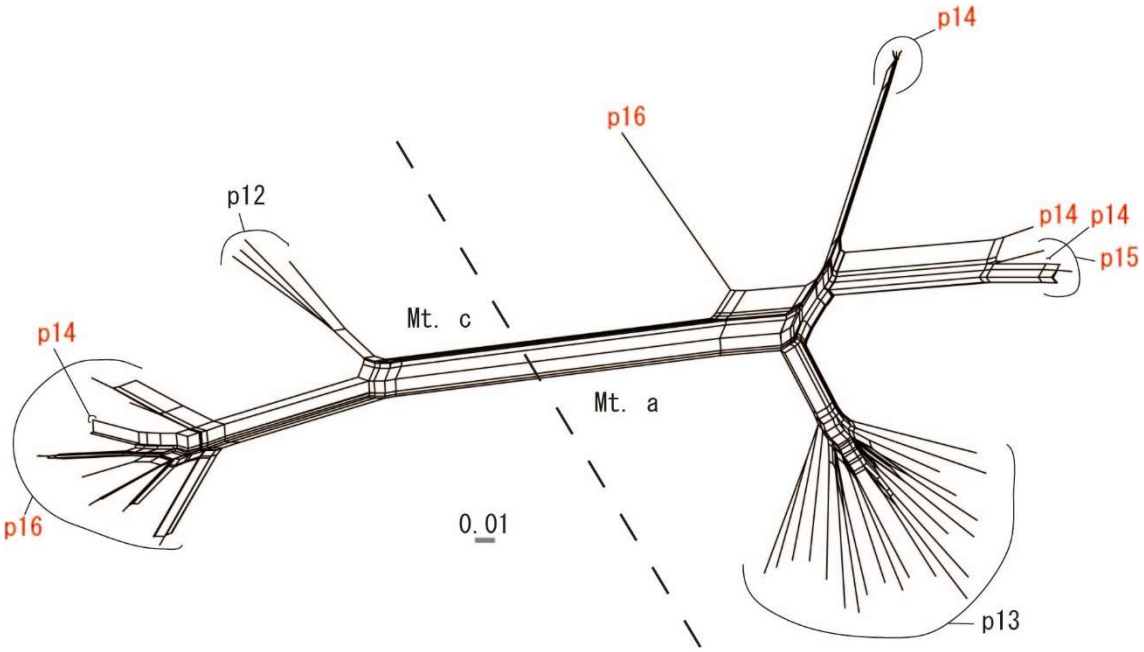

Figure 57. The NeighborNet tree, showing the polyphyly of parthenogenetic populations. Population codes of parthenogenetic populations are indicated by red color. Individuals are separated by a broken line depending on their mitotypes (Mt. a or Mt. c).

Reproductive traits in parthenogens

Fertilization rate

Female gametes from parthenogenetic population p16 were still able to fuse with male gametes; however, most gametophytes from parthenogenetic population p14 released gametes that never fused with male gametes (Fig. 58). In the crossings between individuals from sexual populations, multiple male gametes attached to a settled female gamete with the anterior flagellar tip and formed a clump around the settled female gamete, and only one male gamete fused with each female gamete: fertilization rate was 14.3–88.9% and 81.2–100% in sexual populations p12 and p13, respectively (Fig. 58). In the crossing of a sexual population p12 male × parthenogenetic population p16 females, gamete fusion was observed as in control and fertilization rate was 5.7–72.4% (Fig. 58A). In the crossing between p13 and p14, except for i1 × m1, although male gametes attached on gametes from p14 and formed clumps, gamete fusion was never observed. Gametophytes i6 and i20 were the individuals which were identified as male by the sex check PCR. However, their gametes did not fuse with female gametes from p13, but formed clumps with male gametes (i6 × m1 and i20 × m1). It indicates that gametophytes i6 and i20 are genetically male, but their gametes behave as female gametes from p14. In parthenogenetic population p14, only gametophyte i1 released gametes that fused with male gametes (fertilization rate = 26.6–50.0%; Fig. 58B). Sex pheromone was detectable by olfaction from gametes of gametophyte i1, but not from those from gametophytes i2–i8 and i20.

A

♂ \ ♀		p12 (sexual)		p16 (parthenogenetic)		
		Koi4f	Koi5f	Sz2	Sz7	Sz8
p12 (sexual)	Koi14m	20/38 (52.6%) 17/34 (50.0%) 4/22 (18.2%) 4/28 (14.3%) 16/18 (88.9%)	37/49 (75.5%) 21/34 (61.8%) 2/11 (18.2%)	9/13 (69.2%) 15/30 (50.0%) 2/8 (25.0%) 1/9 (11.1%)	9/26 (34.6%) 7/22 (31.8%) 9/22 (40.9%) 21/29 (72.4%)	2/35 (5.7%)

B

♂ \ ♀		p13 (sexual)			p14 (parthenogenetic)							
		m4	m5	m8	i1	i2	i3	i5	i6	i7	i8	i20
p13 (sexual)	m1	14/14 (100%) 13/16 (81.2%)	10/10 (100%) 16/19 (84.2%)	NA	4/15 (26.6%) 3/6 (50.0%)	0/10 (0.0%) 0/11 (0.0%) 0/13 (0.0%)	0/7 (0.0%) 0/40 (0.0%)	NA	0/22 (0.0%)	0/26 (0.0%)	NA	0/12 (0.0%)
	m2	NA	12/12 (100%)	NA	NA	0/32 (0.0%)	NA	NA	NA	NA	NA	NA
	m3	NA	11/13 (84.6%)	NA	NA	0/29 (0.0%)	NA	NA	NA	NA	NA	NA
	m7	NA	NA	29/33 (87.9%)	NA	NA	NA	0/30 (0.0%)	NA	NA	0/6 (0.0%) 0/25 (0.0%)	NA

Figure 58. The results of crossing experimnets, showing fertilization rates of each trial crossing.
(A) Crossing between p12 and p16. (B) Crossing between p13 and p14. NA: crossing was not performed.

Sex pheromone production

The GCMS analyses could not detect sex pheromones from female gametes of the parthenogenetic populations (p14 and p16) which do not have the smell of sex pheromones (Fig. 59). The compound predicted as ectocarpene (6-[(*Z*)-1-butenyl]-1,4-cycloheptadiene; known as a brown algal sex pheromone; Maier and Müller, 1986) was detected only from the positive control (female gametes from sexual populations) with high intensity at around 12.1 min (Fig. 59). Female gametes from the parthenogenetic populations also had compounds with low intensity at around 12.1 min, but they were not predicted as Ectocarpene. The results indicate that female gametes from parthenogenetic populations p14 and p16 produced little or no sex pheromones.

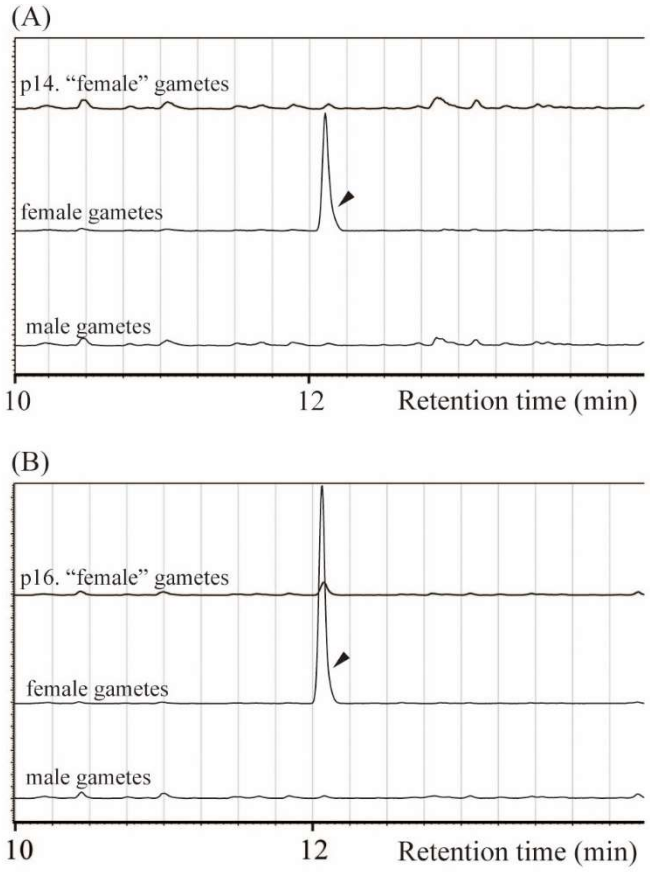

Figure 59. Results of the GCMS analyses of the volatile compounds released from gametes: extracted ion chromatograms = 91–92 m/z. The compound predicted as ectocarpene was detected with high intensity at around 12.1 min from female gametes of sexual populations (arrowheads).

Gamete size and parthenogenetic development

Female gametes of p16 were 4.78 ± 0.15 μm (avg. ± SD of four strains) in diameter and slightly larger than those of p12 which were 4.41 ± 0.18 μm (three strains) in diameter (Fig. 60). The GLMM also predicted that diameter of gamete is slightly smaller in female gametes of p12 than in those of p16 (Estimate = -0.369, P = 0.03; Table 18). While, gametes of p14 were 4.13 ± 0.20 μm (four strains) and slightly smaller than female gametes of p13 which were 4.30 ± 0.09 μm (three strains). The GLMM also predicted that diameter of gamete is slightly lager in female gametes of p13 than in gametes of p14, but the estimate was not statistically significant (Estimate = 0.168, P = 0.223; Table 18).

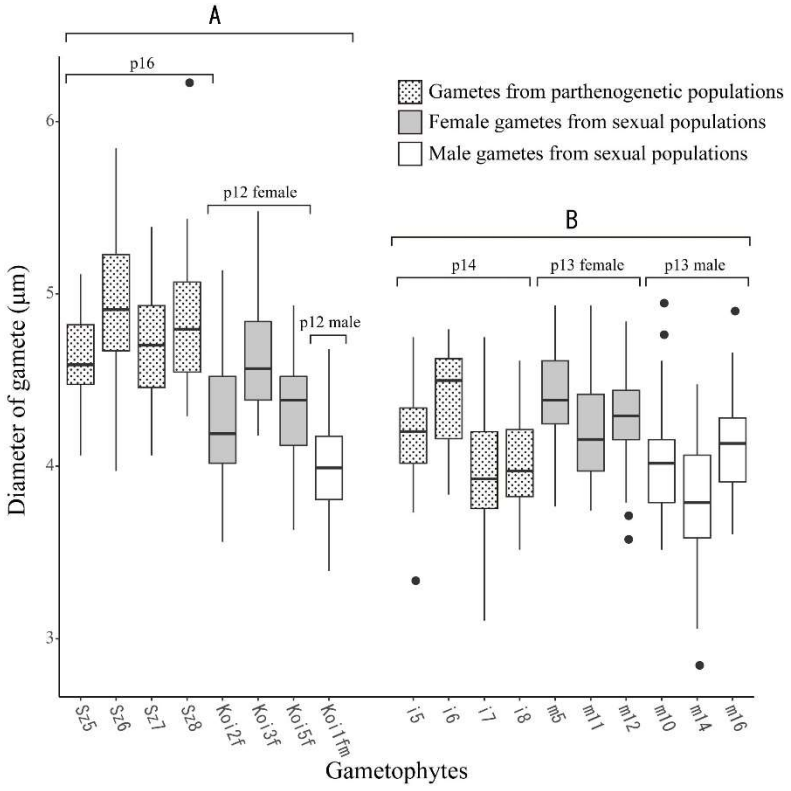

Figure 60. Box-and-whisker plots of diameters of gametes from each strain. The boxes and whiskers represent the interquartile range and the non-outlier ranges and the band near the middle of the box is the median. Black dots represent outliers. “A” and “B” on the box plots indicate genetically close pairs of parthenogenetic and sexual populations.

Table 18. The effects of the experimental groups on gamete size. Negative values for the estimates of the experimental groups (sexual female/sexual male) indicate that female/male gametes of the sexual populations were predicted as smaller than gametes of parthenogenetic populations. Positive value for the estimates of the experimental group indicates that gametes of the experimental groups were predicted as larger than gametes of parthenogenetic populations.

	Gamete size							
	p16 vs p12				p13 vs p14			
	Estimate	SE	df	*P*	Estimate	SE	df	*P*
Intercept	4.779	0.081	5.037	**<0.001**	4.13119	0.08286	6.92552	**<0.001**
Group (sexual female)	-0.369	0.123	5.020	**0.030**	0.16776	0.1247	6.5495	0.223
Group (sexual male)	-0.784	0.180	4.992	**0.007**	-0.15476	0.12486	6.57922	0.258

Both parthenogenetic populations showed more rapid parthenogenetic development than their closely related sexual populations (Fig. 61, Tables 19 and 20). Germination rate after 24 h cultivation was 76.8 ± 9.7% (avg. ± SD of four strains) in female gametes of p16, 19.5 ± 22.9% (three strains) in female gametes of p12, and 51.0 ± 23.1% (five strains) in gametes of p14, 15.7 ± 18.8% (three strains) in female gametes of p13, and 10.2 ± 12.9% (three strains) in male gametes of p13. The GLMM predicted that germination rate is significantly lower in gametes of sexual populations (Table 19).

After 5-day-cultivation, gametes of p16 grew up to ca. 7.5–13 cell-stage, while female gametes from p12 grew up to only ca. 2.0–4.5 cell-stage and most male gametes of p12 were still 1-cell-stage (Fig. 61). Gamete of p14 did not develop as rapid as those of p16. Gamete of p14 grew up to ca. 5.5–7.0 cell-stage, female gametes of p13 grew up to ca. 3.5–6.0 cell-stage, and most male gametes of p13 grew up to 2 cell-stage. The GLMM predicted that the cell numbers of 5-day-old germlings were significantly smaller in gametes of sexual populations (Table 20).

Table 19. The effects of the experimental groups on germination rate of gametes after 24 h cultivation. Negative values for the estimates of the experimental groups (sexual female/sexual male) indicate that the germination rates of female/male gametes of the sexual populations were predicted as lower than those of gametes of parthenogenetic populations.

	Germination rate after 24 h cultivation							
	p16 vs p12				p13 vs p14			
	Estimate	SE	z value	*P*	Estimate	SE	z value	*P*
Intercept	1.265	0.465	2.720	**0.007**	0.05	0.487	0.102	0.919
Group (sexual female)	-3.112	0.742	-4.196	**<0.001**	-2.179	0.81	-2.689	**0.007**
Group (sexual male)	-	-	-	**-**	-2.767	0.823	-3.363	**<0.001**

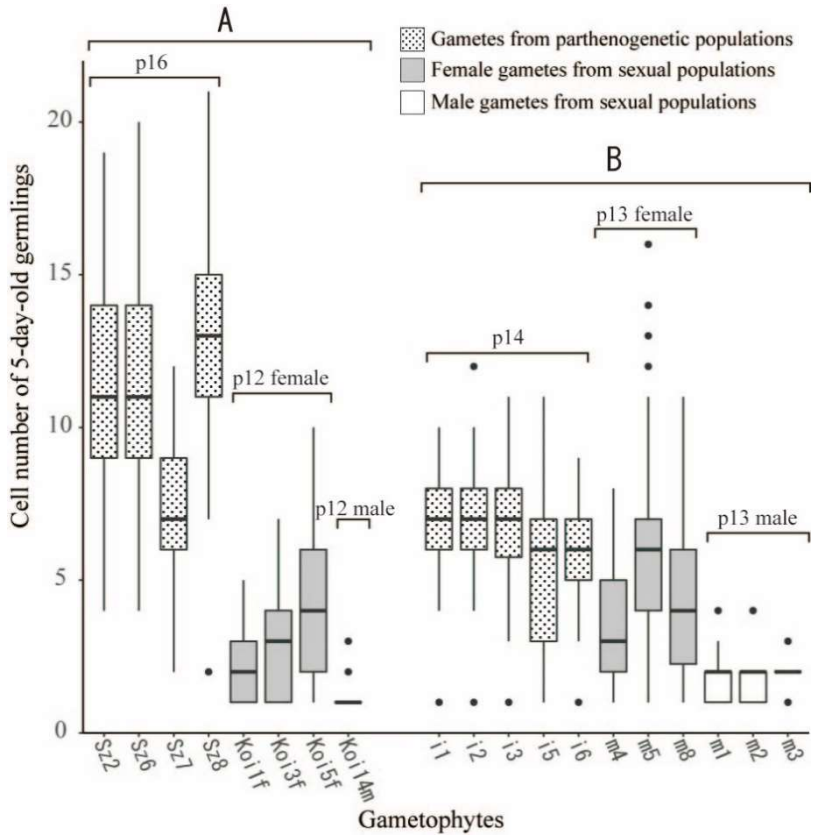

Figure 61. Box-and-whisker plots of cell numbers of 5-day-old germlings of gametes from each strain. The boxes and whiskers represent the interquartile range and the non-outlier ranges and the band near the middle of the box is the median. Black dots represent outliers. “A” and “B” on the box plots indicate genetically close pairs of parthenogenetic and sexual populations.

Table 20. The effects of the experimental groups on cell numbers of 5-day-old germlings. Negative values for the estimates of the experimental groups (sexual female/sexual male) indicate that the germination rates of female/male gametes of the sexual populations were predicted as lower than those of gametes of parthenogenetic populations.

	Cell numbers of 5-day-old germling							
	p16 vs p12				p13 vs p14			
	Estimate	SE	z value	*P*	Estimate	SE	z value	*P*
Intercept	2.361	0.114	20.802	**<0.001**	1.831	0.067	27.149	**<0.001**
Group (sexual female)	-1.260	0.177	-7.106	**<0.001**	-0.361	0.112	-3.225	**0.0013**
Group (sexual male)	-2.292	0.273	-8.384	**<0.001**	-1.246	0.116	-10.699	**<0.001**

DISCUSSION

Phylogenetic and population genetic analyses based on genome-wide SNPs data, suggested that parthenogens have evolved at least twice in the brown alga *S. promiscuus*. Parthenogenetic populations p14–p16 showed low values of genetic diversity *Div* and clonal diversity *R* (gene diversity *He* was also low in p14 and p15), supporting that these populations are maintained by parthenogenesis. Then, to examine how reproductive traits have evolved in these twice transitions to asexuality, I examined four reproductive traits of gametes (sex pheromone production, fertilization rate, gamete size, and parthenogenetic development) in the two parthenogenetic lineages (populations p14 and p16).

Sexual traits under asexuality

Sex pheromone production was suppressed in the most females of both parthenogenetic population p14 and p16. While, the loss of fertilization ability was observed only in p14.

The suppression/decay of these sexual traits are important to understand the evolution of parthenogens for three reasons. (1) Sex pheromone production and fertilization ability are essential for sexual reproduction. Thus, loss of these traits can be considered loss of sexuality and it can be the direct origin of parthenogen. (2) Since parthenogens arise in the midst of or adjacent to its parental sexuals, if any kind of reproductive isolating barriers are absent between them, the initial establishment of parthenogens can be disturbed by hybridization with their parental sexuals (Cuellar, 1977; Lynch, 1984). Suppression/decay of sex pheromone production and fertilization ability are expected to function as strong isolating barriers between parthenogens and its parental sexuals (in our crossing experiments, even female gametes without smell of sex pheromones fused with male gametes, but I guess, in field where female gametes need to attract male gametes, sex pheromone is crucial for efficient fertilization). These trait evolutions might have been necessary for the establishment and the maintenance of parthenogens. (3) In asexual life cycle, since sex pheromone production and fertilization

ability would be useless, these traits can be considered neutral or maladaptive traits depending on the amount of energy cost required for their expression (**Chapter 6**). It has been pointed out that a formerly adaptive trait can become non-fanctional or maladaptive in the new selective environment (Lynch, 1984; Lahti et al., 2009; van der Kooi and Schwander, 2014). Decay of female sexual traits is common in animal parthenogens (van der Kooi and Schwander, 2014).

The nature of brown algal parthenogens reported so far is summarized in Table 21. In the parthenogens of *S. lomentaria*, suppression of sex pheromone production was observed, but reduction of fertilization ability was not observed except for one individual [Hoshino et al., 2019 (**Chapter 5**); **Chapter 6**]. In *Mutimo cylindricus*, fertilization rate of a population showing 1:1 sex ratio was 71%; while, that of a female-dominant population was 9.0% (Kitayama et al., 1992). In *Hapterophycus canaliculatus*, a female-dominant population (six females) and a sexual population (five females and five males) were found at Oshoro Bay, Hokkaido, Japan in 1999. The female-dominant population was found in wave exposed area compared with the sexual population. In crossing experiments, five females from the female-dominant populations showed fertilization rate of 3.1 ± 6.4% (avg. ± SD) which is extremely lower than that of the sexual population: two females, 82.0 ± 6.7% (personal observation by Dr. K.Kogame.). Interestingly, reduction of fertilization ability has been observed when parthenogens and their parental sexuals exist nearby (parapatrically; Table 21). It may suggest that fertilization ability rapidly decayed due to the negative selection against hybridization (i.e. reinforcement of pre-zygotic barrier). In the five brown algal parthenogens, either sex pheromone production or fertilization ability, or both have been reduced (Table 21). Did these reductions occur before the establishment of the parthenogens as direct origin of parthenogens, or after the establishment as the result of changes in selective pressures on the sexual traits? Further investigations on other brown algal parthenogens are necessary to answer this question.

Table 21. Summary and comparison of the known brown algal parthenogens.

Species	Sexual reproduction	Sex of parthenogens	Sex pheromone production reduced?	Fertilization capacity reduced ?	Gamete size enlarged?	Rapid parthenogenetic development?	Geographic distribution of parthenogens	Reference
Scytosiphon lomentaria , The Sea of Japan coast population	isogamy	female	Yes	No	Yes	Yes	Biased to colder waters; when parapatric with sexuals, distributed in more wave-exposed area than sexuals	Hoshino et al., 2019 (**Chapter 5**)
Scytosiphon lomentaria , ThePacific coast population	isogamy	female	Yes	Generalry no	Yes	Yes	Biased to colder waters; when parapatric with sexuals, distributed in more wave-exposed area than sexuals	Hoshino et al., 2019 (**Chapter 5**); **Chapter 6**
S. promiscuus , p14	isogamy	female†	Generalry yes	Yes	No	Yes	Parapatric with sexual populations; distributed in more wave-exposed area than sexuals	This sutudy
S. promiscuus , p16	isogamy	female	Yes	No	Yes	Yes	colder environment than its close sexual population p11	This sutudy
Mutimo cylindricus	anisogamy	female	Not exmained	Yes	Not exmained	Not exmained	Distributed in the northen limit of this species; parapatric with sexual populations	Kitayama et al., 1992; Kogishi et al., 2010
Hapterophycus canaliculatus	anisogamy	female	Not exmained	Yes	Not exmained	Not exmained	Parapatric with sexual populations; distributed in more wave-exposed area than sexuals	Personal observation by K.K.

† Two males possibly parthenogens were found.

Asexual traits under asexuality

The ability to reproduce successfully without fertilization is absolutely necessary for the establishment of parthenogens (Cuellar, 1977). In brown algae, parthenogenetic development of unfused gametes is common in laboratory culture. However, I believe that parthenogenetic ability of sexuals, which is observable in culture, is not enough to maintain a parthenogenetic life cycle in nature. Even in culture condition, parthenogenetic development of gametes of sexuals is often abnormal, accompanied with high mortality, and much slower than the development of zygotes [e.g. Kemp and Cole 1961; Peters and Müller, 1985; Ar Gall et al., 1996; Hoshino and Kogame, 2019 (**Chapter 4**)]. In some taxa, including *Scytosiphon*, it has been shown that parthenogenesis is rare or absent in sexual field populations [Peters and Müller, 1985; Oppliger et al., 2007; Couceiro et al., 2015; Hoshino and Kogame, 2019 (**Chapter 4**)]. Parallel acquisitions of higher parthenogenetic ability (rapid parthenogenesis) in the four parthenogens of *Scytosiphon* (Table 21) may partly support that parthenogenetic ability of sexuals is not enough for a parthenogenetic life. Brown algal parthenogenesis has been mainly studied in sexual entities (e.g., Ar Gall et al., 1996; Bothwell et al., 2010; Mignerot et al., 2019), and studies using parthenogens are rare. In *Scytosiphon*, difference in gene expression was observed between female gametes of a sexual population and those of a parthenogenetic population (as asexual spores; Han et al., 2014). To reveal the evolutionary mechanisms of brown algal parthenogens, studies on genetic bases of parthenogenesis in parthenogens are necessary.

Parthenogenetic population p16 produced slightly larger gametes than those of close sexual population p12. Larger gamete size of parthenogenetic populations has been observed also in *S. lomentaria* [Table 21; Hoshino et al., 2019 (**Chapter 5**)]. It has been hypothesized that gamete size can be considered the resource for early development [Hoshino et al., 2019 (**Chapter 5**)]. In isogamous taxa, a gamete has only half of an initial resource of a zygote. Therefore, in parthenogenetic populations where doubling of the

resource (zygote formation) does not occur, it would be adaptive to produce larger gametes. In fact, gametes of p16 showed rapid parthenogenetic development compared with those of p14 of which gamete size were as large as the close sexual population (Fig. 61). In brown algal parthenogens, larger gamete size is not prerequisite, but may be favored.

Possible explanations for distribution patterns of parthenogens

Parthenogens tend to be biased toward particular environmental settings (e.g., high latitude, high altitude, deserts, islands and 'marginal', 'disturbed' or 'ecotonal' environment) when compared with close sexual relatives, and this pattern is called geographic parthenogenesis (Kearney, 2005; Tilquin and Kokko, 2016). Since I have only five populations in this study, the distributional pattern of parthenogens in *S. promiscuus* is not certain. However, a comparison with the previous studies in other brown algae (Table 21) allows us to infer a general distributional pattern of brown algal parthenogens. That is, in brown algae, parthenogens have been found in higher latitudinal areas (colder waters) or more wave-exposed areas, when compared with sexuals.

In *S. lomentaria*, parthenogens are reported in colder waters, while, sexuals are reported in warm waters (**Chapter 6**). The similar situation was also reported in *Mutimo cylindricus* where sexual populations are common in Japan, but female-dominant populations were found with sexual populations parapatrically in its northern limit in the Tsugaru Strait (the strait between Hokkaido and Honshu; Kitayama et al., 1992; Kogishi et al., 2010). In *S. promiscuus*, sexual reproduction has been widely observed in Japan. However, since individuals having mitotype Mt. a–c had few common SNPs with the other individuals, *S. promiscuus* probably includes at least two distinct species. Among populations having mitotype Mt. a–c, parthenogenetic population p16 was found in the relatively cold environment affected by cold Oyashio current, whereas, its closest sexual relative p12 was found in the warm environment affected by warm Tsushima current. This pattern is consistent with the reports in *S. lomentaria* and *M. cylindricus*. On the other

hand, parthenogenetic populations p14 and p15 were found parapatrically with their closest sexual relative p13 in the warm environment affected by warm Kuroshio current, indicating that parthenogens are not always in colder waters. Interestingly, parthenogenetic populations p14 and p15 were found in wave-exposed area faced to the ocean, and sexual population p13 was found in a bay protected from waves (Fig. 52). Distributions of parthenogens in wave-exposed areas were also observed in *S. lomentaria* (**Chapter 6**), *H. canaliculatus* (Table 21), and *Scytosiphon* species in Oshoro Bay. In Oshoro Bay, four *Scytosiphon* species have been reported [a parthenogenetic population of *S. lomentaria* and sexual population of *S. shibazakiorum*, *S. promiscuus*, and *S. arcanus*; Hoshino et al., 2018, 2019, 2020c (**Chapter 1, 2, 5, 6**)]; *S. lomentaria* was found in more wave-exposed areas compared to the other sexual species (personal observation). Considering the above, in brown algae, parthenogens may tend to be distributed in a colder environment or in wave-exposed area, when compared with sexual relatives.

As I have already pointed out in **Chapter 6**, there are two possible explanations for the brown algal geographic parthenogenesis summarized in Table 21. The first explanation is based on a colonization ability of parthenogens. Parthenogens should have a significant advantage over bi-sexual parents in colonization ability, since they can initiate a new colony by a single individual and its potential increase in numbers per generation is double that of a bi-sexual parent (Cuellar, 1977). In the brown algae listed in Table 21, expansion of distribution might mainly depend on dispersal of zoids (gametes and meiospores) or stranding of gametophytes detached from a substratum. In wave-exposed areas where zoids and drifting gametophytes might have difficulty in reaching, parthenogens may have an advantage in colonization over sexuals. Biased distributions of the brown algal parthenogens toward colder environment can be also explained by a high colonization ability of parthenogens. In many organisms, parthenogens are biased towards previously glaciated areas (Kearney, 2005). It has been speculated that parthenogens occupied these areas after the glaciation partly as a consequence of their

superior colonization ability (Hörandl, 2009). As I discussed in **Chapter 6**, parthenogens in *S. promiscuus* and *S. lomentaria* may have successfully occupied cold waters, the areas possibly became available after the glaciation.

The second explanation presumes niche differentiation of parthenogens. Where sexuals and parthenogens coexist within a species, the parthenogens are often prevalent in marginal habitats, particularly those whose marginal nature is due to abiotic factors (Kawecki, 2008). Lynch (1984) pointed out that since one of the most stringent requirements for the establishment and maintenance of a parthenogen will be the avoidance of backcrosses and competition with parental sexuals, incipient clones that tend to use habitats not normally occupied by the parental sexuals will have an initial selective advantage over other clones. Several culture studies have shown that wavey-condition can disturb interaction between female and male gametes in brown algae (Gordon and Brawley, 2004; Pearson and Serrão, 2006). Thus, wave-exposed areas are possibly marginal habitats for sexuals (i.e., candidate habitat for parthenogens) of *Scytosiphon* and *Hapterophycus*. Regarding colder environment, however, it is unclear whether colder environment disturb sexuals (**Chapter 6**).

Origin of parthenogens

As a cause for the transition to asexuality, inter-species hybridization is often assumed. Many obligate asexual plant and animal taxa are of hybrid ancestry (Simon et al., 2003; Kearney 2005; Neiman et al., 2014). However, the origins of parthenogens in *S. promiscuus* do not seem to be hybrids. The SNPs-based analyses showed that genetic distances between sexuals and parthenogens (p12 vs p16; p13 vs p14 and 15) were smaller than that between sexuals (p12 vs p13), and it is unlikely that these parthenogens have a hybrid-derived genome. My previous studies on parthenogens in *S. lomentaria* also did not support the hybrid origin of parthenogens (**Chapter 6**). Furthermore, multigene analyses using nucleus and mitochondrial markers in Japanese *Scytosiphon* species did not show the evidence for interspecies hybridization (i.e., mitochondrial introgression)

among them (Kogame et al., 2015a). At present, spontaneous loss of sexuality or acquisition of asexuality through mutations (spontaneous origin; Simon et al., 2003) is the most possible candidate for the origin of parthenogens in *Scytosiphon* (**Chapter 6**). To test the spontaneous origin of parthenogens, investigations on the genetic bases of the loss of sexual traits and the acquisition of parthenogenetic ability are necessary.

Brown algal parthenogens reported so far were phenotypically female, including the isogamous species *S. lomentaria* [Kitayama et al., 1992; Kawai et al., 2016; Hoshino et al., 2019 (**Chapter 5**); **Chapter 6**; this study). It is probably due to the inferior parthenogenetic ability of male gametes to female gametes. In brown algae, parthenogenesis is seemed to be a female phenotype. In oogamous and anisogamous taxa, sperms/male gametes usually do not have parthenogenetic ability (Luthringer et al., 2014). In isogamous algae, *Scytosiphon* spp., male gametes show much lower survival rate during parthenogenetic development; although male gametes parthenogenetically develop up to four-celled stage, ca. 95% of them do not develop any further and die [Han et al., 2014; Hoshino et al., 2019 (**Chapter 4**); Hoshino and Kogame, 2019 (**Chapter 5**)]. Male individuals having inferior parthenogenetic ability would have difficulty to evolve to parthenogens compared with female individuals.

In the present study, 84 out of 86 individuals from parthenogenetic populations were genetically identified as female, but two individuals were identified as male by sex-check PCR. Crossing pattern and parthenogenetic development of these two males were the same as those from females from parthenogenetic populations (i6 and i20; Figs. 58 and 61), indicating that they are parthenogens rather than ordinal males introduced from neighbor sexual populations. Furthermore, these parthenogenetic males had unique mitotype Mt. c (unfortunately they were not included in the SNPs discovery). Considering the above, these males probably represent the third parthenogenetic lineage in *S. promiscuus*. If so, this is the first report of male parthenogen in brown algae. Discordance between genetic sex and phenotypic sex has been also reported in the brown alga *Undaria*

pinnatifida. Li et al. (2017) reported genetically male gametophytes which formed both functional antheridia and oogonia. Thus, in brown algae, it may not impossible for males to have a female phenotype without a female sex chromosome. To reveal the precise nature of the individuals which were genetically male but phenotypically female, investigations of its distribution, genome, and gene expression are necessary.

REFERENCES

Agapow P-M, Bininda-Emonds ORP, Grandall KA., Gittleman JI, Mace GM, Marshall JC, Purvis A. 2004. The impact of species concept on biodiversity studies. *The Quarterly Review of Biology* 79:161–179.

Aguilar-Rosas R, Aguilar-Rosas LE, Cho GY, Boo SM. 2006. First record of *Scytosiphon gracilis* Kogame from the Pacific coast of Mexico. *Algae* 21: 11–13.

Ahmed S, Cock JM, Pessia E et al. 2014. A haploid system of sex determination in the brown alga *Ectocarpus* sp. *Current Biology* 24: 1945–1957.

Ar Gall E (Le Gall Y), Asensi A, Marie D, Kloareg B. 1996. Parthenogenesis and apospory in the Laminariales: a flow cytometry analysis. *European Journal of Phycology* 31: 369–380.

Ardehed A, Johansson D, Schagerström E, Kautsky L, Johannesson K, Pereyra RT. 2015. Complex spatial clonal structure in the macroalga *Fucus radicans* with both sexual and asexual recruitment. *Ecology and Evolution* 5: 4233–4245.

Avise JC. 2000. *Phylogeography: the history and formation of species.* Harvard University Press, Cambridge. 447 pp.

Bandelt H-J, Forster P, Röhl A. 1999. Median-joining networks for inferring intraspecific phylogenies. *Molecular Biology and Evolution* 16: 37–48.

Bates D, Mächler M, Bolker B, Walker S. 2015. Fitting linear mixed-effects models using lme4. *Journal of Statistical Software* 67: 1–48.

Bergström L, Tatarenkov A, Johannesson K, Jönsson RB, Kautsky L. 2005. Genetic and morphological identification of *Fucus radicans* sp. nov. (Fucales, Phaeophyceae) in the brackish Baltic Sea. *Journal of Phycology* 41: 1025–1038.

Berthold G. 1881. Die geschlechtliche Fortpflanzung der eigentlichen Phaeosporeen. *Mittheilungen aus der Zoologischen Station zu Neapel* 2: 401–413.

Bierzychudek P. 1985. Patterns in plant parthenogenesis. *Experientia* 41: 1255–1264.

Boo SM, Kim HS, Shin W. et al. 2010. Complex phylogeographic patterns in the freshwater alga *Synura* provide new insights on ubiquity versus endemism in microbial eukaryotes. *Molecular Ecology* 19: 4323–4338.

Boraso de Zaixso AL, Akselman R. 2005. *Anotrichium furcellatum* (Ceramiaceae, Rhodophyta) en Argentina. Una posible especie invasora. *Boletin de la Sociedad Argentina de Botanica* 40: 207–213.

Boraso de Zaixso AL, Negri R. 1997. Presencia de *Sporochnus pedunculatus* (Sporochnales, Phaeophycophyta) en la costa argentina. *Physis (Buenos Aires), Secc. A* 54: 23–24.

Boraso de Zaixso AL. 2013. *Elementos para el estudio de las macroalgas de Argentina.* Universitaria de la Patagonia, Comodoro Rivadavia, 207 pp.

Bothwell JH, Marie D, Peters AF, Cock JM, Coelho SM. 2010. Role of endoreduplication and apomeiosis during parthenogenetic reproduction in the model brown alga *Ectocarpus*. *New Phytologist* 188: 111–121.

Bouckaert R, Heled J, Kühnert D. et al. 2014. BEAST2: a software platform for Bayesian evolutionary analyses. *PLoS Computational Biology* 10: e1003537. DOI: 10.1371/journal.pcbi.1003537.

Brawley SH, Johnson LE. 1992. Gametogenesis, gametes and zygotes: an ecological perspective on sexual reproduction in the algae. *British Phycological Journal* 27: 233–252.

Bringloe TT, Starko S, Wade RM. et al. 2020. Phylogeny and evolution of the brown algae. *Critical Reviews in Plant Science* 39: 281–321.

Bryant D, Moulton V. 2004. Neighbor-Net: an agglomerative method for the construction of phylogenetic network. *Molecular Biology and Evolution* 21: 255–265.

Carstens BC, Pelletier TA, Reid NM, Satler JD. 2013. How to fail at species delimitation. *Molecular Ecology* 22: 4369–4383.

Casas GN, Piriz ML. 1996. Survey of *Undaria pinnatifida* (Laminariales, Phaeophyta) in Golfo Nuevo, Argentina. *Hydrobiologia* 326/327: 213–215.

Castresana J. 2000. Selection of conserved blocks from multiple alignments for their use in phylogenetic analysis. *Molecular Biology and Evolution* 17: 540-552.

Catchen J, Hohenlohe, Bassham S, Amores A, Cresko WA. 2013. Stacks: an analysis tool set for population genomics. *Molecular Ecology* 22: 3124–3140.

Chang CC, Chow CC, Tellier LCAM, Vattikuti S, Purcell SM, Lee JJ. 2015. Second-generation PLINK: rising to the challenge of larger and richer datasets. *GigaScience* 4: 7. DOI: 10.1186/s13742-015-0047-8.

Cheang CC, Chu KH, Fujita D. et al. 2010. Low genetic variability of *Sargassum muticum* (Phaeophyceae) revealed by a global analysis of native and introduced populations. *Journal of Phycology* 46: 1063–1074.

Cho GY, Yang EC, Lee SH, Boo SM. 2002. First description of *Petalonia zosterifolia* and *Scytosiphon gracilis* (Scytosiphonaceae, Phaeophyceae) from Korea with special reference to nrDNA ITS sequence comparisons. *Algae* 17: 135-144.

Cho GY, Kogame K, Boo SM. 2006. Molecular phylogeny of the family Scytosiphonaceae (Phaeophyceae). *Algae* 21: 175–183.

Cho GY, Kogame K, Kawai H, Boo SM. 2007. Genetic diversity of *Scytosiphon lomentaria* (Scytosiphonaceae, Phaeophyceae) from the Pacific and Europe based on RuBisCO large subunit and spacer, and ITS nrDNA sequences. *Phycologia* 46: 657–665.

Clayton MN. 1976. The morphology, anatomy and life history of a complanate form of *Scytosiphon lomentaria* (Scytosiphonales, Phaeophyta) from Southern Australia. *Marine Biology* 38:201–208.

Clayton MN. 1978. Morphological variation and life history in cylindrical forms of *Scytosiphon lomentaria* (Scytosiphonaceae: Phaeophyta) from Southern Australia. *Marine Biology* 47:349–357.

Clayton MN. 1980. Sexual reproduction –a rare occurrence in the life history of the complanate form of *Scytosiphon* (Scytosiphonaceae, Phaeophyta) from southern Australia. *British Journal of Phycology* 15: 105–118.

Clayton MN. 1982. Life history studies in the Ectocarpales (Phaeophyta): contributions toward the understanding of evolutionary processes. *Botanica Marina* 25: 111–116.

Clayton MN. 1987. Isogamy and a fucalean type of life history in the Antarctic brown alga *Ascoseira mirabilis* (Ascoseirales, Phaeophyta). *Botanica Marina* 30: 447–454.

Cock JM, Godfroy O, Macaisne N, Peters AF, Coelho SM. 2014. Evolution and regulation of complex life cycles: a brown algal perspective. *Current Opinion in Plant Biology* 17: 1–6.

Contreras L, Dennett G, Moenne A, Palma RE, Correa JA. 2007. Molecular and morphologically distinct *Scytosiphon* species (Scytosiphonales, Phaeophyceae) display similar antioxidant capacities. *Journal of Phycology* 45: 1320–1328.

Couceiro L, Le Gac M, Hunsperger HM. et al. 2015. Evolution and maintenance of haploid-diploid life cycles in natural populations: the case of the marine brown alga *Ectocarpus*. *Evolution* 69: 1808–1822.

Coyer JA, Hoarau G, Costa JF. et al. 2011. Evolution and diversification within the intertidal brown macroalgae *Fucus spiralis*/*F. vesiculosus* species complex in the North Atlantic. *Molecular Phylogenetic and Evolution* 58: 283–296.

Coyne JA, Orr HA. 2004. *Speciation.* Sinauer Associates Inc., Sunderland, MA. 545 pp.

Cremades J, Pérez-Cirera JL. 1990. Nuevas combinaciones de algas bentónicas marinas, como resultado del estudio del herbario de Simón de Rojas Clemente y Rubio (1777-1827). *Anales del Jardín Botánico de Madrid* 47: 489-492.

Croce ME, Parodi ER. 2014. The Japanese alga *Polysiphonia morrowii* (Rhodomelaceae, Rhodophyta) on the South Atlantic Ocean: first report of an invasive macroalga inhabiting oyster reefs. *Helgoland Marine Research* 68: 241–252.

Cuellar O. 1977. Animal parthenogenesis. *Science* 197: 837–843.

Cánovas FG, Mota CF, Serrão EA, Pearson GA. 2011. Driving south: a multi-gene phylogeny of the brown algal family Fucaceae reveals relationships and recent drivers of a marine radiation. *BMC Evolutionary Biology* 11: 371.

De Clerck O, Gavio B, Fredericq S, Bárbara I, Coppejans E. 2005. Systematics of *Grateloupia filicina* (Halymeniaceae, Rhodophyta), based on *rbc*L sequence analyses and morphological evidence, including the reinstatement of *G. minima* and the description of *G. capensis* sp. nov. *Journal of Phycology* 41: 391–410.

De Wreede RE, Klinger T. 1988. Reproductive strategies in algae. In: *Plant Reproductive Ecology* (Ed. by Doust JL, Doust LL), pp. 267–284, Oxford University Press, New York, USA.

Deshmukhe GV, Tatewaki M. 1993. Occurrence of somatic diploidization in the life history of *Coilodesme japonica* (Dictyosiphonales, Phaeophyta). *Phycologia* 32: 197–203.

Dobzhansky T. 1970. *Genetics of the evolutionary process*. Columbia University Press, New York & London. 505 pp.

Dorken ME, Eckert CG. 2001. Severely reduced sexual reproduction in northern populations of a clonal plant, *Decodonverticillatus* (Lythraceae). *Journal of Ecology* 89: 339–250.

Doty MS. 1947. The marine algae of Oregon. Part I. Chlorophyta and Phaeophyta. *Farlowia* 3: 1–65.

Druehl L, Collins JD, Lane CE, Saunders GW. 2005. An evaluation of methods used to assess intergeneric hybridization in kelp using Pacific Laminariales (Phaeophyceae). *Journal of Phycology* 41: 250–262.

Drummond AJ, Ho SYW, Phillips MJ, Rambaut A. 2006. Relaxed phylogenetics and dating with confidence. *PLoS Biology* 4: e88. DOI: 10.1371/journal.pbio.0040088.

Earl DA, vonHoldt BM. 2012. STRUCTURE HARVESTER: a website and program for visualizing STRUCTURE output and implementing the Evanno method.

Conservation Genetics Resources 4: 359–361.

Edelstein T, Chen LC-M, McLachlan J. 1970. The life cycle of *Ralfsia clavata* and *R. borneti*. *Canadian Journal of Botany* 48: 527–531.

Ence DD, Carstens BC. 2011. SpedeSTEM: a rapid and accurate method for species delimitation. *Molecular Ecology Resources* 11: 473–480.

Engel CR, Daguin C, Serrão EA. 2005. Genetic entities and mating system in hermaphroditic *Fucus spiralis* and its close dioecious relative *F. vesiculosus* (Fucaceae, Phaeophyceae). *Molecular Ecology* 14: 2033–2046.

Evanno G, Regnaut S, Goudet J. 2005. Detecting the number of clusters of individuals using the software STRUCTURE: a simulation study. *Molecular Ecology* 14: 2611–2620.

Excoffier L, Lischer HEL. 2010. Arlequin suite ver 3.5: A new series of programs to perform population genetics analyses under Linux and Windows. *Molecular Ecology Resources* 10: 564–567.

Felsenstein J. 1985. Confidence limits on phylogenies: an approach using the bootstrap. *Evolution* 39: 783–791.

Fletcher RL. 1987. *Seaweeds of the British Isles,* Vol. 3. Fucophyceae (Phaeophyceae) Part 1. British Museum (Natural History), London, UK. 359 pp.

Fu C, Donovan WP, Shikapwashya-Hasser O, Ye X, Cole RH. 2014. Hot fusion: an efficient method to clone multiple DNA fragments as well as inverted repeats without ligase. *PLoS One* 9: e115318. DOI: 10.1371/journal.pone.0115318.

Fu G, Kinoshita N, Nagasato C, Motomura T. 2014. Fertilization of brown algae: flagellar function in phototaxis and chemotaxis. In: *Sexual reproduction in animals and plants* (Ed. by Sawada H, Inoue N, Iwano M). pp. 359–367, Springer, Tokyo, Japan.

Geoffroy A, Mauger S, De Jode A, Le Gall L, Destombe C. 2015. Molecular evidence for the coexistence of two sibling species in *Pylaiella littoralis* (Ectocarpales, Phaeophyceae) along the Brittany coast. *Journal of Phycology* 51: 480–489.

Gordon R, Brawley SH. 2004. Effects of water motion on propagule release from algae with complex life histories. *Marine Biology* 145: 21–29.

Guillemin M-L, Contreras-Porcia L, Ramírez ME. et al. 2016. The bladed Bangiales (Rhodophyta) of the South Eastern Pacific: molecular species delimitation reveals extensive diversity. *Molecular Phylogenetics and Evolution* 94: 814–826.

Guiry MD, Guiry GM. 2020. *AlgaeBase*. World-wide electronic publication, National University of Ireland, Galway. https://www.algaebase.org.

Hall AR, Colegrave N. 2008. Decay of unused characters by selection and drift. *Journal of Evolutionary Biology* 21: 610–617.

Han JW, Klochkova TA, Shim J, Nagasato C, Motomur T, Kim GH. 2014. Identification of three proteins involved in fertilization and parthenogenetic development of a brown alga, *Scytosiphon lomentaria*. *Planta* 240: 1253–1267.

Hanyuda T, Aoki S, Kawai H. 2020. Reinstatement of *Myelophycus caespitosus* (Scytosiphonaceae, Phaeophyceae) from Japan. *Phycological Research* 68: 126–134.

Hanyuda T, Hansen GI, Kawai H. 2018. Genetic identification of macroalgal species on Japanese tsunami marine debris and genetic comparisons with their wild populations. *Marine Pollution Bulletin* 132: 74–81.

Hanyuda T, Suzawa Y, Suzawa T, Arai S, Sato H, Ueda K, Kumano S. 2004. Biogeography and taxonomy of *Batrachospermum helminthosum* (Batrachospermales, Rhodophyta) in Japan inferred from *rbc*L gene sequences. *Journal of Phycology* 40: 581–588.

Harrison RG. 1998. Linking evolutionary pattern and process: the relevance of species concepts for the study of speciation. In: *Endless forms* (Ed. by Howard DJ, Berlocher SH), pp. 19–31. Oxford University Press, New York & Oxford.

Hausdorf B. 2011. Progress toward a general species concept. *Evolution* 65: 923–931.

Hoarau G, Coyer JA, Veldsink JH, Stam WT, Olsen JL. 2007. Glacial refugia and recolonization pathways in the brown seaweed *Fucus serratus*. *Molecular Ecology*

16: 3606–3616.

Hoarau G, Coyer JA, Giesbers MCWG, Jueterbock A, Olsen JL. 2015. Pre-zygotic isolation in the macroalgal genus *Fucus* from four contact zones spanning 100–10000 years: a tale of reinforcement? *Royal Society Open Science* 2: 140538. DOI: 10.1098/rsos.140538.

Hooker WJ. 1833. Div. I. Inarticulatae. In: *The English Flora of Sir James Edward Smith. Class XXIV. Cryptogamia. Vol. V. Part I. Comprising the mosses, Hepaticae, lichens, Characeae and algae* (Ed. by Hooker WJ), pp. 254-63, 268-326. Longman, Brown, Green & Longmans Paternoster-Row, London, UK.

Hori T. 1993. *An illustrated atlas of the life history of algae*. vol. 2. Uchida Rokakuho Publishing, Tokyo, Japan. 345 pp.

Hoshino M, Ishikawa S, Kogame K. 2018. Concordance between DNA-based specie boundaries and reproductive isolating barriers in the *Scytosiphon lomentaria* species complex (Ectocarpales, Phaeophyceae). *Phycologia* 57: 232–242.

Hoshino M, Kogame K. 2019. Parthenogenesis is rare in the reproduction of a sexual field population of the isogamous brown alga *Scytosiphon* (Scytosiphonaceae, Ectocarpales). *Journal of Phycology* 55: 466–472.

Hoshino M, Okino T, Kogame K. 2019. Parthenogenetic female populations in the brown alga *Scytosiphon lomentaria* (Scytosiphonaceae, Ectocarpales): Decay of a sexual trait and acquisition of asexual traits. *Journal of Phycology* 55: 204–213.

Hoshino M, Croce M.E, Hanyuda T, Kogame K. 2020a. Species delimitation of *Planosiphon gracilis* morphospecies (Scytosiphonaceae, Phaeophyceae) from Japan and the description of *Pl. nakamurae* sp. nov. *Phycologia* 59: 116–126.

Hoshino M, Ino C, Kitayama T, Kogame K. 2020b. Integrative systematics approaches revealed that the rare red alga *Schimmelmannia* (Shimmelmanniaceae, Acrosymphytales) from Japan is a new species: the description of *S. benzaiteniana* sp. nov. *Phycological Research* 68: 290–297.

Hoshino M, Tanaka A, Kamiya M, Uwai S, Hiraoka M, Kogame K. 2020c. Systematics, distribution, and sexual compatibility of sex *Scytosiphon* species (Scytosiphonaceae, Ectocarpales) from Japan and the description of four new species. *Journal of Phycology* https://doi.org/10.1111/jpy.13089.

Huang Y, Niu B, Gao Y, Fu L, Li W. 2010. CD-HIT Suite: a web server for clustering and computing biological sequences. *Bioinformatics* 26: 680–682.

Huelsenbeck JP, Ronquist F. 2001. MRBAYES: Bayesian inference of phylogeny. *Bioinformatics* 17: 754–755.

Hurd CL, Harrison PJ, Bischof K, Lobban CS.2014. *Seaweed ecology and physiology*, ed. 2. Cambridge University Press. Cambridge & New York, pp. 551.

Huson DH, Bryant D. 2005. Application of phylogenetic networks in evolutionary studies. *Molecular Biology and Evolution* 23: 254–267.

Hörandl E. 2009. Geographical parthenogenesis: opportunities for asexuality. In: *Lost sex* (Ed. by Schön I, Martens K, van Dijk P), pp. 161-186. Springer, Dordrecht.

Jeffrey SW, Humphrey GF. 1975. New spectrophotometric equations for determining chlorophylls *a*, *b*, c_1 and c_2 in higher plants, algae and natural phytoplankton. *Biochemie und Physiologie der Pflanzen* 167: S191–194.

Kato Y, Kogame K, Nagasato C, Motomura T. 2006. Inheritance of mitochondrial and chloroplast genomes in the isogamous brown alga *Scytosiphon lomentaria* (Phaeophyceae). *Phycological Research* 54: 65–71.

Kawai H, Boland W, Müller D.G. 1994. Sexual reproduction and sexual pheromones in *Myelophycus simplex* (Harvey) Papenfuss (Phaeophyceae). *Japanese Journal of Phycology* 42: 227–231.

Kawai H, Hanyuda T, Draisma SGA, Müller DG. 2007. Molecular phylogeny of *Discosporangium mesarthrocarpum* (Phaeophyceae) with a reinstatement of the order Discosporangiales. *Journal of Phycology* 43: 186–94.

Kawai H, Kogishi K, Hanyuda T. Kitayama T. 2012. Taxonomic revision of the genus *Cutleria* proposing a new genus *Mutimo* to accommodate *M. cylindricus* (Cutleriaceae, Phaeophyceae). *Phycological Research* 60: 241–248.

Kawai H, Hanyuda T, Ridgway LM, Holser K. 2013. Ancestral reproductive structure in basal kelp *Aureophycus aleuticus*. *Scientific Reports* 3: 2491.

Kawai H, Kogishi K, Hanyuda T. et al. 2016. Phylogeographic analysis of the brown alga *Cutleria multifida* (Tilopteridales, Phaeophyceae) suggests a complicated introduction history. *Phycological Research* 64: 3–10.

Kawecki TJ. 2008. Adaptation to marginal habitats. *Annual Review of Ecology Evolution and Systematics* 39: 321–342.

Kearney M. 2005. Hybridization, glaciation and geographical parthenogenesis. *Trends in Ecology & Evolution* 20: 495–502.

Kemp L, Cole K. 1961. Chromosomal alternation of generations in *Nereocystis luetkeana* (Mertens) Postels and Ruprecht. *Canadian Journal of Botany* 39: 1711–1724.

Kimura K, Nagasato C, Kogame K, Motomura T. 2010. Disappearance of male mitochondrial DNA after the four-cell stage in sporophytes of the isogamous brown algae *Scytosiphon lomentaria* (Scytosiphonaceae, Phaeophyceae). *Journal of Phycology* 46: 143–152.

Kitayama T, Kawai H, Yoshida T. 1992. Dominance of female gametophytes in field populations of *Cutleria cylindrica* (Cutleriales, Phaeophyceae) in the Tsugaru Strait, Japan. *Phycologia* 31: 449–461.

Klochkova TA, Klochkova NG, Yotsukura N, Kim GH. 2017. Morphological, molecular, and chromosomal identification of dwarf haploid parthenosporophytes of *Tauya basicrassa* (Phaeophyceae, Laminariales) from the Sea of Okhotsk. *Algae* 32: 15–28.

Kobayashi H, Haino Y, Iwasaki T, Tezuka A, Nagano AJ, Shimada S. 2018. ddRAD-seq based phylogeographic study of *Sargassum thunbergii* (Phaeophyceae, Heterokonta)

around Japanese coast. *Marine Environmental Research* 140: 104–113.

Kogame K, Kawai H. 1993. Morphology and life history of *Petalonia zosteriforia* (Reinke) O. Kuntze (Scytosiphonaceae, Phaeophyceae) from Japan. *The Japanese Journal of Phycology* 41: 29–37.

Kogame K. 1996. Morphology and life history of *Scytosiphon canaliculatus* comb. nov. (Scytosiphonales, Phaeophyceae) from Japan. *Phycological Research* 44: 85–94.

Kogame K. 1997. Sexual reproduction and life history of *Petalonia fascia* (Scytosiphonales, Phaeophyceae). *Phycologia* 36: 389–394.

Kogame K. 1998. A taxonomic study of Japanese *Scytosiphon* (Scytosiphonales, Phaeophyceae), including two new species. *Phycological Research* 46: 39–56.

Kogame K, Horiguchi T, Masuda M. 1999. Phylogeny of the order Scytosiphonales (Phaeophyceae) based on DNA sequences of *rbc*L, partial *rbc*S, and partial LSU *nr*DNA. *Phycologia* 38: 496–502.

Kogame K, Uwai S, Shimada S, Masuda M. 2005. A study of sexual and asexual populations of *Scytosiphon lomentaria* (Scytosiphonaceae, Phaeophyceae) in Hokkaido, northern Japan, using molecular markers. *European Journal of Phycology* 40: 313–322.

Kogame K, Ishikawa S, Yamauchi K, Uwai S, Kurihara A, Masuda M. 2015a. Delimitation of cryptic species of the *Scytosiphon lomentaria* complex (Scytosiphonaceae, Phaeophyceae) in Japan, based on mitochondrial and nuclear molecular markers. *Phycological Research* 63: 167–177.

Kogame K, Rindi F, Peters AF, Guiry MD. 2015b. Genetic diversity and mitochondrial introgression in *Scytosiphon lomentaria* (Ectocarpales, Phaeophyceae) in the north-eastern Atlantic Ocean. *Phycologia* 54: 367–374.

Kogishi K, Kitayama T, Miller KA, Hanyuda T, Kawai H. 2010. Phylogeography of *Cutleria cylindrica* (Cutleriales, Phaeophyceae) in northeastern Asia, and the identity of an introduced population in California. *Journal of Phycology* 46: 553–

558.

Kramer MG, Templeton AR. 2001. Life-history changes that accompany the transition from sexual to parthenogenetic reproduction in *Drosophila mercatorum*. *Evolution* 55: 748–761.

Kumar S, Stecher G, Tamura K. 2016. MEGA7: Molecular Evolutionary Genetics Analysis version 7.0 for bigger datasets. *Molecular Biology and Evolution* 33: 1870–1874.

Kuznetsova A, Brockhoff PB, Christensen RHB. 2016. lmerTest: tests in linear mixed models. R package version 2.0–33.

Kuznetsova A, Brockhoff PB, Christensen RHB. 2017. lmerTest package: tests in linear mixed effects models. *Journal of Statistical Software* 82: 1–26.

Lahti DC, Johnson NA, Ajie BC. et al. 2009. Relaxed selection in the wild. *Trends in Ecology and Evolution* 24: 487–496.

Lane CE, Lindstrom SC, Saunders GW. 2007. A molecular assessment of northeast Pacific *Alaria* species (Laminariales, Phaeophyceae) with reference to the utility of DNA barcoding. *Molecular Phylogenetics and Evolution* 44: 634–648.

Lee KM, Mansilla A, Nelson WA, Boo SM. 2012. *Colpomenia durvillei* (Scytosiphonaceae, Phaeophyceae): its distribution and relationships with other elongate species of the genus. *Botanica Marina* 55: 367–375.

Lee RE. 2008. *Phycology.* Cambridge University Press, New York. 547 pp.

Lehtonen J, Jennions MD, Kokko H. 2012. The many costs of sex. *Trends in Ecology & Evolution* 27: 172–178.

Leliaert F, Verbruggen H, Wysor B, De Cleark O. 2009. DNA taxonomy in morphologically plastic taxa: Algorithmic species delimitation in the *Boodlea* complex (Chlorophyta: Cladophorales). *Molecular Phylogenetics and Evolution* 53: 122–133.

Leliaert F, Verbruggen H, Vanormelingen P, Steen F, López-Bautista JM, Zuccarello GC,

De Clerck O. 2014. DNA-based species delimitation in algae. *European Journal of Phycology* 49: 179–196.

Li J, Pang S, Shan T. 2017. Existence of an intact male life cycle offers a novel way in pure-line crossbreeding in the brown alga *Undaria pinnatifida*. J*ournal of Applied Phycology* 29: 993–999.

Lipinska AP, Ahmed S, Peters AF, Faugeron S, Cock JM, Coelho SM. 2015. Development of PCR-based markers to determine the sex of kelps. *PLoS ONE* 10: e0140535. DOI: 10.1371/journal.pone.0140535.

Lipinska AP, Toda NRT, Heesch S, Peters AF, Cock JM, Coelho SM. 2017. Multiple gene movements into and out of haploid sex chromosomes. *Genome Biology* 18: 104. DOI: 10.1186/s13059-017-1201-7.

Lischer HEL, Excoffier L. 2012. PGDSpider: An automated data conversion tool for connecting population genetics and genomics programs. *Bioinformatics* 28: 298–299.

Luthringer R, Cormier A, Ahmed S, Peters AF, Cock JM, Coelho SM. 2014. Sexual dimorphism in the brown algae. *Perspectives in Phycology* 1: 11–25.

Lynch M. 1984. Destabilizing hybridization, general-purpose genotypes and geographic parthenogenesis. *The Quarterly Review of Biology* 59: 257–290.

Lyngbye HC. 1819. *Tentamen hydrophytologiae danicae*. Heftniae, xxxii + 248pp., 70 pls.

Løvlie A, Bryhni E. 1976. Signal for cell fusion. *Nature* 263:779–781.

Løvlie A, Bryhni E. 1978. On the relation between sexual and parthenogenetic reproduction in haplo-diplontic algae. *Botanica Marina* 21: 155–163.

Lüning K. 1990. *Seaweeds. Their environment, biogeography, and ecophysiology.* John Wiley & Sons, Inc., New York. 527 pp.

Maier I, Müller DG. 1986. Sexual pheromones in algae. *Biological Bulletin* 170: 145–175.

Martin JP, Cuevas JM. 2006. First records of *Undaria pinnatifida* (Laminariales, Phaeophyta) in Southern Patagonia, Argentina. *Biological Invasions* 8: 1399–1402.

Maynard Smith J. 1986. Evolution: contemplating life without sex. *Nature* 324:300–301.

Mayr E. 1996. What is a species, and what is not? *Philosophy of Science* 63: 262–277.

McDevit DC, Saunders GW. 2017. A molecular investigation of Canadian Scytosiphonaceae (Phaeophyceae) including descriptions of *Planosiphon* gen. nov. and *Scytosiphon promiscuus* sp. nov. *Botany* 95: 653–671.

Meirmans PG, Van Tienderen PH. 2004. GENOTYPE and GENODIVE: two programs for analysis of genetic diversity of asexual organisms. *Molecular Ecology* 4: 792–794.

Meirmans PG. 2020. GenoDive version 3.0: easy-to-use software for the analysis of genetic data of diploids and polyploids. *Molecular Ecology Resources* 20: 1126–1131.

Meretta PE, Matula CV, Casas G. 2012. Occurrence of the alien kelp *Undaria pinnatifida* (Laminariales, Phaeophyceae) in Mar del Plata, Argentina. *BioInvasions Records* 1: 59–63.

Mignerot L, Avia K, Luthringer R. et al. 2019. A key role for sex chromosomes in regulation of parthenogenesis in the brown alga *Ectocarpus*. *PLoS Genetics* 15: e1008211. DOI:org/10.1371/journal.pgen.1008211.

Miller MA, Pfeiffer W, Schwartz T. 2010. Creating the CIPRES Science Gateway for inference of large phylogenetic trees. In: *Proceedings of the Gateway Computing Environments Workshop (GCE)*, 14 November 2010, New Orleans, LA, pp. 1–8.

Monaghan MT, Wild R, Elliot M. et al. 2009. Accelerated species inventory on Madagascar using coalescent-based models of species delineation. *Systematic Biology* 58: 298–311.

Montecinos AE, Couceiro L, Peters AF, Desrut A, Valero M, Guillemin M-L. 2017. Species delimitation and phylogeographic analyses in the *Ectocarpus* subgroup

siliculosi (Ectocarpales, Phaeophyceae). *Journal of Phycology* 53: 17–31.

Monteiro CA, Serrão EA, Pearson GA. 2012. Prezygotic barriers to hybridization in marine broadcast spawners: reproductive timing and mating system variation. *PLoS One* 7: e35978. DOI:10.1371/journal.pone.0035978.

Müller DG. 1976. Sexual isolation between a European and an American population of *Ectocarpus siliculosus* (Phaeophyta). *Journal of Phycology* 12: 252–254.

Müller DG. 1977. Sexual reproduction in British *Ectocarpus siliculosus* (Phaeophyta). *British Phycological Journal* 12:131–136.

Müller DG. 1979. Genetic affinity of *Ectocarpus siliculosus* (Dillw.) Lyngb. from the Mediterranean, North Atlantic and Australia. *Phycologia* 18: 312–318.

Müller DG, Eichenberger W. 1995. Crossing experiments, lipid composition, and the species concept in *Ectocarpus siliculosus* and *E. fasciculatus* (Phaeophyceae, Ectocarpales). *Journal of Phycology* 31: 173–176.

Nagasato C, Motomura T, Ichimura T. 1998. Selective disappearance of maternal centrioles after fertilization in the anisogamous brown alga *Cutleria cylindrica* (Cutleriales, Phaeophyceae): paternal inheritance of centrioles is universal in the brown algae. *Phycological Research* 46: 191–198.

Nagasato C, Uemori C, Kato A, Motomura T. 2004. Characterization of centrin genes from *Ochromonas danica* (Chrysophyceae) and *Scytosiphon lomentaria* (Phaeophyceae). *Phycological Research* 52: 266–272.

Nakahara H. 1984. Alternation of generations of some brown algae in unialgal and axenic cultures. *Scientific Papers of the Institute of Algological Research Faculty of Science Hokkaido University* 7: 77–194.

Nakamura Y, Tatewaki M. 1975. The life history of some species of Scytosiphonales. *Scientific Papers of the Institute of Algological Research Faculty of Science Hokkaido University* 6: 57–93.

Nei M, Li WH. 1979. Mathematical model for studying genetic variation in terms of

restriction endonucleases. *Proceedings of the National Academy of Sciences of the United States of America* 76: 5269–5273.

Nei M. 1987. *Molecular Evolutionary Genetics.* Colombia University Press, New York. pp 512.

Neiman M, Sharbel TF, Schwander T. 2014. Genetic causes of transitions from sexual reproduction to asexuality in plants and animals. *Journal of Evolutionary Biology* 27: 1346–1359.

Neiva J, Assis J, Fernandes F, Pearson GA, Serrão EA. 2014. Species distribution models and mitochondrial DNA phylogeography suggest an extensive biogeographical shift in the high-intertidal seaweed *Pelvetia canaliculata*. *Journal of Biogeography* 41: 1137–1148.

Ni-Ni-Win, Hanyuda T, Arai S, Uchimura M, Abbott IA, Kawai H. 2008. Three new records of *Padina* in Japan based on morphological and molecular markers. *Phycological Research* 56: 288–300.

Okamura K. 1931. *Kaisansyokubutsu no chiritekibunpu*. Iwanami Shoten, Tokyo. 86 pp.

Oppliger LV, Correa JA, Peters AF. 2007. Parthenogenesis in the brown alga *Lessonia nigrescens* (Laminariales, Phaeophyceae) from central Chile. *Journal of Phycology* 43: 1295–1301.

Oppliger LV, von Dassow P, Bouchemousse S. et al. 2014. Alteration of sexual reproduction and genetic diversity in the kelp species *Laminaria digitata* at the southern limit of its range. *PLoS ONE* 9: e102518. DOI: org/10.1371/journal.pone.0102518.

Orensanz JM(L), Schwindt E, Pastorino G. et al. 2002. No longer the pristine confines of the world ocean: a survey of exotic marine species in the southwestern Atlantic. *Biological Invasions* 4: 115–143.

Palumbi SR. 1994. Genetic divergence, reproductive isolation, and marine speciation. *Annual Review of Ecology, Evolution, and Systematics* 25: 547–572.

Papenfuss GF. 1958. Notes on algal nomenclature IV. Various Genera and Species of Chlorophyceae, Phaeophyceae and Rhodophyceae. *Taxon* 7: 104–9.

Papenfuss GF. 1964. Catalogue and bibliography of Antarctic and Sub-Antarctic benthic marine algae. In: *Antarctic Research Series. Volume 1. Bibliography of the Antarctic seas* (Ed. by Lee MO). pp. 1–76. American Geophysical Union, Washington D.C.

Payo DA, Leliaert F, Verbruggen H, D'Hondt S, Calumpong HP, De Clerck O. 2013. Extensive cryptic species diversity and fine-scale endemism in the marine red alga *Portieria* in the Philippines. *Proceedings of the Royal Society B* 280: 20122660

Pearson GA, Serrão EA. 2006. Revisiting synchronous gamete release by fucoid algae in the intertidal zone: fertilization success and beyond? *Integrative and Comparative Biology* 46: 587–597.

Pedersen PM. 1980. Culture studies on complanate and cylindrical *Scytosiphon* (Fucophyceae, Scytosiphonales) from Greenland. *British Phycological Journal* 15: 391–398.

Peters AF, Müller DG. 1985. On the sexual reproduction of *Dictyosiphon foeniculaceus* (Phaeophyceae, Dictyosiphonales). *Helgoländer Meeresuntersuchungen* 39: 441–447.

Peters AF. 1987. Reproduction and sexuality in the Chordariales (Phaeophyceae). A review of culture studies. In: *Progress in Phycological Research. Vol. 5* (Ed. by Round FE, Chapman DJ). pp. 223–263. Biopress Ltd. Bistol.

Peters AF, Van Wijk SJ, Cho GY. et al. 2010. Reinstatement of *Ectocarpus crouaniorum* Thuret in Le Jolis as a third common species of *Ectocarpus* (Ectocarpales, Phaeophyceae) in Western Europe, and its phenology at Roscoff, Brittany. *Phycological Research* 58: 157–170.

Peters AF, Couceiro L, Tsiamis K, Küpper FC, Valero M. 2015. Barcoding of cryptic stages of marine brown algae isolated from incubated substratum reveals high diversity in Acinetosporaceae (Ectocarpales, Phaeophyceae) 1. *Cryptogamie*

Algologie 36: 3-29.

Polzin T, Daneshmand SV. 2003. On Steiner trees and minimum spanning trees in hypergraphs. *Operations Research Letters* 31: 12–20.

Pons J, Barraclough TG, Gomez-Zurita J. et al. 2006. Sequence-based species delimitation for the DNA taxonomy of undescribed insects. *Systematic Biology* 55: 595–609.

Pritchard JK, Stephens M, Donnelly P. 2000. Inference of population structure using multilocus genotype data. *Genetics* 155: 945–959.

Provan J, Wattier RA, Maggs CA. 2005. Phylogeographic analysis of the red seaweed *Palmaria palmata* reveals a Pleistocene marine glacial refugium in the English Channel. *Molecular Ecology* 14: 793–803.

Puillandre N, Lambert A, Brouillet S, Achaz G. 2012. ABGD, Automatic Barcode Gap Discovery for primary species delimitation. *Molecular Ecology* 21: 1864–1877.

R Core Team. 2016. R: a language and environment for statistical computing. R foundation for statistical computing, Vienna, Austria. URL https://www.R-project.org/.

R Core Team. 2019. R: A language and environment for statistical computing. R Foundation for Statistical Computing, Vienna, Austria. URL https://www.R-project.org/.

Raffo MP, Lo Russo V, Schwindt E. 2014a. Introduced and native species on rocky macroalgal assemblages: Zonation patterns, composition and diversity. *Aquatic Botany* 112: 57–65.

Raffo MP, Geoffroy A, Destombe C, Schwindt E. 2014b. First record of the invasive red alga *Polysiphonia morrowii* Harvey (Rhodomelaceae, Rhodophyta) on the Patagonian Shores of the Southwestern Atlantic. *Botanica Marina* 57: 21–26.

Rambaut A, Suchard MA, Xie D, Drummond AJ. 2014. Tracer v1.6. http://tree.bio.ed.ac.uk/software/tracer/.

Ramírez ME, Nuñez JD, Ocampo EH, Matula CV, Suzuki M, Hashimoto T, Cledón M. 2012. *Schizymenia dubyi* (Rhodophyta, Schizymeniaceae), a new introduced species in Argentina. *New Zealand Journal of Botany* 50: 51–58.

Reinke J. 1888. Die braunen Algen (Fucaceen und Phaeosporeen) der Kieler Bucht. *Berichte der Deutsche Botanischen Gesellschaft* 6: 14-20.

Ronquist F, Teslenko M. van der Mark P. et al. 2012. MrBayes 3.2: efficient Bayesian phylogenetic inference and model choice across a large model space. *Systematic Biology* 61: 539–542.

Rosenvinge LK. 1893. Grønlands Havalger. *Meddelelser om Grønland* 3: 763–981, pls 1–2.

Santelices B. 2002. Recent advances in fertilization ecology of macroalgae. *Journal of Phycology* 38: 4–10.

Santiañez WJE, Kogame K. 2017. Transfer of *Petalonia filiformis* (Batters) Kuntze to the genus *Planosiphon* McDevit & G.W.Saunders (Scytosiphonaceae, Phaeophyceae). *Notulae algarum* 40: 1–3.

Santiañez WJE, Lee KM, Uwai S. et al. 2018a. Untangling nets: elucidating the diversity and phylogeny of the clathrate brown algal genus *Hydroclathrus*, with the description of a new genus *Tronoella* (Scytosiphonaceae, Phaeophyceae). *Phycologia* 57: 61–78.

Santiañez WJE, Macaya EC, Lee KM, Cho GY, Boo SM, Kogame K. 2018b. Taxonomic reassessment of the Indo-Pacific Scytosiphonaceae (Phaeophyceae): *Hydroclathrus rapanuii* sp. nov. and *Chnoospora minima* from Easter Island, with proposal of *Dactylosiphon* gen. nov. and *Pseudochnoospora* gen. nov. *Botanica Marina* 61: 47–64.

Santiañez WJE, Kogame K. 2019. Proposals to recognize *Petalonia tenella* comb. nov. and to resurrect *Hapterophycus canaliculatus* (Scytosiphonaceae, Phaeophyceae). *Botanica Marina* 62: 149–153.

Schmid CE. 1993. Cell-cell-recognition during fertilization in *Ectocarpus siliculosus* (Phaeophyceae). *Hydrobiologia* 260/261: 437–443.

Schmid CE, Schroer N, Müller DG. 1994. Female gamete membrane glycoproteins potentially involved in gamete recognition in *Ectocarpus siliculosus* (Phaeophyceae). *Plant Science* 102: 61–67.

Schneider CA, Rasband WS, Eliceiri KW. 2012. NIH Image to ImageJ: 25 years of image analysis. *Nature Methods* 9: 671–675.

Schnetter R, Hörnig I, Weber-Peukert G. 1987. Taxonomy of some North Atlantic *Dictyota* species (Phaeophyta). *Hydrobiologia* 151/152: 193–197.

Serrão EA, Brawley SH, Hedman J, Kautsky L, Samuelsson G. 1999. Reproductive success of *Fucus vesiculosus* (Phaeophyceae) in the Baltic Sea. *Journal of Phycology* 35: 254–269.

Setchell WA, Gardner NL. 1925. The marine algae of the Pacific coast of North America. Part III. Melanophyceae. *University of California Publications in Botany* 8: 383–898.

Simon J-C, Delmotte F, Rispe C, Crease T. 2003. Phylogenetic relationships between parthenogens and their sexual relatives: the possible routes to parthenogenesis in animals. *Biological Journal of the Linnean Society* 79: 151–163.

Skottsberg C. 1907. Zur kenntnis der subantarkischen und antarktischen meeresalgen. I. Phaeophyceen. In: *Wissenschaftliche Ergebnisse der Schwedischen Südpolar-Expedition 1901-1903, Vol. 4.* (Ed. by Nordenskjöld O). pp. 1–172. Lithographisches Institut des Generalstabs, Stockholm.

Slatkin M, Hudson RR. 1991. Pairwise comparisons of mitochondrial DNA sequences in stable and exponentially growing populations. *Genetics* 129: 555–562.

Spalding MD, Fox HE, Allen GR. et al. 2007. Marine ecoregions of the world: a bioregionalization of coastal and shelf areas. *BioScience* 57: 573–583.

Stamatakis A. 2014. RAxML version 8: a tool for phylogenetic analysis and post-analysis

of large phylogenies. *Bioinformatics* 30: 1312–1313.

Suyama Y, Matsuki Y. 2015. MIG-seq: an effective PCR-based method for genome-wide single-nucleotide polymorphism genotyping using the next-generation sequencing platform. *Scientific Report* 5: 16963. DOI: https://doi.org/10.1038/srep16963.

Tamura K, Peterson D, Peterson N, Stecher G, Nei M, Kumar S. 2011. MEGA5: Molecular evolutionary genetics analysis using maximum likelihood, evolutionary distance, and maximum parsimony methods. *Molecular Biology and Evolution* 28: 2731–2739.

Tanaka J, Chihara M. 1984. A new species of *Myelophycus* (*M. cavum* sp. nov.) with special reference to the systematic position of the genus (Dictyosiphonales, Phaeophyceae). *Phykos* 23: 152–162.

Tatarenkov A, Bergström L, Jönsson RB, Serrão EA, Kautsky L, Johannsson K. 2005. Intriguing asexual life in marginal populations of the brown seaweed *Fucus vesiculosus*. *Molecular Ecology* 14: 647–651.

Tatewaki M. 1966. Formation of a crustaceous sporophyte with unilocular sporangia in *Scytosiphon lomentaria*. *Phycologia* 6: 62–66.

Thiers BM. 2020 [Continuously updated electronic resource]. Index Herbariorum: A Global Directory of Public Herbaria and Associated Staff. New York Botanical Garden's Virtual Herbarium, New York. http://sweetgum.nybg.org/ih/; searched on 8 October 2020.

Thompson JD, Higgins DG, Gibson TJ. 1994. CLUSTAL W: improving the sensitivity of progressive multiple sequence alignment through sequence weighting, position-specific gap penalties and weight matrix choice. *Nucleic Acids Research* 22: 4673–4680.

Tilquin A, Kokko H. 2017. What does the geography of parthenogenesis teach us about sex? *Philosophical Transactions of the Royal Society B* 371: 20120538. DOI: https://doi.org/10.1098/rstb.2015.0538.

tom Dieck I. 1987. Temperature tolerance and daylength effects in isolates of *Scytosiphon lomentaria* (Phaeophyceae) of the North Atlantic and North Pacific Ocean. *Helgoländer Meeresuntersuchungen* 41: 307–21.

Tronholm A. Leliaert F, Sansón M, Afonso-Carrillo J, Tyberghein L, Verbruggen H, De Clerck O. 2012. Contrasting geographical distributions as a result of thermal tolerance and long-distance dispersal in two allegedly widespread tropical brown algae. *PLoS ONE* 7: e30813. DOI:10.1371/journal.pone.0030813.

Vieira C, Camacho O, Wynne MJ. et al. 2016. Shedding new light on old algae: matching names and sequences in the brown algal genus *Lobophora* (Dictyotales, Phaeophyceae). *Taxon* 65: 689–707.

Vinogradova KL. 1973. Ad anatomiam generis *Petalonia* Derb. et Sol. (Scytosiphonales). *Novitates Systematicae Plantarum non Vascularium* 10: 28-32.

Vrijenhoek RC. 1984. Ecological differentiation among clones: the frozen niche variation model. In: *Population Biology and Evolution* (Ed. by Wöhrmann K, Loeschcke V.). pp. 218–231. Springer, Berlin, Heidelberg.

Watanabe K, Homma Y, Karakisawa H, Ishikawa R, Uwai S. 2018. Haplotypic differentiation between seasonal populations of *Sargassum horneri* (Fucales, Phaeophyceae) in Japan. *Phycological Research* 67: 59–64.

Womersley HBS. 1987. *The marine benthic flora of southern Australia. Part II.* South Australian Government Printing Division, Adelaide, 484 pp.

Wynne MJ. 1969. Life history and systematic studies of some Pacific North American Phaeophyceae (brown algae). *University of California Publications in Botany* 50: 1–88.

Yabu H, Tokida J. 1966. Application of aceto-iron-haematoxylin-chloral hydrate method to chromosome staining in marine algae. *The Botanical Magazine, Tokyo* 79: 381.

Yamagishi Y, Kogame K. 1998. Female dominant population of *Colpomenia peregrina* (Scytosiphonales, Phaeophyceae). *Botanica Marina* 41:217–222.

Yang EC, Peters AF, Kawai H. et al. 2014. Ligulate *Desmarestia* (Desmarestiales, Phaeophyceae) revisited: *D. japonica* sp. nov. and *D. dudresnayi* differ from *D. ligulata*. *Journal of Phycology* 50: 149-166.

Yang Z, Rannala B. 2010. Bayesian species delimitation using multilocus sequence data. *Proceedings of the National Academy of Sciences of the United States of America* 107: 9264–9269.

Yang Z. 2014. *Molecular evolution: a statistical approach.* Oxford University Press, New York. 492 pp.

Yoshizaki M, Tanaka J. 1986. Biogeography of marine algae on the Japan Sea coast of Japan, with special reference to algal flora of the Noto peninsula. *Memoirs of the National Science Museum* 19: 109–119.

Yoshizaki M. 1979. Geographic distribution of marine algae of the Pacific coast of Japan, with special reference to algal flora of the Kii Peninsula. *Memoirs of the National Science Museum* 12: 201–211.

Zanardini G. 1843. *Saggio di classificazione naturale delle Ficee*. Dallo Stabilimento tipographico enciclopedico di Girolamo Tasso, Venice, 64 pp.

Zhang J, Kapli P, Pavlidis P, Stamatakis A. 2013. A general species delimitation method with applications to phylogenetic placements. *Bioinformatics* 29: 2869–2876.

van der Kooi C, Schwander T. 2014. On the fate of sexual traits under asexuality. *Biological Reviews* 89: 805–819.

LIST OF PUBLICATIONS

Hoshino M, Tanaka A, Kamiya M, Uwai S, Hiraoka M, Kogame K. 2020c. Systematics, distribution, and sexual compatibility of six *Scytosiphon* species (Scytosiphonaceae, Ectocarpales) from Japan and the description of four new species. *Journal of Phycology* https://doi.org/10.1111/jpy.13089.

Hoshino M, Ino C, Kitayama T, Kogame K. 2020b. Integrative systematics approaches revealed that the rare red alga *Schimmelmannia* (Shimmelmanniaceae, Acrosymphytales) from Japan is a new species: the description of *S. benzaiteniana* sp. nov. *Phycological Research* 68: 290–297.

Hoshino M, Croce M.E, Hanyuda T, Kogame K. 2020a. Species delimitation of *Planosiphon gracilis* morphospecies (Scytosiphonaceae, Phaeophyceae) from Japan and the description of *Pl. nakamurae* sp. nov. *Phycologia* 59: 116–126.

Hoshino M, Kogame K. 2019. Parthenogenesis is rare in the reproduction of a sexual field population of the isogamous brown alga *Scytosiphon* (Scytosiphonaceae, Ectocarpales). *Journal of Phycology* 55: 466–472.

Hoshino M, Okino T, Kogame K. 2019. Parthenogenetic female populations in the brown alga *Scytosiphon lomentaria* (Scytosiphonaceae, Ectocarpales): Decay of a sexual trait and acquisition of asexual traits. *Journal of Phycology* 55: 204–213.

Hoshino M, Ishikawa S, Kogame K. 2018. Concordance between DNA-based specie boundaries and reproductive isolating barriers in the *Scytosiphon lomentaria* species complex (Ectocarpales, Phaeophyceae). *Phycologia* 57: 232–242.

SUPPLEMENTARY TABLES

Chapter 1

Table S1 is available at: http://dx.doi.org/10.2216/17-77.1.s1.

Chapter 2

Table S2 is available at: https://doi.org/10.1111/jpy.13089 (as Table S1).

Chapter 3

Table S3 and S4 are available at: https://doi.org/10.1080/00318884.2019.1709144 (as Table S1 and S2).

Chapter 4

Table S5–S7 are available at: https://doi.org/10.1111/jpy.12835 (as Table S1–S3).

Chapter 5

Table S8 and S9 is available at: https://doi.org/10.1111/jpy.12812 (as Table S1 and S2).

Table S10. *Scytosiphon lomentaria* samples/sequences used in Chapter 6. f: female, m: male. "fm" is given to samples in which both female and male sex-markers were amplified. For *cox* 1 and *cetn* -int2 sequenences that newly obtained in Chapter 6, numbers are given to each sequence.

Locality	Collection date	Sample code	Sex-check PCR	Sex check by crossing	*cox* 1	*cetn* -int2	MIG-seq
p1. Asari, ♀:♂ = 2:0							
	11 May 1999	990511-2		f		1	used
		990511-3		f		2	used
p2. Oshoro, ♀:♂ = 35:0							
	10 May 2000	000510-17	f	f			used
		000510-19	f	f			used
	27 Apr. 2017	170427-1	f				
		170427-2	f				
		170427-3	f				
		170427-4	f				
		170427-5	f				
		170427-6	f				
		170427-7	f				
		170427-9	f				
		170427-10	f				
		170427-11	f				
		170427-12	f				
		170427-13	f				
		170427-14	f				
		170427-15	f				
		170427-16	f				
		170427-18	f				
		170427-19	f				
		170427-20	f				
		170427-21	f				
		170427-23	f				
		170427-24	f				
		170427-26	f				
		170427-27	f				
		170427-28	f				
	21 Mar. 2018	180321-1	f		1	3	used
		180321-2	f		2	4	used
		180321-3	f		3	5	used
		180321-4	f		4		used
		180321-5	f		5		used
		180321-6	f		6		used
		180321-7	f		7		used
		180321-9	f		8		used
		180321-10	f		9		
p3. Shimamaki, ♀:♂ = 4:1							
	20 Apr. 2000	000420-2	m	m	AB747583	6	used
		000420-6	f	f	AB747584	AB748488	used
		000420-7	f		10	7	used
		000420-9	f		11		used
		000420-10	f		12		used

Table S10. (continued)

Locality	Collection date	Sample code	Sex-check PCR	Sex check by crossing	*cox* 1	*cetn* -int2	MIG-seq
p4. Kamome-o, ♀:♂ = 21:0							
	7 Apr. 2018	180407o-2	f	f	13	8	used
		180407o-3	f		14	9	used
		180407o-4	f		15	10	used
		180407o-5	f		16		used
		180407o-6	f		17		used
		180407o-7	f		18		used
		180407o-8	f		19		used
		180407o-9	f		20		used
		180407o-11	f				
		180407o-12	f				
		180407o-13	f				
		180407o-14	f				
		180407o-15	f				
		180407o-16	f				
		180407o-17	f				
		180407o-18	f				
		180407o-19	f				
		180407o-20	f				
		180407o-21	f				
		180407o-22	f				
		180407o-23	-		21		
		180407o-24	f				
p5. Kamome-u, ♀:♂ = 4:2							
	7 Apr. 2018	180407u-1	f		LC517677	11	used
		180407u-2	f	f	22	12	used
		180407u-3	m		23	13	used
		180407u-4	m	m	24		used
		180407u-5	f		25		used
		180407u-6	f		26		used
p6. Cape Shirakami, ♀:♂ = 5:1							
6	7 Apr. 2018	180407-1	f	f	LC517662	14	used
6		180407-2	f		LC517663	15	used
6		180407-3	f	f	LC517664		used
6		180407-8	f		LC517665		used
6		180407-10	m		LC517666		used
6		180407-13	f		LC517667		used
p7. Fukaura, ♀:♂ = 3:3							
	14 Apr. 2018	180414-1	f		27	16	used
		180414-15	m		28		used
		180414-16	m		29	17	used
		180414-17	m		30		used
		180414-18	f		31		used
		180414-19	f		32		used
p8. Akitashirakami, ♀:♂ = 0:1							
	14 Apr. 2018	180414as-1	m		33	18	used

Table S10. (continued)

Locality	Collection date	Sample code	Sex-check PCR	Sex check by crossing	*cox* 1	*cetn* -int2	MIG-seq
p9. Kosagawa, ♀:♂ = 9:4							
	15 Apr. 2018	180415-3	m		34	19	used
		180415-4	f		35	20	used
		180415-5	m		36	21	used
		180415-6	f		37		used
		180415-7	f		38		used
		180415-8	f		39		used
		180415-9	m		40		used
		180415-10	f		41		used
		180415-11	f		42		
		180415-14	f				
		180415-15	f				
		180415-16	f				
		180415-17	-				
		180415-18	m				
p10. Nagatejima, ♀:♂=4:6							
	29 Mar. 2011	110329-1	m		44	22	used
		110329-2	m		45	23	used
		110329-3	f		46	24	used
		110329-4	m		47		used
		110329-5	f		48		used
		110329-7	f		49		used
		110329-8	m		50		used
		110329-9	m		51		used
		110329-10	f		52		
		110329-11	m		53		
p11. Mihama, ♀:♂ = 6:5							
	18 Mar. 2018	180318-1	m		54	25	used
		180318-2	-		55	26	used
		180318-3	m		56	27	used
		180318-4	m		57		used
		180318-5	f		58		used
		180318-6	f		59		used
		180318-7	f		60		used
		180318-8	m		61		used
		180318-9	m		62		
		180318-10	f		63		
		180318-11	f				
		180318-14	f				
p12. Shikimi, ♀:♂=15:13							
	16 Apr. 2017	170416-1	f		64	28	used
		170416-2	m		65	29	used
		170416-3	f		66	30	used
		170416-4	f		67		used
		170416-5	f		68		used
		170416-6	m		69		used
		170416-8	f		70		used

Table S10. (continued)

Locality	Collection date	Sample code	Sex-check PCR	Sex check by crossing	*cox* 1	*cetn* -int2	MIG-seq
p12. Shikimi, ♀:♂=15:13							
	16 Apr. 2017	170416-9	m		71		used
		170416-10	f		72		
		170416-11	m		73		
		170416-13	f				
		170416-14	m				
		170416-15	f				
		170416-16	f				
		170416-17	f				
		170416-18	f				
		170416-19	m				
		170416-20	f				
		170416-21	m				
		170416-22	m				
		170416-23	m				
		170416-24	f				
		170416-25	f				
		170416-26	m				
		170416-27	m				
		170416-28	m				
		170416-29	m				
		170416-30	f				
p13. Miyatsu, ♀:♂=1:1							
	22 Apr. 2012	13-1	f		74	31	used
		13-2	m		75	32	used
p14. Yurihama, ♀:♂=2:4							
	16 Apr. 2017	170416-1	m		76	33	used
		170416-2	f		77	34	used
		170416-3	m		78	35	used
		170416-4	f		79		used
		170416-5	m		80		used
		170416-6	-		81		used
		170416-7	m		82		used
p15. Kiwado, ♀:♂ = 1:1							
	1 Apr. 2000	kw-2m		m	AB747618	36	used
		kw-5f	f	f	AB747619		
p16. Koinoura, ♀:♂ = 3:8							
	31 Mar. 2000	000331-1	m	m	AB747620		
		000331-2	m	m	AB747621	37	used
		000331-5	f	f	AB747623		
		000331-8	m	m	AB747624	38	used
	23 Mar. 2015	150323-1	f		83	39	used
		150323-3	m		84		used
		150323-4	m		85		used
		150323-6	f		86		used
		150323-9	m		87		
		150323-10	m		88		used
		150323-15	m				used

Table S10. (continued)

Locality	Collection date	Sample code	Sex-check PCR	Sex check by crossing	*cox* 1	*cetn* -int2	MIG-seq
p17. Sakurajima, ♀:♂ = 2:3							
	3 Mar. 2003	030303-1		m			
		030303-2	f	f	AB747625		used
		030303-3		m	AB747626	AB748540	used
		030303-4		f		40	used
		030303-5		m		41	used
p18. Murozumi, ♀:♂ = 2:1							
	23 Apr. 2012	120423-1	f		89	42	used
		120423-2	m		90	43	used
		120423-3	f		91	44	used
p19. Hazumisaki, ♀:♂ = 9:12							
	30 Mar. 2003	030330-1	m				
		030330-2	f				
	29 Mar. 2017	170329-1	m			45	used
		170329-2	m		LC517626	46	used
		170329-3	m		LC517627	47	used
		170329-4	f		LC517628		used
		170329-5	m		LC517629		used
		170329-6	f		LC517630		used
		170329-7	m		LC517631		used
		170329-8	m		LC517632		used
		170329-9	-		LC517633		
		170329-10	f		LC517634		
		170329-11	-				
		170329-12	-				
		170329-13	-				
		170329-14	m				
		170329-15	m				
		170329-16	-				
		170329-17	m				
		170329-18	m				
		170329-19	f				
		170329-20	f				
		170329-21	f				
		170329-22	f				
		170329-23	f				
		170329-24	m				
p20. Shimoda, ♀:♂ = 12:6							
	20 Feb. 2018	180220-1	m		92		
		180220-2	f		93	48	used
		180220-3	f		94	49	used
		180220-4	f		95	50	used
		180220-5	f		96		used
		180220-6	f		97		used
		180220-7	f		98		used
		180220-8	f				used
		180220-9	m		99		used
		180220-10	m		100		

Table S10. (continued)

Locality	Collection date	Sample code	Sex-check PCR	Sex check by crossing	*cox* 1	*cetn* -int2	MIG-seq
p20. Shimoda, ♀:♂ = 12:6							
	20 Feb. 2018	180220-11	f				
		180220-12	m				
		180220-13	f				
		180220-14	f				
		180220-15	m				
		180220-16	f				
		180220-17	m				
p21. Enoshima, ♀:♂ = 15:9							
	18 Feb. 2017	170218-1	f				
		170218-2	f				
		170218-3	-				
		170218-4	m				
		170218-5	m				
		170218-6	m				
		170218-7	f				
		170218-8	f				
		170218-11	f				
		170218-12	f				
		170218-14	f				
		170218-15	-				
		170218-16	-				
		170218-18	m				
		170218-19	m				
		170218-21	m				
		170218-22	f				
	1 Apr. 2018	180401-1	f		101	51	used
		180401-2	f		102	52	used
		180401-3	m		103	53	used
		180401-4	f		104		used
		180401-5	m		105		used
		180401-6	f		106		used
		180401-7	f		107		used
		180401-8	f		108		used
		180401-9	m		109		
		180401-10	f		110		
p22. Kannonzaki, ♀:♂ = 2:3							
	2 Apr. 2002	020402-1		f	AB747631	AB748545	used
		020402-2	f	f	AB747632	AB748546	used
		020402-3		m	AB747633	AB748547	used
		020402-4	m	m	AB747634		used
		020402-5		m			used
p23. Katsuura, ♀:♂ = 3:7							
	5 Mar. 2002	020305-1		m	AB747635		
		020305-2		f	AB747636		
		020305-3		m			
		020305-4		f			
		020305-5		m			

Table S10. (continued)

Locality	Collection date	Sample code	Sex-check PCR	Sex check by crossing	*cox* 1	*cetn* -int2	MIG-seq
p23. Katsuura, ♀:♂ = 3:7							
	5 Mar. 2002	020305-6		m			
		020305-7		m			
		020305-8		m			
		020305-9		f			
		020305-10		m			
p24. Inubouzaki St. 1, ♀ : ♂ : ♀♂ = 12 : 0 : 4							
	31 Mar. 2018	180331st1-1	fm		111	*54/*55	used
		180331st1-2	f	f	112	*56/*57	used
		180331st1-3	f		113	*58/*59	used
		180331st1-4	f		114	*60/*61	used
		180331st1-5	f		115		used
		180331st1-6	fm		116		used
		180331st1-7	f		117		used
		180331st1-8	f		118		used
		180331st1-9	fm		119		used
		180331st1-10	f		120		used
		180331st1-11	f		121		used
		180331st1-12	f		122		used
		180331st1-13	f		123		used
		180331st1-14	fm		124		used
	15 Feb. 2018	180215st1-1	f				used
		180215st1-2	f				used
p25. Inubousaki St. 2, ♀:♂ = 8:6							
	31 Mar. 2018	180331st2-1	m		125	94	used
		180331st2-2	m		126	95	used
		180331st2-3	f		127	96	used
		180331st2-4	f		128		used
		180331st2-5	f		129		used
		180331st2-6	m		130		used
		180331st2-7	-		131		used
		180331st2-8	f		132		used
		180331st2-9	f				used
		180331st2-10	f		133		used
		180331st2-11	m		134		used
		180331st2-12	m		135		used
		180331st2-13	m		136		used
		180331st2-14	f		137		used
		180331st2-15	f		138		used
p26. Shioyazaki, ♀:♂ = 24:0							
	16 Feb. 2017	170216-2	f				
		170216-3	f				
		170216-4	f				
		170216-5	f				
		170216-6	f				
		170216-7	f				
		170216-8	f				
		170216-10	f				

Table S10. (continued)

Locality	Collection date	Sample code	Sex-check PCR	Sex check by crossing	*cox* 1	*cetn* -int2	MIG-seq
p26. Shioyazaki, ♀:♂ = 24:0							
	16 Feb. 2017	170216-12	f				
		170216-13	f				
		170216-14	f				
		170216-16	f				
		170216-20	f				
		170216-21	-				
	25 Mar. 2018	180325-2	-				
		180325-3	f		139	62	used
		180325-4	-				
		180325-5	f		140	63	used
		180325-6	f		141	64	used
		180325-7	-		142		used
		180325-9	f				used
		180325-10	f		143		used
		180325-11	f		144		used
		180325-12	-				
		180325-13	f		145		used
		180325-14	f		146		
		180325-15	f				
p27. Azukihama, ♀:♂:♀♂ = 7:0:26							
	15 Feb. 2017	170215-1	fm				
		170215-2	fm				
		170215-3	fm				
		170215-6	fm				
		170215-7	fm				
		170215-8	fm				
		170215-9	fm				
		170215-10	f				
		170215-11	f				
		170215-12	f				
		170215-13	fm				
		170215-14	fm				
		170215-15	fm				
		170215-16	fm				
		170215-17	fm				
	14 Feb. 2018	180214-1	fm	f	147	65/*66	used
		180214-2	fm	f	148		used
		180214-3	fm	f	149	*67/*68	used
		180214-4	fm	f	150	*69/*70	used
		180214-5	fm	f	151		used
		180214-6	fm	f			used
		180214-7	-				
		180214-8	-				
		180214-9	f	f	152		used

Table S10. (continued)

Locality	Collection date	Sample code	Sex-check PCR	Sex check by crossing	*cox* 1	*cetn* -int2	MIG-seq
		180214-10	fm	f	153		used
	23 Mar. 2018	180323-1	fm	f			
		180323-2	fm				
		180323-3	f	f			
		180323-4	f	f			
		180323-5	fm	f			
		180323-6	f				
		180323-7	-				
		180323-8	-				
		180323-9	fm				
		180323-10	fm				
		180323-11	fm				
p28. Jodogahama, ♀:♂ = 14:0							
	5 May 2018	180505-1	f		154	97	used
		180505-2	f	f	155	98	used
		180505-3	f		156	99	used
		180505-4	f		157		used
		180505-5	f		158		used
		180505-6	f		159		used
		180505-7	-		160		used
		180505-8	f		161		used
		180505-9	f		162		
		180505-10	f		163		
		180505-11	f				
		180505-12	f				
		180505-13	f				
		180505-14	f				
p29. Kabushima, ♀:♂ = 28:0							
	6 May 2018	180506-1	f		164	71	used
		180506-2	f		165	72	used
		180506-3	f		166	73	used
		180506-4	f		167		used
		180506-5	f		168		used
		180506-6	f		169		used
		180506-7	f		170		used
		180506-8	f		171		used
		180506-9	f		172		
		180506-10	f		173		
		180506-11	f				
		180506-12	f				
		180506-13	f				
		180506-14	f				
		180506-15	f				
		180506-16	f				
		180506-17	f				
		180506-18	f				
		180506-19	f				
		180506-20	-				

Table S10. (continued)

Locality	Collection date	Sample code	Sex-check PCR	Sex check by crossing	*cox* 1	*cetn* -int2	MIG-seq
p29. Kabushima, ♀:♂ = 28:0							
	6 May 2018	180506-21	f				
		180506-22	f				
		180506-23	f				
		180506-24	f				
		180506-25	f				
		180506-26	f				
		180506-27	f				
		180506-28	f				
		180506-29	f				
p30. Nanaehama, ♀:♂ = 39:0							
	9 Apr. 2017	170409-1	f				
		170409-2	f				
		170409-3	f				
		170409-4	f				
		170409-5	f				
		170409-6	f				
		170409-7	f				
		170409-9	f				
		170409-10	f				
		170409-11	f				
		170409-12	f				
		170409-13	f				
		170409-14	f				
		170409-15	f				
		170409-16	f				
		170409-17	f				
		170409-19	f				
		170409-20	f				
		170409-21	f				
		170409-22	f				
		170409-23	f				
		170409-24	f				
		170409-25	f				
		170409-26	f				
		170409-27	f				
		170409-28	f				
		170409-29	f				
		170409-30	f				
		170409-31	f				
		170409-32	f				
	6 Apr. 2018	180406-1	f		174	74	used
		180406-2	f		175	75	used
		180406-3	f		176	76	used
		180406-4	f		177		used
		180406-5	f		178		used
		180406-6	f		179		used
		180406-7	f		180		used

Table S10. (continued)

Locality	Collection date	Sample code	Sex-check PCR	Sex check by crossing	*cox* 1	*cetn* -int2	MIG-seq
p30. Nanaehama, ♀:♂ = 39:0							
	6 Apr. 2018	180406-8	-		181		used
		180406-9	f		182		
		180406-10	f		183		
p31. Cape Tachimachi, ♀:♂ = 28:0							
	6 Apr. 2018	180406t-1	f	f	LC517668	77	used
		180406t-2	f		LC517669	78	used
		180406t-3	f	f	LC517670	76	used
		180406t-4	f		LC517671		used
		180406t-5	-		LC517672		used
		180406t-6	f		LC517673		used
		180406t-7	f		LC517674		used
		180406t-8	f		LC517675		used
		180406t-9	f				
		180406t-10	f		LC517676		
		180406t-11	f				
		180406t-12	f				
		180406t-13	f				
		180406t-14	f				
		180406t-15	f				
		180406t-16	f				
		180406t-17	f				
		180406t-18	f				
		180406t-19	f				
		180406t-20	f				
		180406t-21	f				
		180406t-22	f				
		180406t-23	f				
		180406t-24	-				
		180406t-25	f				
		180406t-26	f				
		180406t-27	f				
		180406t-28	f				
		180406t-29	f				
		180406t-30	f				
p32. Muroran, ♀:♂ = 38:0							
	10 Mar. 2000	000510-13	f	f			
		000510-20	f				
	24 May 2016	160524-4	f				
		160524-5	f				
		160524-6	f				
		160524-14	f				
		160524-15	f				
		160524-26	f				
		160524-27	f				
		160524-28	f				
		160524-29	f				
		160524-31	f				

Table S10. (continued)

Locality	Collection date	Sample code	Sex-check PCR	Sex check by crossing	*cox* 1	*cetn* -int2	MIG-seq
p32. Muroran, ♀:♂ = 38:0							
	24 May 2016	160524-32	f				
	28 May 2017	170528-1	-				
		170528-2	f				
		170528-3	-				
		170528-4	f				
		170528-5	f				
		170528-6	f				
		170528-7	f				
		170528-8	f				
		170528-9	f				
		170528-10	f				
		170528-11	f				
		170528-12	f				
		170528-13	f				
		170528-14	f				
		170528-15	f				
		170528-16	f				
		170528-17	f				
		170528-18	f				
		170528-19	f				
		170528-20	f				
		170528-21	-				
		170528-22	f				
	17 May 2018	180517-1	f		184	80	used
		180517-3	f		185	81	used
		180517-4	-		186	82	used
		180517-6	f		187		used
		180517-8	f		188		used
		180517-9	f		189		used
		180517-10	f		190		used
		180517-11	-				used
p33. Aikappu, ♀:♂ = 21:0							
	9 July 2017	170709-1	-				
		170709-5	f				
		170709-6	f		LC517654	83	used
		170709-7	f		LC517655	84	used
		170709-9	f		LC517656	85	used
		170709-10	f	f	LC517657		used
		170709-11	f		LC517658		used
		170709-13	f		LC517659		used
		170709-19	f		LC517660		used
		170709-21	f		LC517661		used
		170709-30	f				
		170709-38	f				
		170709-58	f				
		170709-63	f				
		170709-67	f				

Table S10. (continued)

Locality	Collection date	Sample code	Sex-check PCR	Sex check by crossing	*cox* 1	*cetn* -int2	MIG-seq
p33. Aikappu, ♀:♂ = 21:0							
	10 July 2017	170710-6	f				
		170710-7	f				
		170710-11	f				
		170710-13	f				
		170710-16	f				
		170710-19	f				
		170710-20	f				
		170710-23	f				
		170710-27	f				
		170710-29	f				
		170710-30	f				
		170710-35	f				
		170710-36	f				
		170710-40	f				
Europe, ♀:♂ = 4:0							
Ona		Ona1	f		LC517610	86	used
Ona		Ona2	f		LC517611	87	used
Portrush		Portrush	f	f	LC517609		used
Slead Head		SH	f	f	LC517608		used
Argentina, ♀:♂:♀♂ = 12:0:5							
SAO		SAO140			191	88	used
SAO		SAO244	f		192	89	used
SAO		SAO245	f		193	90	used
SAO		SAO246	f		194		used
SAO		SAO247	f		195		used
SAO		SAO248	f		196		used
SAO		SAO249	fm		197		used
SAO		SAO250	fm		198		used
SAO		SAO251	f		199		
PM		PM254	fm		200	91	used
PM		PM255	fm		201	92	used
PM		PM256	f		202	93	used
PM		PM257	f		203		used
PM		PM258	f		204		used
PM		PM259	f		205		used
PM		PM260	f		206		used
PM		PM261	fm		207		used
PM		PM266	f		208		
North America: *cox* 1 sequences generated in McDevit and Saunders (2017)							
Canada		HQ990464			HQ990464		
Canada		HM891000			HM891000		
Canada		HM891096			HM891096		
Canada		HM891134			HM891134		
Canada		HM891164			HM891164		
Canada		HM891175			HM891175		
Canada		HM891209			HM891209		

Table S10. (continued)

Locality	Collection date	Sample code	Sex-check PCR	Sex check by crossing	*cox* 1	*cetn* -int2	MIG-seq
North America: *cox* 1 sequences generated in McDevit and Saunders (2017)							
Canada		HM890851			HM890851		
USA		HQ990541			HQ990541		
Canada		HM890965			HM890965		
Canada		HM891011			HM891011		
Canada		HM891130			HM891130		
Canada		HM891131			HM891131		
Canada		KF281328			KF281328		
Canada		HM891171			HM891171		
Canada		KF281311			KF281311		
Canada		KF281300			KF281300		
Canada		HM891214			HM891214		
Canada		HM891213			HM891213		
USA		HQ990515			HQ990515		
USA		HQ990514			HQ990514		
Canada		HQ990552			HQ990552		
Canada		HM891030			HM891030		
Canada		KF281312			KF281312		
Canada		KF281319			KF281319		
USA		HQ990540			HQ990540		
USA		HQ990509			HQ990509		
Canada		HQ990665			HQ990665		
Canada		HQ990657			HQ990657		
Canada		HQ990656			HQ990656		
Canada		HQ990648			HQ990648		
Canada		HQ990615			HQ990615		
Canada		HQ990575			HQ990575		
Canada		KF281333			KF281333		
Canada		HM891215			HM891215		
Canada		HM890857			HM890857		
Canada		HM890850			HM890850		
Canada		HM891210			HM891210		
Canada		HM890849			HM890849		
Canada		HM890848			HM890848		
Canada		KF281332			KF281332		
Canada		HM890847			HM890847		
Canada		HM891204			HM891204		
Canada		HM891202			HM891202		
Canada		HM891200			HM891200		
Canada		HM891183			HM891183		
Canada		HM891174			HM891174		
Canada		HM891173			HM891173		
Canada		HM891170			HM891170		
Canada		KF281331			KF281331		
Canada		HM891169			HM891169		
Canada		HM891166			HM891166		

Table S10. (continued)

Locality	Collection date	Sample code	Sex-check PCR	Sex check by crossing	*cox* 1	*cetn* -int2	MIG-seq
North America: *cox* 1 sequences generated in McDevit and Saunders (2017)							
Canada		KF281330			KF281330		
Canada		HM891149			HM891149		
Canada		KF281329			KF281329		
Canada		KF281327			KF281327		
Canada		HM891147			HM891147		
Canada		KF281310			KF281310		
Canada		HM891137			HM891137		
Canada		HM891136			HM891136		
Canada		HM891135			HM891135		
Canada		HM891129			HM891129		
Canada		HM891128			HM891128		
Canada		HM891127			HM891127		
Canada		HM891126			HM891126		
Canada		KF281326			KF281326		
Canada		HM891125			HM891125		
Canada		KF281301			KF281301		
Canada		KF281299			KF281299		
Canada		KF281308			KF281308		
Canada		HM891115			HM891115		
Canada		KF281298			KF281298		
Canada		HM891105			HM891105		
Canada		HM891102			HM891102		
Canada		KF281309			KF281309		
Canada		KF281322			KF281322		
Canada		HM890988			HM890988		
Canada		KF281321			KF281321		
Canada		KF281325			KF281325		
Canada		KF281313			KF281313		
Canada		KF281320			KF281320		
Canada		KF281324			KF281324		
USA		KF281307			KF281307		
USA		KF281306			KF281306		
USA		KF281305			KF281305		
USA		KF281304			KF281304		
USA		KF281303			KF281303		
Canada		KF281318			KF281318		
Canada		KF281317			KF281317		
Canada		KF281302			KF281302		
USA		KF281289			KF281289		
USA		KF281290			KF281290		
USA		KF281291			KF281291		
USA		KF281296			KF281296		
USA		KF281294			KF281294		
Canada		HM891230			HM891230		
Canada		HM891228			HM891228		

Table S10. (continued)

Locality	Collection date	Sample code	Sex-check PCR	Sex check by crossing	*cox* 1	*cetn* -int2	MIG-seq
North America: *cox* 1 sequences generated in McDevit and Saunders (2017)							
Canada		HM891220			HM891220		
Canada		HM891154			HM891154		
Canada		HM891153			HM891153		
Canada		HM891152			HM891152		
Canada		KF281316			KF281316		
Canada		KF281315			KF281315		
Canada		KF281323			KF281323		
Canada		HM891110			HM891110		
France		KF281293			KF281293		
Canada		KF281314			KF281314		
USA		KF281288			KF281288		

Table S11. *Scytosiphon promiscuus* samples used in **Chapter 7**. Results of sex check are shown: f, female; m, male; fm, samples in which both female and male sex-markers were amplified. For *cox* 1 sequenences that newly obtained in **Chapter 7**, numbers (1–82) are given to each sequence. Culture codes are corresponde to those in Figure 58–61. References for *cox* 1 data/specimens are also shown.

Locality	Collection date	Sample code	Sex-check PCR	Sex check by crossing	Mitotype	*cox* 1	MIG-seq	GCMS	Culture code	Reference
Populations used for sex ratio investigations										
p12, Koinoura (GPS: 33.802968, 130.450711), ♀:♂ = 5:1										
	23 Mar. 2015	150323-5	f	f	Mt. c	LC517751	used		koi5f	Hoshino et al., 2020c
		150323-14		m	Mt. c	1	used	used	koi14m	This study
	24 Mar. 2015	150324-1	f		Mt. c	2	used		koi1f	This study
		150324-2	f		Mt. c	3	used		koi2f	This study
		150324-3	f		Mt. c	4	used		koi3f	This study
		150324-4	f	f	Mt. c	5	used		koi4f	This study
p13, Inshiri-M (33.434433, 133.439520), ♀:♂ = 24:23										
	21 Feb. 2019	190221-1	m	m		LC517763	used			Hoshino et al., 2020c
		190221-2	m	m			used			This study
		190221-3	f	f			used			This study
		190221-4		f						This study
		190221-5		f						This study
		190221-6		m						This study
	7 Mar. 2019	190307m-1	f	f	Mt. a	6	used			This study
		190307m-2	m	m	Mt. a	7	used			This study
		190307m-3	f		Mt. a	8	used			This study
		190307m-4	m	m	Mt. a	9	used			This study
		190307m-5	f	f	Mt. a	10	used			This study
		190307m-6	f	f	Mt. a	11	used			This study
		190307m-7	f	f	Mt. a	12	used			This study
		190307m-8	f	f	Mt. a	13	used			This study
		190307m-9	m	m	Mt. a	14	used			This study
		190307m-10	m	m	Mt. a	15	used			This study
		190307m-11	f				used			This study
		190307m-12	m				used			This study
		190307m-13	f				used			This study
		190307m-14	m				used			This study
		190307m-15	f				used			This study
		190307m-16	f				used			This study
		190307m-17	m				used			This study
		190307m-18	f				used			This study
		190307m-19	m				used			This study
		190307m-20	f				used			This study
		190307m-21	f				used			This study
	13 Feb. 2020	200213-1	m	m	Mt. a	16			m1	This study
		200213-2	m	m	Mt. a	17			m2	This study
		200213-3	m	m	Mt. a	18			m3	This study
		200213-4	f	f	Mt. a	19			m4	This study
		200213-5	f	f	Mt. a	20			m5	This study

Table S11. (continued)

Locality	Collection date	Sample code	Sex-check PCR	Sex check by crossing	Mitotype	*cox* 1	MIG-seq	GCMS	Culture code	Reference
p13, Inshiri-M (33.434433, 133.439520), ♀:♂ = 24:23										
	13 Feb. 2020	200213-6	m	m	Mt. a	21			m6	This study
		200213-7	m	m	Mt. a	22			m7	This study
		200213-8	f	f	Mt. a	23			m8	This study
		200213-9		f					m9	This study
		200213-10	m	m					m10	This study
		200213-11	f	f					m11	This study
		200213-12	f	f					m12	This study
		200213-13	m	m					m13	This study
		200213-14	m	m					m14	This study
		200213-15	m	m					m15	This study
		200213-16	m	m					m16	This study
		200213-17	f							This study
		200213-18	m							This study
		200213-19	f							This study
		200213-20	m							This study
	14 Feb. 2020	200214m-1	f	f				used		This study
		200214m-2	m					used		This study
		200214m-5	m	m				used		This study
		200214m-6	m	m				used		This study
		200214m-8	f	f				used		This study
p14, Inoshiri-I (33.439514, 133.443991), ♀:♂ = 53:2**										
	20 Feb. 2019	190220-1	f		Mt. a	LC517764				Hoshino et al., 2020c
		190220-2	f		Mt. a	24				This study
		190220-3	f		Mt. a	25				This study
		190220-4	f		Mt. a	26				This study
		190220-5	f		Mt. a	27				This study
		190220-6	f		Mt. a	28				This study
		190220-7	f		Mt. a	29				This study
		190220-8	f		Mt. a	30				This study
		190220-9	f	f	Mt. a	31				This study
		190220-10	f		Mt. a	32				This study
		190220-11	f		Mt. a	33				This study
		190220-12	f		Mt. a	34				This study
		190220-13	f		Mt. c	35				This study
		190220-14	f		Mt. a	36				This study
		190220-15	f		Mt. a	37				This study
		190220-16	f		Mt. a	38				This study
		190220-17	f		Mt. a	39				This study
		190220-18	f		Mt. a	40				This study
		190220-19	f		Mt. a	41				This study
		190220-20	f		Mt. a	42				This study
	7 Mar. 2019	190307i-1	f	f						This study
		190307i-2	f	f						This study
		190307i-3	f	f						This study

Table S11. (continued)

Locality	Collection date	Sample code	Sex-check PCR	Sex check by crossing	Mitotype	*cox* 1	MIG-seq	GCMS	Culture code	Reference
p14, Inoshiri-I (33.439514, 133.443991), ♀:♂ = 53:2**										
	7 Mar. 2019	190307i-4	f	f						This study
		190307i-5	f	f						This study
		190307i-6	f							This study
		190307i-7	f							This study
		190307i-8	f							This study
		190307i-9	f							This study
		190307i-10	f							This study
		190307i-11	f							This study
	14 Feb. 2020	200214i-1	f	f	Mt. a	43			i1	This study
		200214i-2	f	f	Mt. a	44			i2	This study
		200214i-3	f	f	Mt. a	45			i3	This study
		200214i-4	f	f	Mt. a	46		used	i4	This study
		200214i-5	f	f	Mt. a	47			i5	This study
		200214i-6	m	f	Mt. b	48			i6	This study
		200214i-7	f	f	Mt. a	49		used	i7	This study
		200214i-8	f	f					i8	This study
		200214i-9	f							This study
		200214i-10	f	f				used	i10	This study
		200214i-11	f							This study
		200214i-12	f							This study
		200214i-13	f							This study
		200214i-14	f							This study
		200214i-15	f							This study
		200214i-16	f							This study
		200214i-17	f							This study
		200214i-18	f							This study
		200214i-19	f							This study
		200214i-20	m	f	Mt. b	50			i20	This study
		200214i-21	f							This study
		200214i-22	f							This study
		200214i-23	f							This study
		200214i-24	f							This study
p15, Shiranohana (33.430102, 133.462658), ♀:♂ = 6:0										
	26 Mar. 2017	p13-1	f		Mt. a	LC517749	used			Hoshino et al., 2020c
		p13-2	f				used			This study
		p13-3	f		Mt. a	51	used			This study
		p13-4	f		Mt. a	52	used			This study
		p13-5	f		Mt. a	53	used			This study
		p13-6	f				used			This study
p16, Shioyazaki (36.995939, 140.981575), ♀:♂ = 25:0										
	16 Feb. 2017	170216-9	f		Mt. a	54	used			This study
		170216-17	f		Mt. c	55	used			This study
		170216-22	f		Mt. c	56	used			This study
		170216-23	f		Mt. c	57	used			This study

Table S11. (continued)

Locality	Collection date	Sample code	Sex-check PCR	Sex check by crossing	Mitotype	*cox* 1	MIG-seq	GCMS	Culture code	Reference
	16 Feb. 2017	170216-24	f		Mt. c	58	used			This study
	25 Mar. 2018	180325-8	f		Mt. c	59	used			This study
		180325-15	f		Mt. c	LC517766	used			Hoshino et al., 2020c
	21 Mar. 2019	190321-1	f		Mt. c	60	used			This study
		190321-2	f	f	Mt. c	61	used			This study
		190321-3	f	f	Mt. c	62	used	used	sz2	This study
		190321-4	f		Mt. c	63	used			This study
		190321-5	f		Mt. c	64	used		sz5	This study
		190321-6	f	f	Mt. c	65	used	used	sz6	This study
		190321-7	f	f	Mt. c	66	used	used	sz7	This study
		190321-8	f	f	Mt. c	67	used	used	sz8	This study
		190321-9	f		Mt. c	68	used			This study
		190321-10	f	f	Mt. c	69	used	used	sz10	This study
		190321-12	f		Mt. c	70	used			This study
		190321-13	f		Mt. c	71	used			This study
		190321-14	f		Mt. c	72	used			This study
		190321-15	f		Mt. c	73	used			This study
		190321-16	f		Mt. c	74	used			This study
		190321-17	f				used			This study
		190321-18			Mt. c	75				This study
		190321-19	f		Mt. c	76				This study
		190321-20	f		Mt. c	77				This study
Populations which did not used for sex ratio investigations										
p1, Asari (43.176829, 141.065947)										
	11 May 1999	Asari 6m			others	AB747562	used			Kogame et al. 2015a
		Asari 7f			others	AB747563				Kogame et al. 2015a
		Asari 8f			others	AB747564				Kogame et al. 2015a
		Asari 9f			others	AB747565	used	used		Kogame et al. 2015a
		Asari 10f			others	LC328912	used			Hoshino et al. 2018
p2, Otamoi (43.229847, 140.955387)										
	9 Apr. 2011	Otamoi 12f			others	LC328920				Hoshino et al. 2018
		Otamoi 15f			others	LC328921				Hoshino et al. 2018
		Otamoi 16m			others	LC328922				Hoshino et al. 2018
p3, Oshoro (43.213412, 140.856422)										
	6 Apr. 2010	Oshoro 100406 4m			others	LC328916	used			Hoshino et al. 2018
		Oshoro 100406 5f					used			Hoshino et al. 2018
		Oshoro 100406 6f			others	LC328918	used			Hoshino et al. 2018
	14 Nov. 2016	OshoroSt3 14Nov2016Cr7			others	78	used			This study
		OshoroSt3 14Nov2016Cr8			others	79	used			This study
		OshoroSt3 14Nov2016Cr9					used			This study
	21 Mar. 2018	OshoroSt3_fsl			others	LC517756	used			Hoshino et al., 2020c

Table S11. (continued)

Locality	Collection date	Sample code	Sex-check PCR	Sex check by crossing	Mitotype	*cox* 1	MIG-seq	GCMS	Culture code	Reference
p4, Shimamaki (42.712833, 140.064056)										
	20 Apr. 2000	Shimamaki_3			others	LC517736	used			Hoshino et al., 2020c
p5, Setana (42.382004, 139.815914)										
	18 Mar. 1987	Setana			others	AB747585	used			Kogame et al. 2015a
p6, Esashi (41.868377, 140.111927)										
	7 Apr. 2018	Kamome_o10			others	LC517755	used			Hoshino et al., 2020c
p7, Cape Shirakami (41.397622, 140.197348)										
	7 Apr. 2018	CapeShirakami180407_6			others	LC517754	used			Hoshino et al., 2020c
p8, Unosaki (39.855810, 139.815278)										
	6 Apr. 2017	Unosaki_2			others	LC517750	used			Hoshino et al., 2020c
		Unosaki_4					used			This study
p9, Himi (36.916241, 137.026745)										
	26 Feb. 2004	Himi 1			Mt. C	AB747609				Kogame et al. 2015a
p10, Mitsumatsu (35.500403, 135.514516)										
	29 Mar. 2005	Mitsumatsu 1m			others	AB747611	used			Kogame et al. 2015a
		Mitsumatsu 2f			others	AB747612	used			Kogame et al. 2015a
		Mitsumatsu 3m			others	AB747613	used			Kogame et al. 2015a
		Mitsumatsu 8f			others	AB747615	used			Kogame et al. 2015a
		Mitsumatsu 9f			others	AB747616				Kogame et al. 2015a
		Mitsumatsu 11m			others	AB747617				Kogame et al. 2015a
p11, Mihama (35.612000, 135.891900)										
	18 Mar. 2018	Mihama_kg5			others	LC517765				Hoshino et al., 2020c
p12, Koinoura (33.803136, 130.450803), samples that did not have mitotype mt. a–c.										
	23 Mar. 2015	Koinoura150323_7			others	LC517752	used			Hoshino et al., 2020c
		Koinoura150323_8			others	LC517753	used			Hoshino et al., 2020c
		Koinoura150323_11			others	80	used			This study
		Koinoura150323_13			others	81	used			This study
p16, Shioyazaki (36.995939, 140.981575), samples that did not have mitotype mt. a–c.										
	21 Mar. 2019	190321-11			others	82	used			This study
p17, Jodogahama (39.650400, 141.980200)										
	14 Feb. 2017	Jodogahama170214_1			others	LC517735	used			Hoshino et al., 2020c
p18, Muroran (42.305800, 140.983600)										
	24 May 2016	Muroran160524_30			others	LC517737				Hoshino et al., 2020c

Table S11. (continued)

Locality	Collection date	Sample code	Sex-check PCR	Sex check by crossing	Mitotype	*cox* 1	MIG-seq	GCMS	Culture code	Reference
p18, Muroran (42.305800, 140.983600)										
	10 Mar. 2016	Muroran 1f			others	AB747589				Kogame et al. 2015a
		Muroran 5f			others	LC330915	used	used		Hoshino et al. 2018
		Muroran 6f			others	AB747590				Kogame et al. 2015a
		Muroran 7f			others	AB747591	used			Kogame et al. 2015a
		Muroran 8m			others	AB747592	used			Kogame et al. 2015a
p19, Erimo (41.925571, 143.249360)										
	16 May 1987	Erimomisaki			others	AB747594	used			Kogame et al. 2015a
p20, Shoya (42.054294, 143.311783)										
	16 May 1987	Shoya			others	AB747595	used			Kogame et al. 2015a
p21, Aikappu (43.015100, 144.833000)										
	26 Apr. 2016	Aikappu160426_1			others	LC517738	used			Hoshino et al., 2020c
		Aikappu160426_2			others	LC517739	used			Hoshino et al., 2020c
		Aikappu160426_3			others	LC517740	used			Hoshino et al., 2020c
		Aikappu160426_4			others	LC517742	used			Hoshino et al., 2020c
		Aikappu160426_5			others	LC517741				Hoshino et al., 2020c
		Aikappu160426_6			others	LC517743				Hoshino et al., 2020c
		Aikappu160426_7			others	LC517744				Hoshino et al., 2020c
		Aikappu160426_8			others	LC517745				Hoshino et al., 2020c
		Aikappu160426_9			others	LC517746				Hoshino et al., 2020c
		Aikappu160426_10			others	LC517747				Hoshino et al., 2020c
		Aikappu160426_11			others	LC517748				Hoshino et al., 2020c
p22, Hanasaki (43.278596, 145.589844)										
	18 May 1991	Hanasaki 1			others	AB747599				Kogame et al. 2015a
Russia										
	15 July 2016	Magadan160715_5_1			others	LC517731	used			Hoshino et al., 2020c
		Magadan160715_5_3			others	LC517732	used			Hoshino et al., 2020c
		Magadan160715_5_4			others	LC517733	used			Hoshino et al., 2020c
		Magadan160715_5_5			others	LC517734	used			Hoshino et al., 2020c
	22 July 2005	Vilkova050722			others	LC517730	used			Hoshino et al., 2020c

Table S11. (continued)

Locality	Collection date	Sample code	Sex-check PCR	Sex check by crossing	Mitotype	*cox* 1	MIG-seq	GCMS	Culture code	Reference
North America										
		KF281367			others	KF281367				McDevit & Saunders 2017
		KF281361			others	KF281361				McDevit & Saunders 2017
		KF281363			others	KF281363				McDevit & Saunders 2017
		KF281359			others	KF281359				McDevit & Saunders 2017
		KF281349			others	KF281349				McDevit & Saunders 2017
		HM891182			others	HM891182				McDevit & Saunders 2017
		HQ990463			others	HQ990463				McDevit & Saunders 2017
		HQ990595			others	HQ990595				McDevit & Saunders 2017
		HQ990462			others	HQ990462				McDevit & Saunders 2017
		HM891140			others	HM891140				McDevit & Saunders 2017
		HM891221			others	HM891221				McDevit & Saunders 2017
		KF281343			others	KF281343				McDevit & Saunders 2017
		HM891168			others	HM891168				McDevit & Saunders 2017
		KF281353			others	KF281353				McDevit & Saunders 2017
		KF281352			others	KF281352				McDevit & Saunders 2017
		KF281356			others	KF281356				McDevit & Saunders 2017
		KF281364			others	KF281364				McDevit & Saunders 2017
		KF281369			others	KF281369				McDevit & Saunders 2017
		KF281368			others	KF281368				McDevit & Saunders 2017
		HM891181			others	HM891181				McDevit & Saunders 2017
		HM891226			others	HM891226				McDevit & Saunders 2017
		HM891227			others	HM891227				McDevit & Saunders 2017
		KF281360			others	KF281360				McDevit & Saunders 2017
		KF281354			others	KF281354				McDevit & Saunders 2017
		KF281362			others	KF281362				McDevit & Saunders 2017
		KF281355			others	KF281355				McDevit & Saunders 2017

Table S11. (continued)

Locality	Collection date	Sample code	Sex-check PCR	Sex check by crossing	Mitotype	*cox* 1	MIG-seq	GCMS	Culture code	Reference
North America										
		HM891145			others	HM891145				McDevit & Saunders 2017
		HM891144			others	HM891144				McDevit & Saunders 2017
		KF281378			others	KF281378				McDevit & Saunders 2017
		KF281357			others	KF281357				McDevit & Saunders 2017
		HQ990633			others	HQ990633				McDevit & Saunders 2017
		HQ990594			others	HQ990594				McDevit & Saunders 2017
		HM891172			others	HM891172				McDevit & Saunders 2017
		HM891163			others	HM891163				McDevit & Saunders 2017
		HM891162			others	HM891162				McDevit & Saunders 2017
		HM891159			others	HM891159				McDevit & Saunders 2017
		KF281366			others	KF281366				McDevit & Saunders 2017
		KF281344			others	KF281344				McDevit & Saunders 2017
		KF281346			others	KF281346				McDevit & Saunders 2017
		KF281347			others	KF281347				McDevit & Saunders 2017
		KF281348			others	KF281348				McDevit & Saunders 2017
		KF281341			others	KF281341				McDevit & Saunders 2017
		HM890830			others	HM890830				McDevit & Saunders 2017
		HM891499			others	HM891499				McDevit & Saunders 2017
		HM891179			others	HM891179				McDevit & Saunders 2017
		HM891178			others	HM891178				McDevit & Saunders 2017
		HM891177			others	HM891177				McDevit & Saunders 2017
		KF281340			others	KF281340				McDevit & Saunders 2017
		HM891158			others	HM891158				McDevit & Saunders 2017
		HM891151			others	HM891151				McDevit & Saunders 2017
		KF281351			others	KF281351				McDevit & Saunders 2017
		KF281350			others	KF281350				McDevit & Saunders 2017

Table S11. (continued)

Locality	Collection date	Sample code	Sex-check PCR	Sex check by crossing	Mitotype	*cox* 1	MIG-seq	GCMS	Culture code	Reference
North America										
		HM891109			others	HM891109				McDevit & Saunders 2017
		HM891071			others	HM891071				McDevit & Saunders 2017
		HM891034			others	HM891034				McDevit & Saunders 2017
		KF281358			others	KF281358				McDevit & Saunders 2017
		KF281375			others	KF281375				McDevit & Saunders 2017
		HM890986			others	HM890986				McDevit & Saunders 2017
		KF281371			others	KF281371				McDevit & Saunders 2017
		KF281370			others	KF281370				McDevit & Saunders 2017
		KF281376			others	KF281376				McDevit & Saunders 2017
		KF281380			others	KF281380				McDevit & Saunders 2017
		KF281365			others	KF281365				McDevit & Saunders 2017
		KF281342			others	KF281342				McDevit & Saunders 2017
		KF281379			others	KF281379				McDevit & Saunders 2017
		KF281373			others	KF281373				McDevit & Saunders 2017
		KF281345			others	KF281345				McDevit & Saunders 2017
		HQ990589			others	HQ990589				McDevit & Saunders 2017
		HM891500			others	HM891500				McDevit & Saunders 2017